Results and Findings from the Joint Enhanced Ozone and PM Precursor - $PM_{2.5}$ Technology Assessment and Characterization Study in New York (PMTACS-NY)

Final Report 09-10
July 2009

New York State
Energy Research and
Development Authority

NYSERDA

NYSERDA New York State Energy Research and Development Authority

The New York State Energy Research and Development Authority (NYSERDA) is a public benefit corporation created in 1975 by the New York State Legislature.

NYSERDA derives its revenues from an annual assessment levied against sales by New York's electric and gas utilities, from public benefit charges paid by New York rate payers, from voluntary annual contributions by the New York Power Authority and the Long Island Power Authority, and from limited corporate funds.

NYSERDA works with businesses, schools, and municipalities to identify existing technologies and equipment to reduce their energy costs. Its responsibilities include:

- Conducting a multifaceted energy and environmental research and development program to meet New York State's diverse economic needs.
- The **New York Energy $mart**[SM] program provides energy efficiency services, including those directed at the low-income sector, research and development, and environmental protection activities.
- Making energy more affordable for residential and low-income households.
- Helping industries, schools, hospitals, municipalities, not-for-profits, and the residential sector, implement energy-efficiency measures. NYSERDA research projects help the State's businesses and municipalities with their energy and environmental problems.
- Providing objective, credible, and useful energy analysis and planning to guide decisions made by major energy stakeholders in the private and public sectors.
- Since 1990, NYSERDA has developed and brought into use successful innovative, energy-efficient, and environmentally beneficial products, processes, and services.
- Managing the Western New York Nuclear Service Center at West Valley, including: overseeing the State's interests and share of costs at the West Valley Demonstration Project, a federal/State radioactive waste clean-up effort, and managing wastes and maintaining facilities at the shut-down State-Licensed Disposal Area.
- Coordinating the State's activities on energy emergencies and nuclear regulatory matters, and monitoring low-level radioactive waste generation and management in the State.
- Financing energy-related projects, reducing costs for ratepayers.

For more information, contact the Communications unit, NYSERDA, 17 Columbia Circle, Albany, New York 12203-6399; toll-free 1-866-NYSERDA, locally (518) 862-1090, ext. 3250; or on the web at www.nyserda.org

Results and Findings from the Joint Enhanced Ozone and PM Precursor - $PM_{2.5}$ Technology Assessment and Characterization Study in New York (PMTACS-NY)

Final Report

Prepared for the
New York State
Energy Research and
Development Authority
Albany, NY
www.nyserda.org

Barry Liebowitz
Senior Project Manager

Prepared by:
Atmospheric Sciences Research Center
University at Albany
State University of New York

Kenneth L. Demerjian,
James J. Schwab
Utpal Roychowdhury
Olga Hogrefe

NYSERDA
Report 09-10

NYSERDA 4918

July 2009

NOTICE

This report was prepared by Atmospheric Sciences Research Center, University at Albany, State University of New York in the course of performing work contracted for and sponsored by the New York State Energy Research and Development Authority and the U.S. Environmental Protection Agency (hereafter the "Sponsors"). The opinions expressed in this report do not necessarily reflect those of the Sponsors or the State of New York, and reference to any specific product, service, process, or method does not constitute an implied or expressed recommendation or endorsement of it. Further, the Sponsors and the State of New York make no warranties or representations, expressed or implied, as to the fitness for particular purpose or merchantability of any product, apparatus, or service, or the usefulness, completeness, or accuracy of any processes, methods, or other information contained, described, disclosed, or referred to in this report. The Sponsors, the State of New York, and the contractor make no representation that the use of any product, apparatus, process, method, or other information will not infringe privately owned rights and will assume no liability for any loss, injury, or damage resulting from, or occurring in connection with, the use of information contained, described, disclosed, or referred to in this report.

ABSTRACT AND KEYWORDS

The Joint Enhanced Ozone and PM Precursor/$PM_{2.5}$ Technology Assessment and Characterization Study in New York (PMTACS-NY) was designed to improve our understanding of ozone/$PM_{2.5}$-precursor relationships and to assess methods for tracking the effectiveness of emission control programs using new air quality monitoring systems.

The study was designed around three major objectives: 1) Measure the temporal and spatial distribution of the O3, $PM_{2.5}$/ co-pollutant complex[1] and its precursors to support regulatory requirements to develop cost effective mitigation strategies for O3, $PM_{2.5}$ and its co-pollutants and to establish trends in the relevant precursor concentrations to assess the impact of recent and future emission reductions in terms of emission control effectiveness and air quality response; 2) Monitor the effectiveness of new emission control technologies [i.e. Compressed Natural Gas (CNG) bus deployment and Continuously Regenerating Technology (CRT)] introduced in New York City and its potential impact on ambient air quality; and 3) Test, evaluate, and identify operationally robust new measurement technologies for future network operation that will improve understanding of atmospheric processes affecting air quality and support health-based exposure assessments.

This report summarizes the key accomplishments and findings of the study and associated published scientific results.

Keywords – Particulate matter**,** aerosols, air quality, criteria pollutants, vehicle emissions, photochemical production, secondary pollutants, measurement technology, monitoring

[1] The $PM_{2.5}$/co-pollutant complex refers to the co-existing ambient particulate matter and gaseous pollutants, for example O_3, SO_2, and NO_2, which are also known to effect health outcomes.

ACKNOWLEDGEMENTS

The findings and results reported in his final report would not have been possible without the dedicated efforts of many research groups and teams of scientists that participated in this program. We would like to acknowledge our research partners: Pennsylvania State University; Aerodyne Research Inc., New York State Department of Environmental Conservation; New York State Department of Health; Rupprecht and Patashnick Co., Inc.; Aerosol Dynamics, Inc.; Clarkson University; Georgia Institute of Technology; Max Plank Institute and the scores of researchers who have participated in this program over the past six years.

University at Albany: Kenneth L. Demerjian, PI, Gar Lala, Jim Schwab, Frank Drewnick, Olga Hogrefe, Yongquan Li, Volker Mohnen, Sarah Peters, Bob Kerr, Silke Weimer, Mingu Tang, Chenxia Cai, Rachael Jenkins, Kevin Rhoads, Utpal Roychowdhury, Richard Lamica, Ken Eckhardt, Doug Wolfe, John Spicer, Charles Schirmer, Matt Novak

Pennsylvania State University: Bill Brune, PI, Xinrong Ren, Robert Lesher, Jen Adams Angelique Oliger, Hartwig Harder, Monica Harder, Terry Shirley

Aerodyne Research Inc.: Charles Kolb, PI, John Jayne, Scott Herndon, Mark Zahniser Doug Worsnop, Joanne Shorter, Manjula Canagaratna, David Nelson, Hacene Boudries, Joda Wormhoudt, Quan Shiq

New York State Department of Environmental Conservation: Phil Galvin, PI, Dick Gibbs, Garry Boynton, Dirk Felton, Thomas Lanni, Oliver Rattigan, Brian Frank, Shida Tang, Anthony Tagliaferro, Robert Elburn, Edward Marion, Mike Christophersen

New York State Department of Health: Lee Husain, PI, Vince Dutkiewicz, Xianliang Zhou, Yi He, Jiangun Li, Sumizah Qureshi

Rupprecht and Patashnick Co., Inc.: Harvey Patashnick, PI, Jeff Ambs, A. Bicknese

Brookhaven National Laboratory: Dan Imre, PI**,** Alla Zelenyuk, Logan Chieffo, Cynthia Randles

University of California at Riverside: Kim Prather, PI, Lara Gertler, Anne Johnson, Michele Sipin**, Hiroshi Furutani**

Aerosol Dynamics, Inc.: Susanne Herring, PI,

Clarkson University: Philip Hopke, PI, Prasanna Venkatachari, Eugene Kim, Liming Zhou, Zheng Li

Georgia Institute of Technology: Rodney Weber, PI, Dan Diamond, Doug Orsini

University of Colorado: Jose Jimenez, PI, Qi Zhang

Max Plank Institute: Frank Drewnick, PI, Silke Hinges

TABLE OF CONTENTS

FIGURES

Figure

Appendix Figures

TABLES

Table

Appendix Table

BOXES

Box

EXECUTIVE SUMMARY

The Joint Enhanced Ozone and PM Precursor/$PM_{2.5}$ Technology Assessment and Characterization Study in New York (PMTACS-NY) was designed to improve our understanding of ozone/$PM_{2.5}$-precursor relationships and to assess methods for tracking the effectiveness of emission control programs using new air quality monitoring systems. The long-term monitoring of the $PM_{2.5}$/co-pollutant complex[1] and related precursors provides the opportunity to track the progress of the air quality management approach and provides a basis for its accountability. Such data can be used to assess whether emission controls for $PM_{2.5}$ primary and secondary precursor (including ozone precursor) are performing to our expectations and to verify that $PM_{2.5}$ and ozone air quality has responded to achieved emission changes as expected. Without adequate monitoring systems to track the progress and effectiveness of control programs, the air quality management approach remains unaccountable.

The PMTACS-NY study was designed around three major objectives. As part of the U.S. EPA request for application RFA guidance, investigators were asked to develop their target program objectives using test hypotheses and questions as an organizing approach in building the integrated study plan. The science policy relevant questions and associated hypotheses provided the framework and rationale for the study design and implementation. The detailed framework used in preparing the proposal is presented in Appendix A. This report summarizes the key accomplishments and findings of the study and associated published scientific results in the context of the following three targeted proposal objectives:

Objective 1. Measure the temporal and spatial distribution of the O3, $PM_{2.5}$/co-Pollutant complex and its precursors to support regulatory requirements to develop cost effective mitigation strategies for O3, $PM_{2.5}$ and its co-pollutants and to establish trends in the relevant precursor concentrations to assess the impact of recent and future emission reductions in terms of emission control effectiveness and air quality response.

Objective 2. Monitor the effectiveness of new emission control technologies [i.e. Compressed Natural Gas (CNG) bus deployment and Continuously Regenerating Technology (CRT)] introduced in New York City and its potential impact on ambient air quality.

Objective 3. Test, evaluate, and identify operationally robust new measurement technologies for future network operation that will improve understanding of atmospheric processes affecting air quality and support health-based exposure assessments.

ROUTINE MONITORING AND SPECIAL FIELD INTENSIVE CAMPAIGNS

Comprehensive measurements of $PM_{2.5}$ mass, chemical speciation, and gaseous precursors have been performed at monitoring sites located in the New York City metropolitan area and at regional representative locations in Upstate NY: Whiteface Mountain (Wilmington, NY),

[1] The $PM_{2.5}$/co-pollutant complex refers to the co-existing ambient particulate matter and gaseous pollutants, for example O_3, SO_2, and NO_2, which are also known to effect health outcomes.

operational since 1973 for ozone and since 1988 for other precursor species and Pinnacle State Park (Addison, NY), operational since 1995, both upstate; and Intermediate School I.S. 52 (South Bronx, NY), and Queens College/Public School PS219 (Queens, NY) in New York City, operational for select parameters and with some interruptions since 1990.

These measurement sites constituted the backbone of the PMTACS-NY "Supersite Network" and provided not only the routine measurements of criteria pollutants[1] and the mandated $PM_{2.5}$ mass and chemical speciation measurements, but they also were designed to operate advanced instrumentation that would complement and provide more chemical and temporal specificity of the gas and particulate matter air quality at these locations. Details regarding measurement parameters, techniques, and frequency are presented in Table B.1 of Appendix B. The enhanced measurements performed over the course of this program have provided substantial data associated with the characterization of the chemical composition of $PM_{2.5}$ within New York City and background of upstate NY.

In addition to the measurement network, which has operated throughout most of the 6-year program period (2000-2005), four special intensive field studies were carried out over the course of this program. These studies occurred in the summer of 2001 and winter of 2004 at Queens College, the summer of 2002 at Whiteface Mountain, and the summer of 2004 at Pinnacle State Park. The intensive field studies were four to six weeks in duration, and involved many research groups performing research grade measurements using emerging measurement technologies.

KEY RESULTS AND FINDINGS WITHIN PROGRAM OBJECTIVES

The findings presented are associated with citations to papers from research conducted within the program objectives, the ten science policy questions and related hypotheses (Appendix A). Some results are inconclusive and those questions that remain outstanding require additional data and/or further analyses to address.

The extensive Ozone, $PM_{2.5}$, and precursor measurement data set collected and complied over this five-year program provides a rich data base that has not yet been fully utilized. There are significant opportunities for further analyses; some are underway and will be reported in a subsequent report. Additional analyses, however, will depend on the further support. The results and findings summarized in this report highlight the most prominent and expeditious analyses that support the identified program objectives and related science policy questions and hypotheses posed.

Data sets have been posted on the NARSTO permanent archive web-site: http://eosweb.larc.nasa.gov/PRODOCS/narsto/table_narsto.html#new_york. The archive includes metadata details and all measurements collected under the NYSERDA/U.S. EPA sponsored program.

[1] Criteria pollutants designated by the U.S. Environmental Protection Agency include: ozone, carbon monoxide, nitrogen dioxide, sulfur dioxide, particulate matter and lead.

Objective 1: Measure the temporal and spatial distribution of the $PM_{2.5}$/co-Pollutant complex in urban and rural locations across New York.

Finding ES-1: *The average composition of PM at urban New York City sites indicates that the bulk of PM mass is attributed as follows: Carbon-based (~40%), Sulfate-based (~27%), Nitrate-based (~14%) and Ammonium (~13%); the remaining ~6% is metals/soil related and particle bond water (Schwab et al., 2004a).*

Figure ES.1 shows bulk chemical composition at four areas in New York State for the period ending February 2003. The data record for these plots ranges from about 21 months of data for Whiteface Mountain to 36 months of data for the urban sites. The major components at all sites are carbon, nitrate, sulfate, and ammonium, but there is a systematic change in the distribution of these components from the urban to the rural and remote locations. Carbon is proportionally highest in the New York City area and lowest in the rural and remote locations. Nitrate is highest in the large urban (New York City) and small urban (Rochester) locations and significantly lower in the rural and remote locations. Sulfate is proportionally highest at Pinnacle State Park, presumably due to its proximity to the Ohio Valley source region, and lowest in New York City. The absolute mass concentration of the "Other" component is quite similar for the urban and rural locations, but it is proportionally largest at the Whiteface Mountain location.

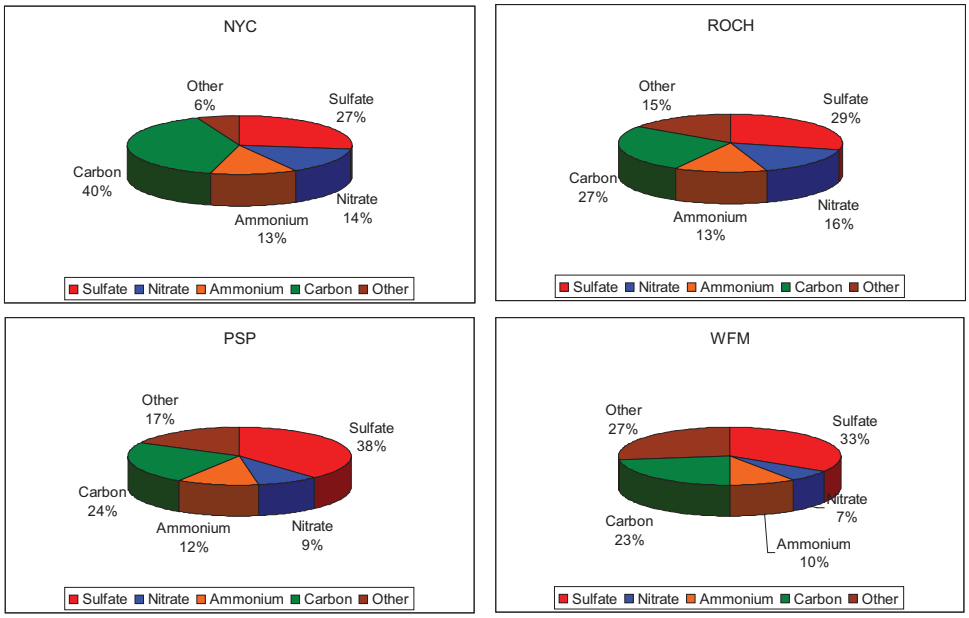

Figure ES.1. Average three-year composition of $PM_{2.5}$ at New York State sites. The NYC chart is the average of three sites (New York Botanical Garden, South Bronx IS52, and Queens College). The other sites are Rochester, Pinnacle State Park and Whiteface Mountain Lodge level. Mean $PM_{2.5}$ mass concentrations for NYC, ROCH, PSP and WFM are 15.70, 13.13, 11.26 and 7.40 $\mu g/m^3$ respectively.

Finding ES-2: *Although the contributions to the annual PM mass by season are comparable for cold and warm season months (16.6 and 15.4 ug/m,^{3} respectively) based on filter based measurement data averaged over three New York city sites in 2002, the PM species composition differs significantly by cold vs. warm season (SO_4, 22%/34%; NO_3, 23%/8%; NH_4,*

*14%/13%; OC*1.4, 28%/34%; EC, 9%/6%; and soil, 4%/5%), (Drewnick et al., 2004a,b; Schwab et al., 2004a, Weimer et al., 2006).*

Unlike rural sites where PM mass is highly seasonal, urban i.e. New York City sites show little seasonal mass variability, but show considerable variability in composition with season as shown in Figure ES.2. The measurements presented are based on three NYC sites averaged over a three-year period. Nitrate shows the most dramatic change with season, contributing a nearly equal amount of mass as sulfate during the winter, but contributes only roughly ¼ as much during the summer. Elemental carbon (EC) is also lower during the summer months, but it contributes a roughly equal percentage during the other three seasons. Sulfate and OC show greater percent contributions during the summer period, which is consistent with appreciable secondary production of these species.

The total organic mass is approximated by application of a correction factor to the measured organic carbon mass to account for the mass contribution of oxygen, nitrogen, and sulfur associated with the molecular structure of the organic particulate matter. The specific value of this factor remains uncertain and likely varies from 1.4 to 2.0 (Zhang et al., 2005a, 2005b, Turpin et al., 2001) depending on the location of the measurement site (e.g. urban vs. rural), local source emission contributions, and season. For consistency with past analyses, the 1.4 multiplier was used in the results reported in Figures ES-1-3 from Schwab et al., 2004a. Follow-on analyses presented in this report have all used a multiplier of 1.6, which is more consistent with research findings on organic particulate matter reported in this study.

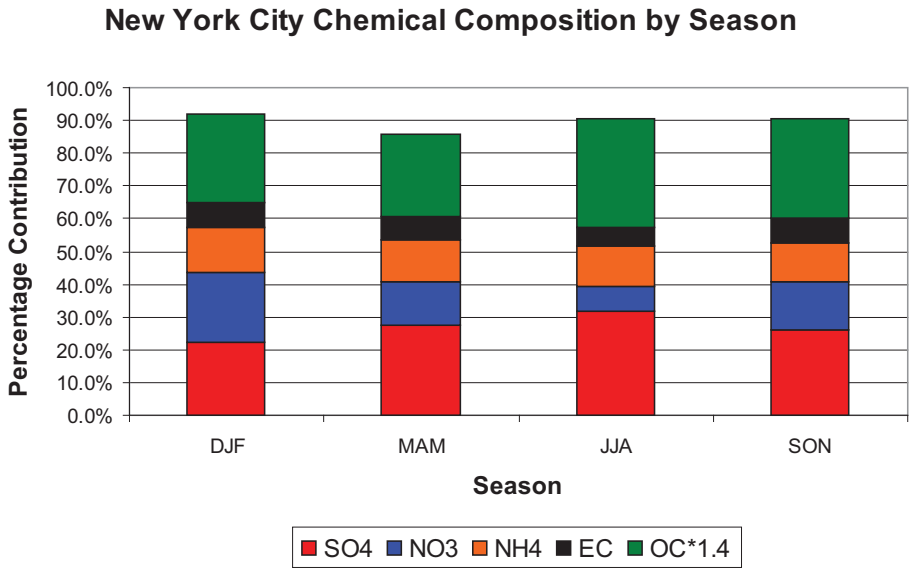

Figure ES.2. Percent contribution, by season, of five major chemical components to the $PM_{2.5}$ mass concentrations measured at three New York City sites for a three-year period from March 2000 through February 2003.The mean mass concentrations for reported months are as follows: DJF = 15.57 µg/m^3; MAM = 14.35 µg/m^3 ; JJA = 18.00 µg/m^3; SON = 13.83 µg/m^3.

Finding ES-3: *Seasonal composition differences observed based on AMS measurements during intensive field campaigns are consistent with seasonal composition differences observed from filter based measurements, but AMS measurements also show that there is significant temporal*

variation in the minute to hourly averaged time scales that are likely critical to source attribution and exposure assessment studies (Drewnick et al., 2004b; Weimer et al., 2006).

The 10-minute averaged time series of PM species composition measured by the AMS (averaged on an hourly basis) for the summer and winter campaigns are shown in figures ES.3 and ES.4. These data indicate that both the summer and winter seasons are dominated by clean and polluted episodes lasting several days in duration and with limited diurnal variation within these events. The pollution episodes are mainly characterized by south – south-westerly wind flows under somewhat stagnant conditions which suggest a regional contribution to these aerosol episodes with a significant local component under low-wind conditions.

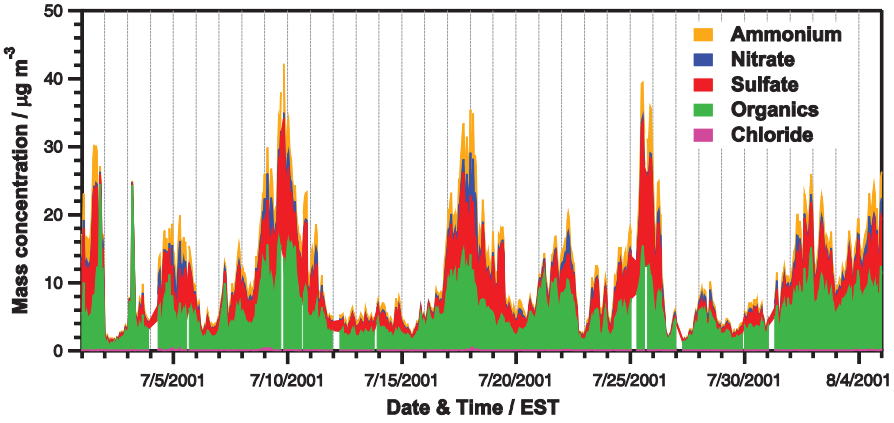

Figure ES.3 AMS one hour averaged mass concentration time series of nitrate, sulfate, ammonium, organics, and chloride for PMTACS-NY 2001 Field Intensive Campaign for the period 1 July until 5 August 2001.

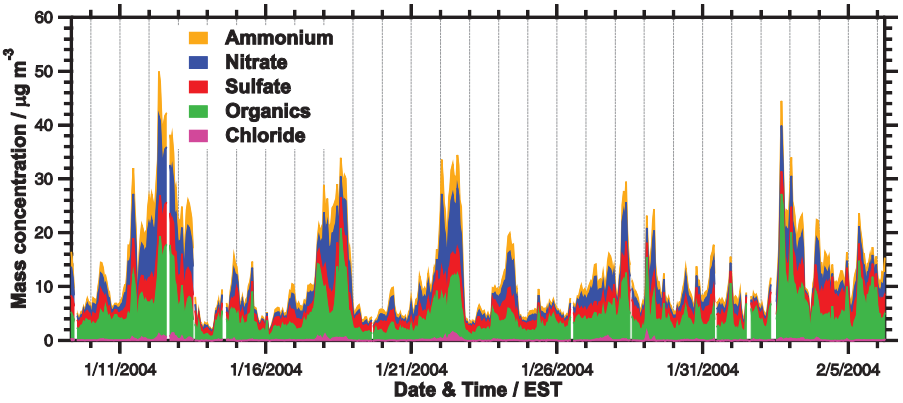

Figure ES.4 AMS one hour averaged mass concentration time series of nitrate, sulfate, ammonium, organics and chloride for PMTACS-NY 2004 Field Intensive Campaign for the period 6 January until 6 February 2004.

Finding ES-4: *Summer vs. winter AMS compositional size distribution measurements in Queens, NY, indicated a significant shift in mean mode volume size distribution ranging from 350-400nm to 150-200nm for summer and winter, respectively. The observed difference in mean mode size distributions is likely the result of significant summertime photochemical production (Drewnick et al., 2004b; Weimer et al., 2006; Canagaratna et al., 2004).*

The average of the fixed site AMS size distribution measurements as a function of composition performed during the entire Queens College Summer 2001 field intensive campaign (Figure ES.5) shows a bimodal distribution in organic PM indicative of relatively fresh aerosol emission, likely produced by highway traffic in the vicinity of the measurement site. Vehicle chase studies also performed during this same summer campaign, but not in the vicinity of this site, showed a strong small mode organic component as well, which has been associated with condensed lube oil. AMS measurements performed during the winter 2004 intensive field campaign, shown in figure ES.6, indicate a distinct shrinkage in the wintertime aerosol size distribution that likely masks the small mode organic contribution, which appears on the left shoulder of the organic distribution in figure ES.6.

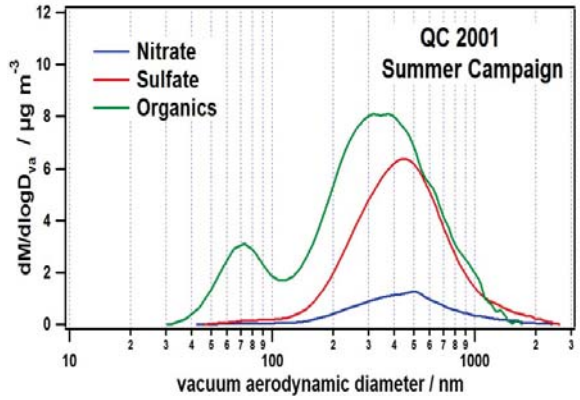

Figure ES.5 Aerosol Mass Spectrometer average PM composition as a function of size measurements for the Queens College 2001 summer field intensive study.

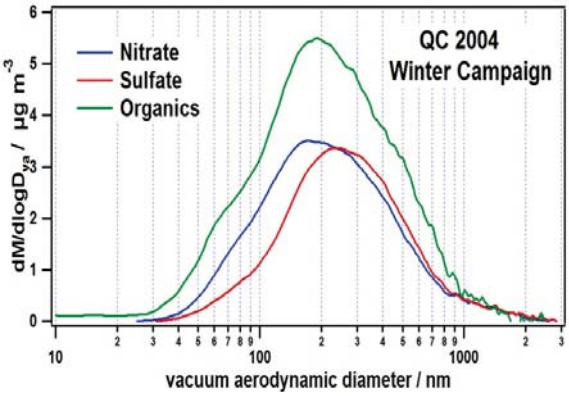

Figure ES.6 Aerosol Mass Spectrometer average PM composition as a function of size measurements for the Queens College 2004 winter field intensive study

In addition to seasonal compositional differences, the mean mode PM mass size distributions in summer are greater than those measured in winter**.** This distinct difference in aerosol size (i.e. larger mean mode aerosol particles in summer), we believe, is the result of the accumulation of secondary aerosols by way of photochemical production. The mean mode aerosol size is also likely associated with the age of the aerosol, which is more likely to accumulate mass through condensation and coagulation growth processes with time.

Finding ES-5: *AMS (Aerosol Mass Spectrometer) measurements observed at Queens College during the summer of 2001 showed that carbon-based PM contributes up to 45% of the daily PM mass; empirical estimates of PM production based on OH+VOC measurements suggests that ~ 40% of the total PM organic carbon is generated by photochemical oxidation processes (most likely of local origin), (Drewnick et al., 2004ab; Weimer, et al. 2005; Drewnick et al., 2005).*

Finding ES-6: *Summertime PM secondary organic aerosol (SOA) contributions correlate with photochemical oxidant formation and will vary (i.e. the % SOA contributions to PM mass) as function of the severity of the oxidant season. Estimates of photochemical production of SOA from the direct measurement of OH and VOC are consistent with estimates from AMS analyses that attribute PM organic carbon into hydrocarbon-like organic aerosol (HOA) and oxygenated organic aerosol (OOA) species. (Tang, 2006; Ren et al., 2003ab, 2005; Zhang et. al., 2005).*

Applying AMS data analysis techniques developed by Zhang et al., 2005, it is possible to distinguish, within the total PM organic mass concentrations, two classes of organic materials: hydrocarbon-like organic aerosol (HOA) and oxygenated organic aerosol (OOA). HOA is thought to be predominantly associated with primary emissions (fossil fuel combustion), while OOA, which has a primary emissions component, is thought to be predominantly associated with secondary oxidized products of VOC precursors or photochemical aged HOA. This analysis performed on the AMS data sets for both the 2001 summer and 2004 winter intensive field campaigns are presented in Figures ES.7 and ES.8, respectively.

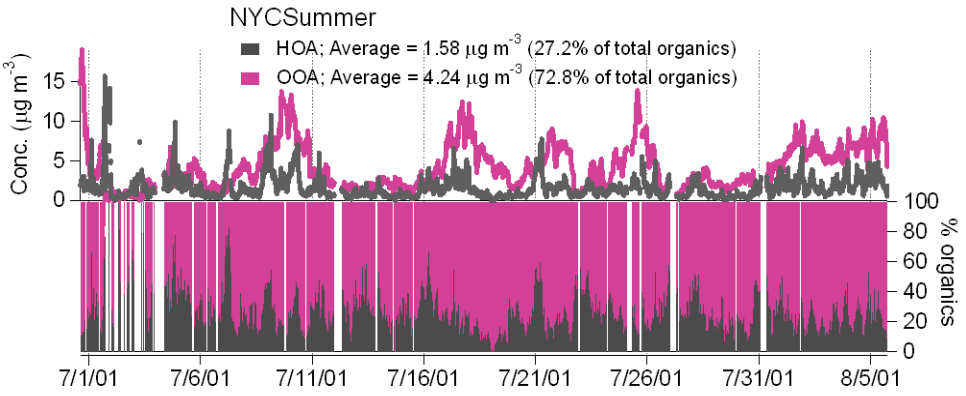

Figure ES.7 Time series of HOA and OOA mass and weight percent contributions to PM organic measurements from an aerosol mass spectrometer performed at Queens College in the summer 2001.

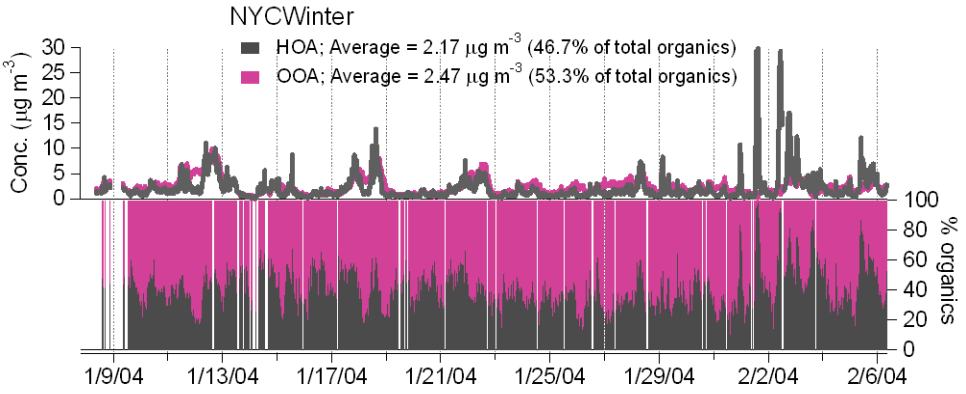

Figure ES.8 Time series of HOA and OOA mass and weight percent contributions to PM organic measurements from an aerosol mass spectrometer performed at Queens College in the winter 2004.

The mean contributions of the HOA and OOA for summer versus winter PM organic contributions in Queens are consistent with the hypothesis that photochemical production is a significant source of summertime OOA. The mass concentration of HOA summer vs. winter is 1.58 and 2.17μg/m^3 , respectively. In an independent methodology for estimating the production of SOA using measurements of hydroxyl radical (OH) and VOC SOA precursors and applying empirical reaction kinetic and smog chamber aerosol yield data (*Tang,* 2006),

hourly production rate of SOA has been estimated for individual VOC precursors as well as the total class of identified and unidentified VOC species measured under the Photochemical Assessment Monitoring Stations (PAMS) VOC measurement protocol.

Figure ES.9 provides the diurnal distribution for the summer and winter season integrated average SOA mass production as contributed by identified and unidentified VOC SOA precursor compound as described above. These results suggest that there is a clear and significant contribution from unidentified VOC (i.e. unresolved GC peaks in the PAMS analysis) to the SOA production in this urban atmosphere, and although the details of these contributions remain somewhat speculative, we believe that the approximations used in these estimates are likely conservative (i.e. lower limits).

The summer time carbon-based PM contributes ~47% (5.79 μg/m^3) of the PM mass; empirical estimates of the mean PM organic production based on OH+VOC measurements suggests that ~ 40% (2.33 μg/m^3) of the total PM organic carbon is generated by photochemical oxidation processes (most likely of local origin). Summertime PM SOA contributions correlate with photochemical oxidant formation and will vary (i.e. the % SOA contributions to PM mass) as a function of the severity of the oxidant season.

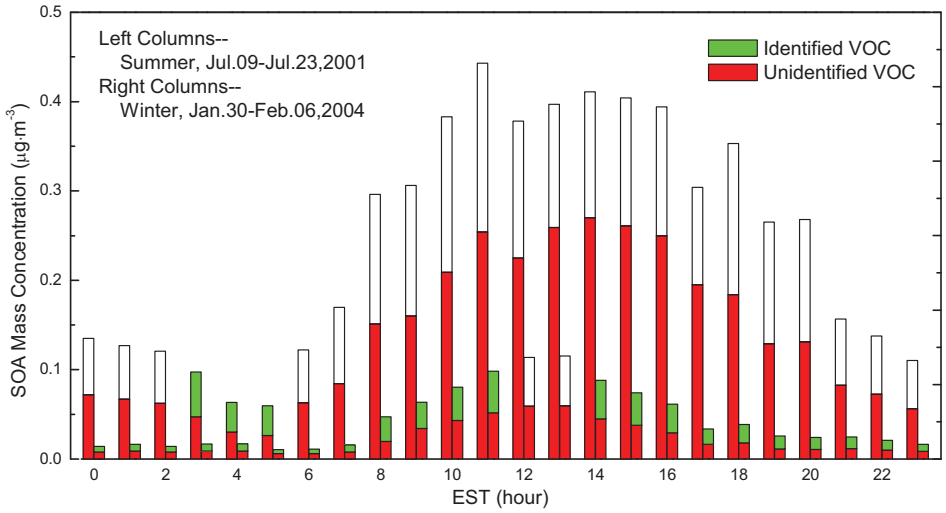

Figure ES.9 Diurnal averaged empirical estimate of secondary organic aerosol (SOA) production based on the reaction of measured identified and unidentified Volatile Organic Compound SOA precursors with measured OH.

Finding ES-7: *Estimates of summer PM SO_4 photochemical production based measurements in Queens, NY, in the summer of 2001 and reactions kinetics OH + SO_2 indicated a mean production rate of 0.14μg/m^3-hr^{-1} or 3.38μg/m^3-day^{-1}. These results indicate that 15-60% of observed PM SO_4 at Queens, NY, is generated by photochemical oxidation processes (most likely of local origin). These results are consistent with source apportionment estimates that suggest on average ~ 50% of the observed warm season sulfate in New York City is transported into the metropolitan region. Summertime PM SO_4 contributions correlate with local photochemical oxidant formation, and the % SO_2 conversion contributing to PM SO_4 mass is in part a function of the severity of the oxidant event (Ren et al., 2003ab, 2005; Dutkiewicz et al., 2004; Kim and Hopke, 2004).]*

The local production of PM sulfate has been estimated for the Queens College summer 2001 field campaign (Figure ES.10) using the ambient measurements of OH and SO_2 and applying the reaction rate kinetics for the OH + SO_2 reaction to estimate PM sulfate production. Using these hourly estimates, Figure ES.11 compares the daily production estimates of sulfate (upper boxplot) with daily observed PM sulfate from R&P8400S (lower boxplot). In most cases, high ambient PM sulfate concentrations correlate with high production rates (e.g. circled event) and indicate local contributions of > 50% of observed PM SO4 at Queens College. High PM sulfate levels with low sulfate production rates would indicate transport dominated events.

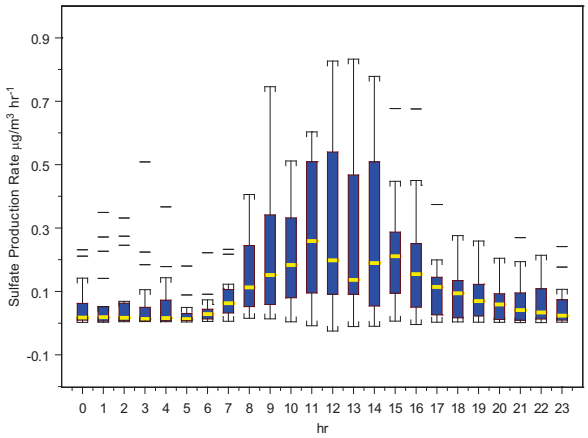

Figure ES.10 Mean diurnal boxplots of PM sulfate production estimates via OH + SO_2 for measurement days (1 July until 5 August) at Queens College in the summer 2001.

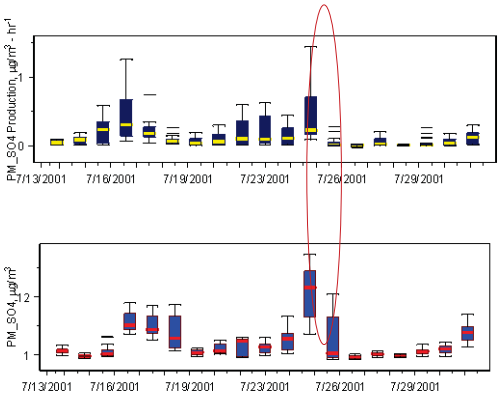

Figure ES.11 Daily boxplots based on hour average estimates of PM sulfate production rates (top) and PM sulfate hour average measurements (bottom).

Finding ES-8: *Particle counting showed higher number concentrations at the urban location compared with the regional/rural sites with higher number counts on average in urban winter than urban summer, which suggests that primary particle emissions are an important source contributing to the particle concentration, which varies by season with mixing height. In addition, the sizing measurements in Queens, NY, show little evidence of major new particle formation (nucleation) events, suggesting preferential condensation of secondary semi-volatile products on existing aerosol surfaces; only under very clean urban and rural aerosol background conditions (e.g. at Whiteface Mountain)was some evidence of possible nucleation indicated.*

A striking feature of the urban campaigns is the absence of significant nucleation events. This could be related to typically high regional background concentration of particles in urban environment, which leads to preferential condensation of gaseous compounds on already existing particle surfaces rather than forming new ones. Time series of particle number concentration during summer and winter at Queens College are shown in ES.12a, 12b. The higher average number concentrations in winter versus summer and the similar diurnal patterns observed with both suggest a common primary emissions source that is likely modulated by variation in mixing height on a daily and seasonal basis.

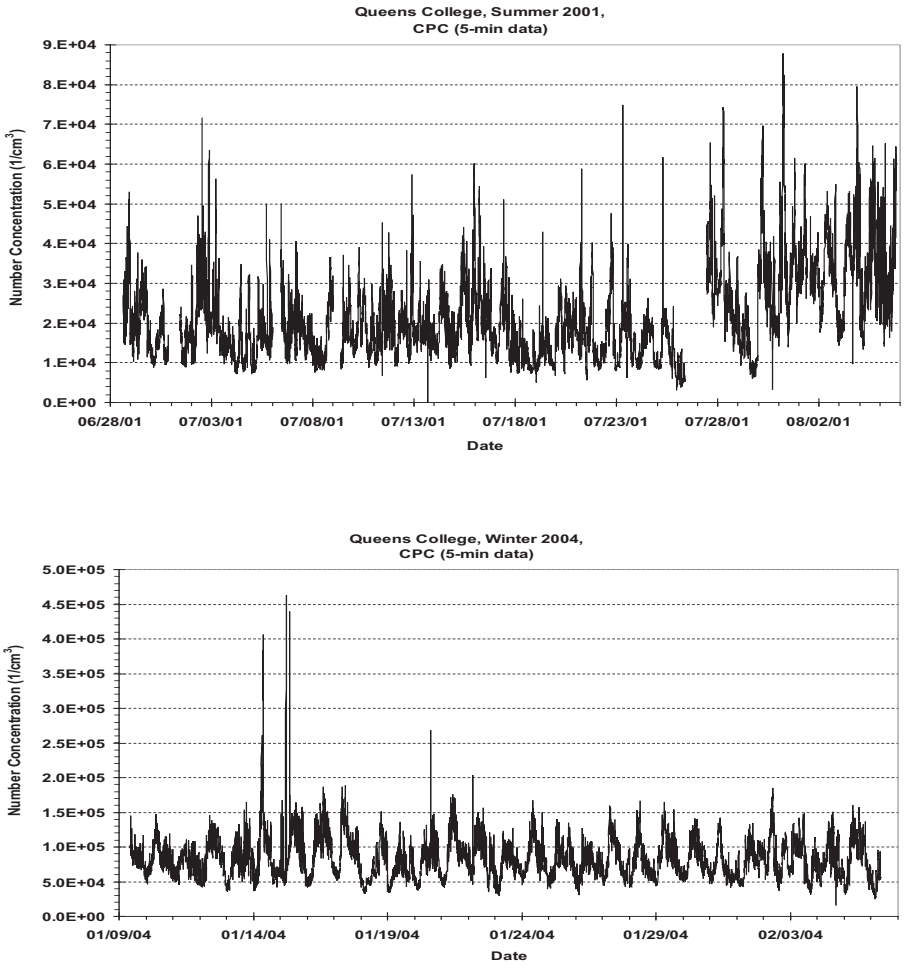

Figure ES.12a and ES.12b Time series of five-minute particle total number concentrations from the CPC during the QC 2100 summer and QC2004 winter campaigns.

Objective 2: Monitor the effectiveness of new emission control technologies [i.e. Compressed Natural Gas (CNG) bus deployment and Continuously Regenerating Technology (CRT) –Diesel Particle Filter (DPF)] introduced in New York City and its impact on ambient air quality.

Finding ES-9: *On-road vehicle emissions flux measurements of residual gases and PM mass and chemical composition using a mobile measurement platform has been demonstrated as a viable means to sample large populations of in-use vehicle emissions (Kolb et al., 2004, Canagaratna et al., 2004).*

Finding ES-10*: CNG-powered and CRT-DPF- equipped diesel buses show significant reduction in PM emissions as compared to their standard diesel counterparts (Herndon et al., 2005).*

Finding ES-11: *The comparison of vehicle chase study and dynamometer emissions for PM are consistent in the mean, but real-world in situ emission measurements suggest significantly more variation than dynamometer tests (Shorter et al., 2005).*

A proof-of–concept measurement technique for monitoring on-road, in-use, in situ vehicle exhaust emissions (*Canagaratna et al.,* 2004) was demonstrated during this program. A mobile van equipped with fast response gas and particle measurement was deployed to follow and sample targeted vehicles, predominantly heavy duty trucks and buses, with preference given to MTA buses as characterization of this fleet. A database provided by the MTA, which contained the vehicle information such as engine type, age, and fuel, was used to categorize each MTA bus. The chase of an individual vehicle generally ranged from four to seven minute and included continuous measurements of particle size and composition, CO_2 and typically two other gases (including combinations of the following: CH_4, H_2CO, SO_2, NO_2, and NO). Measurement of the correlated changes in PM and CO_2 is essential to the experiment as CO_2 is used as a tracer for the exhaust plume. The measurement technique provides unique on-road vehicle emission characterizations that will assist in the evaluation of emissions models and an implemented emission control program.

Results of all the PM emissions ratios calculated and categorized by vehicle type are summarized in figure ES.13. The height of each bar denotes the average emission ratio calculated over all the relevant chase events that represent the particular vehicle class, while the error bar represents one standard error of the mean. The vehicle classes are broadly categorized as MTA buses, non-MTA buses, and other heavy-duty vehicles. Within the MTA fleet, buses were divided into diesel, CRT, and CNG categories, with each diesel bus further separated according to the Detroit Diesel Corporation engine model (6V-92 or Series 50). The "Non-MTA buses" category consists of passenger buses used in the city that are operated by companies other than the MTA. The "other heavy-duty" vehicle category contains trucks as well as school and charter buses. The emission ratios calculated for the "dirty car" category emitting a large amount of blue smoke, where its emission index[1] (EI) is divided by 10 to place it on scale with the other vehicles, and for mixed-traffic emissions in the Midtown tunnel, are also presented. The reported non-refractory PM (NRPM) refers to PM components that volatize at temperature ≤ 600ºC, which in this case, is principally organic PM and does not include elemental carbon.

Although the bulk of the vehicles sampled were diesel fueled, it is worth noting that on the occasions that CNG buses were sampled, their PM emissions were quite low and comparable to the CRT-DF equipped diesels.

[1] The emission index reported in units of grams of NRPM per kilogram of fuel burned, is derived from the measured emissions ratio (ER) in $\mu g/m^3$ of NRPM per ppm of CO_2 based on the following conversion factor: $EI = (ER/490.8)(10^3)(W_c)$, where W_c is the weight fraction of carbon in the fuel. In the case of diesel fuel the typical value of W_c is 0.87.

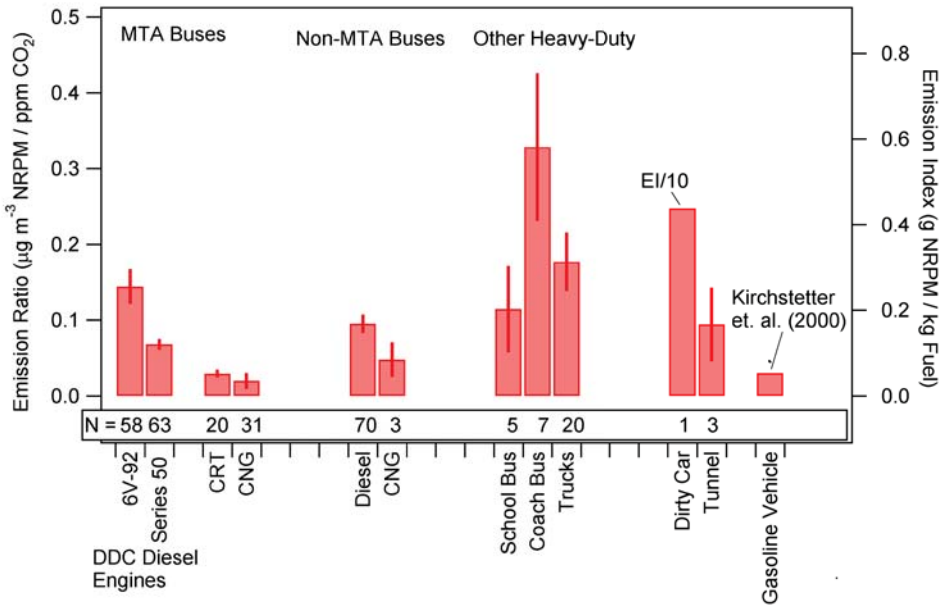

Figure ES.13 Classification of average, non-refractory PM emissions by Vehicle Type. The height of each bar reflects the average emission ratio calculated over all the relevant chase events that represent the particular vehicle class. "N" represents the number of chase runs included in the average. The error bar represents ± 1 standard error of the mean (*Canagaratna et al., 2004).*

Finding ES-12: *CNG- powered buses have significant methane emissions that are likely the result of engine misfiring and would likely require additional controls (EGR, oxy-catalyst) (Herndon et al., 2005).*

Finding ES-13: *CNG- powered buses have significant formaldehyde emissions that will likely require additional controls (e.g. oxy-catalyst after treatment) (Herndon et al., 2005).*

A summary of the overall findings for methane, formaldehyde, and sulfur dioxide emissions for each individual chase study event performed is presented in ES.14 and shows that CNG-powered buses emit considerable amounts of CH_4 per CO_2 compared to diesel buses. There is also evidence that a significant fraction of these emissions occur as a result of engine misfiring, which is also noted in dynamometer tests (*Lanni et al.,* 2003). Over the course of chasing 21 CNG buses on typical routes, the elevated CH_4 with no concomitant CO_2 enhancements occurred nine times, which suggests that the CNG buses sampled emit ~0.5% of their carbon as unburned fuel during normal operation. It is unclear from this work what the potential magnitude of these methane releases is relative to other emissions associated with CNG vehicles, such as losses during refueling, but given CH_4 significant greenhouse gas potential, a large fleet conversion to CNG would suggest careful consideration of this CH_4 emission source.

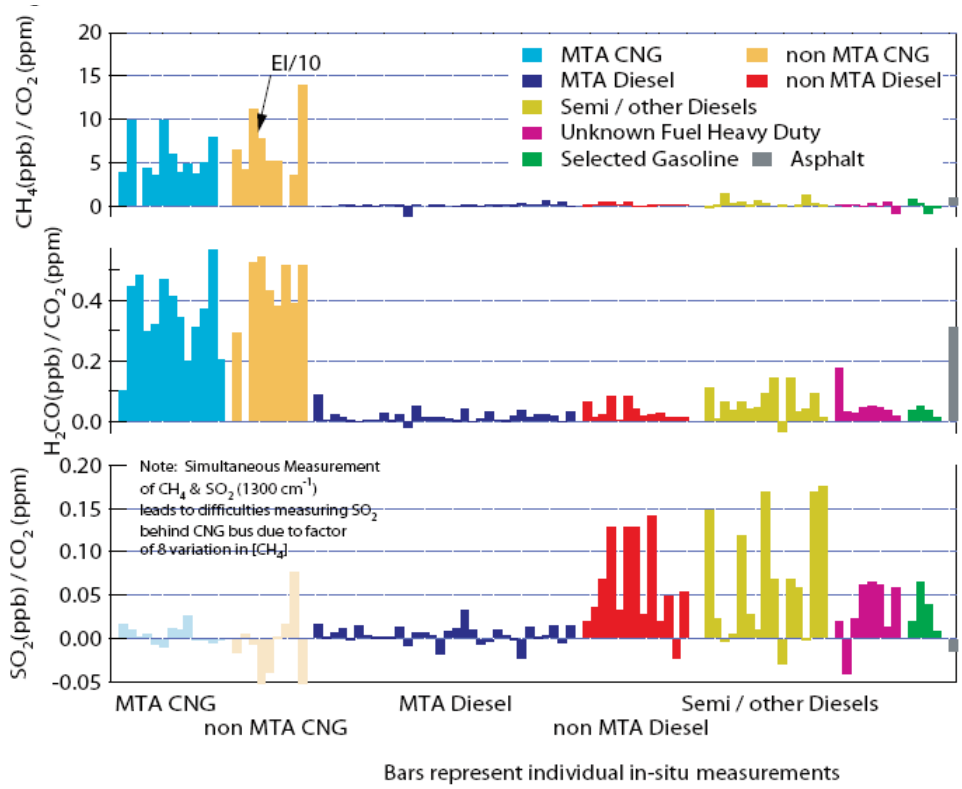

Figure ES.14 Molar Emission Ratios for Methane, Formaldehyde, and Sulfur Dioxide of Individually 'Chased' Vehicles The emission ratios for CH4, H_2CO, and SO_2 determined from the chase period for individual vehicles are depicted in three different panels from top to bottom, respectively. The classes of vehicles from left to right are; MTA CNG, non-MTA CNG, MTA Diesel, non-MTA Diesel, 'Semi' and other Diesel, Other Heavy Duty, Heavy Duty Gasoline, and Asphalt Paving fumes. The results for SO_2 while chasing CNG vehicles are presented, but they are not considered valid due to SO_2 spectral line masking at high CH4 levels *(Herndon et al., 2005)*.

Formaldehyde emissions measured during chase studies were one tenth of the methane emissions on a per molecule basis. The general finding that CNG- powered buses emit high levels of H_2CO (Figure ES.13) has been observed in other chassis-dynamometer studies. *(Lanni et al.* 2003 and *Kado et al.*, 2005.) In the case of Kado et al., 2005, H_2CO emissions were greatly reduced as a result of the presence of an oxidation catalyst, suggesting a possible remedy for this potential toxic exhaust emission product from CNG fueled vehicles.

Finding ES-14: *CRT-DPF equipped diesel buses significantly change the NO_2/NO_x ratio, which may have to be addressed in the long term (Shorter et al., 2005). [Q8]*

Chase studies performed using fast response measurements of CO_2 and NO and NO_2 technologies to characterize the fleet emissions of MTA, non-MTA buses and trucks are consistent with chassis- dynamometer experiments in the mean, but they show significantly more vehicle-to-vehicle variability. A particular interesting finding relates to the NO_2 slip issues associated with the diesel CRT-DF trap control technology. The results presented in Figure ES.15 suggest NO_2/NO_x of up to 50% on average are observed from in situ in-uses exhaust plume sampling. These higher fractions of NO_2 will likely increase on and near road NO_2 traffic exposures and may increase local ozone production efficiencies in urban areas.

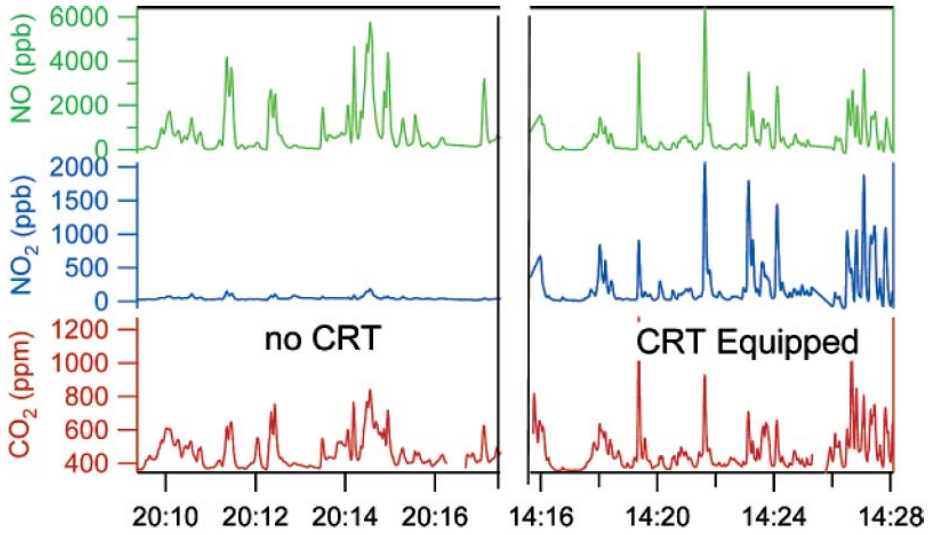

Figure ES.15 Comparison of typical NO, NO_2, and CO_2 chase data from a standard diesel bus (on left) and a CRT equipped diesel bus (on right). While the CO_2 and NO levels in the exhaust of both buses were comparable, the NO_2 emissions from the CRT bus are clearly higher *(Shorter et al., 2005).*

The introduction of CNG- powered and DF-CRT retrofitted vehicles during the course of this study was principally associated with actions taken by the New York Metropolitan Transit Authority (MTA) to reduce emissions from its bus fleet. It is clear from the vehicle chase studies reported above that these actions do reduce $PM_{2.5}$ exhaust emissions and subsequently population exposures in the vicinity of these sources. These control actions involved only a very small number (<<1%) of the trucks and buses operating in the New York City, and their impact on $PM_{2.5}$ mass measurements at central urban monitors is not distinguishable. As the population of controlled vehicles increases (most assuredly with the introduction of the of 2007 heavy duty diesel vehicle emission standard), the opportunity to track changes in ambient air concentrations at urban central monitors as affected by diesel emissions will improve. The significant time associated with diesel vehicle fleet turnover rates (20 years or longer) suggests that measurements will be required for a decade or more to track the effectiveness of this control program on $PM_{2.5}$ mass and its organic components, elemental and organic carbon.

Objective 3: Test and evaluate new measurement technologies and provide tech-transfer of demonstrated operationally robust technologies for network operation.

Finding ES-15: *Continuous PM mass measurement technologies (SES TEOM, FDMS-TEOM, and BAM) have shown continued progress in achieving the "true" measurement of PM mass. The designation of FRM as the mass measurement standard for the "true" ambient PM mass is now being challenged. Recent measurements based on FDMS technology indicates that the "true" PM mass is underestimated by the FRM that loses NH_4NO_3 and semi-volatile organics, and these losses exhibit significant seasonal dependence (Schwab et al., 2003; Schwab et al., 2004bc; Schwab et al., 2005a).*

The Filter Dynamics Measurement System (FDMS) TEOM, developed to account for volatilization and condensation artifacts in the TEOM monitor and to match the FRM standard measurements more closely, is based the differential measurement method described by Patashnick et al. (2001). An attractive feature of this instrument is the simultaneous reporting of volatile and nonvolatile mass concentrations. This measurement method and a continuous mass measurement method based on beta attenuation by PM (the Beta Attenuation Monitor or BAM) were evaluated and compared to the FRM filter- based measurements (*Schwab et al.* (2006a). The correlation of the FDMS and BAM methods at Queens (not shown) was very high, with a regression slope of 1.02, and an R^2 coefficient of 0.93. Figure ES.16 shows the correlation scatter plots for each of these instruments versus the FRM measurements, again at the Queens site for the calendar year of 2004. The regression slopes indicate that the FRM method missed ~25% of the particle mass as measured by the FDMS at the Queens site in New York City during 2004.

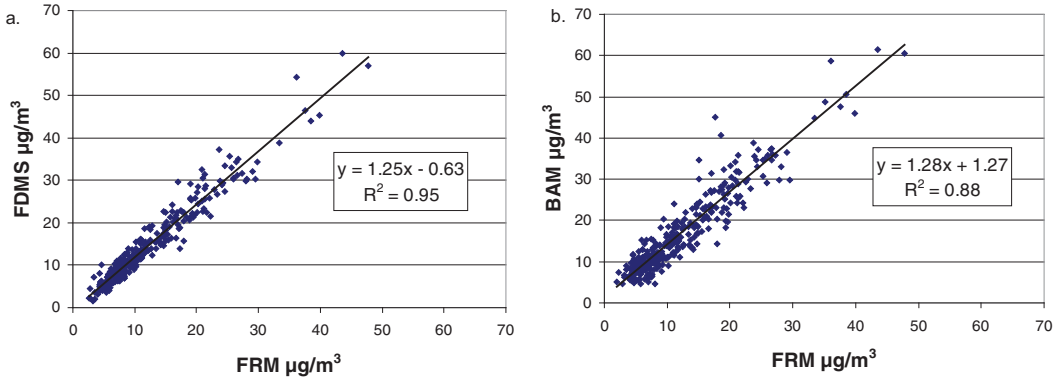

Figure ES.16. a.) Correlation plot for the 2004 24-hour averaged FDMS TEOM measurements vs. the FRM measurements at Queens. The fitted linear regression line and coefficients are also shown. b.) Correlation plot for the 2004 24-hour averaged BAM measurements vs. the FRM measurements at Queens. The fitted linear regression line and coefficients are also shown.

It has been observed that the seasonally averaged analyses do not, in general, give a good picture of the true nature of the aerosol amount and composition, nor of our ability to measure it with known precision. To capture the simplest seasonal variation in $PM_{2.5}$ mass and various chemical components, Schwab et al. (2006a) calculated second order polynomial fits to various quantities, including FDMS, FRM, standard TEOM mass concentrations, and major chemical species form Speciation Trends Network (STN) filter samples. A reconstruction of $PM_{2.5}$ mass from the chemical species, along with an estimate for particle bound water, as described in Swab et. al. (2006a), agreed to within about 10% of the FDMS measurement as shown in Figure ES.17, while agreement with the BAM is not as good. A reconstruction of the FRM mass using the same major species and using estimates of the amount of semi-volatile nitrate and OC lost from the FRM filter (and retained by the STN filters) have also been performed at Queens and shown to be close but systematically low.

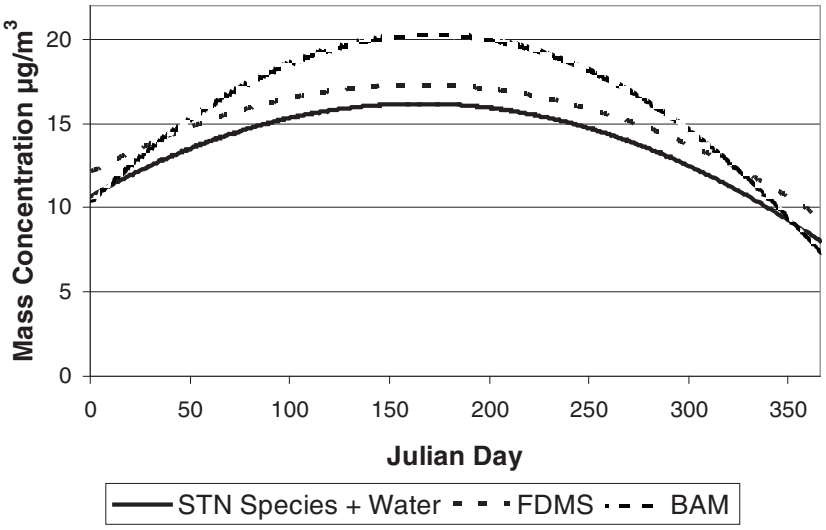

Figure ES.17. Reconstruction of the species mass contributions at Queens using the polynomial fits for individual species compared with the polynomial fit for the FDMS TEOM and the BAM. Species included in the reconstruction are sulfate, nitrate, ammonium, EC, OC*1.6, trace elements, and calculated water.

Finding ES-16: *Continuous PM sulfate measurement technologies (8400S and Thermo 5020) show promise for routine network deployment. Sulfate measurements are in good agreement with collocated instruments and consistently recover about 80% as much sulfate as 24 hr STN filters. Outstanding operational/maintenance issues with some systems remain to be resolved (Drewnick et al., 2003; Hogrefe et al., 2004; Rattigan et al., 2005; Schwab et al., 2005b).*

Finding ES-17: *Continuous PM nitrate measurement technology (8400N) shows promise for routine network deployment, but measured PM NO_3 levels are significantly lower (30-40%) than other collocated semi-continuous instruments and 24 hr STN filters. Some measurement data indicate a non-linear response with increasing PM nitrate levels suggesting a changing or limiting reductive capacity of the flash conversion system (Hogrefe et al., 2004; Hering et al., 2004;Rattigan et al., 2005).*

Comparisons of R&P 8400S data with filter samples collected every third day as part of the EPA STN program and daily as part of the PMTACS-NY activity are presented as a correlation scatter plot in Figure ES.18 (with R&P 8400S data averaged up to 24-hours). The significant intercepts reported from the linear regression also fits shown in Figure ES.18 suggest a possibility of an unknown positive artifact in the 8400S data. The slopes of these regression fits are quite consistent with other semi-continuous measurements performed during the summer intensive campaigns. Although the 8400S is capable of providing a high data capture (>80%), its requirement for frequent (bi-weekly and often weekly) maintenance by trained personnel makes its deployment at remote monitoring sites impractical.

In a similar manner, comparison studies with R&P 8400N PM nitrate monitor were performed (*Rattigan et al.,* 2006) at the South Bronx with the correlation scatter plots presented in Figure ES.19. The regression slope of 0.59 for this site is quite similar to the value of 0.65 obtained for the filter comparison obtained in the summer 2001 Queens campaign.

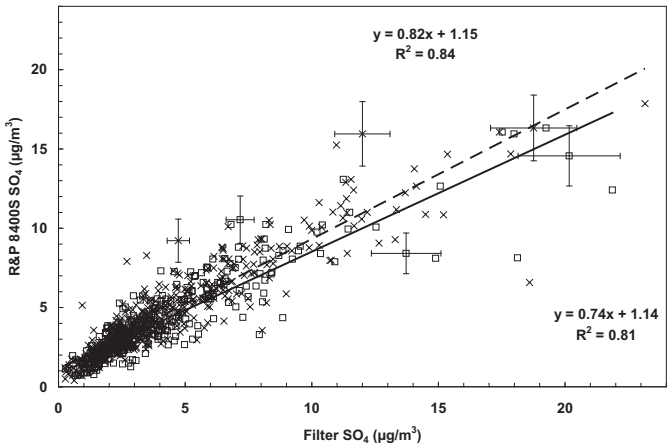

Figure ES.18. Comparison of 24-hr average R&P 8400S SO4 data at the South Bronx site with the corresponding colocated R&P ACCU (crosses) and R&P 2300 (open squares) 24-hr integrated filter data. The dashed and solid lines indicate the linear least squares regression fits to the crosses and squares, respectively.

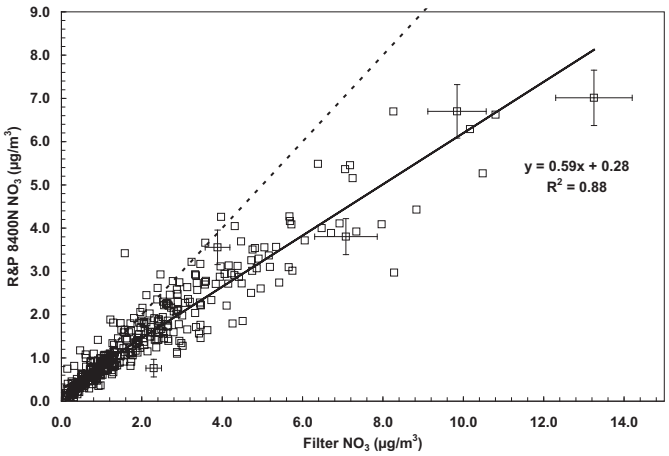

Figure ES.19. Comparison of 24-hr average R&P 8400N NO_3 at the South Bronx site with the corresponding colocated R&P 2300 24-hr integrated filter data. The solid and dashed lines indicate the linear least squares regression fit to the data set and the 1:1 line.

As with the 8400S, the instrument is capable of providing a high data capture (>80%) and a reasonable correlation with filter measurements, but its requirement for frequent (bi-weekly and often weekly) maintenance by trained personnel makes its deployment at remote monitoring sites quite difficult. Comparison of the R&P 8400N with 24-hr integrated filter measurements shows that the R&P 8400N is on average biased low by 30%-40% compared to the filter data, which indicates that the R&P 8400N NO_3 to NO_x conversion process is sensitive to aerosol composition or suffers from a systematic shortfall.

Finding ES-18: *Continuous PM carbon measurement technology (Sunset Labs - EC/OC) shows promise for routine network deployment which indicates good agreement with collocated instruments and 24 hr STN filters and AMS – OC measurements. R&P 5400 EC/OC tracks total relative carbon well, but it is not quantitative, as it does not provide comparable EC/OC with 24 hr STN filters (Venkatachari et al., 2006; Weimer, et al., 2006).*

An intercomparison of measurement methods for carbonaceous aerosol (*Venkatachari et al.,* 2006b, *Weimer at al.,* 2006)) using data collected during the Queens Winter 2004 campaign included the Sunset Labs EC/OC field instrument (EC and OC), the R&P 5400 Monitor (EC and OC), the Aerodyne Q-AMS (organic matter, OM, only), Magee Scientific AE-20 Aethalometer (BC only), and STN and ASRC 24-hour filters (EC and OC). They observed that the R&P 5400 total carbon (TC) tracked the filter measurements reasonably well (r = 0.91), but EC and OC from the 5400 did not compare as well (r = 0.76 for OC and r = 0.88 for EC). The Sunset Labs EC/OC instrument compared to the filter measurements yielded correlation coefficients of 0.88 for TC, 0.82 for OC, and 0.97 for EC. All of these comparisons are based on between 15 and 17 24-hr average samples collected during January and February 2004.

The AMS cannot be compared in quite the same way because it does not measure EC, and because it reports OM, or organic matter including oxygen, hydrogen and other elements chemically bonded to it. Comparison PM organic carbon mass measurements from an aerosol mass spectrometer and the Sunset Labs analyzer (*Weimer et al.,* 2006) indicated a linear correlation of paired hourly data with an $R^2 = 0.66$ and slope = 3.28 and intercept = -4.18. This rather significant negative intercept is likely due to a sampling artifact of the Sunset Labs analyzer resulting from the loss of volatile organic PM from the filter surface that typically runs above ambient temperatures during the sampling cycle.

The regression of the AMS OM to the Sunset Labs OC gives an indication of the nature of the organic aerosol, that is, whether it is fresh hydrocarbon dominated or more aged oxygenated material. The slope of the regression line for a zero intercept is 2.06; a number in agreement with recent results, which suggests that standard accepted multiple of 1.4 may be significantly under estimated (Zhang et al., 2005a, 2005b, Turpin et al., 2001).

IMPLICATIONS FOR AIR QUALITY MANAGEMENT AND KNOWLEDGE GAPS

PMTACS-NY findings have provided insight into several aspects of the air quality management of $PM_{2.5}$ and photochemical oxidants. These include:

Control and Measurement Technologies for Mobile Sources

The results from chase studies of heavy duty diesel buses retrofitted with diesel filter trap oxidation catalyst control technology suggest that implementation of a diesel truck retrofit filter trap control program would be an extremely effective means of reducing organic PM in major metropolitan areas (e.g. Boston to Washington corridor) through the reduction of direct primary EC/OC emission as well as the reduction of gas phase precursor VOCs contributing to SOA. In planning such a program, the impact on ambient air quality needs to be assessed and measurement strategies identified that allow tracking of air quality changes in response to the implementation of emission controls.

The demonstration of instrumentation for the measurement of on-road vehicle emissions fluxes of residual gases and PM mass and chemical composition, using aerosol mass and tunable

diode laser differential absorption spectrometers provides a viable means to sample large populations of in-use vehicles and effectively evaluate the performance. The instrumentation could also be used to collect data to assess the overall uncertainty of mobile emission model predictions. Overall, our studies suggest that the comparison of vehicle chase study and dynamometer emissions for PM are consistent in the mean, although real-world in situ emission measurements are significantly more variable than dynamometer tests (*Shorter et al.,* 2005). In-use testing also offers the opportunity to assess the impact of gross emitters of PM (poorly maintained high pollution vehicles) from both diesel and gasoline-fueled vehicles.

Atmospheric Processes and Secondary Aerosol Formation

Our studies have shown the strong linkage between summer ozone and OH concentrations in the atmosphere and the importance of OH reactions with precursors (e.g., SO_2, VOC and NO_2) in the secondary formation of PM sulfates, organics, and nitrates. The results indicate that the oxidant and PM control strategies must be considered in an integrated framework recognizing that ozone mitigation directly effects (i.e. reduces) PM secondary production. It must be noted that strategies that consider controls only during the oxidant season (e.g. NO_x SIP call) do not benefit, such as PM winter time nitrate mitigation in the northeast. Although recent studies have indicated that biogenic emissions of isoprene and terpenes can be significant precursors to secondary organic aerosol (SOA) production, we did not see evidence of this in our studies. Although significant levels of isoprene were observed in New York City (terpenes were not measured), theoretical estimates of SOA production based on empirical laboratory yields of aerosol from the reaction of OH and isoprene suggested much larger SOA productions that were not consistent with the aerosol mass spectrometric measurements of PM organic. The production of SOA from these biogenic species may be quite sensitive to ambient NO levels, where NO/VOC ratios/levels must fall below a certain threshold, before aerosol formation can occur. It is clear that further field studies are needed to study the SOA production in the presence of biogenic compounds under a variety of ambient environmental conditions.

In addition, when secondary PM production is attenuated due to low photochemical activity during the cold season in the northeast, we find comparable PM mass levels and only a slight reduction in the percentage contribution of sulfate. This result suggests the presence of a significant cold season SO_2 transformation processes (likely heterogeneous reactions) to sulfate, processes that remain unevaluated (in summer or winter) in models due to very limited measurement studies.

Promising Methods for Ambient Air Quality Monitoring

Several new measurement systems were deployed and evaluated over the course of the PMTACS_NY Supersite program including the following commercial monitors: Sunset Labs-EC/OC, Magee Scientific AE20-BC, R&P 5400-EC/OC, TECO 5020-$PM_{2.5}$ Sulfate, R&P 8400S –$PM_{2.5}$ Sulfate, R&P 8400N-$PM_{2.5}$ Nitrate, R&P FDMS-$PM_{2.5}$ mass, and Met One BAM- $PM_{2.5}$ mass. The deployment experience gained by NYSDEC, our collaborative partner in this study, and the published results from intercomparison and evaluation studies of these monitoring systems have benefitted air quality monitoring agencies in making informed

decisions regarding the selection of advanced semi-continuous PM mass and PM component monitoring systems.

Over the course of the PMTACS-NY Supersite program and as a result of findings therein, additional scientific questions as well as areas of uncertainty have surfaced that will need further attention. These findings, the knowledge gaps, and suggested recommendations for future work are briefly summarized as follows.

Characterization Fine Particle Emission Sources

The warm season AMS diesel PM organic emissions measured in chase studies show a bimodal distribution (70nm and 400nm modes) that was also reflected in ambient AMS measurements in Queens, NY (Herndon et al., 2005, Drewnick et al., 2004a,b). Similar AMS chase studies of heavy duty diesel vehicles under cold season conditions should be performed to characterize the size distribution of diesel PM organic in the source plume. This would help resolve if the loss of the distinct bimodal size distribution in the AMS PM organic fixed site measurements during the 2004 winter intensive field study was emissions related or the result of masking, due to an overall downward shift in mean mode size distribution of ambient PM.

Implications for health effects research

The accurate determination of ambient $PM_{2.5}$ mass concentration is critically important to the development and implementation of $PM_{2.5}$ National Ambient Air Quality Standards. Recent instrumentation evaluation and intercomparison studies of $PM_{2.5}$ mass measurement devices performed as part of the PMTACS-NY Supersite program indicate that the "true" ambient PM mass is underestimated by the FRM and that the likely source of these differences is the loss of NH_4NO_3 and semi-volatile organics, which exhibit significant seasonal dependencies (*Schwab et al.,* 2003; *Schwab et al.,* 2004bc; *Schwab et al., 2005a*). These findings have significant implications in exposure assessment and in the interpretation of the epidemiological time series studies used in the development of the $PM_{2.5}$ NAAQS. Understanding the seasonal and regional differences in $PM_{2.5}$ mass as well as any associated measurement artifacts that may exist, is critically important to the health effects community that corrects for confounders (e.g. temperature), which also correlates with volatile $PM_{2.5}$ losses. The systematic loss of seasonally averaged semi-volatile components of $PM_{2.5}$ mass by the FRM measurement technique also raises questions as to the composition and toxicological importance of the volatized species.

Implications for accountability

Tracking the trends in $PM_{2.5}$, photochemical oxidants, and their precursor species in response to regulatory actions is critically important to the demonstration of accountability in air quality management systems. Some notable examples of important measurement/analysis activities that must be sustained to address key air quality accountability issues include: 1) tracking the impact of the NO_x SIP call on trends in NO_y and ozone air quality; 2) tracking the impact of the national 2007 diesel sulfur rule regulation on local and regional SO_2, PM (sulfate and organic size) air quality, and in the case of New York City, where additional fuel sulfur regulations are

being contemplated (in heating oil and off road and marine diesel), designed experiments to demonstrate the effectiveness of these interventions; and 3) tracking the introduction of new control technologies (e.g. 2007 diesel engine standard, CRT-DF diesel engine retrofits, and the use of alternate fuels, such as CNG, ethanol, gasoline-oxygenate blends, and biodiesel) for anticipated improvements and potential negative impacts on air quality.

The accountability of the air quality management process entails maintaining measurement programs to track progress made in improving the air quality in urban and regional environments in response to regulatory actions. Such measurement programs require routine monitoring as well as strategic intensive measurement studies to track the actions outlined above.

Achieving accountability in this process requires a commitment to support several strategically placed "PM Supersite like" monitoring systems capable of supporting advanced field intensive studies as needed. These sites would be placed within and downwind of affected source regions and kept operational for a decade or longer over the course of the regulations expected effectiveness. The Pinnacle State Park and Whiteface Mountain monitoring stations represent two such regional sites that have measurement records approaching decade time scales and that will be applied, for example, to track air quality trends in response to emission reductions in SO_2 and NO_x as mandated under Title IV and NOx SIP call regulations.

1 INTRODUCTION

Background and Objectives of the Research Program

In 1999, the New York State Energy Research Development Authority (NYSERDA), under the Systems Benefits Charge (SBC) I, funded a research measurement program titled "Enhanced Measurements of Oxidants, $PM_{2.5}$ and their Precursors: Elucidating Air Quality Issues Facing New York State", Contract #4918-ERTER-ES-99. The program initiated studies to characterize regional air quality and to advance understanding of the precursor relationships pertaining to the formation of photochemical oxidants and particulate matter. This work continued and augmented trace gas and $PM_{2.5}$ measurements at two regional research sites, Whiteface Mountain, in Wilmington, NY, and Pinnacle State Park in Addison, NY. These enhanced measurements were designed to help address major gaps in understanding of photochemical oxidants and the chemical composition of particulate matter in regional environments and their formation pathways. The linkage between photochemical oxidation processes and $PM_{2.5}$ composition were of major interest in light of the anticipated and now promulgated revised PM NAAQS (i.e. $PM_{2.5}$ National Ambient Air Quality Standard (15 $\mu g/m^3$ annual and 65 $\mu g/m^3$ 24-hr average; Federal Register, 1997).

This NYSERDA supported research effort, in part, provided the opportunity for the University at Albany to compete for an EPA solicitation that proposed to establish several so called "$PM_{2.5}$ Supersites" across the nation (Albritton and Greenbaum, 1998). The "Supersites" are intended to provide enhanced measurement data on chemical and physical composition PM and its associated precursors so as 1) to characterize the $PM_{2.5}$/Co-pollutant complex[1] and its related sources and sinks; 2) support health effects and exposure research; 3) evaluate new measurement technologies and establish their potential for routine monitoring; and establish and demonstrate the use of these data analyses to track mitigation progress and support an accountable air quality management process. The significant foundation of air quality research established in New York State by the ASRC/University at Albany, its long-standing collaboration with the NYS Department of Environmental Conservation, and NYSERDA's commitment to ongoing research programs as part of the cost sharing in the "Supersite" activity, were all major assets to our success in receiving the U.S. EPA "PM Supersite" award. The report covers activities under NYSERDA contract #4918-ERTER-ES-99, which started in January of 1999 and was renewed as part of the $PM_{2.5}$ Supersite collaboration through December 2005.

The Joint Enhanced Ozone and PM Precursor/$PM_{2.5}$ Technology Assessment and Characterization Study in New York (PMTACS-NY) was designed to enhance our understanding of ozone/$PM_{2.5}$-precursor relationships and to assess methods for tracking the effectiveness of emission control programs using new air quality monitoring systems.

The long-term monitoring of the $PM_{2.5}$/co-pollutant complex and its precursors at urban and regional representative sites provides the opportunity to track the impact of emission controls

[1] The $PM_{2.5}$/co-pollutant complex refers to the co-existing ambient particulate matter and gaseous pollutants, for example O_3, SO_2, and NO_2, which are also known to effect health outcomes.

and their effectiveness on air quality. Such data can be used to verify that implemented $PM_{2.5}$ primary and secondary precursor (including ozone precursor) emission controls are performing according to specifications and verify that $PM_{2.5}$ and ozone air quality have responded to achieved emission changes as expected. Without adequate monitoring systems to track the progress and effectiveness of implemented control programs, the air quality management approach remains unaccountable.

$PM_{2.5}$, like O_3, has a regional component that must be characterized to determine its source and its potential role in the development of mitigation strategies for non-attainment areas. Chemical speciation measurements of $PM_{2.5}$ at urban and regional representative sites are essential in support of analyses to help elucidate our understanding of: 1) the chemical and physical processes that couple urban and regional air quality; 2) the role that anthropogenic and biogenic sources of VOC, NO_x, SO_2 , and primary particulate play in the production of the $PM_{2.5}$/co-pollutant complex in time (diurnal, seasonal, and inter annual) and space (local to regional); and 3) the effectiveness of emission control technologies on air quality.

Addressing the scientific and technical uncertainties associated with the mitigation of the warm season $PM_{2.5}$ /co-pollutant complex and its interdependence with O_3 air quality through coupled photochemical pathways, common precursors, and similar dependencies upon meteorology is critical if effective control strategies are to be implemented.

The PMTACS-NY study was designed around three major objectives. As part of the U.S. EPA RFA guidance, investigators were asked to develop their target program objectives using test hypotheses and questions as an organizing approach in building the integrated study plan. The science policy relevant questions and associated hypotheses provided the framework and rationale for the study design and implementation. The detailed framework used in preparing the proposal is presented in Appendix A. This report summarizes the key accomplishments and findings of the study and associated published scientific results in the context of the following three targeted proposal objectives:

Objective 1. Measure the temporal and spatial distribution of the O3, $PM_{2.5}$/co-Pollutant complex, and its precursors to support regulatory requirements to develop cost effective mitigation strategies for O3, $PM_{2.5}$, and its co-pollutants and to establish trends in the relevant precursor concentrations to assess the impact of recent and future emission reductions in terms of emission control effectiveness and air quality response.

Objective 2. Monitor the effectiveness of new emission control technologies [i.e. Compressed Natural Gas (CNG) bus deployment and Continuously Regenerating Technology (CRT)] introduced in New York City and its potential impact on ambient air quality.

Objective 3. Test, evaluate, and identify operationally robust new measurement technologies for future network operation that may improve understanding of atmospheric processes affecting air quality and support health based exposure assessments.

2 ROUTINE MONITORING AND SPECIAL FIELD INTENSIVE CAMPAIGNS

Comprehensive measurements of $PM_{2.5}$ mass, chemical speciation, and gaseous precursors have been performed at monitoring sites located in the New York City metropolitan area and at regional representative locations in Upstate NY. These sites shown in Figure 2.1 include two research regional monitoring sites, Whiteface Mountain (Wilmington, NY), operational since 1973, and Pinnacle State Park (Addison, NY), operational since 1995 and two urban monitoring sites Intermediate School I.S. 52 (South Bronx, NY), Queens College/Public School PS219 (Queens, NY). See text box TB-2-1 for details. The measurements from one additional site (NY Botanical Garden in the Bronx) operated by NYS DEC have also been incorporated in specific analyses performed over the metropolitan region.

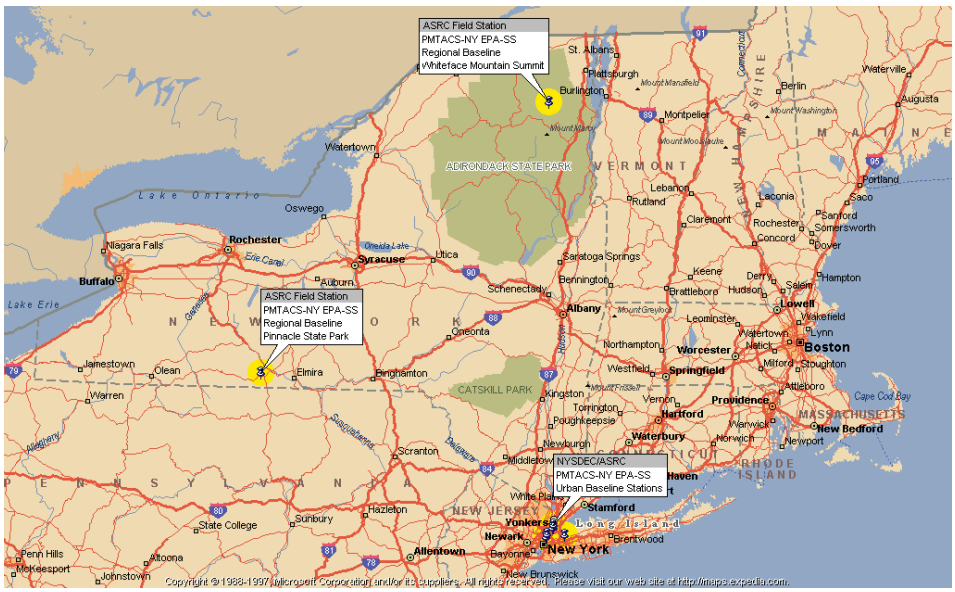

Figure 2.1. PMTACS-NY Supersite Network

These measurement sites constituted the backbone of the PMTACS-NY "Supersite Network" and provided not only the routine measurements of criteria pollutants and the mandated $PM_{2.5}$ mass and chemical speciation measurements, but they were also designed to operate advanced instrumentation that would complement and provide more chemical and temporal specificity of the gas and particulate matter air quality at these locations. Details regarding measurement parameters, techniques and frequency are presented in Table B.1 of Appendix B. The enhanced measurements performed over the course of this program provided substantial data associated with the characterization of the chemical composition of $PM_{2.5}$ within New York City and the transport-impacted regional background of Upstate NY.

In addition to the measurement network, which has operated throughout most of the six-year program period (2000-2005), four special intensive field studies were carried out over the course of this program. These studies occurred in the summer of 2001 and winter of 2004 at Queens College, the summer of 2002 at Whiteface Mountain, and the summer of 2004 at Pinnacle State Park. The intensive field studies were four to six weeks in duration and involved

many research groups performing research grade measurements using emerging measurement technologies. Details of intensive field campaigns are presented in Section VI.

Whiteface Mountain (44.4° N, 73.9° W) summit is located in the Adirondack Mountains of northern New York at an elevation of 1500 m and is forested from the base to ~1400m altitude. A conifer forest region from ~ 900m to 1400m is made up balsam fir mixed with an increasing percentage of red spruce with increasing elevation. The summit is ~ 90m above the tree line. Measurement facilities are maintained at the lodge facility at 600m, situated in clearing within a deciduous forest canopy on the eastern shoulder of the mountain and the summit facility housed in a three-story observatory at the mountaintop. The nearest major urban centers are Montreal ~ 130 km to the north; Albany ~ 180 km to the south; Syracuse ~ 220 km to southwest.

Pinnacle State Park (42.1°N, 72.2°W) in Addison, NY is located in a rural area in the New York/Pennsylvania Twin Tiers Region at an elevation of 515m. The site is located in an open clearing on Orr Hill, which is ~12m below and about 100m east of the highest hill in the park. The closest trees are ~50m away and the surrounding areas include a 50 acre pond, pastures, undeveloped state forest lands and a 9-hole golf course. The instrumentation is housed in an Eco shelter, with a 10m meteorological tower installed at the site. The village of Addison (pop. ~1,800) is 4 km to the northwest and the town of Corning (pop. ~12,000) is 15 km to the northeast.

I.S. 52 (40.8° N, 73.9° W) in South Bronx, NY is located at 470 Jackson Avenue. The gas monitoring systems are located in Room #342 on the third floor on the north side of the school. Gases are sampled from a 3" glass manifold that extends through a window and approximately one meter above roof level. PM monitoring systems are place outside on the roof.

PS219/Queens College (40.7° N, 73.8° W) is located at New York City Public School 219 (PS 219) between the Flushing and Forest Hills neighborhoods in the borough of Queens. The school is directly adjacent to the southeast corner of the Queens College C.U.N.Y. campus, where field intensive studies were carried out as well. The site is about 750 m south of the Long Island Expressway and about 1 km east of the Van Wyck Expressway, two of the busiest highways in New York City. The site is adjoined to the east by a cemetery, and Flushing Meadow Corona Park and Kissena Park (both large urban parks), each less than 2 km from the site.

TEXT BOX TB 2-1. Monitoring Site Descriptions

The measurements from the special field intensive, along with the routine measurements performed at these sites, have provided detailed real-time chemical and physical characterization of the PM/co-pollutant complex to 1) help elucidate the operative gas-to-particle transformation processes occurring in urban and regional environments; 2) enhance the chemical source signature data base in support of source attribution studies; and 3) compare emerging technologies and evaluate their performance and their performance in comparison with operational routine measurement systems.

3 PINNACLE STATE PARK MEASUREMENTS AND RESULTS

One very valuable opportunity afforded us by the multi-year data record from this site is the ability to look for trends in the trace gas and particulate matter concentrations. It is a little risky to read too much into trends based on only eight years of data (and about six and a half years for $PM_{2.5}$). At the same time, eight years is long enough to observe significant changes and strong trends. In this section, we present several analyses including running monthly averages, and annual and monthly box plots with brief commentary for the following measured parameters: ozone, sulfur dioxide, NO_x (NO plus NO_2), NO_y (total oxides of nitrogen), carbon monoxide, and $PM_{2.5}$ mass. The boxplot summaries presented in this report are described as follows: the solid boxes indicate the inter-quartile (i.e. 25th and 75th percentiles) with median line (separating the quartiles) and whiskers attached to the vertical line identifies the 5th and 95th percentiles. All values outside of the 5th and 95th percentiles are reported as horizontal lines. In addition, we present resultant slopes of scatter plots of ozone versus NO_z (defined as NO_y minus NO_x).

Ozone

The monthly averaged ozone concentrations for the eight- year period are shown in Figure 3-1. The monthly boxplot distribution averaged over the eight- year period presented in Figure 3-2, indicates that the highest ozone levels are observed in spring and summer seasons and lowest ozone in late fall and winter. The outliers in the boxplot distributions, that is, those levels exceeding the 95th percentile, are ozone events typically associated with stagnating synoptic conditions with warm temperatures and high solar irradiance. There is significant year-to-year variation in ozone concentrations, particularly in the spring-summer "ozone season" as can be seen in Figures 3-3 and 3-4, where the ozone annual and monthly box plot distribution by year are presented. The highest monthly averaged values in 2000 and 2004 are more than 10 ppbv lower than those in the more typical years of 1998, 2001, 2002, and 2005. 2000 and 2004 were wet and cool summers, which highlight the strong dependence of seasonal ozone on meteorology. The year-to-year and seasonal variations also complicate any attempt to identify long-term trends in the overall ozone concentration.

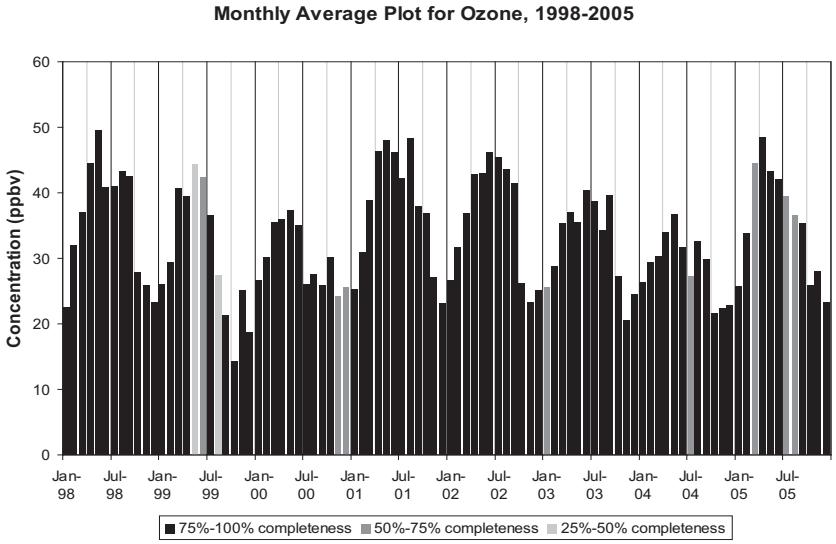

Figure 3-1. Monthly averaged ozone concentrations at the Pinnacle State Park site in Addison, NY. Shadings of the bars indicate levels of data completeness for the month as indicated in the legend.

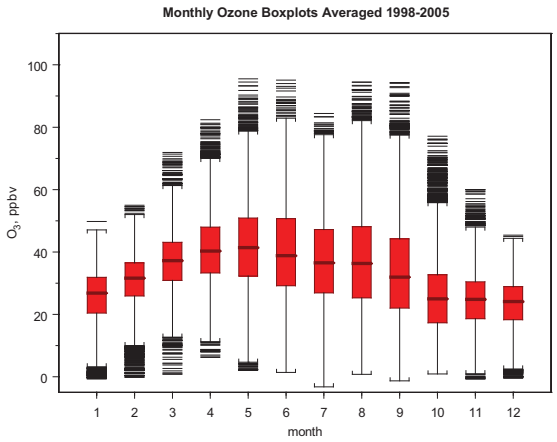

Figure 3-2. Monthly ozone concentration boxplots averaged from 1998-2005 at Pinnacle State Park in Addison, NY.

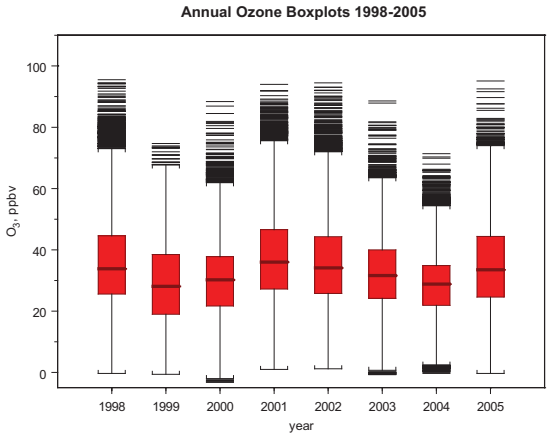

Figure 3-3. Annual ozone concentration boxplots 1998-2005 at Pinnacle State Park in Addison, NY.

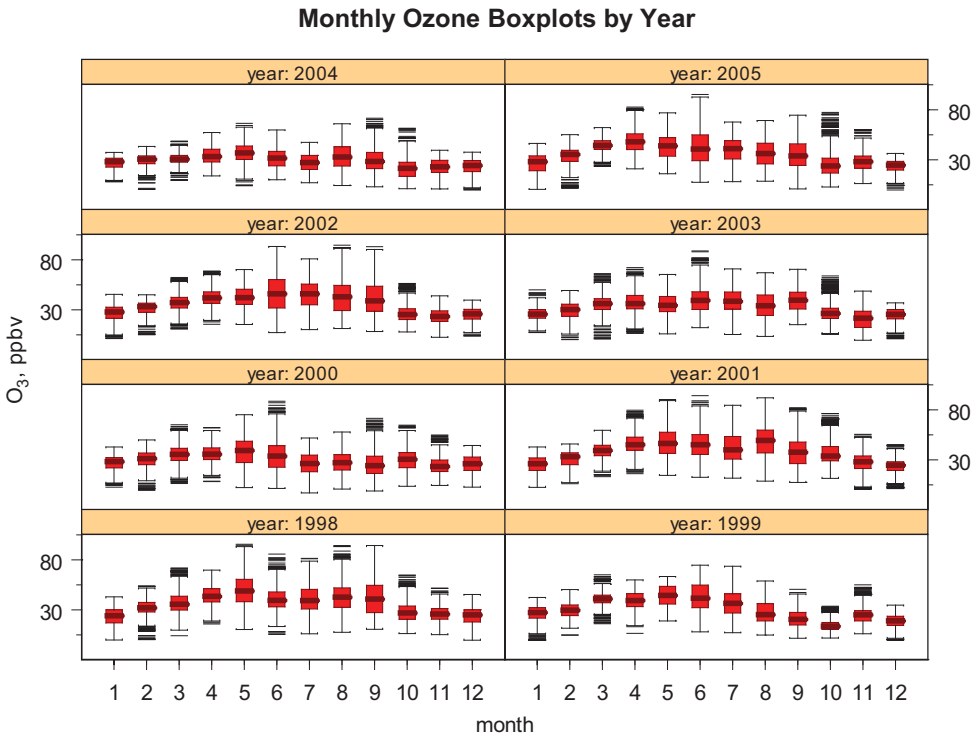

Figure 3-4. Monthly ozone concentration boxplots by year 1998-2005, at Pinnacle State Park in Addison, NY.

Sulfur Dioxide

The monthly averaged sulfur dioxide concentrations for the eight- year period are shown in Figure 3-5. The highest average sulfur dioxide is observed in winter months as indicated in Figures 3-5 and 3-6, which also shows the significant number of outliers, i.e., concentration values exceeding the 95th percentile. The outliers are the result of elevated point source plumes

impacting the site as a result of vertical entrainment. These point sources may be local or distant in origin. Plume impacts are dependent on wind direction and speed, atmospheric stability, and insulation, as well as parameters that affect the plume rise of the source itself. The observed seasonal distribution in the intensity of the SO_2 outliers (i.e., concentrations and frequency of outliers), as shown in Figure 3-6, is consistent with the expected variations in these parameters. For example, summer time photochemical conditions and deeper vertical mixing in the planetary boundary layer will attenuate plume impacts; while reduced photochemical activity and enhanced atmospheric stability during winter contribute to increases in mean concentrations and those concentrations associated with impacts from elevated plumes. Generally speaking, midwinter monthly averages reach as high as 4-6 ppbv and midsummer monthly values as low as 1 ppbv. The high time resolution data during the winter is dominated by plumes of SO_2 with concentrations reaching 20-40 ppbv fairly frequently. Plumes greater than 20 ppbv are quite infrequent during summer months.

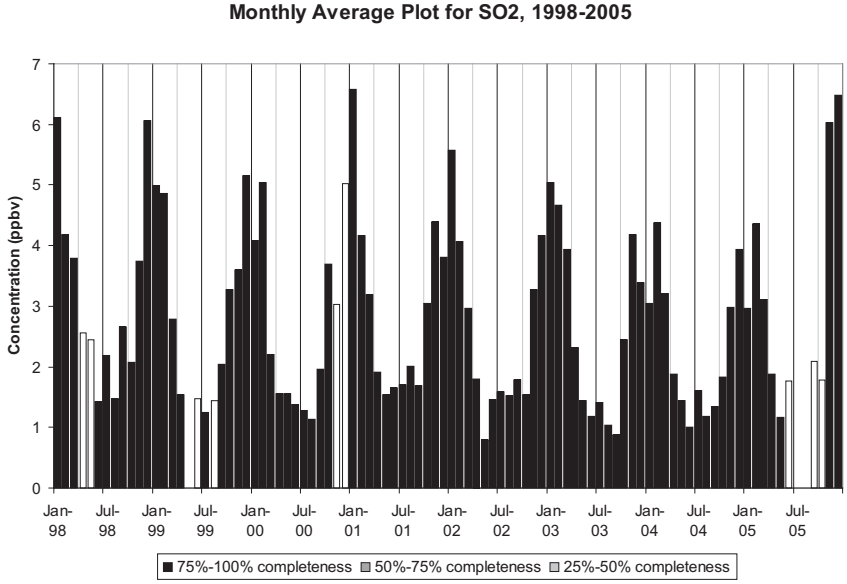

Figure 3-5. Monthly averaged sulfur dioxide concentrations at Pinnacle State Park in Addison, NY. Shadings of the bars indicate levels of data completeness for the month as indicated in the legend. Missing bars indicate less than 25% data completeness.

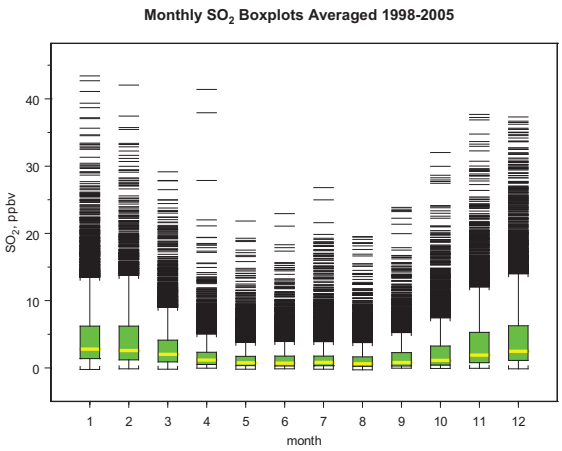

Figure 3-6. Monthly sulfur dioxide concentration boxplots averaged from 1998-2005 at Pinnacle State Park in Addison, NY.

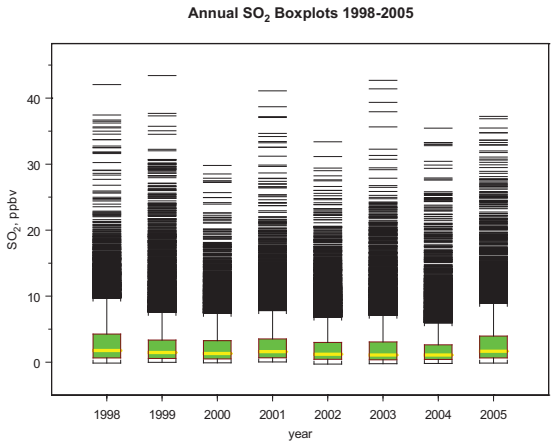

Figure 3-7. Annual sulfur dioxide concentration boxplots from 1998-2005 at Pinnacle State Park in Addison, NY.

It is difficult to discern any trend in the annual boxplots presented in Figure 3-7. This is partially the result of the scaling due to the plume impactions. Figures 3-8a and 3-8b present boxplots of the January-February and May-June SO_2 data by year, respectively. The boxplots consider all the data, but the outliers are not plotted on the y-axis which are rescaled to better visualize any trend in the distribution. The winter data presented in Figure 3-8a indicate a downward trend in SO_2 but with significant inter-annual variability. The winter time trend is more perceptible likely due to the higher concentrations resulting from SO_2's longer lifetime. These trends seem to be consistent with the effect of mandated SO_2 emissions reductions introduced under Title IV acid rain regulations. Further analyses are under consideration to quantify the likely causes of the inter-annual variability (source vs. meteorological/chemical lifetime)

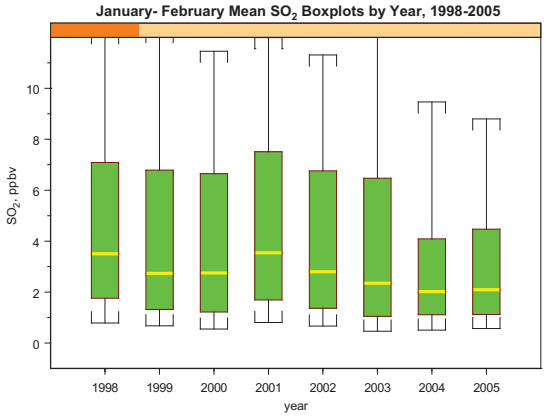

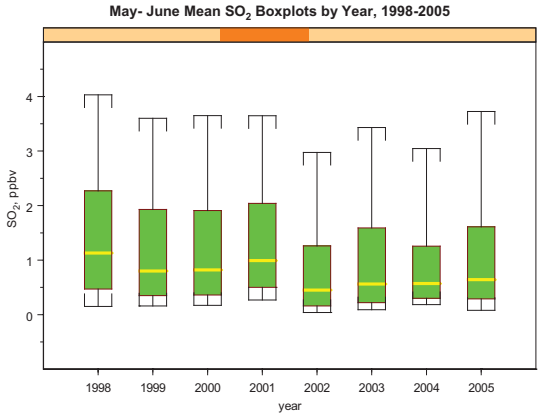

Figures 3-8a and 3-8b sulfur dioxide boxplots of the January-February and May-June concentration data by year (outliers are included but not plotted) at Pinnacle State Park in Addison, NY.

NO_x ($NO + NO_2$)

NO_x here is reported as the sum of NO and NO_2. NO is measured directly by the chemiluminescence analyzer, and NO_2 is measured by the same analyzer after photolysis to NO

by a xenon arc lamp system. Monthly averages for this quantity are shown as Figure 3-9. The arc lamp system is rather high maintenance. Arc lamp lifetime ranges from three to six months, and we have been through four arc lamp power supplies at this site. Power supply failures account for the majority of the missing data which is evident from Figure 3-9. The seasonal pattern for NO_x is similar to that for SO_2, which is, significantly higher in the winter months and lower during the summer.

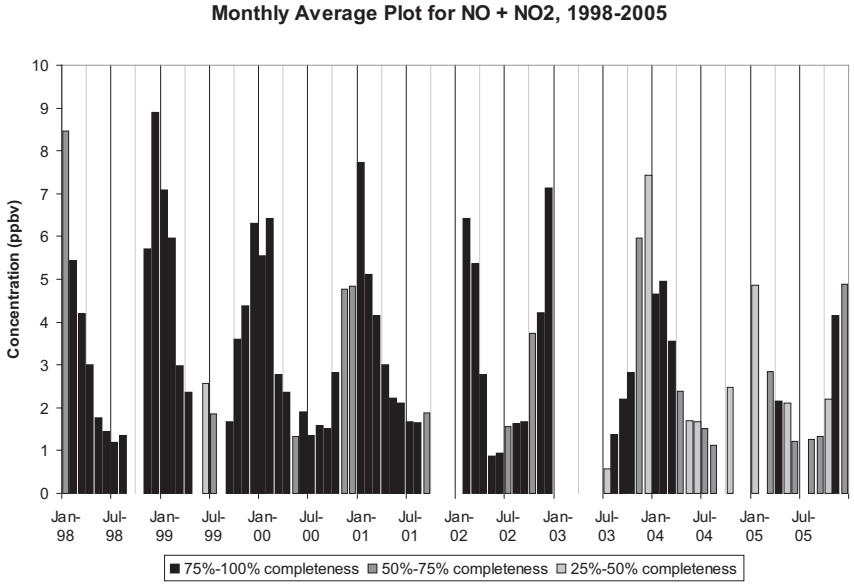

Figure 3-9. Monthly averaged NO_X ($NO + NO_2$) concentrations at the Pinnacle State Park site in Addison, NY. Shadings of the bars indicate levels of data completeness for the month as indicated in the legend. Missing bars indicate less than 25% data completeness.

Total Oxides of Nitrogen (NO_y)

Total oxides of nitrogen, or NO_y, include NO_x and higher oxides, including nitric and nitrous acids (HNO_3, HONO), and organic nitrates ($RONO_2$). Monthly averages for this quantity are shown as Figure 3-10.There is better data completeness for NO_y than for NO_x. As with SO_2 and NO_x, the concentrations are higher in winter and lower in summer due to the reduced photochemical activity in the winter and higher planetary boundary layer heights in summer.

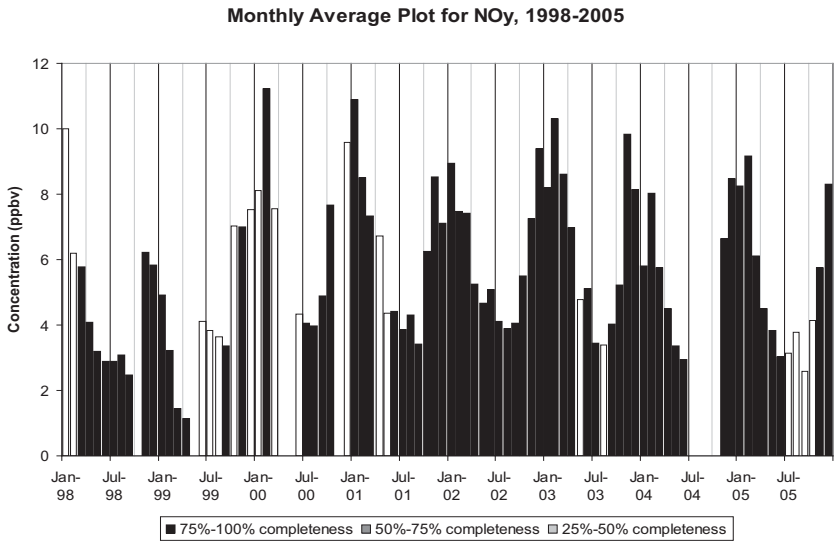

Figure 3-10. Monthly averaged NO_Y (total oxides of nitrogen) concentrations at Pinnacle State Park in Addison, NY. Shadings of the bars indicate levels of data completeness for the month as indicated in the legend. Missing bars indicate less than 25% data completeness.

May through August boxplots of NO_x and NO_y ,presented in Figures 3-11a and 3-11b, show little indication of a downward trend in NO_x, but NO_y levels suggest a downward trend into 2004 after a 2002 maximum. Regional NO_x emission estimates indicate a downward trend from 1998 to 2004 with little change between 2004 and 2005. The post 2001 ambient NO_y ambient summertime concentrations are consistent with reported emission reductions, but that is not the case for prior years. It is not clear as to the source of these inconsistencies, but potential factors include: 1) the spatial and temporal variations in the application of emission controls under title IV and the NO_x SIP call; and 2) meteorological inter-annual variability, which affect the transport, deposition, and chemical lifetime of NO_y component species.

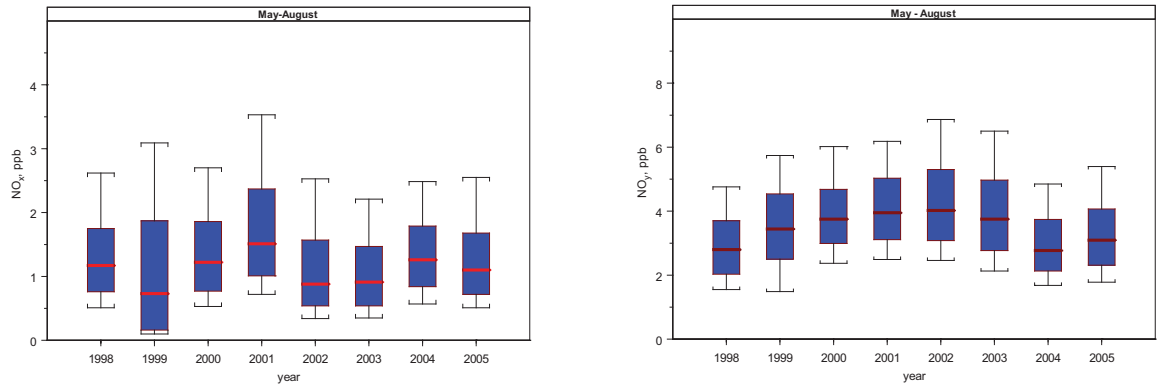

Figure 3-11a and 3-11b Boxplots of May-August averaged NO_x and NO_y by Year

Carbon Monoxide

Monthly averaged carbon monoxide concentrations for the eight- year period are shown in Figure 3-12. As with sulfur dioxide, carbon monoxide concentrations are highest in the winter months (see Figure 3-13) for pretty much the same reasons: longer chemical lifetimes and more

stable and lower mixed layer heights in the winter months. It also appears from the annual boxplots, shown in Figure 3-14, that CO mean concentrations were somewhat lower in the years 2000-2002 and larger before and after that period. We do not have an explanation for this apparent dip. Since 2000 was a cool and wet year, as noted above, the lower average values for this year cannot be explained by increase average oxidation activity in the atmosphere. Likewise the somewhat higher levels for the years 2003 – 2005 do not lend themselves to an easy explanation[1]. It is worth noting that, although less distinct, similar annual trends have also been observed at Whiteface Mountain and are discussed in the next section.

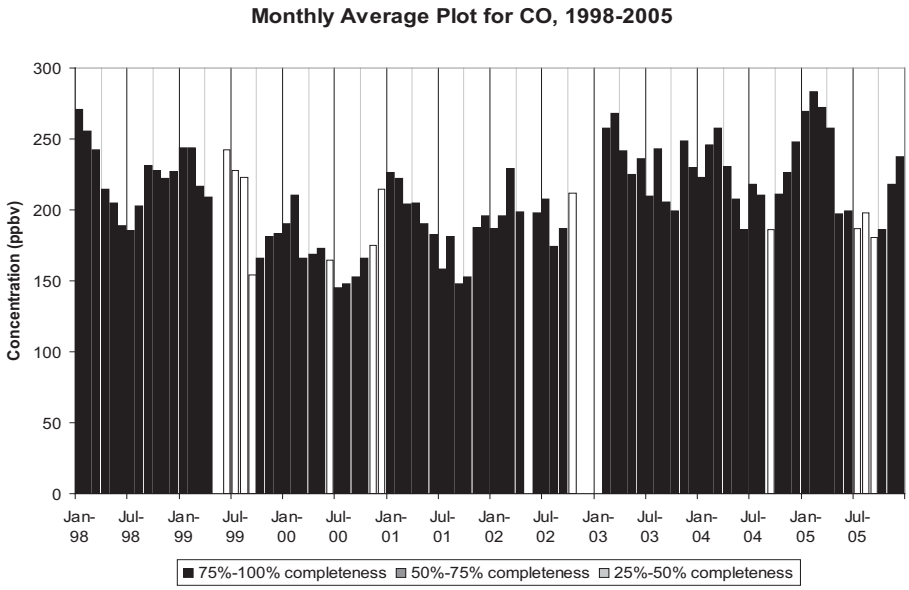

Figure 3-12. Monthly averaged carbon monoxide concentrations at Pinnacle State Park in Addison, NY. Shadings of the bars indicate levels of data completeness for the month as indicated in the legend. Missing bars indicate less than 25% data completeness.

[1]The CO instrument malfunctioned in late 2002 and was returned to the manufacturer for repair. It was reinstalled in January 2003. While the QA/QC procedures for the instrument operation and data handling did not change, there is a possibility that a slight systematic change in the instrument could be responsible for the perceived change. The apparent change before and after servicing is not much more than the specified lower detection limit of 20 ppbv.

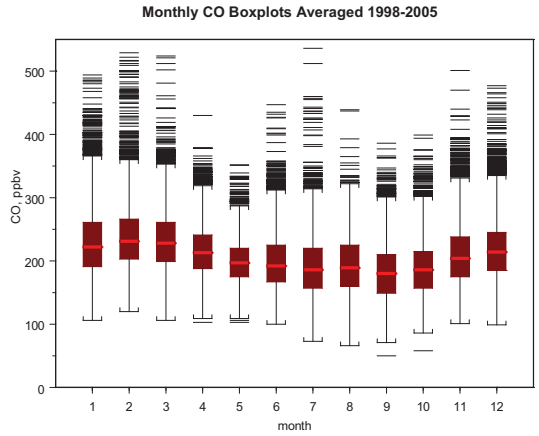

Figure 3-13. Monthly carbon monoxide concentration boxplot averaged from 1998-2005 at Pinnacle State Park in Addison, NY.

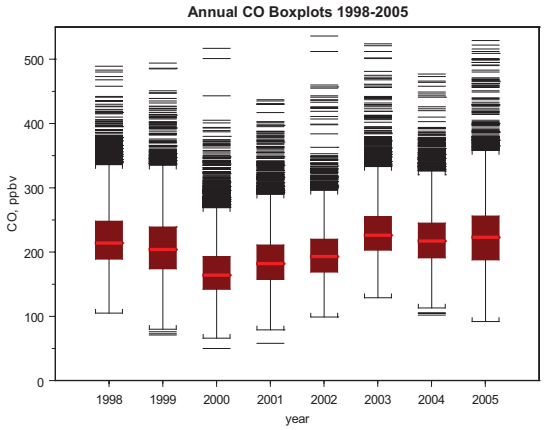

Figure 3-14. Annual carbon monoxide concentration boxplot from 1998-2005 at Pinnacle State Park in Addison, NY.

$PM_{2.5}$ Mass Concentration

The continuous (and filter-based) measurements of $PM_{2.5}$ mass began in 1999, so the period covered in Figure 3-15 is shorter than the period of Figures 3-1 through 3-5. The PM mass concentrations are very strongly seasonally dependent, with a clear summer maximum. The year-to-year variation is perhaps most strongly visible for this pollutant, particularly if one compares the "clean" year of 2000 with the "polluted" year of 2001. The winter fine PM concentrations are consistently quite low, reaching values near 4µg/m^3. While ozone concentrations often peak in the spring months (see 1998, 2001, 2005 in Figure 3-1 above), $PM_{2.5}$ definitely is highest in the summer months of July and August at this site. Continuous $PM_{2.5}$ mass measurement methods and instrument performance are discussed elsewhere in this report.

By way of comparison, Figure 3-16 shows the $PM_{2.5}$ mass concentrations measured using the filter based Federal Reference Method (FRM) sampler at the site. As discussed in detail elsewhere in this report, the FRM measurements report mass concentrations that are systematically higher than those reported from the standard TEOM monitor. This is evident as a nearly 3 µg/m^3 difference during some winter months. Comparison and simultaneous evaluation of these $PM_{2.5}$ measurement technologies has helped us to significantly inform the debate about appropriate measurement methods for this criteria pollutant.

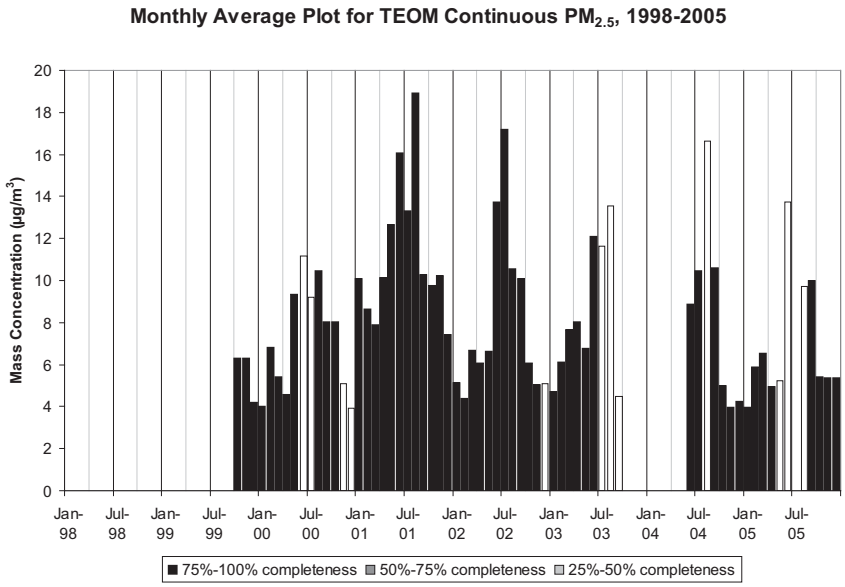

Figure 3-15. Monthly averaged $PM_{2.5}$ mass concentrations measured with the continuous TEOM mass monitor at the Pinnacle State Park site in Addison, NY. Shadings of the bars indicate levels of data completeness for the month as indicated in the legend. Missing bars indicate less than 25% data completeness.

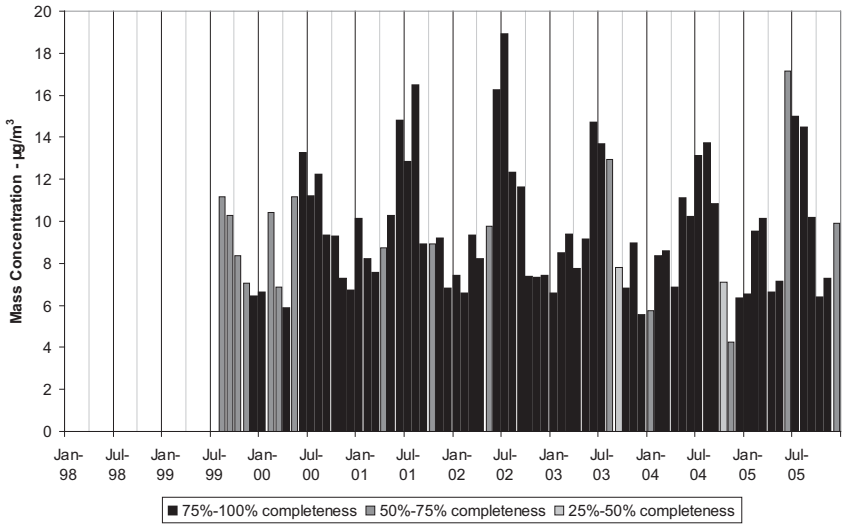

Figure 3-16. Monthly averaged $PM_{2.5}$ mass concentrations measured with the Federal Reference Method filter based sampler at the Pinnacle State Park site in Addison, NY. Shadings of the bars indicate levels of data completeness for the month as indicated in the legend. Missing bars indicate less than 25% data completeness.

Ozone Production Efficiency – Empirical Estimates

Atmospheric photochemical processes, which form ozone, also process other chemically active species. Species that are formed and processed along with ozone are often used as "indicators" of ozone formation and photochemical oxidation processes. The use of NO_y and NO_z as indicators for ozone production is well established (Sillman, 1995; Seinfeld and Pandis, 1998; NARSTO, 2000). NO_z is defined as (NO_y – NO_x) and interpreted as the more highly oxidized

oxides of nitrogen than NO and NO_2 – product species like nitric acid and organic nitrates. In fact, due to the intimate connection between NO_x and ozone formation, the slope of the correlation scatter plot with NO_y or NO_z plotted on the x-axis and O_3 plotted on the y-axis is sometimes referred to as the ozone production efficiency (OPE). In the case of O_3 versus NO_z, the simple interpretation is as follows: the slope is ΔO_3 divided by ΔNO_z, or the number of ozone molecules formed before the NO_x molecule is oxidized to NO_z and stops forming ozone. This interpretation is complicated by other loss processes, most notably surface deposition, which is significantly larger for NO_z (and particularly nitric acid) than it is for ozone. Still the OPE values (correlation slopes) offer a valuable zeroth order picture of the ozone production regime at a given site.

Figure 3-17 shows the monthly correlation slopes for plots of ozone versus NO_y at the Pinnacle State Park site for the time period 1998 – 2005. (Missing bars indicate that there is data missing for one or the other species.) As expected, these slopes are highest in the photochemically active "warm" season of May through October, typically peaking in July, August, or September. The winter slopes are negative, due to surface deposition processes and titration of the already low ozone levels by fresh NO_x plumes. All hourly data are included in this analysis, and one can see that there is a large variation in the R^2 values (the so-called "coefficient of determination"). Restricting the data by time-of-day, or solar light levels, or dry conditions, or by wind direction should improve the R^2 values and may allow additional interpretation of these data. These approaches will be explored, as this data is prepared for publication in the peer-reviewed literature.

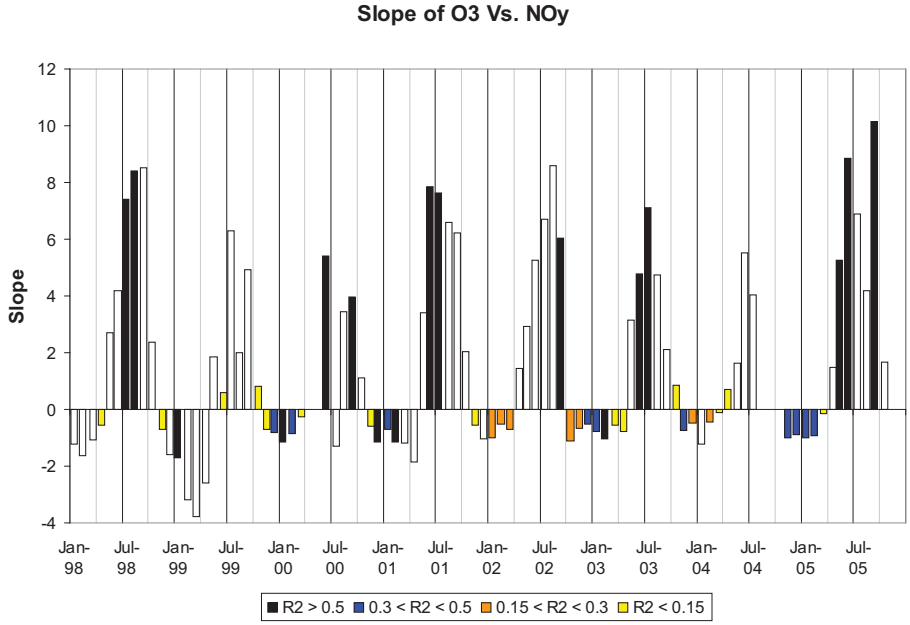

Figure 3-17. Regression slopes for the monthly correlation scatter plots of hourly averaged O_3 versus NO_y data at Pinnacle State Park in Addison, NY. The bars are color coded based on the R^2 (coefficient of determination) value – the black bars have the highest R^2 values and the yellow bars have the lowest R^2 values.

Figure 3-18 shows the monthly correlation slopes for plots of ozone versus NO_z at the Pinnacle State Park site for the time period 1998 – 2005. (Missing bars indicate that there is data missing

for one or the other species.). Comparison with Figure 3.17 is instructive. There is more missing data due to the repeated failures of the arc lamp system discussed above. Still, the R^2 values are generally higher for Figure 3-18, which indicates a higher degree of correlation of O_3 with NO_z than with NOy. As noted above, this makes scientific sense, since NO_z is only higher oxides of nitrogen and not NO_x plus higher oxides. This plot gives values of the O_3 to NO_z slope of 7-10 for the summer months that are typical of those observed in North America (NARSTO, 2000). Figure 3.18 seems to indicate that there is some low level of ozone production even during most winter months – a result that is not clear for Figure 3.17. Investigation of these correlation slopes and their relation to ozone production efficiency is underway and continuing.

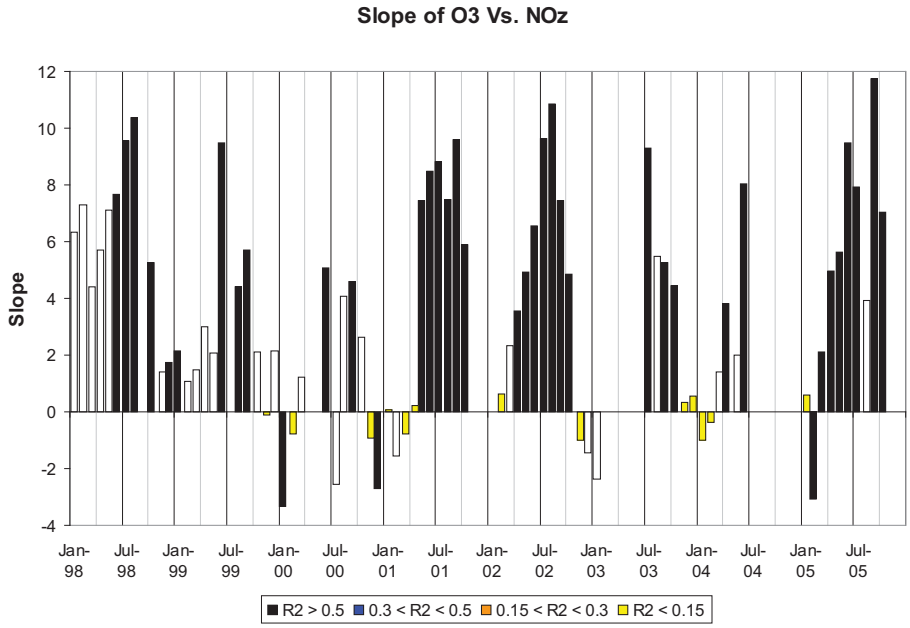

Figure 3-18. Regression slopes for the monthly correlation scatter plots of hourly averaged O_3 versus NO_z data at Pinnacle State Park in Addison, NY. The bars are color coded based on the R^2 (coefficient of determination) value – the black bars have the highest R^2 values, and the yellow bars have the lowest R^2 values

4 WHITEFACE MOUNTAIN MEASUREMENTS AND RESULTS

For comparison purposes, we provide monthly summaries similar to those presented for Pinnacle State Park in Section 3. In general, the Whiteface Mountain seasonal and inter-annual trends are consistent with those observed at Pinnacle State, but it is important to note that there are systematic differences between the sites. Whiteface Mountain is more isolated from emission source regions than is Pinnacle State Park, and the reported gas concentration measurements at Whiteface are from the summit at ~ 4800ft. These two factors are the main reason for the systematically lower observed mean concentrations at Whiteface Mountain as compared to Pinnacle State Park. There are other features of gas phase concentration measurements that are accentuated as a result of the high elevation monitoring, and these are discussed in the individual species sections.

Ozone

The monthly averaged ozone concentrations at Whiteface Mountain for the eight-year period are shown in Figure 4-1. The seasonal ozone pattern (Figure 4-1) is similar to that observed at Pinnacle State Park, which is highest in spring and summer and lowest in late fall and winter. The dynamic range of the Whiteface seasonal averages are substantially attenuated compared to those at Pinnacle State Park. This stems mainly from the fact that, as a result of its elevation, Whiteface does not experience diurnal variations as it is typically at or above the top of the planetary boundary layer. The year-to-year variation in, annual ozone concentrations (Figure 4-3) is also less than that observed at Pinnacle State Park, and it is even more difficult to identify long-term trends in the overall ozone concentration.

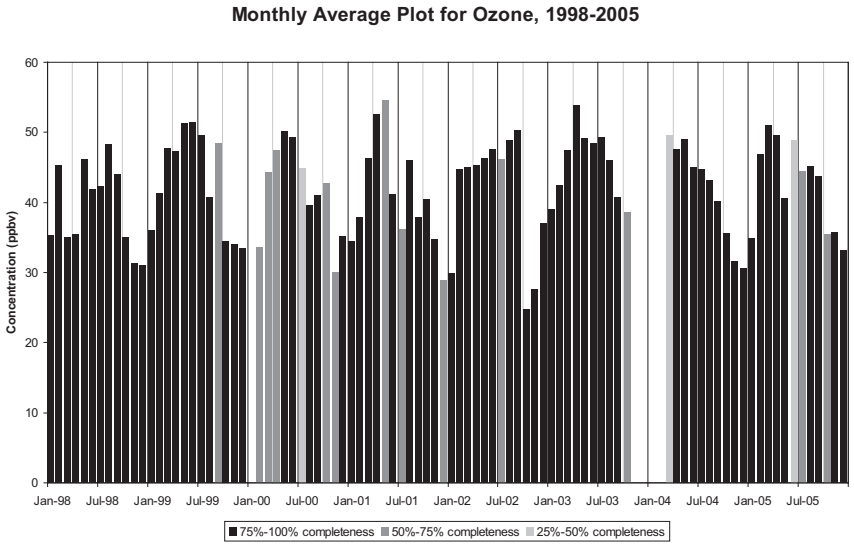

Figure 4-1. Monthly averaged ozone concentrations at the Whiteface Mountain summit in Wilmington, NY. Shadings of the bars indicate the level of data completeness for the month as indicated in the legend.

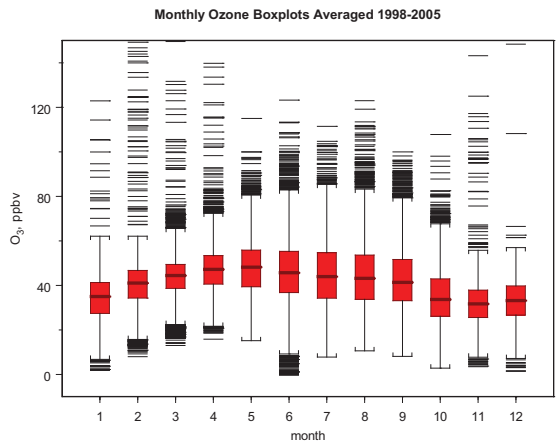

Figure 4-2. Monthly ozone concentration boxplots averaged from 1998-2005 at Whiteface summit in Wilmington, NY.

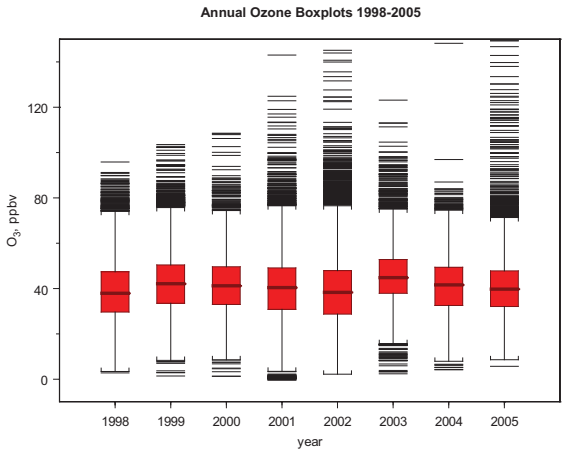

Figure 4-3. Annual ozone concentration boxplots 1998-2005 at the Whiteface summit in Wilmington, NY.

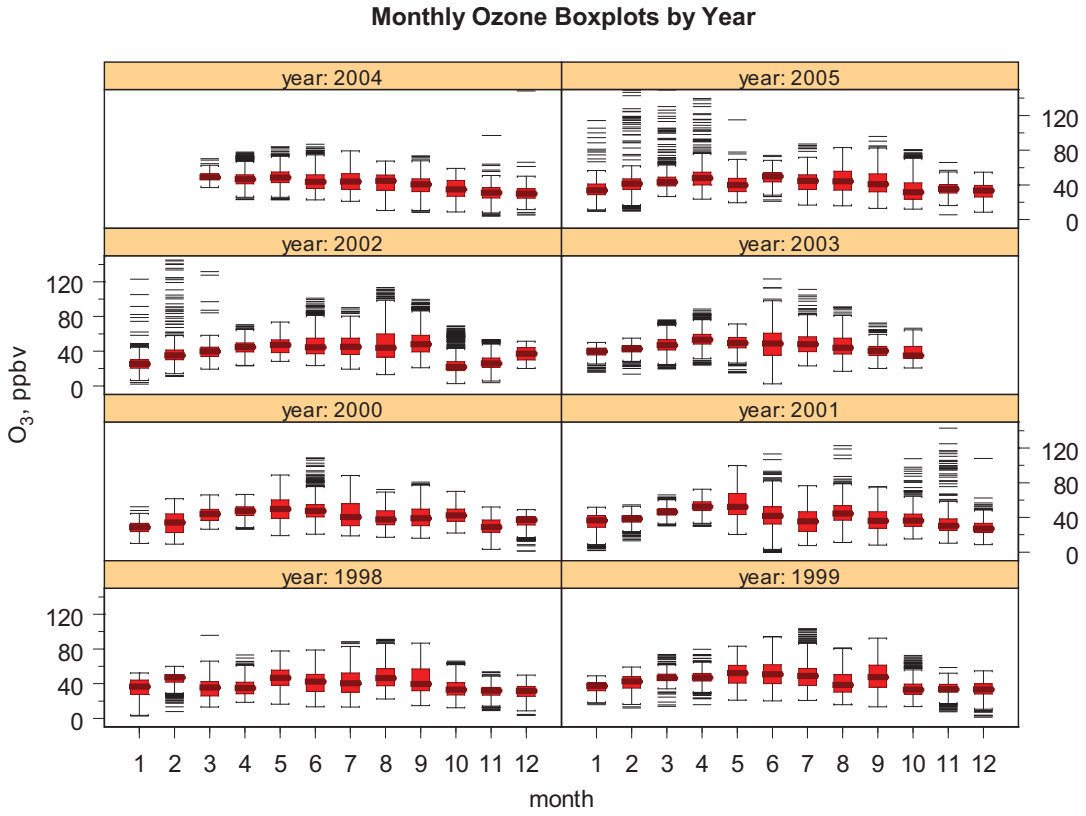

Figure 4-4. Monthly ozone concentration boxplots by year 1998-2005, at the Whiteface summit, Wilmington, NY.

Sulfur Dioxide

The monthly averaged sulfur dioxide concentrations for the eight-year period are shown in Figure 4-5. The highest average sulfur dioxide is observed in winter months as indicated in Figures 4-5 and 4-6, which also shows the significant number of outliers, i.e., concentration values exceeding the 95th percentile. As with Pinnacle State Park, the outliers are associated with plume impacts, but the outliers and mean values at Whiteface Mountain are systematically lower than those observed at Pinnacle State Park. This difference is mainly due to the

substantially larger source-to-receptor distances at Whiteface Mountain, which are otherwise seasonal distribution that follow similar patterns as observed at Pinnacle State Park. In the case of Whiteface Mountain, midwinter monthly averages reach only as high as 1.5 ppbv, and midsummer monthly values were < 0.5 ppbv. The high-time resolution data during the winter is also attenuated as compared to Pinnacle State Park, with winter plumes of SO_2 reaching 10 ppbv fairly frequently and summer plumes greater than 7.5 ppbv quite infrequent.

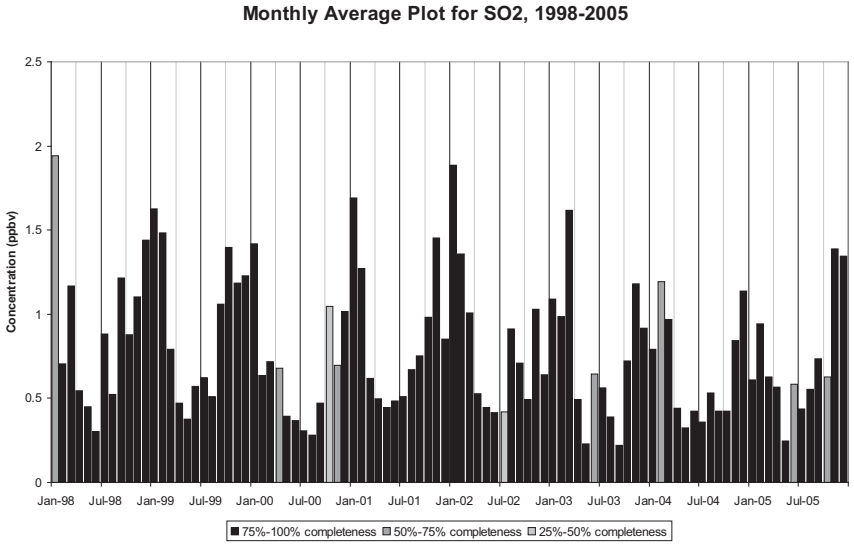

Figure 4-5. Monthly averaged SO_2 concentrations at the Whiteface Mountain summit in Wilmington, NY. Shadings of the bars indicate the level of data completeness for the month as indicated in the legend.

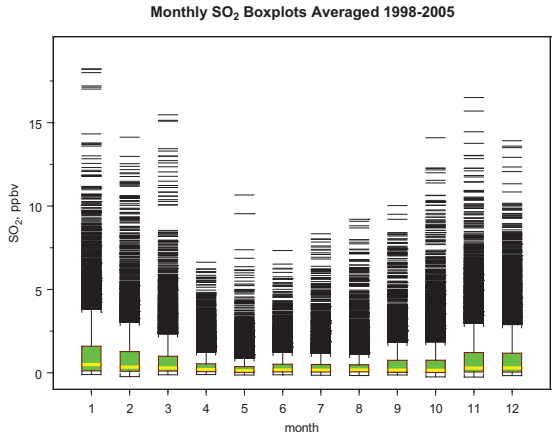

Figure 4-6. Monthly sulfur dioxide concentration boxplots averaged from 1998-2005 at the Whiteface Mountain Summit, Wilmington, NY.

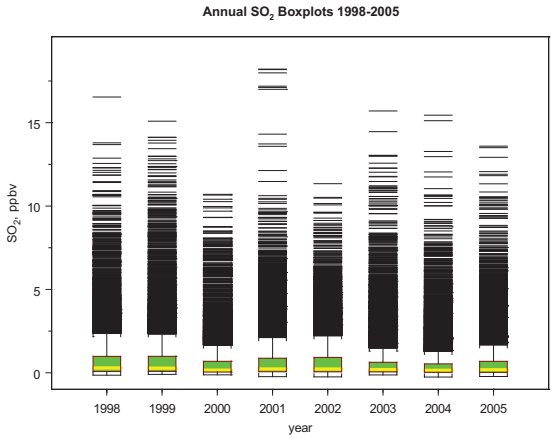

Figure 4-7. Annual sulfur dioxide concentration boxplots from 1998-2005 at the Whiteface Mountain summit, Wilmington, NY.

It is even more difficult to discern any trend in the annual boxplots of SO_2 as presented in Figure 4-7 and the January-February and May-June SO_2 boxplots, presented in Figures 4-8a and 4-8b by year, respectively. Further analysis needs to be performed to determine if the significant inter-annual variability observed in the wintertime boxplots (Figure 4-8b) is associated with changes in emissions or is due to meteorological variability.

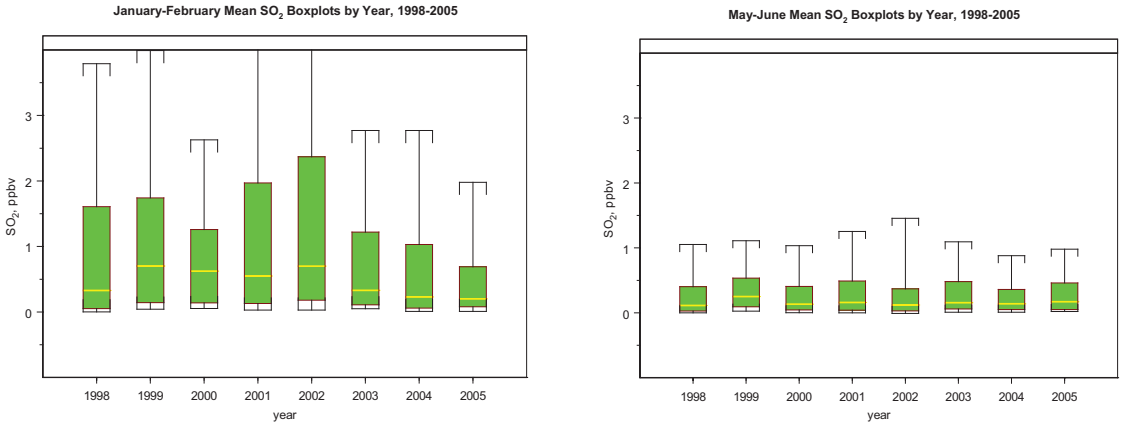

Figures 4-8a and 4-8b sulfur dioxide boxplots of the January-February and May-June concentration data by year (outliers are included but not plotted) at the Whiteface Mountain summit in Wilmington, NY.

NO_X ($NO + NO_2$)

As with Pinnacle State Park, the reported NO_x ($NO+NO_2$)is based on NO which is measured directly by the chemiluminescence analyzer and NO_2 measured by the same analyzer after photolysis to NO by a xenon arc lamp system. Monthly average NO_x at the Whiteface Mountain summit is shown in Figure 4-9, and as with Pinnacle State Park, high maintenance issues are associated with the NO_2 photolysis method and significant amounts of missing data are experienced. In general, as with Pinnacle State Park, the seasonal pattern for NO_x is similar to that for SO_2, with significantly higher values in the winter months as compared to the summer months, which is consistent with NO_x's significantly shorter chemical lifetime under high summer time photochemical conditions.

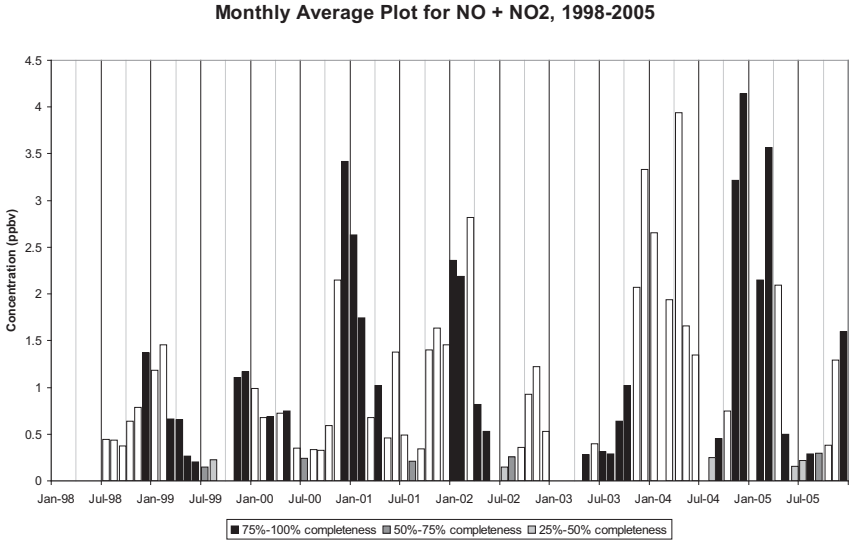

Figure 4-9. Monthly averaged $NO+NO_2$ concentrations at the Whiteface Mountain summit in Wilmington, NY. Shadings of the bars indicate the level of data completeness for the month as indicated in the legend.

Total Oxides of Nitrogen (NO_y)

The monthly average NO_y ppbv concentrations for Whiteface Mountain are presented in Figure 4-10. The persistent levels of data completeness in the summer are a result of operational difference in the measurement over the course of the seasons. In the summer time, the NO_y catalytic converter box is placed outside on the summit roof and the flows through the converter must be turned off when the summit is in cloud (which can be as much as 50% of the time). Cloud water diminishes the conversion efficiency of the catalytic converter and ultimately destroys its ability to reduce oxidized nitrogen species to NO. In the winter, the converter box must be brought inside, as it cannot tolerate icing conditions. In this instance, disruption of flow is not necessary, as any liquid water present is lost through impaction within the sampling manifold and sampling lines. One might ask why the converter unit is placed outside at all. The purpose for that placement is to achieve the shortest sampling distance to the converter to avoid the loss of HNO_3 (an extremely sticky gas) on manifold walls and sampling lines. The current sampling protocol is the best compromise for the unique conditions at the summit. As with SO_2 and NO_x, the NO_y concentrations are higher in winter and lower in summer due to longer lifetimes as a result of reduced photochemical activity in the winter.

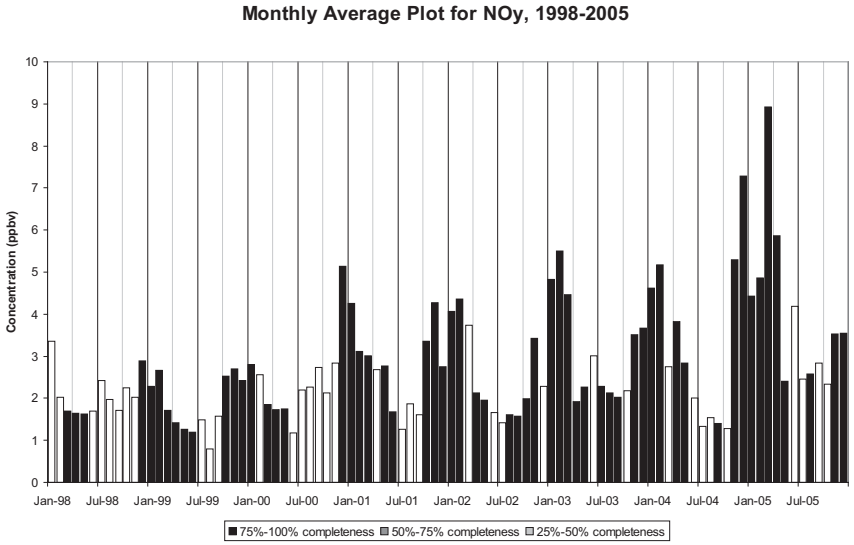

Figure 4-10. Monthly averaged NO_y concentrations at the Whiteface Mountain summit in Wilmington, NY. Shadings of the bars indicate the level of data completeness for the month as indicated in the legend.

Carbon Monoxide

The monthly average carbon monoxide concentrations for Whiteface Mountain over the eight-year period are presented in Figure 4-11. The monthly boxplot distributions presented in Figure 4-12 do not show a seasonal pattern as observed at Pinnacle State Park or as observed at Whiteface Mountain for SO_2 or NO_y (not shown). This seems puzzling at first, but a possible explanation may lie in elevation of the summit measurements. Since the Whiteface summit does not experience diurnal variations, as it is typically at or above the top of the planetary boundary layer, it is much less influenced by ground level sources (the predominant level for CO emissions). It is a reasonable assumption the bulk of the SO_2 and NO_y plume impactions at the summit are from elevated emission sources. In the winter months, the summit resides at the

top or above the planetary boundary layer, which means ground -level emission sources likely have little influence on ambient concentrations at the summit elevation and likely are typical of free troposphere levels. Elevated emissions from tall stacks with significant plume rise are likely to penetrate the higher levels of the atmosphere, which result in the observed plume impacts of SO_2 and NO_y at the summit.

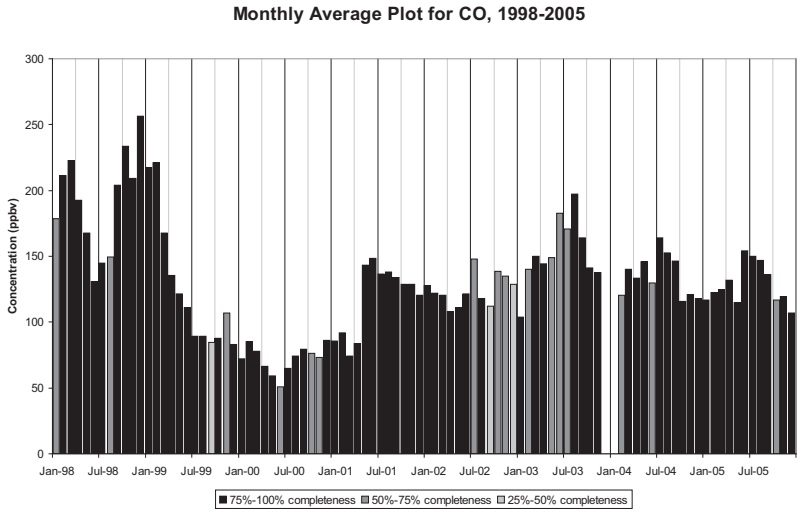

Figure 4-11. Monthly averaged CO concentrations at the Whiteface Mountain summit in Wilmington, NY. Shadings of the bars indicate data completeness for the month as indicated in the legend.

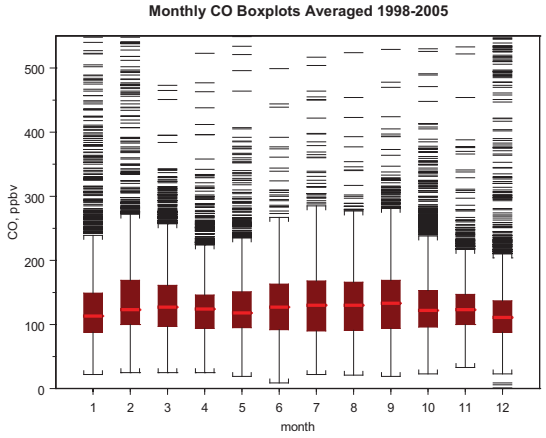

Figure 4-12. Monthly carbon monoxide concentration boxplot averaged 1998-2005 at the Whiteface Mountain summit in Wilmington, NY.

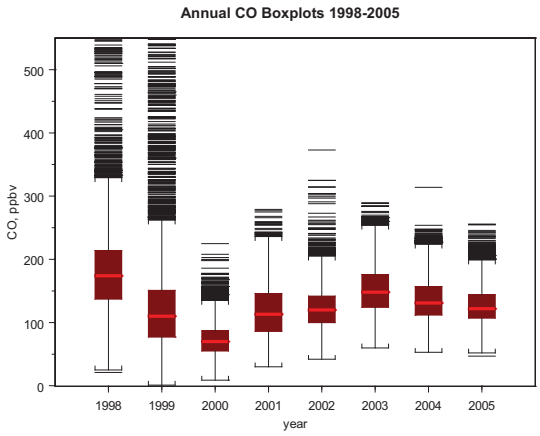

Figure 4-13. Annual carbon monoxide concentration boxplot 1998-2005 at the Whiteface Mountain summit in Wilmington, NY.

The annual mean concentrations at Whiteface Mountain, shown in the Figure 4-13, are on average lower than those observed at Pinnacle State Park. It is important to note that the anomalously low CO concentrations in the year 2000 at Pinnacle State Park were also observed at Whiteface Mountain. As mentioned previously, 2000 was a cool and wet year, so it is unlikely that the lower average values are due to enhanced photochemical processes. It is also unlikely this is the result of a reduction in anthropogenic emissions, as we are unaware of any

major changes in fuel consumption or new emission control programs. In addition, the latter would be permanent and would be expected to be sustained in the years to follow, which is not the case. It is conceivable that forest fires and biomass burning during this year were anomalously low, but we have no evidence at this time to support this hypothesis. We hope to explore this issue further in future work.

5 OVERVIEW OF SPECIAL FIELD INTENSIVE CAMPAIGNS

Over the course of the PMTACS-NY program three intensive field campaigns were performed. These campaigns were performed at Queens College in the summer of 2001 and winter of 2004 (see map Figure 5.1) and at Whiteface Mountain in the summer of 2002. The campaigns, which operated over ~ 4 week periods, involved many research groups performing research grade measurements using emerging measurement technologies. In addition, a mini-intensive, not part of the original plan, was also performed at Pinnacle State Park in the summer of 2004, in part to participate in the regional component of the International Consortium for Atmospheric Research on Transport and Transformation (ICARTT). This intensive was performed with limited resources and involved only University at Albany participants. These measurements have provided detailed real-time chemical and physical characterization of the PM/co-pollutant complex that has been extremely useful in 1) the elucidation of the operative gas-to-particle transformation processes occurring in urban centers; 2) the enhancement of the chemical source signature data base in support of source attribution studies; and 3) the comparison and evaluation of emerging advanced measurement technologies with operational routine measurement systems. Participating research groups in the field intensives included: Aerodyne Research, Inc.; Aerosol Dynamics, Inc.; Brookhaven National Laboratory; Clarkson University; Georgia Institute of Technology; Penn State University; Max Planck Institute for Chemistry; NYS Department of Environmental Conservation; NYS Department of Health; Rupprecht and Patashnick, Co., Inc.; University of California; Irvine; and U.S. Environmental Protection Agency. A brief description of each of the field intensive campaigns is provided in the Text Boxes TB-5.1 – TB-5.4.

Figure 5.1 Map of Queens College measurement site and surrounding NY metropolitan area

View from PS 219

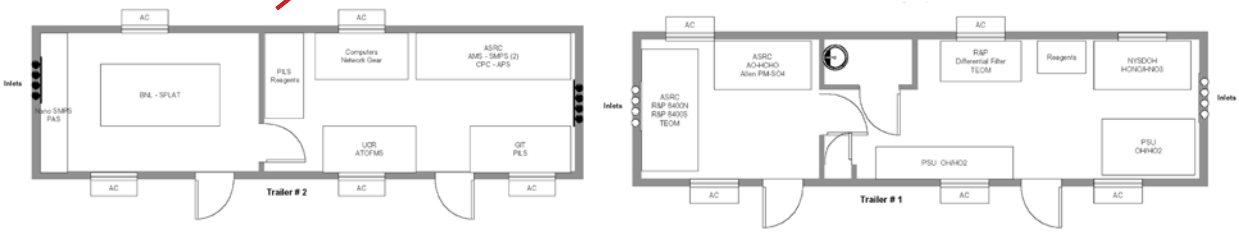

The PMTACS-NY 2001 summer intensive field study was located at the edge of parking field # 6 of Queens College in Queens/New York, adjacent to a running track/athletic field. Queens College is located in the heart of Queens, a few hundred meters south of Long Island Expressway and ca. 1 km east of Van Wyck Expressway, two of the busiest highways in eastern New York City. The primary measurement period of this campaign was June 30th until July 31st, but most instruments were operated through August 4th.

The majority of instrumentation was housed in two trailers located next to each other. Each instrument was equipped with a $PM_{2.5}$ cyclone. The inlets were all located at a height of approximately five meters above ground and not more than 2 m apart from each other.

Two filter based samplers (six-hour and one of three 24-hour filter samplers) were located adjacent to the trailer at the Queens College site. The inlets of these samplers were at a height of approximately 3 meters above the parking level, located ca. 10 m from the inlets of the semi-continuous instruments. The other two 24-hour filter samplers were located on the roof of Public School 219, ca. 100 m west of the Queens College site with a running track between the two locations. Due to a difference in ground elevation between the two sites, the inlets of these samplers were approximately at the same height as the inlets of the semi-continuous instruments located at Queens College.

TEXT BOX TB-5-1 Summer 2001 Queens College Field Intensive Campaign

The PMTACS-NY 2002 Summer field intensive campaign operated from 7/10/2002 to 8/7/2002 at the Whiteface Mountain base station of the ASRC, University at Albany, SUNY facility located in the northeastern Adirondack Mountains, New York (44° 23.6' N, 73° 51.5' W). The base lodge (2080 ft above msl), is situated northeast of the summit on Marble Mountain and located at the end of a dead end street. The traffic in the approach road to the base station is minimal and was generally limited to the participants of the campaign. An uphill graveled road (approximately 200 ft) leads to the sampling location from the parking lot, where advanced measurement systems (TDLAS, AMS, PILS and SMPS) and all other measurements were deployed within several trailers located in the forest clearing approximately 300 ft x 100 ft in area (see schematic of the instrument deployment below).

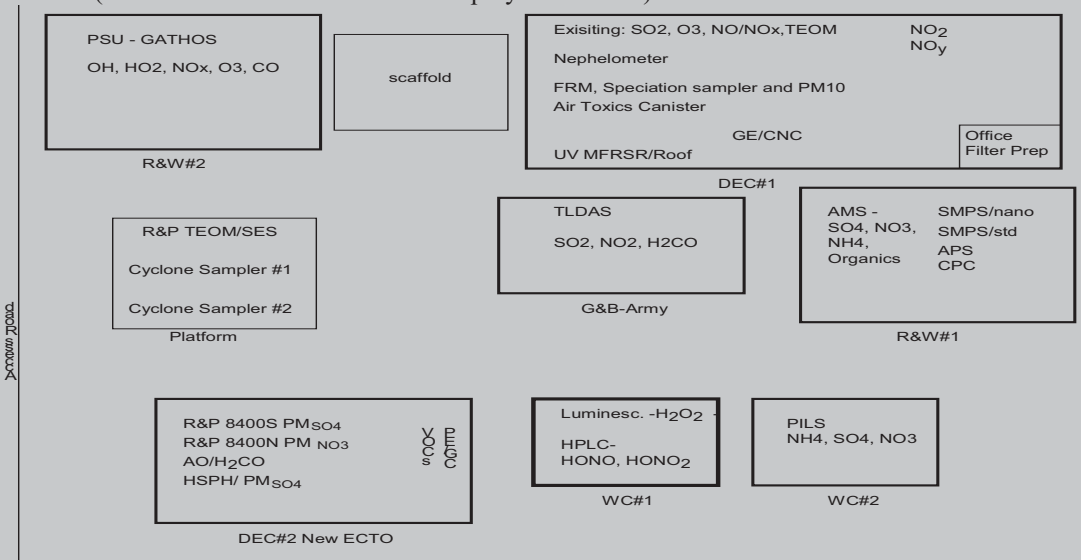

The surrounding forest is identified as 'Transition Zone' forest and is comprised of a mix of hardwood and conifer species. These include white and yellow birch, sugar maple, beach, and some red spruce and balsam fir. During the summer months the prevalent wind direction at Whiteface Mountain is from the southwest. A strong inversion was observed at the Lodge at most nighttimes during the measurement period. Winds were observed to be mostly from south through to the northwest. Relatively low wind speeds were predominant at the Lodge base station (average ~ 2m s^{-1}).

TEXT BOX TB-5-2 Summer 2002 Whiteface Mountain Field Intensive Campaign

The $PM_{2.5}$ Technology Assessment and Characterization Study – New York (PMTACS-NY) 2004 winter intensive field campaign operated at the Queens College measurement site in Queens, New York from 6 January through 6 February 2004. The measurement site is located on campus of Queens College (40.74° N, 73.82° W, ~25 m a.m.s.l.), adjacent to parking field # 6, which is approximately 300 meters south of Long Island Expressway (I-495) and 1 km east of Van Wyck Expressway (I-678), two high-traffic highways in the New York City metropolitan area.

The majority of measurement systems were situated in a one-story building complex, with sample inlets configured at a height ~6.5 m above ground level, 1 m above the roof of the building. Aerosols measurements were sampled through a $PM_{2.5}$ cyclone (URG-2000-30EN) and transported into the building using thermally insulated 14.1 mm ID copper tube or carbon based aerosol tubing. The tube diameter (ID 14.1 mm) was chosen to minimize losses by impaction and gravitational settling for the given flow rate.

TEXT BOX TB-5-3 Winter 2004 Queens College Field Intensive Campaign

The $PM_{2.5}$ Assessment and Characterization Study – New York (PMTACS-NY) 2004 mini-intensive study at Pinnacle State Park was performed as part of our participation in the International Consortium for Atmospheric Research on Transport and Transformation– ICARTT http://www.al.noaa.gov/ICARTT/. The PSP site is located in Addison, NY at 42.09°N, 77.21°W in the southwestern part of New York State, at an elevation of 504 m above sea level on Orr Hill, which is part of the Allegheny Plateau. The site is bounded by a golf course, a 50 acre pond, pastures, and coniferous and deciduous undeveloped state forest lands. The village of Addison, with a population of approximately 1,800, is located 4 km to the northwest, and Corning, with a population of approximately 12,000, is located 15 km to the northeast.

This special field intensive operated for four weeks (July 14 – August 11, 2004) within the overall ICARTT study period, which operated from July 1 – August 15, 2004. During the intensive study period, in addition to routine measurements performed at this site (see Table B.1 Appendix B), an Aerosol Mass Spectrometer (AMS), Particle In Liquid Sampler – Ion Chromatograph(PILS IC), Tunable infrared laser diode absorption spectrometer (TILDAS), and particle sizing and counting instrumentation (SMPS, APS and CPC) were deployed. To accommodate the additional instrumentation for the special study an 8'x8' monitoring shelter was provided by NYS DEC and placed on the south side adjacent to our permanent monitoring shelter as shown above. In addition, a Sunset Labs EC-OC carbon analyzer and TEI – prototype semi-continuous PM Sulfate analyzer were also deployed.

TEXT BOX TB-5-4 Summer 2004 Pinnacle State Park Mini-Field Intensive Campaign

6 KEY RESULTS AND FINDINGS WITHIN PROGRAM OBJECTIVES

This section provides a summary of key results and findings based on measurements provided under the routine backbone monitoring network established as part of this research program as well as the extensive research measurements carried out as part of the special field intensive campaigns. The results and findings are presented within the context of the program objectives identified in the project plan, which in turn, as previously discussed (section I), are linked to hypothesis and science policy questions presented in Appendix A.

6.1. Objective 1: Measure the temporal and spatial distribution of the $PM_{2.5}$/co-Pollutant complex in Urban and Rural Locations across New York.

Filter Based $PM_{2.5}$ Measurements

Figure 6.1-1 generated from data presented in Schwab et al. (2004a) shows bulk chemical composition at four areas in New York State for the period ending February 2003. The data record for these plots ranges from about 21 months of data for Whiteface Mountain to 36 months of data for the New York City site of New York Botanical Gardens. The major components at all sites are carbon, nitrate, sulfate, and ammonium, but there is a systematic change in the distribution of these components from the urban to the rural and remote locations. Carbon is proportionally highest in the New York City area and lowest in the rural and remote locations. Nitrate is highest in the large urban (New York City) and small urban (Rochester) locations and significantly lower in the rural and remote locations. Sulfate is proportionally highest at Pinnacle State Park, presumably due to its proximity to the Ohio Valley source region, and lowest in New York City. The absolute mass concentration of the "Other" component is quite similar for the urban and rural locations, but it is proportionally largest at the Whiteface Mountain location.

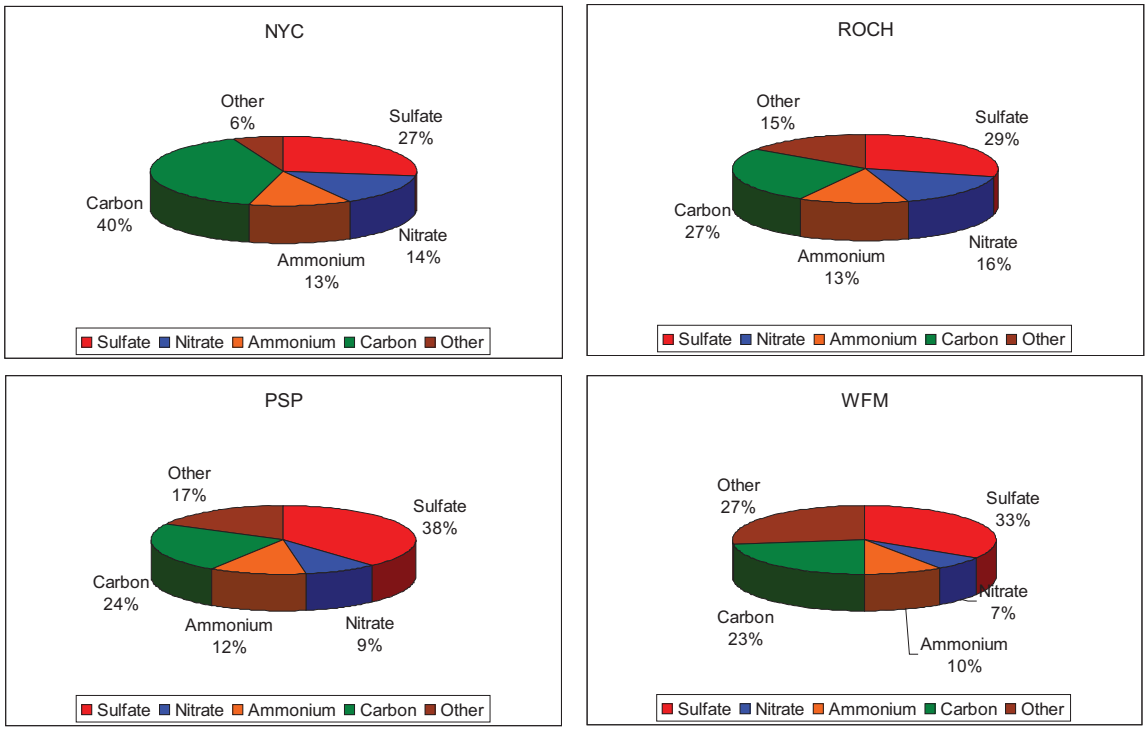

Figure 6.1-1. Average three-year chemical composition of $PM_{2.5}$ at New York State sites. The NYC chart is the average of three sites (New York Botanical Garden, South Bronx IS52, and Queens College). The other sites are Rochester, Pinnacle State Park, and Whiteface Mountain Lodge level. Mean $PM_{2.5}$ mass concentrations for NYC, ROCH, PSP, and WFM are 15.70, 13.13, 11.26 and 7.40 $\mu g/m^3$, respectively.

Finding 6.1-1: *The average composition of PM at urban New York City sites suggests that the bulk of PM mass is attributed as follows: Carbon-based (~40%), Sulfate-based (~27%), Nitrate-based (~14%), and Ammonium (~13%); the remaining ~6% is metals/soil related and particle bond water (Schwab et al., 2004a).*

As seen from the multi-year time series of $PM_{2.5}$ mass concentration at Pinnacle State Park elsewhere in this report, PM mass is highly seasonal at rural sites. This is much less true for the urban sites, particularly New York City, as seen in Figure 6.1-2 (Schwab et al., 2004a). However, in this same paper, the chemical composition in the New York City sites does vary considerably with season as shown in Figure 6.1-3 based on three NYC sites averaged over a three- year period. Nitrate shows the most dramatic change with season, contributing a nearly equal amount of mass as sulfate during the winter, but only roughly ¼ as much during the summer. Elemental carbon (EC) is also lower during the summer months but contributes a roughly equal percentage during the other three seasons. Sulfate and OC show greater percent contributions during the summer period, which is consistent with appreciable secondary production of these species. The "other" component, including mineral dust and sea salt, is highest in the spring season, which is also consistent with this period being the most meteorological active and turbulent season.

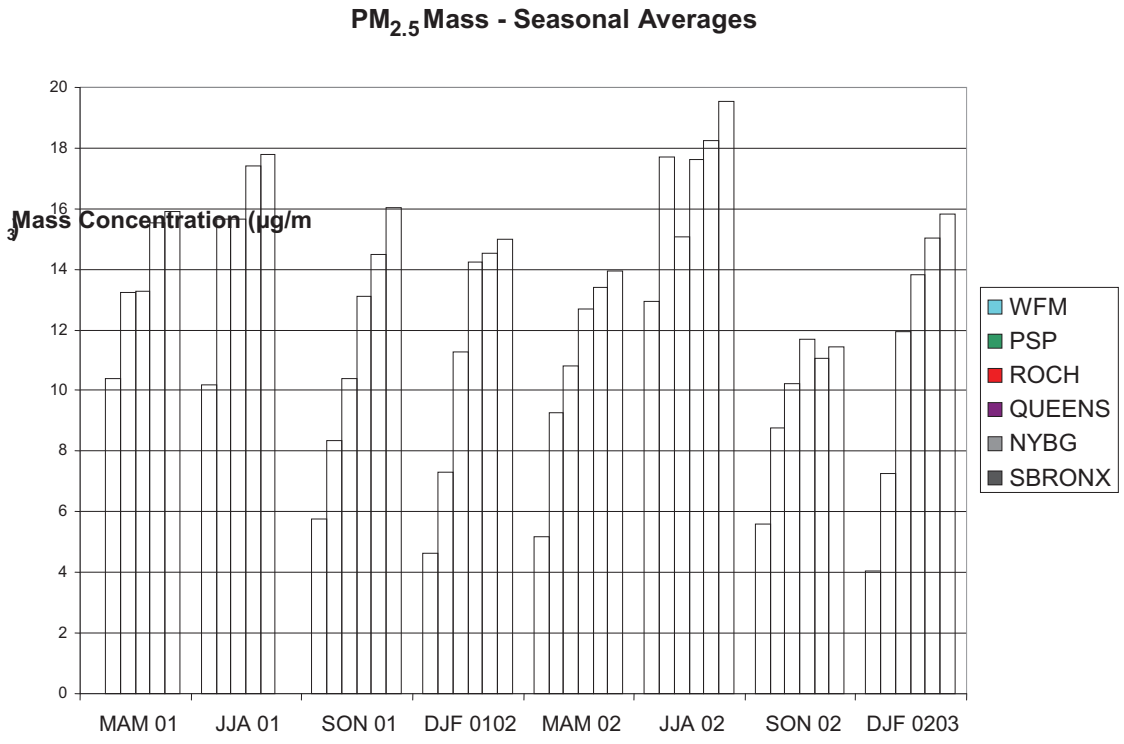

Figure 6.1-2. Seasonally averaged $PM_{2.5}$ mass concentrations for six New York State sites.

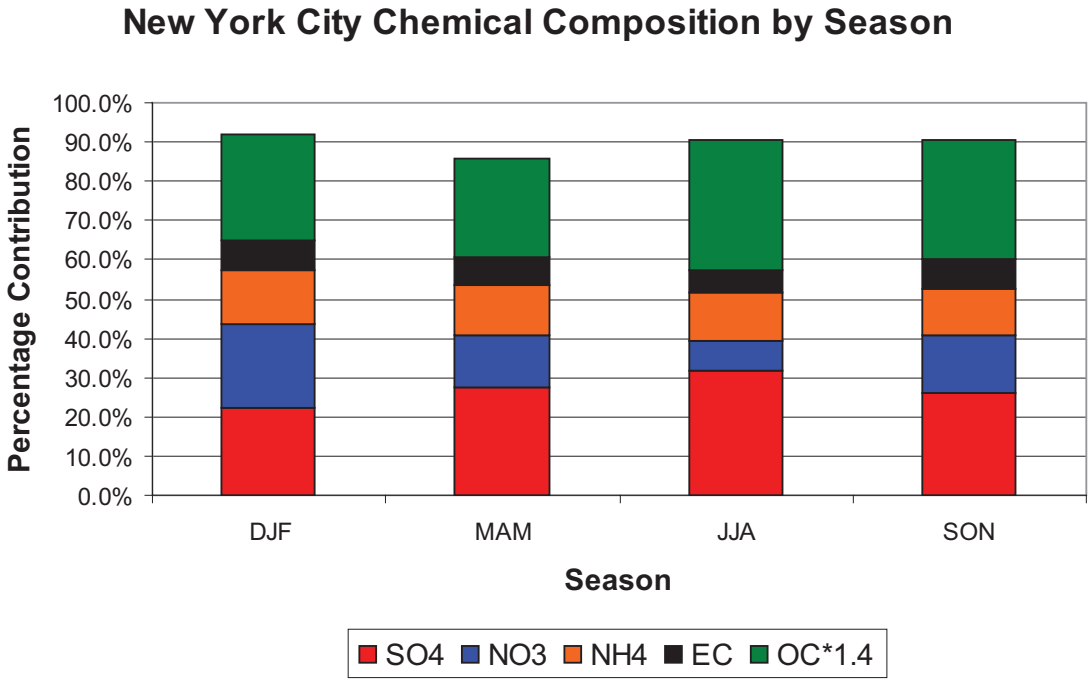

Figure 6.1-3. Percent contribution, by season, of five major chemical components to the $PM_{2.5}$ mass concentrations measured at three New York City sites for a three-year period from March 2000 through February 2003. The mean mass concentrations for reported months are as follows: DJF = 15.57 µg/m^3; MAM = 14.35 µg/m^3 ; JJA = 18.00 µg/m^3; SON = 13.83 µg/m^3.

Finding 6.1-2: *Although the contributions to the annual PM mass by season are comparable for cold and warm season months (16.6 and 15.4 μg/m^3, respectively) based on filter based measurement data averaged over three New York city sites in 2002, the PM species composition differs significantly by cold vs. warm season (SO_4, 22%/34%; NO_3, 23%/8%; NH_4, 14%/13%; OC*1.4, 28%/34%; EC, 9%/6%; and soil, 4%/5%), (Drewnick et al., 2004a,b; Schwab et al., 2004a, Weimer et al., 2006).*

AMS PM Measurements

A quadrupole aerosol mass spectrometer (Q-AMS), developed and manufactured by Aerodyne Research, Inc. [*Jayne et al.*, 2000; *Jimenez et al.*, 2003a], was applied to measure mass concentration and species-resolved mass size distributions for non-refractory aerosol components like nitrate, sulfate, ammonium, chloride, and total organics in near real-time during the Queens College Summer 2001 and Winter 2004 field intensive campaigns.
The Q-AMS vacuum system consists of three major parts: an aerosol sampling chamber, a particle sizing chamber, and an analysis chamber. The aerosol is introduced into the vacuum system through an aerodynamic particle beam-forming lens (Figure 6.1-4) (Drewnick et al., 2004a).

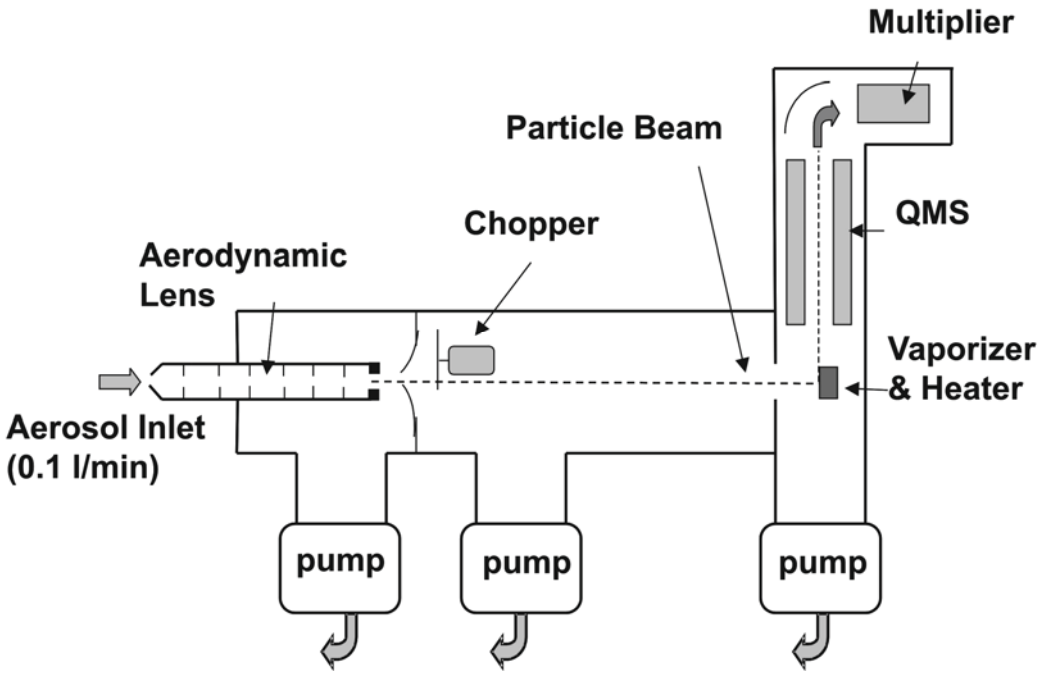

Figure 6.1-4 Schematic of the Aerosol Mass Spectrometer

The flow into the inlet system is set to 0.1 l minute^{-1} by a 100 μm critical orifice before the lens. Particles in the range of approximately 50-700 nm are focused with almost 100% efficiency into a narrow beam that passes a skimmer and the particle sizing chamber, before it impacts onto the vaporizer which is heated to approximately 500-700 °C. Non-refractory particle components are flash vaporized, and the generated vapor is ionized by electron impact

(70 eV). Positive ions are extracted into a quadrupole mass spectrometer (QMS, Balzers QMG 422) for mass analysis and subsequent detection with a calibrated electron multiplier.

The AMS measures the vacuum aerodynamic diameter (d_{va}), defined as $d_{va} = (\rho_p/\chi_v\rho_0)d_{ve,}$, where ρ_p is the particle density, χ_v is the dynamic shape factor in the free molecular regime, ρ_0 is the unity density (= 1 g cm^{-3}), and $d_{ve,}$ is the volume-equivalent diameter (*DeCarlo et al.*, 2005; *Takegawa et al.*, 2005). The aerodynamic lens (Zhang et al., 2002, 2004) transmits particles with ~100% efficiencies in the d_{va} range from 50 – 600nm and drops off significantly for D_{va} >1.The characteristic operational mean particle diameter size sampling range of the AMS is 30nm - 1500nm and has similar characteristics to PM_1 size selective inlets used in filter- based measurements.

In both the summer 2001 and winter 2004 field campaigns, the Q-AMS operated in two modes, the *Particle Time-of-Flight Mode* (P-TOF) and the *Mass Spectra Mode* (MS). The P-TOF mode is used for the measurement of species resolved aerosol mass-size distributions. For particle sizing a mechanical chopper wheel, which is situated right after the skimmer at the beginning of the particle sizing chamber (l = 39 cm), is moved into the particle beam to chop the beam with a frequency of about 120 Hz. The chopper wheel has two radial slits, covering 1 % of the wheel area. An equivalent fraction of particles pass the chopper when the flight path is open, which result in a common starting time of all particles at the position of the chopper. During the expansion of the sampled air into the vacuum, aerosol particles are accelerated according to their aerodynamic properties and reach the vaporizer at different times. By setting the QMS on a fixed mass and measuring the time resolved ion signal, the particle velocities can be mapped out. The velocity distribution can be transformed into a particle size distribution for the selected species using a P-TOF calibration.

In the MS mode, the average composition of the non – refractory aerosol components is determined by scanning the complete mass spectrum (1 – 300 amu) with the QMS at a frequency of 3 Hz. In order to maximize particle transmission, the chopper is moved completely out of the particle beam (‘beam open’ position). The instrument background signal is measured routinely by moving the chopper wheel far into the particle beam to completely block it (‘beam closed’ position). The difference of the signal at ‘beam open’ and ‘beam closed’ position is used for the calculation of aerosol mass concentrations for non-refractory species that are extracted from the averaged mass spectra.

These measurements have provided significant insight into the time resolved composition of PM and the size distribution of PM as a function of composition. The time series of PM species composition measured by the AMS for the summer and winter campaigns are shown in figures 6.1-5 and 6.1-6 (Drewnick et al., 2004b; Weimer et al., 2006).

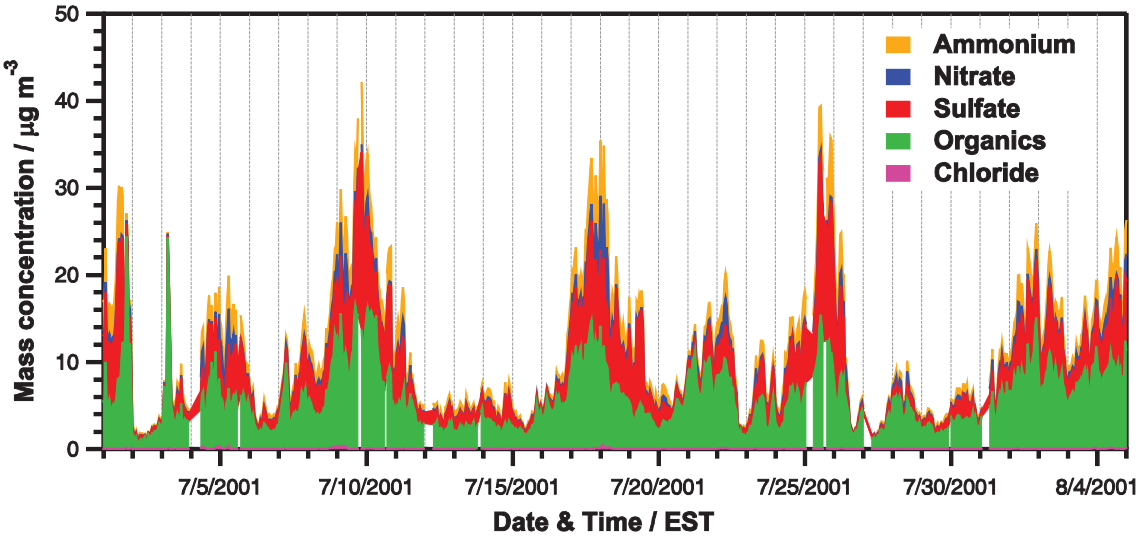

Figure 6.1-5 AMS one hour averaged mass concentration time series of nitrate, sulfate, ammonium, organics and chloride, PMTACS-NY 2001 Field Intensive Campaign, Queens College for the period 1 July- 5 August 2001.

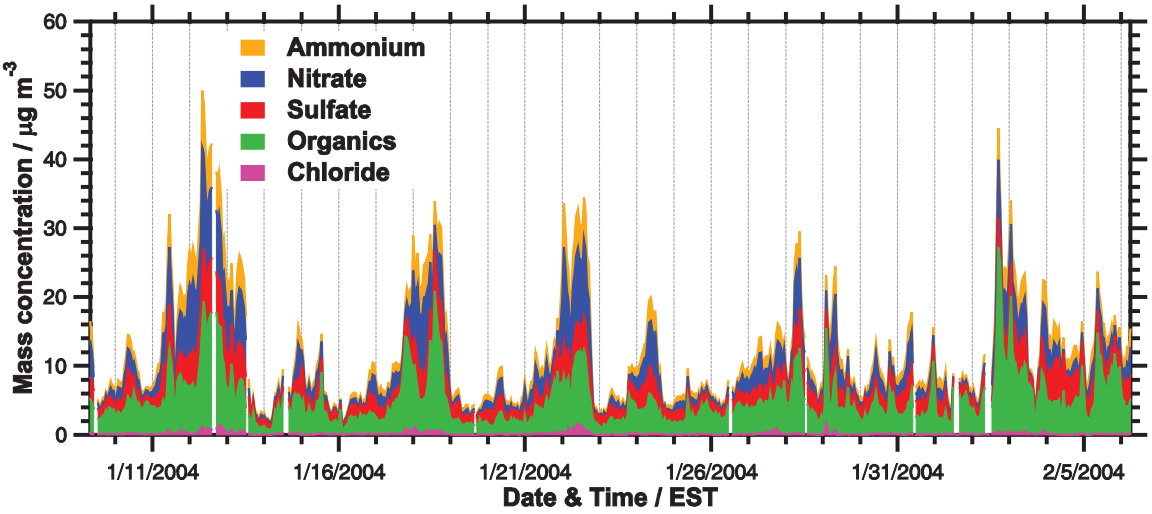

Figure 6.1-6 AMS one hour averaged mass concentration time series of nitrate, sulfate, ammonium, organics, and chloride, PMTACS-NY 2004 Field Intensive Campaign, Queens College for the period 6 January- 6 February 2004.

The PM composition time series data shown in Figures 6.1-5 and 6.1-6 indicate that both the summer and winter seasons are dominated by clean and polluted episodes lasting several days in duration and with limited diurnal variation within these events. The pollution episodes are mainly characterized by south – south-westerly wind flows under somewhat stagnant conditions, suggesting a regional contribution to these aerosol episodes with a significant local component under low wind conditions.

Summer vs. winter PM composition and size distributions

The average AMS PM composition by species over the respective summer and winter field intensive campaigns in Queens, NY, are presented in a pie chart format in Figures 6.1-7 and 6.1-8. Although during these campaigns the average mass concentration of PM indicates a significantly (~45%) larger mass concentration (13 μg/m^3) in summer compared to winter (9 μg/m^3) season, this distinction is far less when reviewing a larger statistical sample of warm versus cold season data as reported from the filter based measurements (see finding 6.1-1). The seasonal compositional distributions observed from the AMS measurements and filter- based measurements are quite consistent.

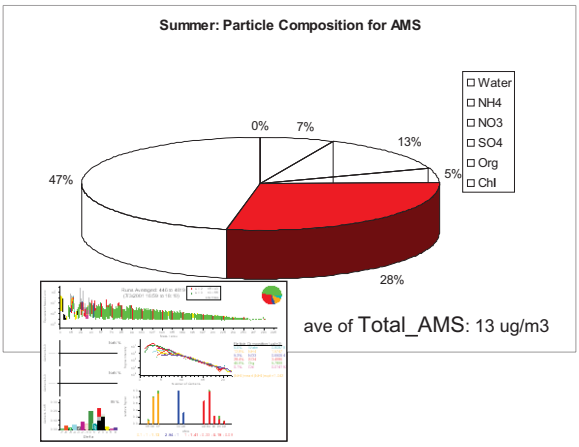

Figure 6.1-7 Aerosol Mass Spectrometer average PM composition measurements for the Queens College 2001 summer field intensive study.

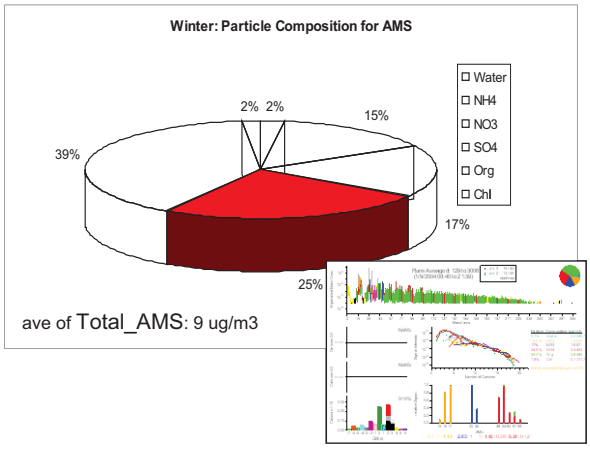

Figure 6.1-8 Aerosol Mass Spectrometer average PM composition measurements for the Queens College 2004 winter field intensive study.

Finding 6.1-3: *Seasonal composition differences observed based on AMS measurements during intensive field intensive campaigns are consistent with seasonal composition differences observed from filter based measurements, but AMS measurements also show that there is significant temporal variation in the minutes to hourly averaged time scales that are likely critical to source attribution and exposure assessment studies .*

The average of the fixed site AMS size distribution measurements, as a function of composition performed during the entire Queens College Summer 2001 field intensive campaign ,are presented in Figure 6.1-9. The bimodal distribution in organic PM shown in figure 6.1-9 is indicative of relatively fresh aerosol emission, likely produced by highway traffic in the vicinity of the measurement site. Vehicle chase studies also performed during this same summer campaign, but not in the vicinity of this site, showed a strong small mode organic component, which has been associated with condensed lube oil (*Canagaratna et al*., 2004). Similar AMS measurements performed during the winter 2004 intensive field campaign are shown in figure 6.1-10. These measurements indicate a distinct shrinkage in the wintertime aerosol size distribution that likely masks the small mode organic contribution, which appears on the left shoulder of the organic distribution in figure 6.1-10.

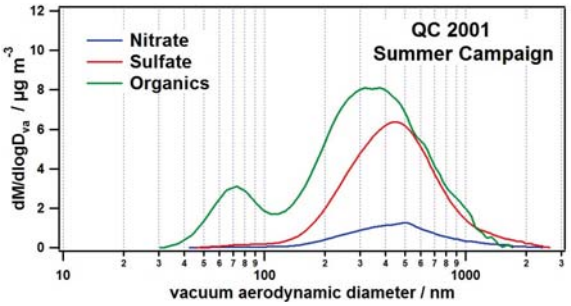

Figure 6.1-9 Aerosol Mass Spectrometer average PM composition as a function of size measurements for the Queens College 2001 summer field intensive study.

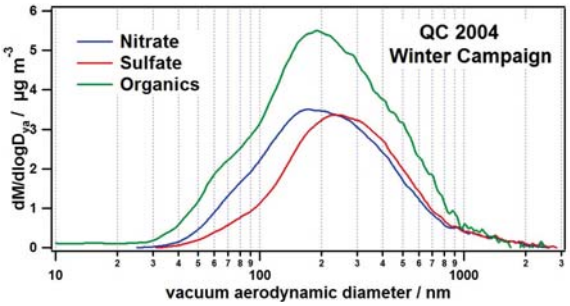

Figure 6.1-10 Aerosol Mass Spectrometer average PM composition as a function of size measurements for the Queens College 2004 winter field intensive study.

A summary of AMS measurement results from the four intensive field campaigns performed across three sites is presented in Table 6.1-1. The summary results indicated that, in addition to seasonal compositional differences, the mean mode PM mass size distributions in summer are greater than those measured in winter**.** The distinct difference in aerosol size (i.e. larger mean mode aerosol particles in summer), we believe, is the result of the accumulation of secondary aerosols by way of photochemical production. The mean mode aerosol size is also likely associated with the age of the aerosol, as particles grow in size through condensation and coagulation processes with time. A quantitative estimate of the local summer time contribution of secondary aerosol production from photochemical processes in the NYC urban environment (Queens College) is discussed in a later section of this report.

Table 6.1-1 Mean composition mass mode size from aerosol mass spectrometer measurements performed at three sites in New York State (QC = Queens College; WFM = Whiteface Mountain, PSP = Pinnacle State Park).

Mode / nm	QC 2001S	QC 2004W	WFM 2002S	PSP 2004S
Ammonium	-	200	-	480
Nitrate	400	170	400	480
Sulfate	400	240	450	490
Organics	70 and 350	200	400	490

Finding 6.1-4: *Summer vs. winter AMS compositional size distribution measurements in Queens, NY, indicated a significant shift in mean mode volume size distribution ranging from 350-400nm to 150-200nm for summer and winter, respectively. The observed difference in mean mode size distributions is likely the result of significant summertime photochemical production of secondary aerosol and its condensation/coagulation on the background aerosol (Drewnick et al., 2004ab; Weimer, et al., 2006; Drewnick et al., 2005).*

Estimates of the primary and secondary organic carbon in $PM_{2.5}$ mass.

Applying AMS data analysis techniques developed by Zhang et al., 2005, it is possible to distinguish within the total PM organic mass concentrations two classes of organic materials.

These compound classes of aerosol organics have been labeled hydrocarbon organic aerosol (HOA) and oxidized organic aerosol. HOA is thought to be predominantly associated with primary emissions (fossil fuel combustion), while OOA, which has a primary emissions component, is thought to be predominantly associated with secondary oxidized products of VOC precursors or aged photochemical HOA.

This analysis has been performed on the AMS data sets for both the 2001 summer and 2004 winter intensive field campaigns, and the results are presented in Figures 6.1-11 and 6.1-12, respectively.

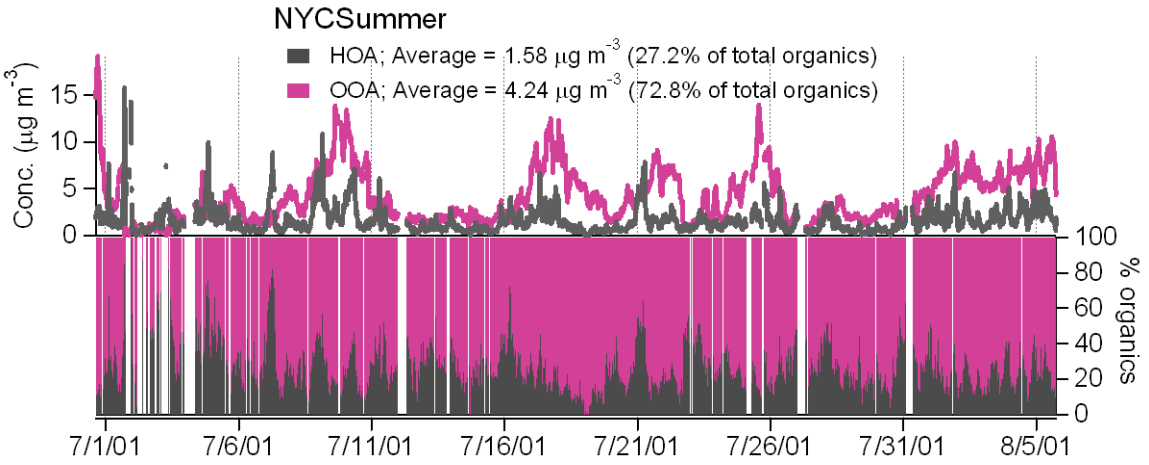

Figure 6.1-11 Time series of HOA and OOA mass and weight percent contributions to PM organic measurements from an aerosol mass spectrometer performed at Queens College in the summer 2001.

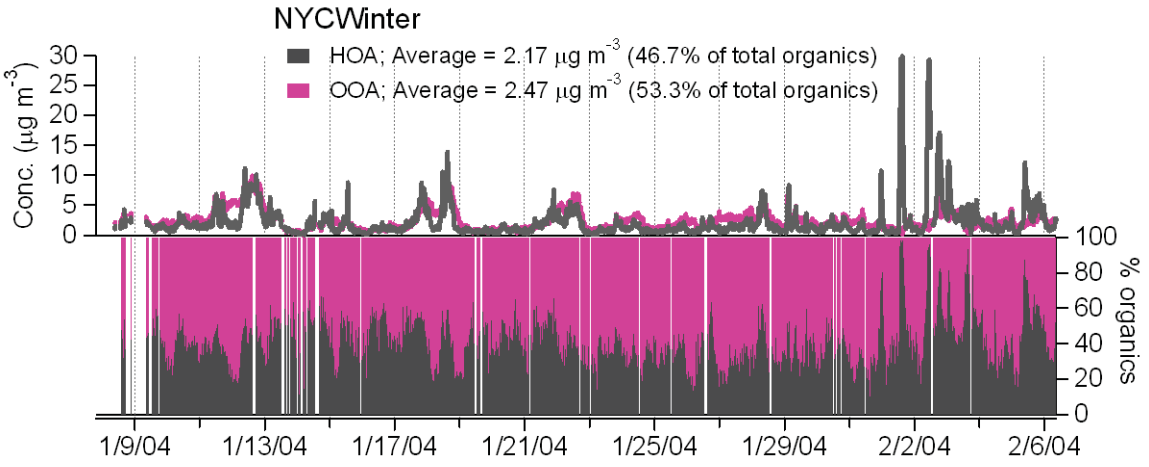

Figure 6.1-12 Time series of HOA and OOA mass and weight percent contributions to PM organic measurements from an aerosol mass spectrometer performed at Queens College in the winter 2004.

The mean contributions of the HOA and OOA for summer versus winter PM organic contributions in Queens are consistent with the hypothesis that photochemical production is a significant source of summertime OOA. The mass concentration of HOA summer vs. winter is 1.58 and 2.17μg/m^3 ,respectively. If we assume that primary emissions of HOA is

approximately constant with season(not quite true as residential heating increases and off road diesel decreases in winter), we speculate that the reduced summertime HOA is due to enhanced dilution through a higher summer time mixed layer and from the photochemical oxidation of the HOA itself. The increase in summer time OOA is consistent with the assumption of photochemical production of SOA and a likely ubiquitous increase in the regional background of OOA through cloud processing and photochemical aging of air masses.

The mass concentration of OOA summer vs. winter is 4.24 and 2.47 $\mu g/m^3$,respectively. If we assume that the winter time value represents the primary emission and regional contribution of OOA, then the incremental 1.77 $\mu g/m^3$ or ~72% increase in summer time OOA might be attributed to secondary production processes within the region. In the section to follow, we apply an independent means for estimating the production of secondary organic aerosol (assumed all as OOA) from VOC gaseous precursors based on the work by Tang, 2006 for comparison purposes.

SOA Estimates from Hydroxyl Radical (OH) – VOC Precursor Reactions

The production of secondary organic aerosol (SOA) in the atmosphere occurs when selected volatile organic compounds (SOA VOCs precursors) undergo chemical oxidation reactions to form compounds of higher polarity and molecular weight, results in lower volatility products that may then condense on existing aerosols, or in some cases, self-condense (i.e. undergo homogeneous nucleation), thereby contributing to the mass of particulate matter in the atmosphere. The secondary organic aerosol production processes involves two distinct steps: (Figure 6.1-13).

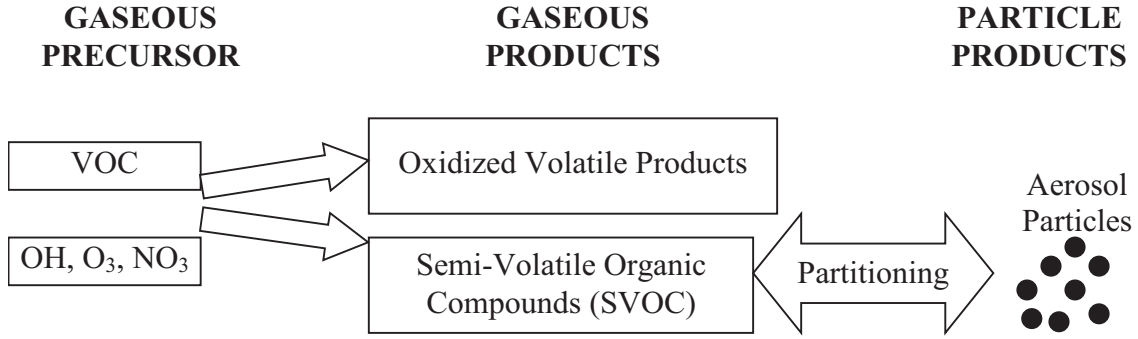

Figure 6.1-13. Oxidation of Volatile Organic Compound and its Products.

First, the precursor VOC reacts to form the oxidized, higher molecular weight, semi-volatile organic compounds in gas phase, as well as lower molecular weight, oxidized, volatile organic compounds. Second, the semi volatile organic product begins to condense, and mass is transferred from the gas phase to the particulate phase. The partitioning of the semi-volatile material is complex and depends on the nature of the ambient aerosol present (composition and surface area) in the production environment, and the production rate of the SOA. Its volatility is being of particular significance.

According to *Pandis et al.* [1992], the formation of SOA has been empirically derived and expressed by the following reaction pathway:

VOC + oxidants → Semi-Volatile Organic Compounds → Gas + Particle.

Based on this expression, a simple measure, the fractional mass yield *Y*, can be introduced to estimate the SOA formation:

$$Y = \frac{M_o}{\Delta \mathrm{VOC}}, \qquad 1$$

where *Y* (yield) is the amount of aerosol produced from the atmospheric oxidation of a specific amount of parent hydrocarbon gas, and M_o ($\mu g \cdot m^{-3}$) is the mass production of SOA produced for a given amount of VOC, ΔVOC ($\mu g \cdot m^{-3}$) reacted. The particulate phase mass production of condensable products can be roughly estimated with this single-valued yield. Obviously, yield *Y* is a dimensionless value and can be considered as the molar stoichiometric coefficient for all particle phase products. From Equation 1, M_o can expressed as

$$M_o = Y \cdot \Delta \mathrm{VOC} = Y \cdot C \cdot k_{OH} \cdot [\mathrm{Oxidant}][\mathrm{VOC}] \cdot \Delta \mathrm{time}, \qquad 2$$

where [Oxidant] ($molecule \cdot cm^{-3}$) can be the concentration of OH, O_3, or NO_3, and [VOC] ($molecule \cdot cm^{-3}$) is the concentration of precursor volatile organic compounds. C is a unit converter that converts $molecule \cdot cm^{-3}$ to $\mu g \cdot m^{-3}$. K_{OH} ($cm^3 \cdot molecule^{-1} \cdot s^{-1}$) is the rate constant of the oxidation of specific VOCs. *Atkinson and Calvert* summarized the rate constants for gas-phase reactions of alkenes, aromatic hydrocarbons with OH, O_3, NO_3 [*Atkinson*, 1997; *Atkinson*, 2003; *Calvert*, 2000; *Calvert*, 2002].

Yields (*Y*) for dozens of individual VOCs have been empirically determined in smog chamber studies by numerous researchers [*Forstner et al.*, 1997; *Grosjean and Seinfeld*, 1989; *Kleindienst et al.*, 1999; *Pandis et al.*, 1992]. Usually, the experiments are conducted in a smog chamber and are based on the oxidation of a single parent volatile organic compound. The photooxidation process is usually driven by either natural or artificial sunlight. The experiments involve simultaneously monitoring the consumption of VOC reactant and the formation aerosol product to calculate an aerosol yield *Y*.

The yields of secondary organic aerosol are relatively constant for individual precursor gases within specified temperature ranges and only depend on the reacted mass of volatile organic gases. This method does not elucidate the complex pathways, partitioning processes, and identification and quantification of the semi-volatile organic products and only considers the relationship between the reacted precursor gas and the final PM product. Using the single-valued yields [*Hoffmann et al.*, 1997; *Odum et al.*, 1996; *Odum et al.*, 1997], relative aerosol formation potentials can be estimated in a fast and efficient way.

Using the above procedures, Tang, 2006 has drawn upon the measurements of volatile organic compounds and OH radicals performed during the Queens College special field intensive campaigns to estimate the contribution of each measured known VOC SOA precursor to the PM organics mass contribution and also provided an estimate of the contributions from those unidentified species likely to contribute to SOA production.

Figure 6.1-14 provides the diurnal distribution for the summer and winter season integrated average SOA mass production as contributed by each known identified VOC SOA precursor compound. A clear distinct difference between summer and winter production (SOA production is ~ a factor of 4 lower in winter) is observed in these data and is directly associated with seasonal changes in photochemical activity, which is directly reflected in differences in OH concentrations, the main driver of the seasonal changes in SOA production.

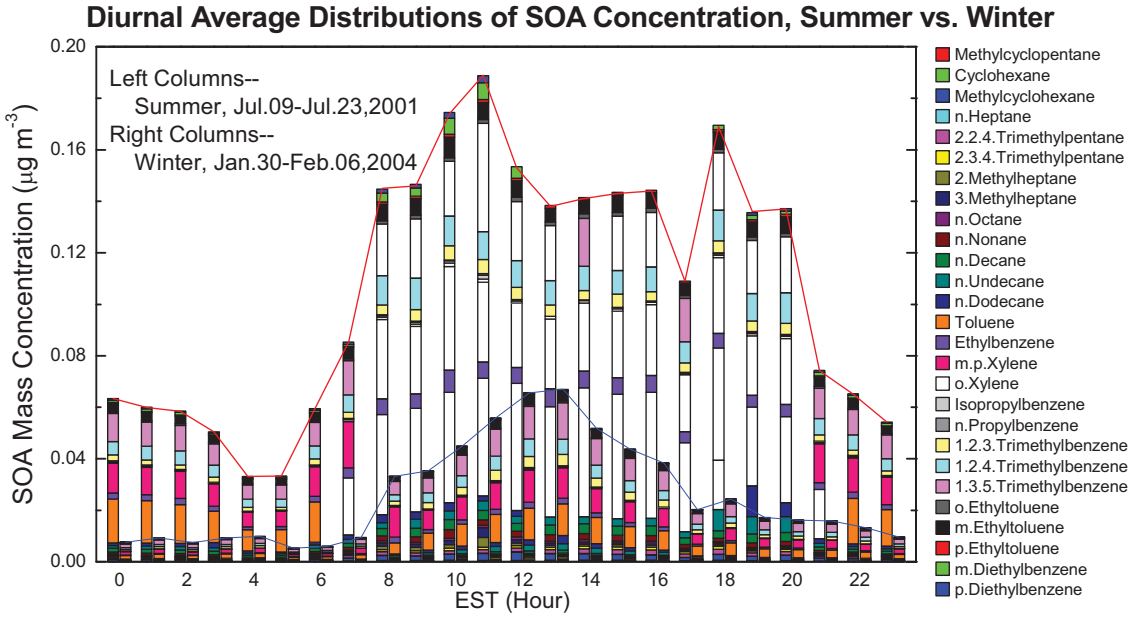

Figure 6.1-14 Diurnal averaged empirical estimate of secondary organic aerosol (SOA) production based on the reaction of measured Volatile Organic Compound SOA precursors with measured OH.

The VOC measured during the Queens summer and winter field intensive campaigns used the PAMS VOC GC measurement protocol, which is designed to measure 56 targeted hydrocarbons on an hourly basis during the O_3 season within the constrained sampling cycle (about 45 minute). The unresolved peaks observed within the analyzed chromatogram and the final unresolved peak observed with the purging of the column at the end of the analysis cycle are assigned as unidentified VOC. This unidentified VOC constitutes a significant portion ~60% (Figure 6.1-15) of total PAMS VOCs. It should be noted that the target PAMS hydrocarbons do not include biogenic terpene compounds that are known to contribute significantly to SOA formation. Also, recent studies have reported SOA formation from biogenic isoprene as well, which is measured in the PAMS suite of compounds. We plan to study the potential contribution of biogenic compounds on SOA production in urban environments in future follow-on work.

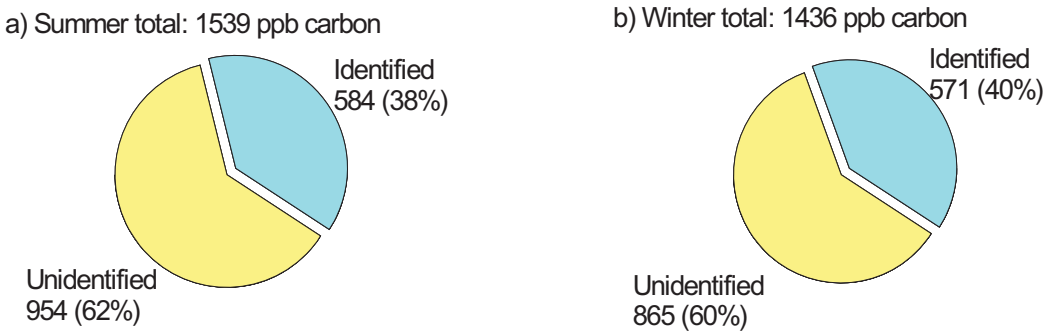

Figure 6.1-15. Fractions of daily averaged unidentified and identified precursor VOCs in two campaigns.

Excluding the low molecular weight VOCs that do not generate SOA, the total measured VOCs, considered as SOA precursor VOCs, are classified into identified and unidentified VOCs (Figure 6.1.15). The SOA precursor VOC measurements indicate minor differences in total amount and composition with season. The daily averaged SOA precursor VOC concentration was 1539 ppb carbon in summer and 1436 ppb carbon in winter. SOA precursor VOC in summer was only 7% more than that in winter.

The bulk of the unidentified VOCs are high molecular weight, slow eluting compounds that remaining on the chromatographic column prior to purging in preparation for the analysis of the next sample. The composition is associated with molecule weights greater than 10 carbon atoms [*Heard and Pilling*, 2003], or possibly more polar organic compounds, but in either case they are considered available for oxidation to generate condensable compounds. As a first approximation, we have assumed that the unidentified VOCs are molecules with an average carbon number of 10.

Since the unidentified VOC are assumed to be a mixture of higher molecular weight VOCs than that of the identified SOA precursors, it is necessary to parameterize/estimate their SOA forming ability. It is assumed that unidentified VOCs should include both alkanes and aromatics. The SOA yields and reaction rate constants of 27 SOA precursor VOCs were used to calculate the yield and rate constant of unidentified VOC. The weight of each VOC contributing to the unidentified VOC is decided from the percentage (ppb carbon) of each SOA precursor VOC in total identified VOCs. The weights in summer and winter are slightly different; therefore the aerosol yields and rate constants of unidentified VOCs are different in summer and winter. In summer, the yield is 6.4% and rate constant is 10.57×10^{-12} $cm^3\cdot molecule^{-1}\cdot s^{-1}$; in winter, the yield is 6.6% and rate constant is 12.47×10^{-12} $cm^3\cdot molecule^{-1}\cdot s^{-1}$.

Figure 6.1-16 provides the diurnal distribution for the summer and winter season integrated average SOA mass production as contributed by identified and unidentified VOC SOA precursor compound as described above. These results suggest that there is a clear and significant contribution from unidentified VOCs (i.e. unresolved GC peaks in the PAMS analysis) to the SOA production in this urban atmosphere, and although the details of these contributions remain somewhat speculative, we believe that the approximations used in these estimates are likely conservative (i.e. lower limits).

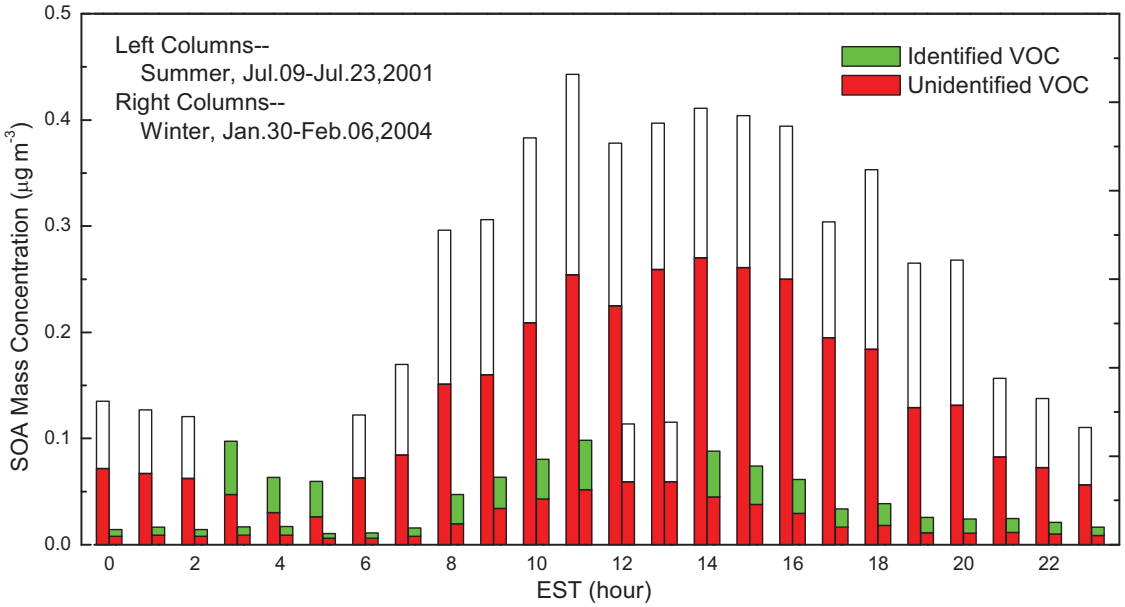

Figure 6.1-16 Diurnal averaged empirical estimate of secondary organic aerosol (SOA) production based on the reaction of measured identified and unidentified Volatile Organic Compound SOA precursors with measured OH.

The summertime carbon-based PM contributes ~47% (5.79 μg/m^3) of the PM mass; empirical estimates of the mean PM organic production based on OH+VOC measurements suggests that ~ 40% (2.33 μg/m^3) (see Figure 6.1-17) of the total PM organic carbon is generated by photochemical oxidation processes (most likely of local origin).

Summertime PM SOA contributions correlate with photochemical oxidant formation and will vary (i.e. the % SOA contributions to PM mass) as a function of the severity of the oxidant season.

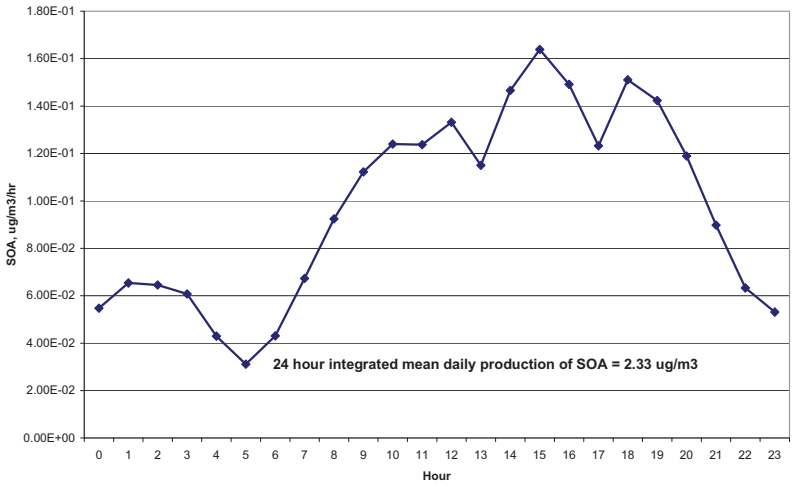

Figure 6.1-17 Mean diurnal SOA production estimates via OH + organic for all measurement days at Queens College in the summer 2001.

Finding 6.1-5: *AMS (Aerosol Mass Spectrometer) measurements observed that the summer time carbon-based PM contributes up to 45% of the daily PM mass; empirical estimates of PM production based on OH+VOC measurements suggests that ~ 40% of the total PM organic carbon is generated by photochemical oxidation processes (most likely of local origin), (Drewnick et al., 2004ab; Weimer, et al. 2005; Drewnick et al., 2005).*

Finding 6.1-6: *Summertime PM secondary organic aerosol (SOA) contributions correlate with photochemical oxidant formation and will vary (i.e. the % SOA contributions to PM mass) as function of the severity of the oxidant season. Estimates of photochemical production of SOA from the direct measurement of OH and VOC are consistent with estimates from AMS analyses that attribute PM organic carbon into Hydrocarbon-based Organic Aerosol (HOA) and Oxidized Organic Aerosol (OOA) species (Tang, 2006, Demerjian et al., 2005; Ren et al., 2003ab, 2005).*

The local production of PM sulfate has been estimated for the Queens College summer 2001 field campaign using the ambient measurements of OH and SO_2 and applying the reaction rate kinetics for the OH + SO_2 reaction. The sequence of reactions to form PM sulfate involve the rate limiting reaction step of OH + SO_2 to form SO_3 and its subsequent reaction with water to form H_2SO_4, which may react in the gas phase with NH_3 to form ammonium nitrate (NH_4NO_3) or condense on existing aerosol surfaces where it is subsequently neutralized by NH_3 or other alkaline materials contained in the aerosol. Figure 6.1-18 shows the calculated mean diurnal boxplots for PM sulfate production based on the measurement of OH and SO_2 and reaction rate constant for all measurement days (at Queens College in the summer 2001).

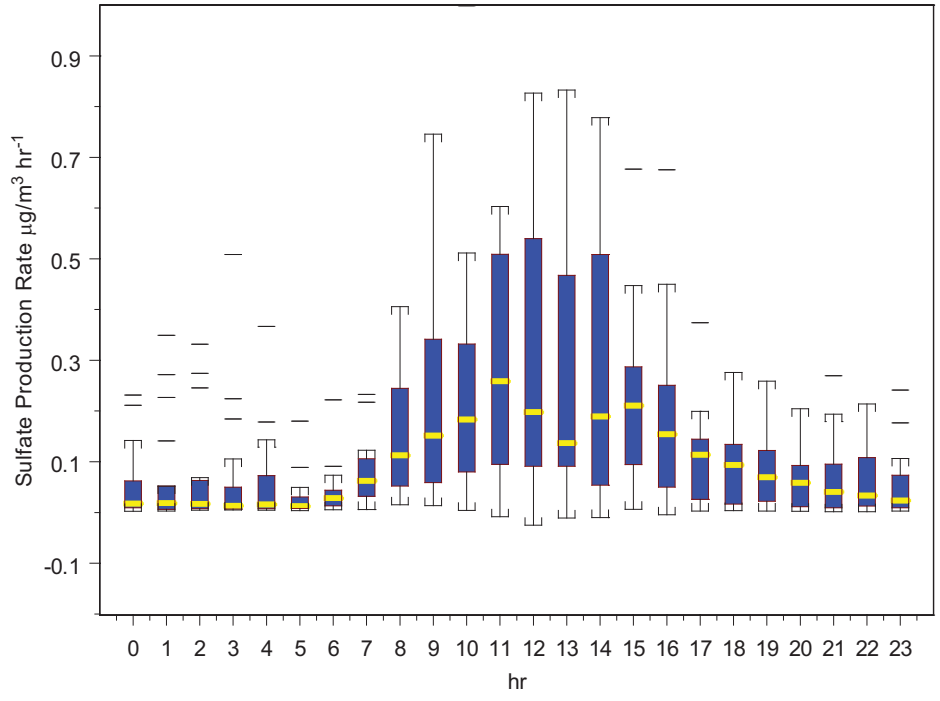

Figure 6.1-18 Mean diurnal boxplots of PM sulfate production estimates via OH + SO_2 for all measurement days (1 July until 5 August) at Queens College in the summer 2001.

Using these same hourly estimates, Figure 6.1-19 shows boxplots of the daily production of sulfate are compared with boxplots daily PM sulfate based on hourly observations from R&P8400S. In most cases, high ambient PM sulfate concentrations correlate with high production rates and indicate local contributions of > 50% of observed PM SO_4 at Queens College. High PM sulfate levels with low sulfate production rates indicate transport dominated events. A final indication of the role local photochemical sulfate production (i.e. within a diurnal cycle) can also be seen in Figure 6.1-20, which shows good correlation between PM sulfate production and the product concentration of O_3 and SO_2.

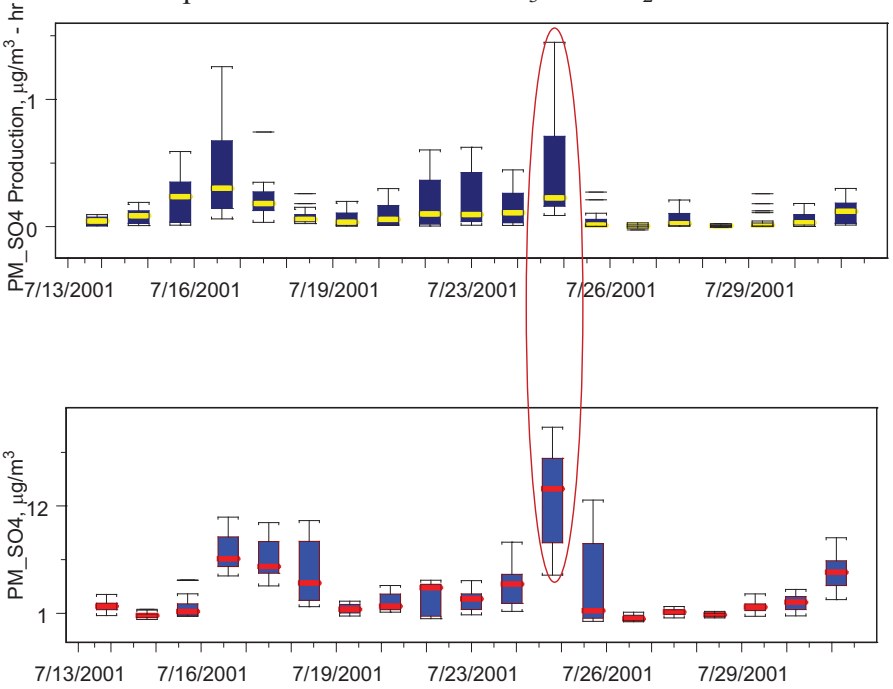

Figure 6.1-19 Daily boxplots based on hour average estimates of PM sulfate production rates (top) and PM sulfate hour average measurements (bottom).

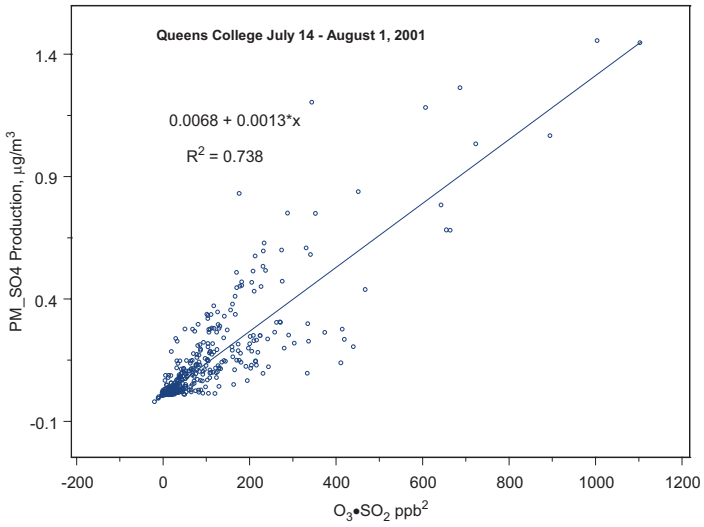

Figure 6.1-20 Correlation of PM sulfate hourly production and product of hourly average concentrations of O_3 and SO_2 at Queens College Summer 2001.

Finding 6.1-7: *Estimates of summer PM SO_4 photochemical production based measurements in Queens, NY in the summer of 2001 and reactions kinetics OH + SO_2 indicated a mean production rate of 0.14μg/m^3-hr^{-1} or 3.38μg/m^3-day^{-1}. These results indicate that 15-60% of observed PM SO_4 at Queens, NY, is generated by photochemical oxidation processes (most likely of local origin). These results are consistent with source apportionment estimates that suggest ~ 50% on average ,of the observed warm season sulfate in New York City is transported into the metropolitan region. Summertime PM SO_4 contributions correlate with local photochemical oxidant formation and the % SO_2 conversion contributing to PM SO_4 mass is in part a function of the severity of the oxidant event (Demerjian et al., 2005; Ren et al., 2003ab, 2005; Dutkiewicz et al., 2004; Kim and Hopke, 2004).*

Particle Counting and Sizing

A variety of particle counting and sizing instrumentation (both conventional and newly developed) was deployed during PMTACS-NY intensive field studies. Conventional instruments were a butanol-based Condensation Particle Counter (CPC), Scanning Mobility Particle Sizers (SMPS), and an Aerodynamic Particle Sizer (APS). The evaluation of new instrument technology performed during a Queens College, Winter 2004 field study included a "single box" SMPS and a water-based CPC and is discussed under objective 3 in section 6.3 of this report.

The CPC 3022 (TSI Inc.) measured total number concentration of particles with diameter greater than 7 nm during all intensive field campaigns. Figures 6.1-21 – 6.1-24 show five-minute time series of particle number concentrations measured during four intensive field campaigns (Queens College, Summer 2001 and Winter 2004 (QC2001 and QC2004); Whiteface Mountain, Summer 2002 (WFM2002 and Pinnacle State Park, Summer 2004 (PSP2004)).

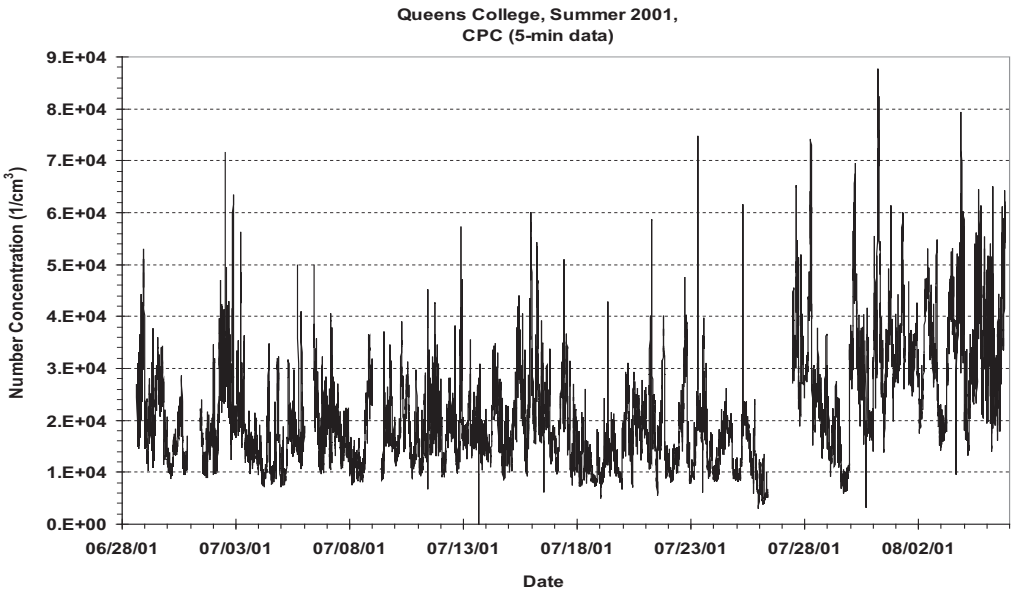

Figure 6.1-21. Time series of five-minute particle total number concentrations from the CPC during the QC2001 summer campaign.

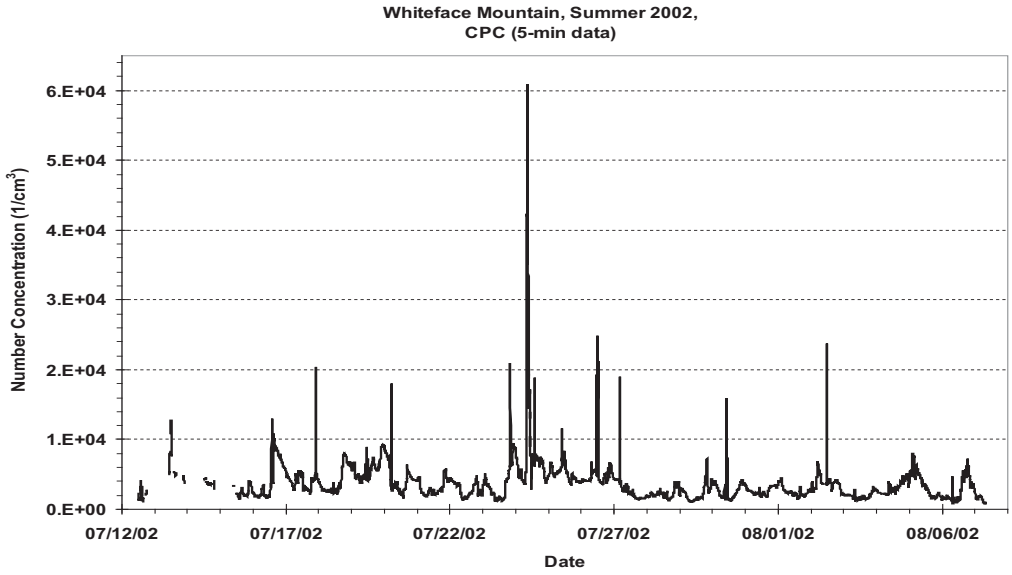

Figure 6.1-22. Time series of five-minute particle total number concentrations from the CPC during the WFM2002 summer campaign.

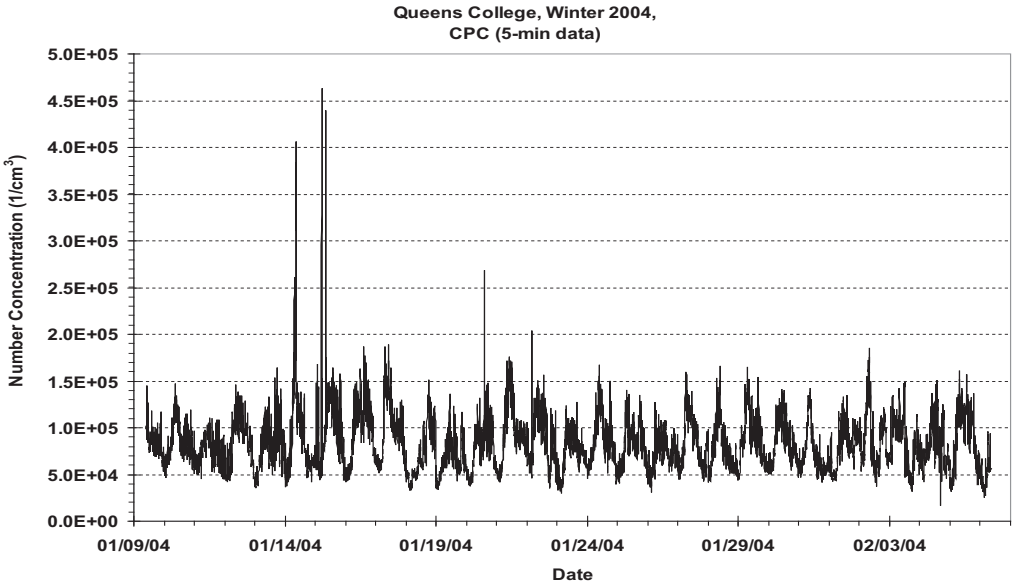

Figure 6.1-23. Time series of five-minute particle total number concentrations from the CPC during the QC2004 winter campaign.

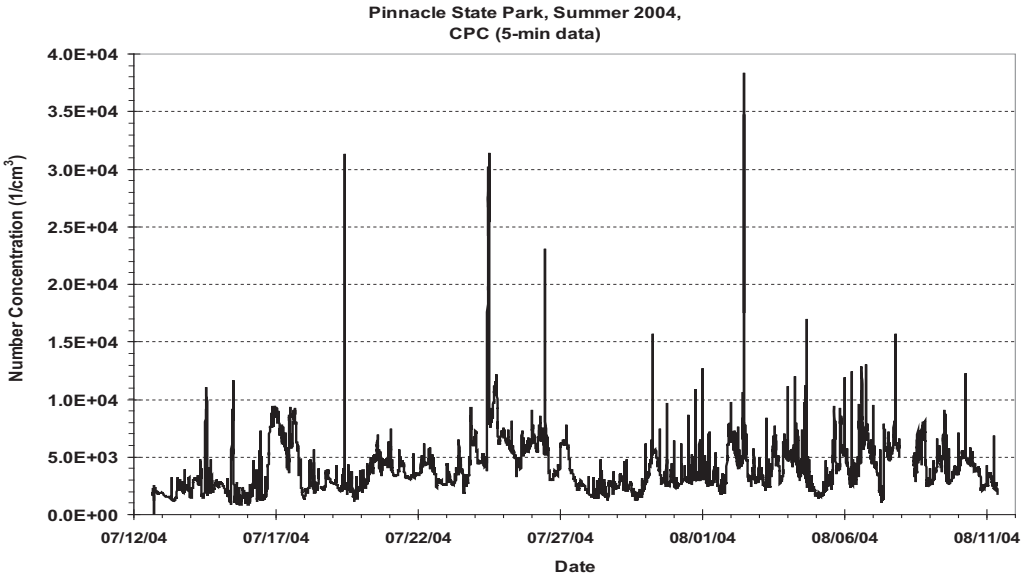

Figure 6.1-24. Time series of 5-minute particle total number concentrations from the CPC during the PSP2004 summer campaign.

During both summer and winter urban field campaigns (QC2001 and QC2004,) high total concentrations of particles were observed: during the QC 2001, particle concentrations rarely fell below 1 x 10^4 1/cm^3; during the QC2004 the "baseline" was even higher – 5 x 10^4 1/cm^3. During summer campaign particle concentrations almost never exceeded 9 x 10^4 1/cm^3, while during winter, campaign particle concentrations periodically reached 1.5 x 10^4 1/cm^3. In addition, a clearer diurnal pattern was observed during the winter study.

In contrast, during rural field campaigns (WFM2002 and PSP2004) total concentrations of particles rarely reached 1 x 10^4l/cm^3. Both rural campaigns were characterized by a presence of relatively extended "clean" periods and by much fewer short-term particle events, compared to the urban campaigns. The latter can be attributed to a much heavier traffic in urban areas. It is worth mentioning that during the QC01 the CPC 3022 was used up to July 27th, after which time it was replaced by the CPC 3025. The latter is capable of measuring smaller particles (down to 3 nm). This CPC switch can explain an increase in total number concentration measured after July 28th.

Particle size distributions - intensive field studies

A Scanning Mobility Particle Sizer (SMPS) measures the number concentration of ultrafine particles of individual sizes using an electrical mobility separation technique. The SMPS 3936 (TSI Inc.) is based on an Electrostatic Classifier (ESC), which includes a Differential Mobility Analyzer (DMA), and a butanol-based CPC. The particle size range over which the SMPS measures particle number concentrations is dependent on the type of the DMA deployed and its operating parameters. Two SMPSs were deployed during all four campaigns: a NanoSMPS (with a short DMA, upper size is slightly above 100 nm) and an LDMA SMPS (a long DMA, upper particle size around 600 nm). Exact size range is determined by the sampling flow rate.

Number concentrations of particles with diameter larger than 500 nm were measured by the Aerodynamic Particle Sizer (APS, TSI Inc.). The APS is a time-of-flight spectrometer that measures the particle number concentration and their velocity in an accelerating airflow (and thus their aerodynamic diameters). Hourly particle size distributions measured by the three instruments during the four campaigns are shown in figures 6.1-25 – 6.1-36.

Queens College, Summer 2001

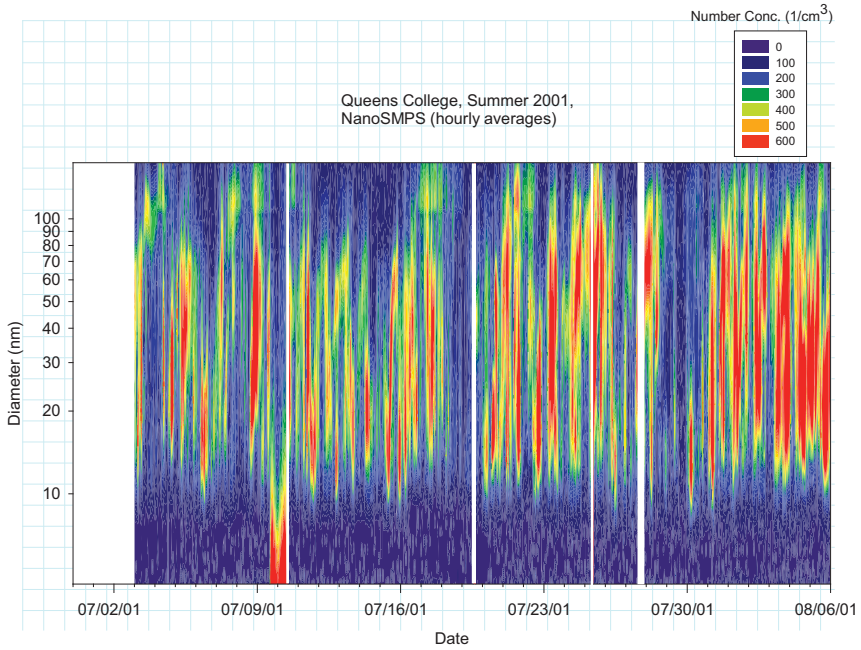

Figure 6.1-25. Time series of hourly particle size distributions from the NanoSMPS during the QC2001 summer campaign.

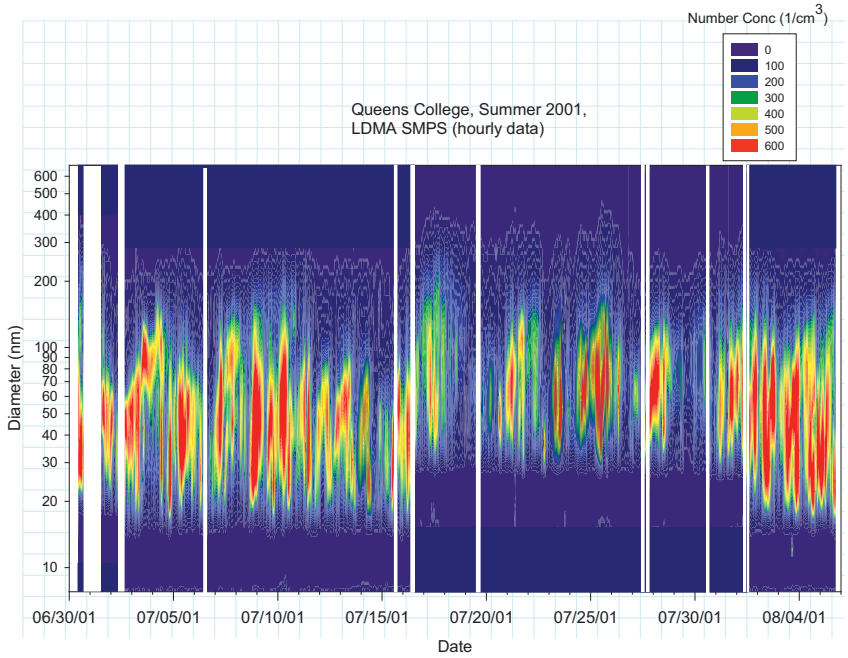

Figure 6.1-26. Time series of hourly particle size distributions from the LDMA SMPS during the QC2001 summer campaign.

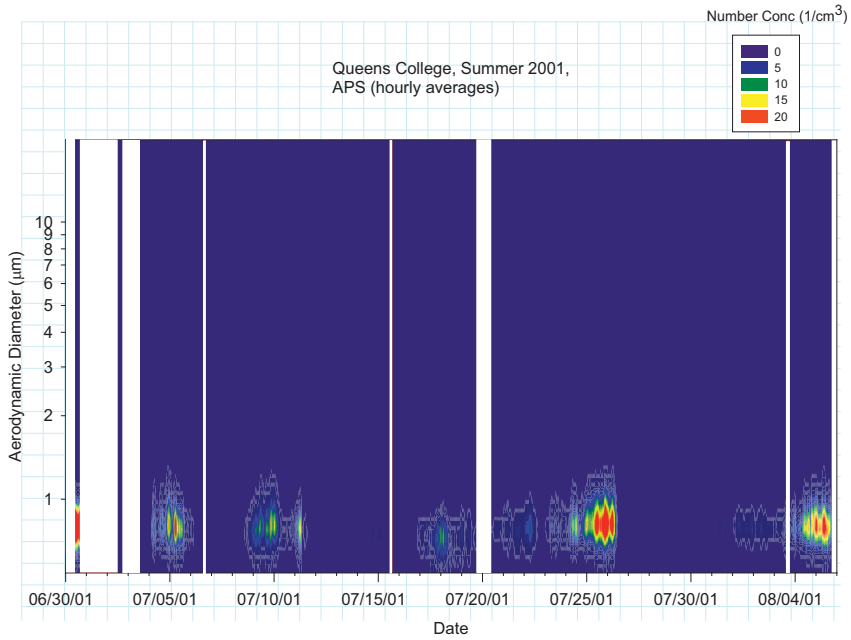

Figure 6.1-27. Time series of hourly particle size distributions from the APS during the QC2001 summer campaign.

Whiteface Mountain, Summer 2002

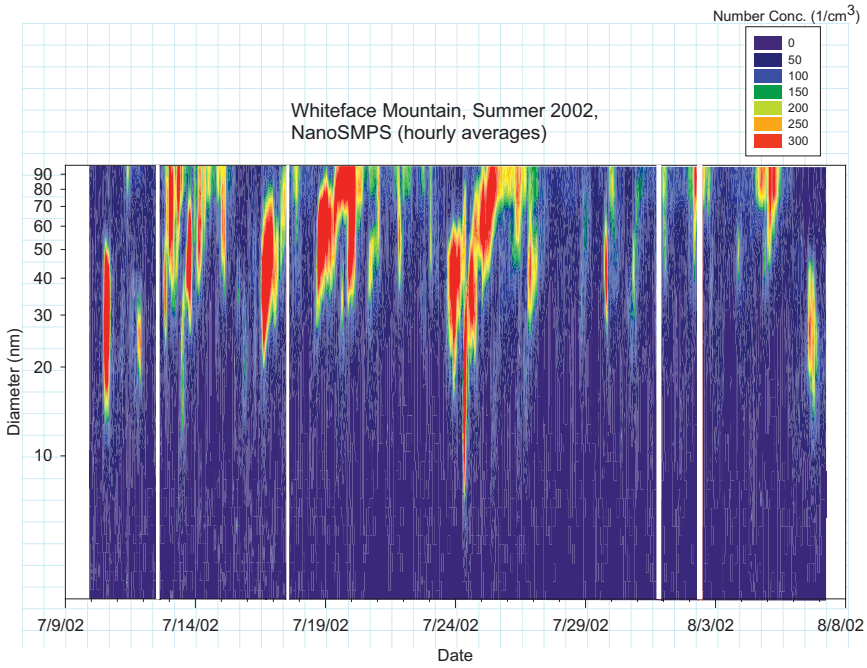

Figure 6.1-28. Time series of hourly particle size distributions from the NanoSMPS during the WFM2002 summer campaign.

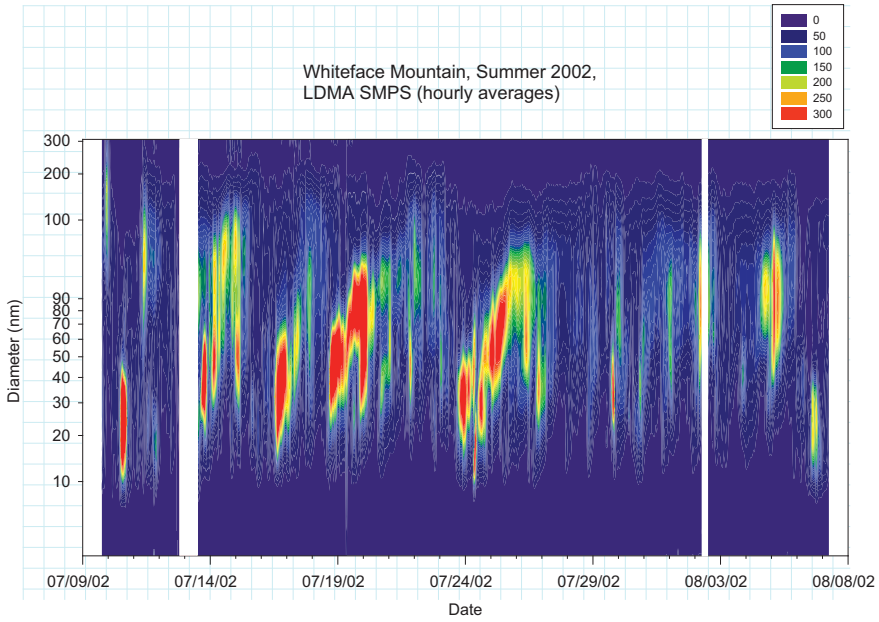

Figure 6.1-29. Time series of hourly particle size distributions from the LDMA SMPS during the WFM2002 summer campaign.

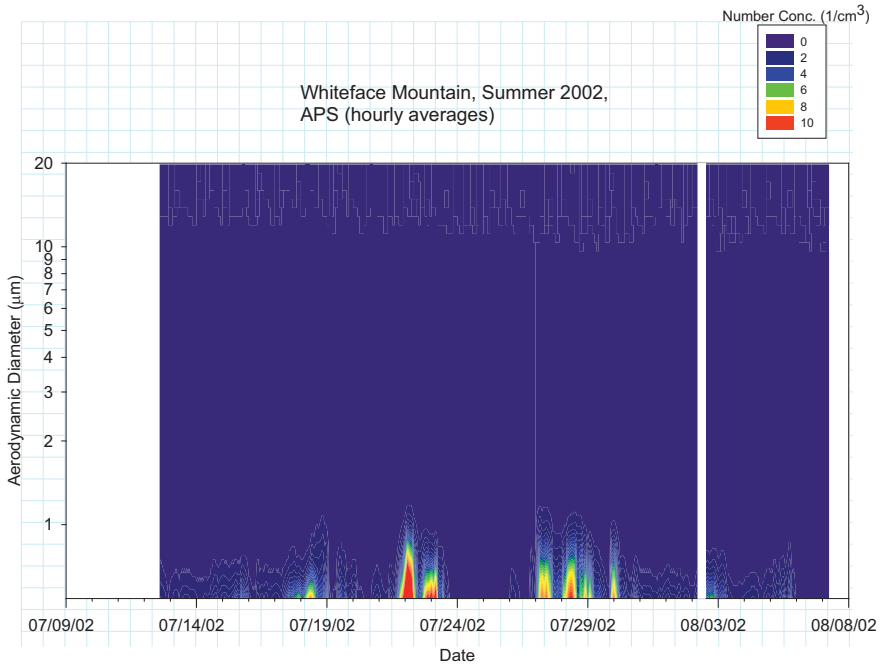

Figure 6.1-30. Time series of hourly particle size distributions from the APS during the WFM2002 summer campaign.

Queens College, Winter 2004

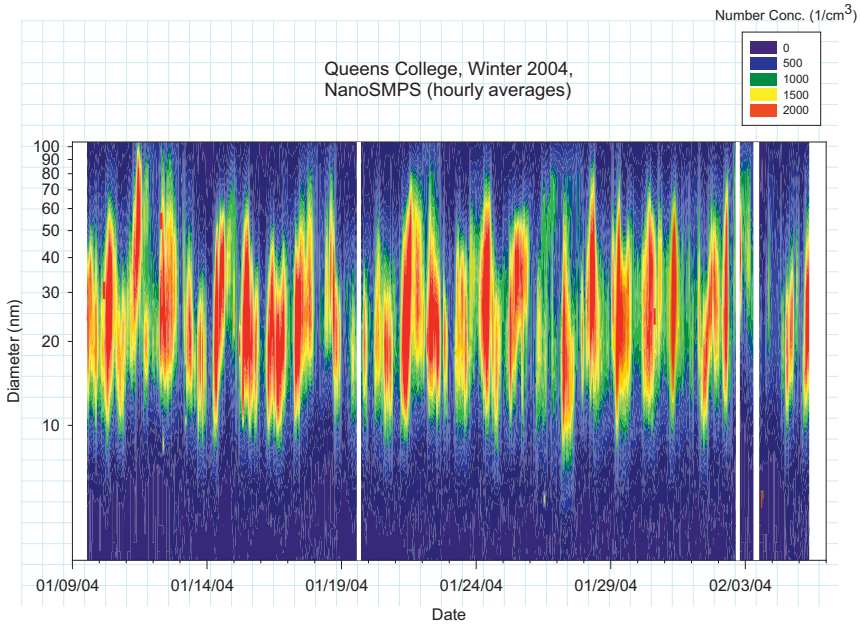

Figure 6.1-31. Time series of hourly particle size distributions from the NanoSMPS during the QC2004 winter campaign.

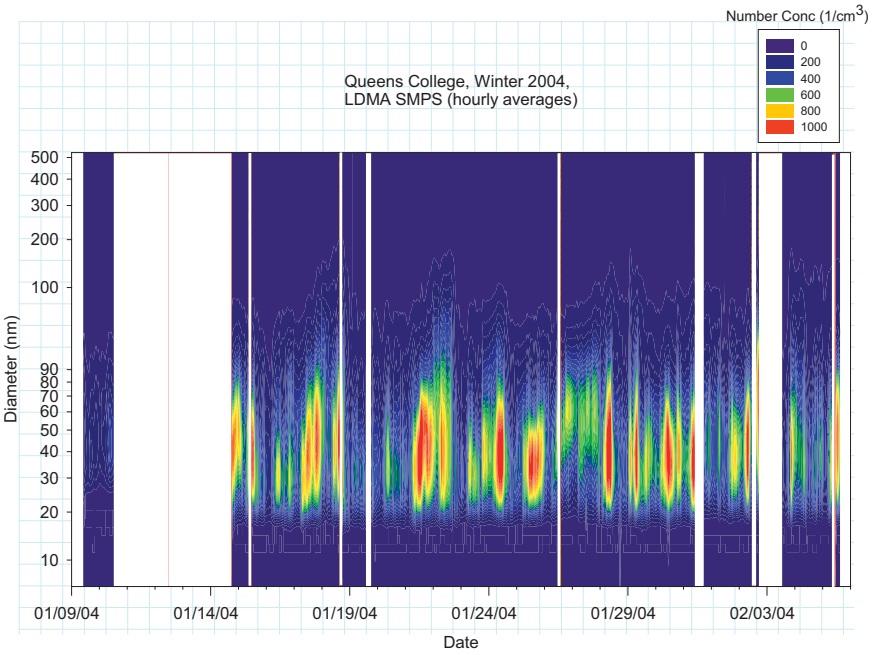

Figure 6.1-32. Time series of hourly particle size distributions from the LDMA SMPS during the QC2004 winter campaign.

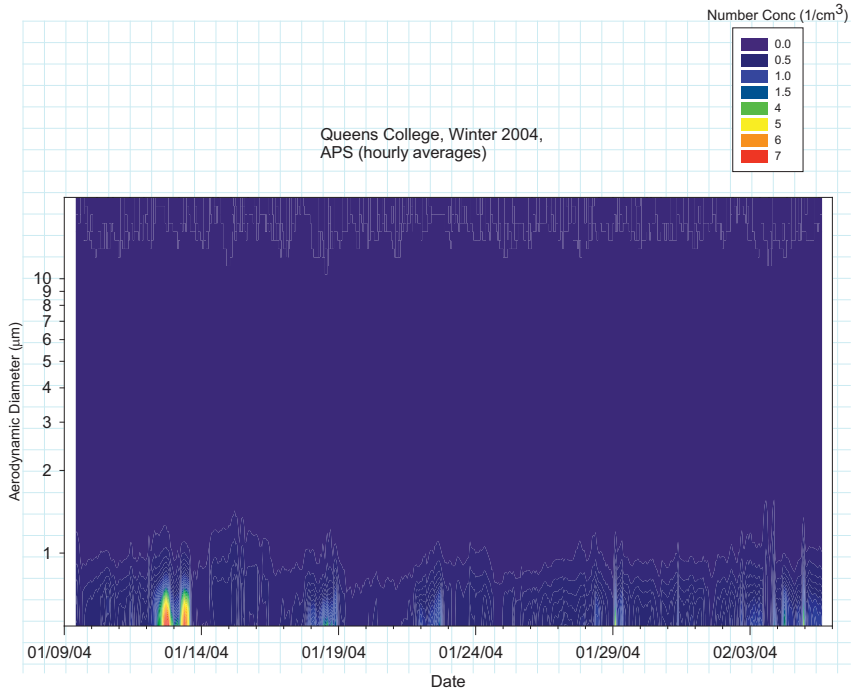

Figure 6.1-33. Time series of hourly particle size distributions from the APS during the QC2004 winter campaign.

Pinnacle State Park, Summer 2004

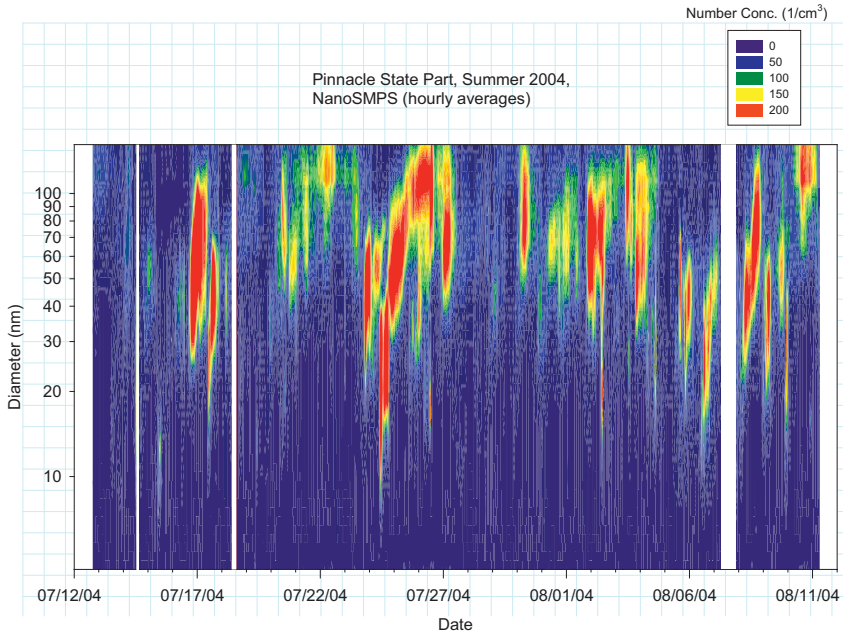

Figure 6.1-34. Time series of hourly particle size distributions from the NanoSMPS during the PSP2004 summer campaign.

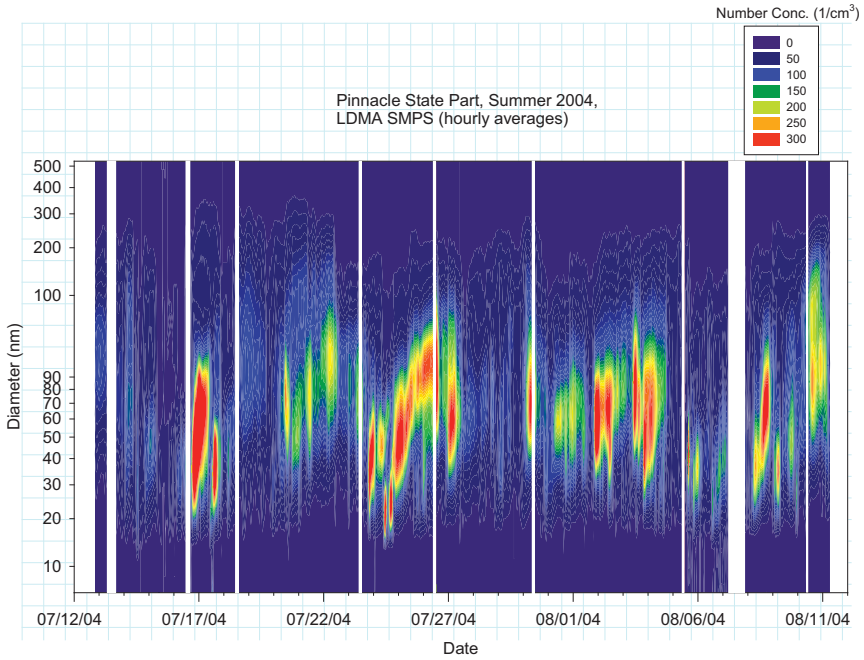

Figure 6.1-35. Time series of hourly particle size distributions from the LDMA SMPS during the PSP2004 summer campaign**.**

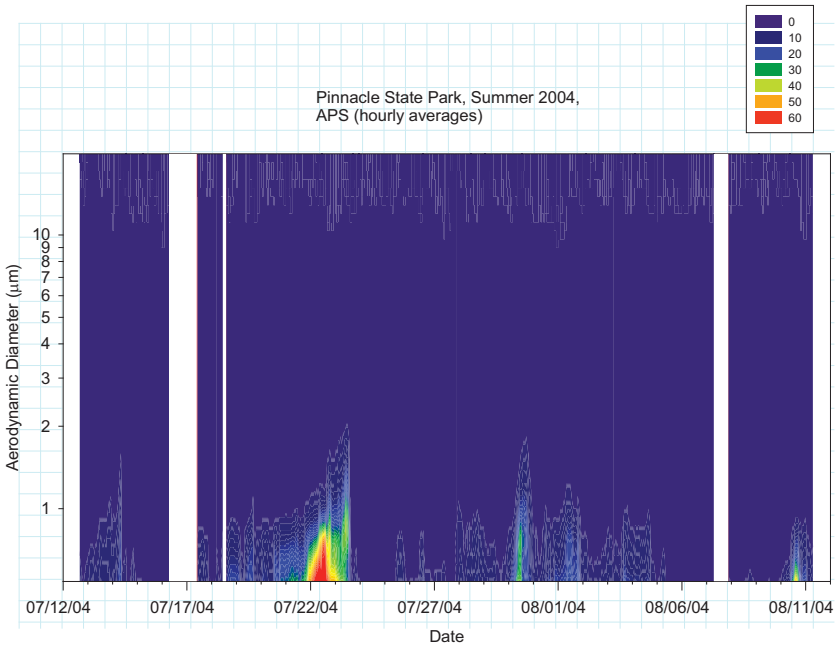

Figure 6.1-36. Time series of hourly particle size distributions from the APS during the PSP2004 summer campaign.

Size distributions based on LDMA SMPS measurements from all campaigns exhibit a persistent diameter mode. In 95% of cases, the mean mode diameter did not exceed 100 nm in urban campaigns (QC2001 and QC2004). During the WFM2002 campaign, the mean mode diameter rarely exceeded 150 nm. The PSP2004 particles were characterized by much larger size with a median mode of approximately 300 nm.

During both summer and winter urban field campaigns higher concentrations of ultrafine particles (D< 100 nm) were measured, compared to rural campaigns. While the urban winter campaign was characterized by the highest concentration of particles with D< 100 nm, the summer urban campaign was the only one when appreciable concentrations of particles with 100 nm <D < 200 nm were detected.

The highest concentration of large particle (D> 500 nm) was observed during the PSP2004 campaign. During other campaigns, number concentration of large particles in individual size bins was very small and was the lowest during the QC2004 campaign. It should be noted, however, that while being rather scarce, large particles account for a large fraction of total particle mass.

A striking feature of urban campaigns was the absence of easily detectable nucleation events. This could be related to a high background concentration of particles in Queens, leading to preferential condensation of gaseous compounds on already existing particle surfaces rather than forming new ones. Several possible nucleation events can be seen in WFM2002 and PSP2004 NanoSMPS and LDMA SMPS data time series (they are characterized by a gradual increase of particle diameter over a time period of several hours). More details on particle size distributions from the QC2001 and WFM2002 campaigns can be found in Lala et al., 2003, 2005.

Finding 6.1-8: *Particle counting and sizing measurements in Queens, NY, show little evidence of major new particle formation (nucleation) events, which suggest preferential condensation of secondary semi-volatile products on existing aerosol surfaces; only under very clean urban and rural aerosol background conditions (e.g. at Whiteface Mountain) is there some evidence of possible nucleation.*

Source Apportionment Applications

A number of methods of estimating and attributing sources of $PM_{2.5}$ and its chemical components have been applied by groups using the data obtained under this project. Dutkiewicz et al. (2004) used wind sectors and back trajectories to evaluate the regional sources of sulfate in New York State. Finer time resolution data from six-hour filter samples and AMS and PILS data averaged to six hours from the summer 2001 intensive were studied using positive matrix factorization to determine source categories (*Li et al.*, 2004). An empirical method examining ratios of mass ratios for chemical components is described and applied to New York State data by Schwab et al. (2004a). Regional and local sources affecting the New York City metropolitan area are examined using sulfate and trace metals data obtained under this project (*Qureshi et al.*, 2006; *Dutkiewicz et al.*, 2006). These authors use statistical methods and air trajectories on a seasonal basis to elucidate sources for these components of fine PM. Finally, a related project that examined more than nine years worth of data from the Brigantine IMPROVE site along the New Jersey coast used potential source contribution function (PCSF) analysis and back trajectories to examine source identification (*Kim and Hopke*, 2004). This study is included in this report because it was partially funded by the EPA Supersites award.

Dutkiewicz et al. (2004) used daily sulfate data collected under this project, in conjunction with additional data from CASTNet and an NYSDOH site, to determine the sources of fine particle sulfate at Queens, Pinnacle State Park, and Whiteface Mountain (lodge location). Figure 6.1-37 shows the wind sector analysis for these three sites during the summer of 2001. The apportionment panel of the figure shows the highest sulfate focused toward the Ohio River Valley and the Great Lakes Basin. The authors present the following three conclusions: 1) Sulfate concentrations over broad regions of the Northeast are highly correlated; 2) Human activities do not appear to contribute significantly to the $PM_{2.5}$ sulfate, since sites with grossly different population densities can have essentially the same concentrations; and 3) Based on air trajectories and on an annual basis at Queens, 44-55% of the fine particle sulfate is transported from distant sources. This value for Pinnacle State Park and Whiteface Mountain Lodge is 60%.

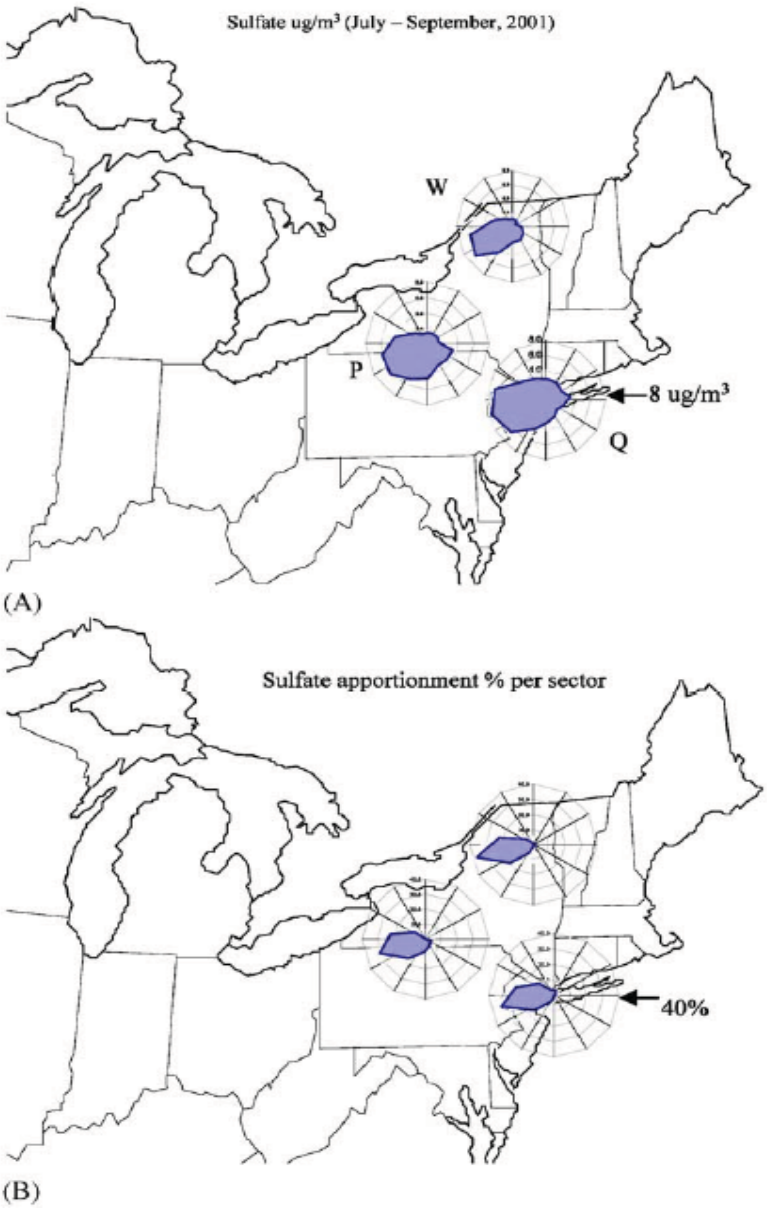

Figure 6.1-37. (A) Radial plot of sulfate as a function of the 12 sector directions (C_j) superimposed onto a map of the Northeast. The largest ring at each site is 8 μg/m^3 and there is 2 μg/m^3 between each ring. **(B)** Same as A except sulfate are normalized to the frequency of the air masses and expressed as percent. The largest ring at each site is 40% and there is 10% between each ring. (From Dutkiewicz et al., 2004).

The rich data set collected during the summer 2001 Supersites intensive at Queens College in New York City was studied using positive matrix factorization (PMF) by Li et al. (2004). Twenty-three chemical species averaged over and measured at 6-hour intervals were used in the analysis. Data for sulfate and 16 additional trace elements were obtained from six-hour integrated filters collected by the NYSDOH cyclone sampler and analyzed in their laboratory. Data for fine particle organic carbon, nitrate, ammonium, and chloride were obtained from six-hour averages of AMS data; and data for sodium and potassium were obtained from PILS-IC data. The authors identified six sources at the site: secondary sulfate with high concentration of sulfate; secondary nitrate with the presence of high concentration nitrate; motor vehicle

emissions with high concentrations of OC and zinc; road dust represented by Al, Ca, Fe, and K; sea salt with high concentrations of Na and Cl, and oil combustion marked by the presence of Ni and V. Figure 6.1-38 summarizes the results of their PMF calculations. The road dust source is larger than expected and may be due to large relative uncertainties for the elements used to identify its factor, or be due to a missing factor.

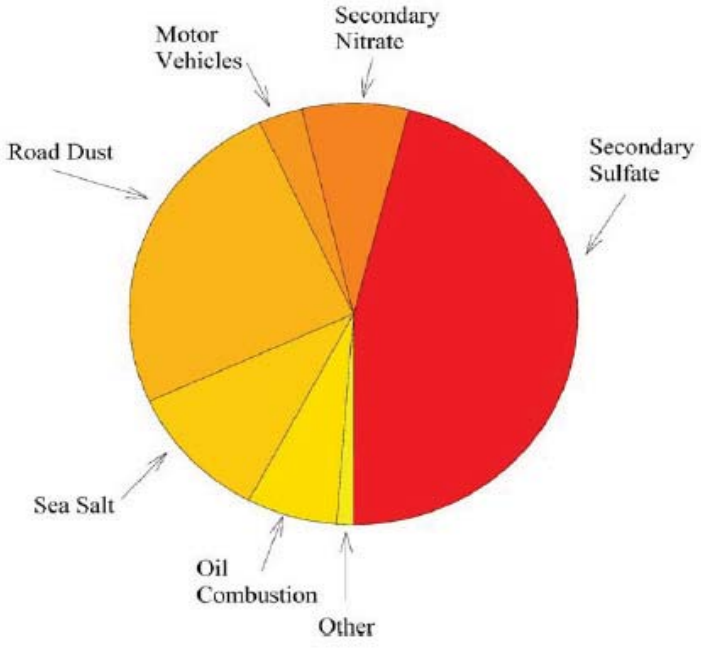

Figure 6.1-38. Averaged contributions to $PM_{2.5}$ mass concentrations measured at the Queens College site during July 2001. (From Li et al., 2004)

Schwab et al. (2004a) applied ratio analysis techniques to provide insight into the sources of selected chemical components of $PM_{2.5}$ relative to the sources of total $PM_{2.5}$ mass. This empirical method relies on 1) having data from a number of locations influenced by different sources; and 2) being able to select one of the locations as a background, or "closest to background" site. In this study, the Whiteface Mountain Lodge site was selected as the background site, and the sources of $PM_{2.5}$ to this site were assumed to be purely regional. With this designation, base ratios for the other sites (Pinnacle State Park, Rochester, and the three New York City sites of New York Botanical Gardens, South Bronx, and Queens College) are computed as seasonal averages of all selected quantities to the seasonal average of the same quantity for the same season measured at Whiteface Mountain (WFM). If the base ratio of sulfate, for example, is divided by the base ratio for mass, the resulting ratio of ratios indicates the relative variation of sulfate compared to total $PM_{2.5}$ mass. A ratio of ratios (RR) greater than 1 gives indication of sources for the selected species that are more local than the sources of $PM_{2.5}$ mass, while an RR less than 1 indicates sources that are more regional. Quantities that showed the highest RRs, and therefore the strongest indication of local sources in the New York City area, included elemental carbon (EC); iron; and a sum of first row transition metals including Ti, V, Cr, Mn, Ni, and Cu. The ratio of ratio plots for these quantities (referenced to $PM_{2.5}$ mass) are shown in Figure 6.1-39.

Note that the PSP site does not show strong enhancements of these quantities, while the New York City sites do, to varying degrees. Rochester shows summertime enhancements of EC, and year round enhancements of iron, but little or no enhancements of the first row transition metals. While this method is relatively crude, it is clearly capable of highlighting strong local sources of components or groups of components.

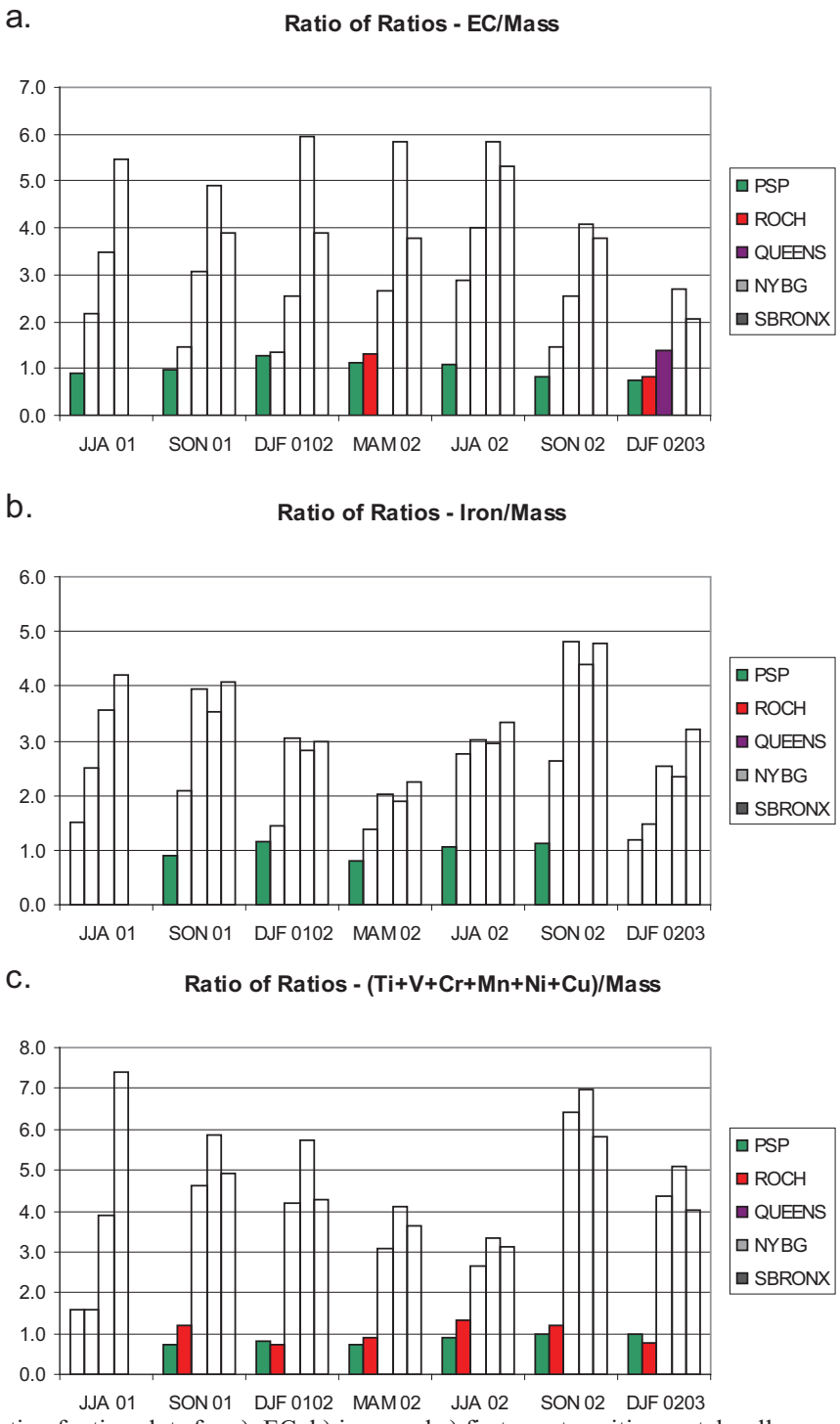

Figure 6.1-39. Ratio of ratios plots for a). EC; b) iron; and c) first row transition metals, all computed with $PM_{2.5}$ base ratios as the denominator.

The papers by Qureshi et al. (2006) and Dutkiewicz et al. (2006) are two of a series of three publications describing the instrumentation and methods used by the NYSDOH group as part of the Supersites program and some analysis of the data obtained by their group. Relevant to this discussion are the source attribution results from these studies. Figure 6.1-40 from Dutkiewicz et al. (2006) shows angular concentration profiles used in the wind sector analysis similar to their 2004 paper (Dutkiewicz et. al., 2004). Based on this analysis of data from Queens, the authors conclude: 1) selenium is most like sulfate, with a strong single peak in the westerly direction; 2) antimony and vanadium also show strong westerly components, but each showed additional influences – possibly Bronx, upstate NY, or New England for antimony, and local area sources for vanadium; and 3) nickel showed the strongest seasonal variation, with a 5-7 ng/m^3 increase in nickel mass concentrations over all directions. The authors also estimated the regional coal contribution to arsenic, lead, vanadium, and antimony based on correlation with selenium. They concluded that regional coal combustion was dominantly associated with winds from the southwest and west sectors (SW = 15, W = 18) and contributed about 50% of the arsenic, 25% of the lead, and 10-15% of the vanadium and antimony at the Queens College site.

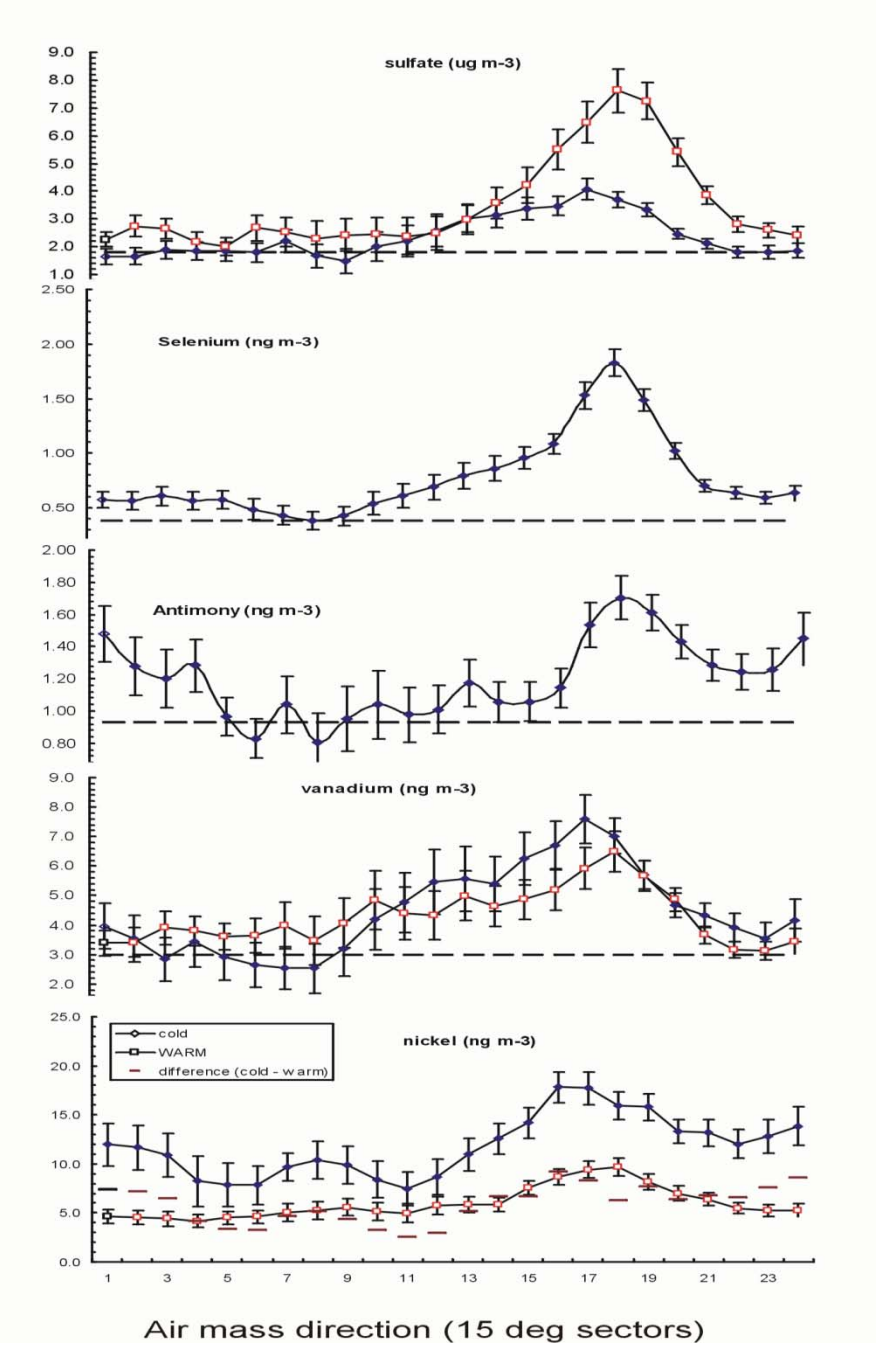

Figure 6.1-40. Angular concentration profiles (15 deg sectors, where N=1 and S=12) for sulfate, Se, Sb, Mg, V, and Ni at Queens based on air trajectories. The heavy horizontal bars in the Ni plot show the difference between the cold minus the warm season concentrations. (From Dutkiewicz et al., 2006).

The Li et al. (2004) study, using a single measurement of carbonaceous aerosol, attributed only 3.1% of the aerosol mass to motor vehicle emissions and almost ten times as much (25%) to road dust. Kim and Hopke (2004) attempted to improve upon the ability of the PMF model to identify traffic-related carbonaceous sources by including eight individual carbon fractions reported by the IMPROVE network. They choose the Brigantine site in southern New Jersey

and included data from March 1992 and May 2001. $PM_{2.5}$ mass and 35 species were used for the PMF analysis. For this data set the authors reported 11-source factors. The average contributions for the summer and winter seasons are shown in figure 6.1-41, reproduced from their paper. Averaged over the whole time period, they find a nearly 60% contribution from the three sulfate-rich secondary aerosol factors. However, in contrast to the Queens paper (Li et al., 2004), the motor vehicle factor contributes more than 15%, and the soil factor contributes less than 4%.

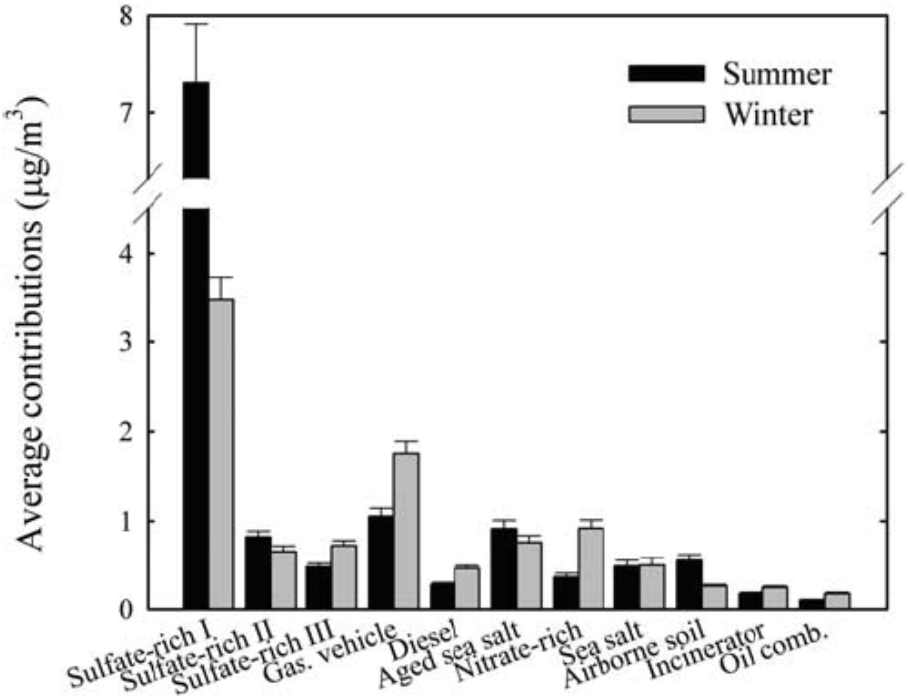

Figure 6.1-41 Seasonal comparison of the source contributions to $PM_{2.5}$ mass concentration (mean ±95% confidence interval). (From Kim and Hopke, 2004).

Finding 6.1-9: *Source apportionment techniques using speciation trends network compositional data and enhanced six-hr filter sampler metals analysis data collected during PMTACS-NY intensive field studies suggest that these methods are hampered by inconsistencies that limited their ability to resolve fuel based combustion sources (Li et al., 2004; Qureshi et al., 2005; Schwab et al., 2004a).*

Atmospheric Ammonia (NH_3) Measurements

Ammonia plays an important role in the atmosphere in the neutralization of acid gases (e.g. HNO_3 and H_2SO_4) and in the formation of aerosol particles (e.g. NH_4NO_3 and $(NH_4)_2SO_4$). Robust routine measurement techniques for ambient ammonia monitoring remain elusive. During the Queens College winter 2004 field campaign, a Tunable Infrared Laser Diode

Absorption Spectrometer (TILDAS) was deployed to measure ambient NH_3 concentrations. The fast response of the TILDAS instrument provides the opportunity to measure ambient concentrations with high temporal and spatial resolution and combined with other fast response measurements. In the case of this study, a Licor CO_2 instrument was used to characterize exhaust emissions from vehicles passing by the measurement site.

The TDLAS system employed in the field campaign was developed by Aerodyne Research Inc. and has been described previously (*Zahniser et al*., 1995; *Nelson et al*., 1996; *Horii et al*., 1999; *Li et al*., 2004a). The system consists of an optical module and an electronic module. The optical module is built on a two by four foot aluminum optical table and contains one liquid-nitrogen-cooled Dewar for temperature control of tunable diode lasers and detectors, optics for laser beam collection and transport, and one reduced pressure multi-pass absorption cell. The optical module processes the light from each of the infrared laser diodes into a pair of beams (main beam and reference beam), directing the main beam into the multi-pass absorption cell that provides a long path length of 153.50 m in a volume of 5 liter and then exiting the cell to a detector. The reference beam is sent through a short reference cell containing a high concentration of the gas of interest (in this experiment, NH_3) in order to give a high-contrast spectral signal for line position locking. A key element of the optical module is the low volume, long path length Astigmatic Herriott multi-pass absorption cell [McManus et al., 1995], which with high speed pumping achieves fast time response (> 1 Hz) and reduces the pressure broadening of the absorption lines by operating the absorption cell at 25 torr sampling pressure across the inlet orifice. A schematic of the TILDAS system is shown in Figure 6.1-42.

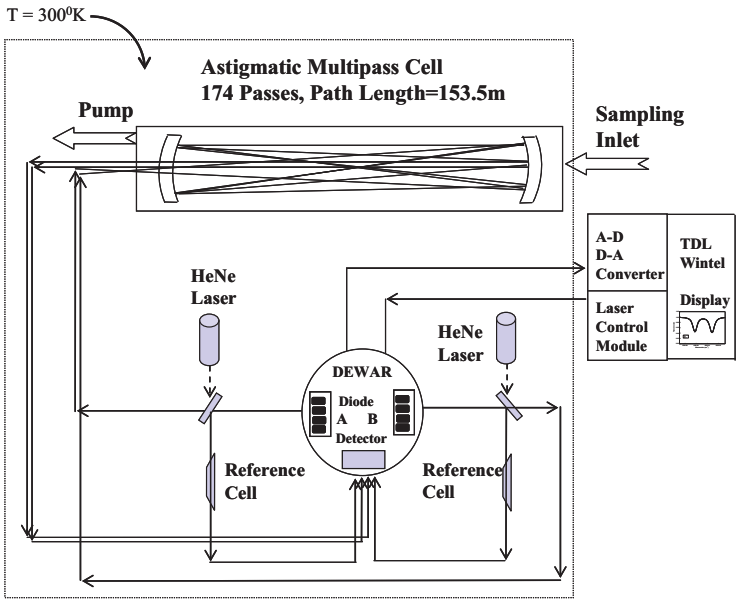

Figure 6.1-42 Schematic of Tunable Infrared Laser Diode Absorption Spectrometer (TILDAS) *(Li et al., 2004a).*

The electronics module comprises a fast computer with two data acquisition boards (National Instruments) and a dual laser control unit (Laser Analytics, Inc.). The electronics module controls the laser diode frequency and processes the detected absorption signals to return trace gas concentrations. Both of these functions are controlled via a Windows based TDL Wintel

data acquisition program. The computer sends commands to the laser controller, which in turn adjusts the laser diode temperature and average current and provides a fast ramp sweeping the laser frequency across the trace gas absorption feature. The laser light exiting from the absorption cell or the reference cell is detected and converted to electrical signals digitalized by a fast data acquisition board. As the laser frequency is swept across the spectral feature of interest, TDL Wintel program calculates the change in absorption by fitting to a calculated line shape based on the tabulated spectral parameters, the measured sample temperature and pressure, and then yields an absolute trace gas concentration.

The strong NH_3 absorption feature at 1065.5654cm^{-1} was employed to measure NH_3 concentrations in the field campaign. In this region, three strong absorption lines at 1065.5654 cm^{-1}, 1065.5817 cm^{-1} and 1065.5943 cm^{-1} compose a distinctive triplet. The strongest line at 1065.5654cm^{-1} has an integrated cross section of 2.60 x 10^{-19} cm^2 $molecule^{-1}$ cm^{-1}. Figure 6.1-43 shows the NH_3 spectrum acquired from sampling a diluted mixture of the certified NH_3 source. In the data analysis, all three lines were included in the fitting for NH_3 concentration measurement. Fitting multiple absorption lines assures that retrieved concentrations are less susceptible to potential interferences from other species and enhances the overall specificity and sensitivity of the measurement.

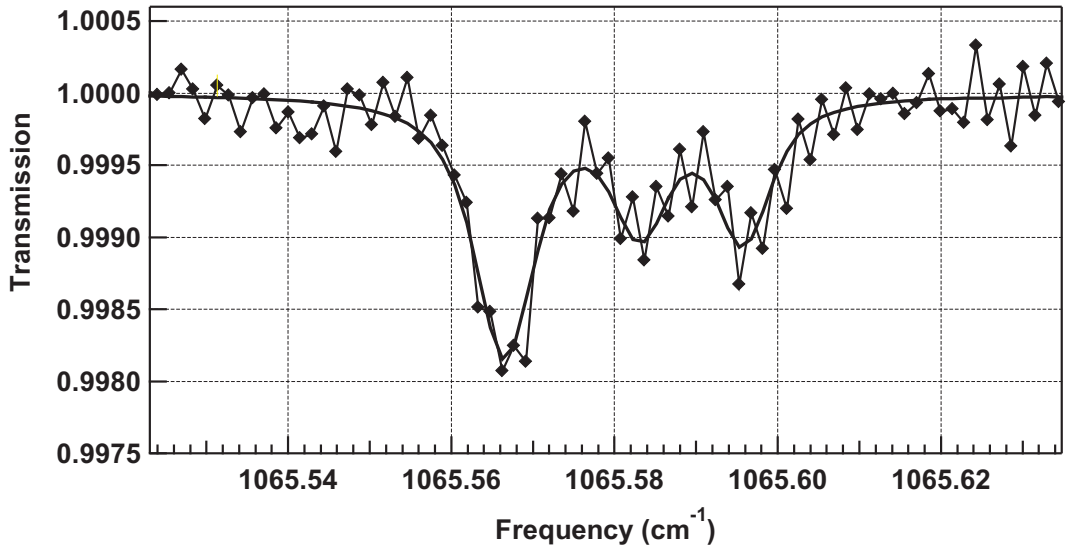

Figure 6.1-43 The one- second average NH_3 spectrum acquired from sampling the certified NH_3 source. The fitting result yields a concentration of 4.7 ppbv *(Li et al., 2006).*

The measured NH_3 ranged from below the detection limit to a maximum of 60.80 ppbv, with 70% of the NH_3 data less than 1ppb and mean concentration value of 0.76 ppbv. The NH_3 data show significant structure (spikes) in the one-second data and suggest the potential influence of local emission sources. We anticipated that this emission might be mobile source based and operated a fast response Licor CO_2 monitor simultaneously with TILDAS NH_3 measurements to look for correlations between the parameters. The measurements and the analysis performed are similar to those applied in mobile laboratory chase studies where the mobile laboratory is placed in the path of the vehicle exhaust plume, tracking and measuring exhaust components on the fly. In the fixed-site mode employed here, the mobile source plumes must pass by the

sampling site, and where we are limited by the luck of the draw in terms of types of vehicles sampled.

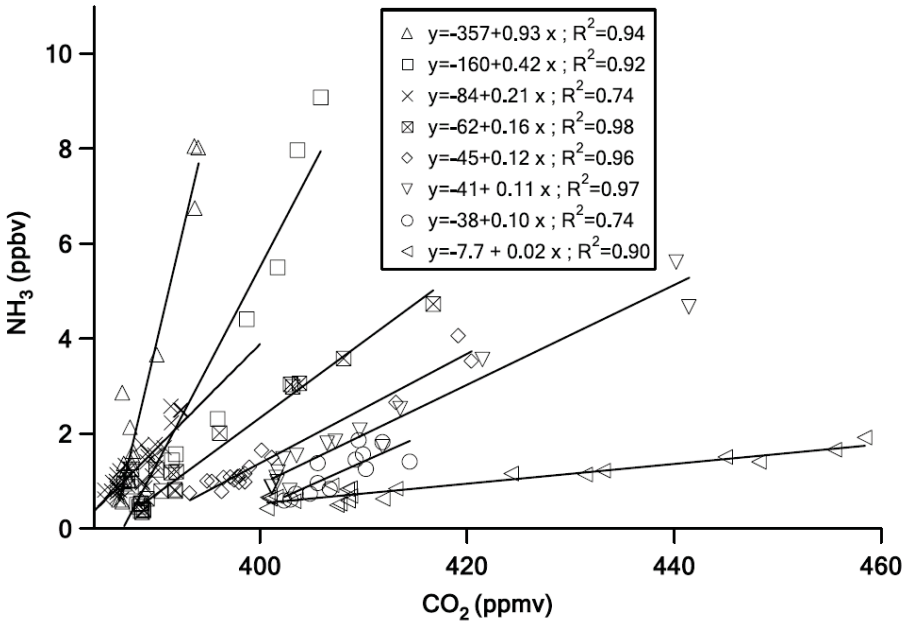

Figure 6.1-44. Scatterplots of NH_3 concentration versus CO_2 concentrations for eight plumes sampled on 4 February 2004, during the winter field intensive campaign at Queens College. Linear regression fitting parameters are listed in the box. *(Li et al., 2006).*

The NH_3 to CO_2 emission ratio varied by vehicle, as shown in Figure 6.1-44, where the linear regression of eight plumes sampled on 4 February 2004 indicates the NH_3 to CO_2 emission ratios ranged from 0.02 to 0.93 ppbv/ppmv. The highest single plume ratio observed was 2.7 ppbv/ppmv. Each plume shows a very tight correlation between NH_3 and CO_2 concentrations with R^2 ranging from 0.74 to 0.97. The observed difference in the emission ratios for individual plumes is likely associated with many parameters including engine/catalyst type, engine state (hot vs. cold), fuel type, and ambient conditions.

Finding 6.1-10: *Wintertime ambient NH_3 measurements are correlated with CO_2 vehicle emissions, but show significant variation by vehicle and are likely affected by a variety of parameters including engine/catalyst type, engine state (hot vs. cold), fuel type, and ambient conditions. These results indicate that motor vehicle exhaust is a significant source of NH_3 emissions, and its subsequent contributions to ambient NH_3 concentrations immobile source impacted urban environments. (Li et al., 2006).*

6.2 Objective 2: Monitor the effectiveness of new emission control technologies [i.e. Compressed Natural Gas (CNG) bus deployment and Continuously Regenerating Technology (CRT) –Diesel Particle Filter (DPF)] introduced in New York City and its impact on ambient air quality.

The conversion of diesel fueled heavy duty engines to compressed natural gas fueled systems or the introduction of retrofit diesel emission control technologies [e.g. Continuously Regenerating Technology (CRT) –Diesel Particle Filter (DPF)] have both been considered by NYC Transit Authority in its proactive efforts to reduce diesel emissions of its bus fleets

operating in the metropolitan area. The implementation of these technologies provided an opportunity to assess their effectiveness. Central elements of the PMTACS-NY program were to demonstrate how advanced measurement technologies could be applied to monitor in-use vehicle emissions and to document the effectiveness of these emission control technologies in reducing PM emissions (the primary main goal), and to identify other positive benefits and negative consequences that may arise as a result of the introduction of these technologies.

The Mobile laboratory used in these studies, described in detail in Canagaratna et. al., 2004, consisted of an instrumented 1989 Ford Econoline 350 (gasoline powered) box truck, with cargo dimensions with approximately 14' L x 7' W x 6' H in size, which is used to house all the instrumentation. When in the mobile operation mode, instrumentation is powered by a 5 kW gasoline fueled generator (Honda EZ5000) mounted on the rear bumper of the truck. The instrumentation package included: 1) a tunable infrared laser differential absorption spectroscopy (TILDAS) instruments using lead salt diode lasers [*Shorter et al.*, 2001; *Zahniser et al.*, 1995] for real time measurements of selected trace gases such as NO, NO_2, CO, N_2O, CH_4, SO_2 ,and H_2CO; 2) a commercial LICOR non-dispersive infrared unit provided real time CO_2 measurements; 3) a commercial TSI Model 3022 condensation particle counter (CPC) provided total number densities for particles with diameters between 10 and 1000 nm. A video camera directed out the front windshield provided a multipurpose record of the vehicles being sampled and overall characterization of the environment (e.g. traffic level, vehicle mode, and mix). A Global Positioning Sensor (GPS) provided a highly accurate record of the lab's position, while a driveshaft monitor provided an accurate measurement of the velocity of the mobile lab. Data from the individual instrument was logged on a central onboard computer, which enabled all data streams to be viewed in real-time and stored synchronously.

Mobile Lab "Chase" Experiments

A typical chase experiment entailed following a selected vehicle at a distance of approximately 3-15 m with the mobile lab, while the target vehicle drove through city traffic or through quiet neighborhoods making stops to pick-up or discharge passengers. In most cases, the drivers of the target vehicles were not aware that their vehicle's emissions were being measured, which suggested that the driving conditions and style encountered in the study can be assumed to be representative of typical driving conditions. Target vehicles were chosen randomly among heavy duty vehicles with preference given to MTA buses as characterization of this fleet was a major objective of the program. A database provided by the MTA, which contained the vehicle information such as engine type, age, and fuel, was used to categorize each MTA bus. Automated preliminary analysis of the data was used to display the results of the emission measurements in real-time on the on-board computers. Chases of an individual vehicle generally ranged from four to seven minute with the duration of a chase decided by on-board scientists. This decision was based on the measurement of a sufficient number of intense CO_2 plumes from the target vehicles or the inability to maintain the chase due to vehicle cut-offs and heavy traffic. The start and end points of the chase together with notes on the drive conditions and pertinent chase details were written to text files and automatically tagged with the appropriate time for later use during data analysis.

Synthesis of Vehicle Chase Event Data

The term "vehicle chase event" refers to the entire time period during which a single target vehicle was chased by the mobile lab. The calculation of volatile $PM_{1.0}$ emission indices for a single vehicle begins with the synthesis of the time trends of continuously measured AMS data together with the other data collected on the mobile lab during the chase event for that particular vehicle. Figure 6.2-1 shows the AMS time trend of total volatile PM as well as analogous trends in the one-second measurements of CO_2 mixing ratio, total particle number concentration, and mobile lab speed during a single vehicle chase event (Canagaratna et. al., 2004). The mobile lab speed is used as a proxy for the target vehicle's speed. The baseline signal levels in the gas and particle time trends represent ambient concentrations of the various species during the chase event. The sharp dips in CO_2 concentrations correspond to time periods when N_2 was blown through the sampling inlet to measure zero-signal levels for the various instruments. The peaks in the particle and gas phase signals, which usually last for approximately 10- 20 seconds, represent separate instances during the chase when the sampling inlet of the mobile lab continuously captured the single target vehicle's exhaust plume. Thus, a single vehicle chase event is made up of a series of "plume captures" that reflect the emissions of the target vehicle under a range of driving conditions.

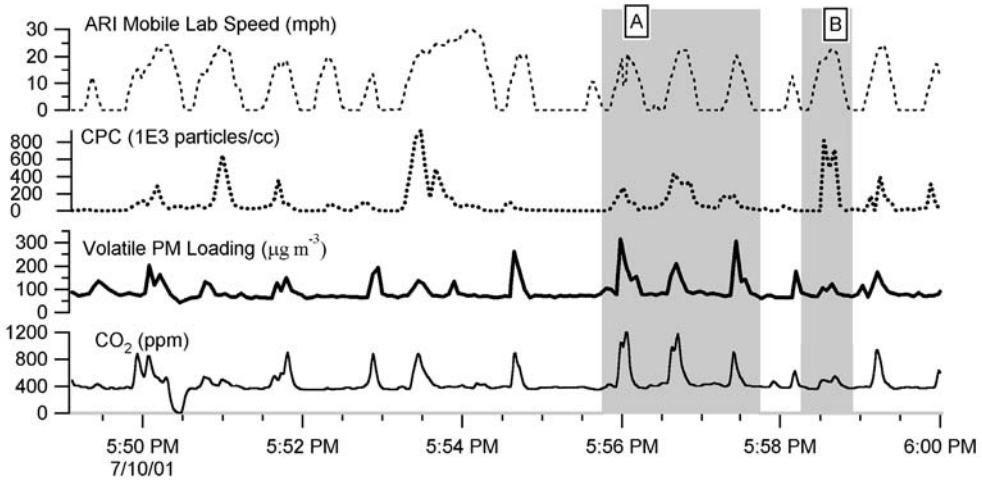

Figure 6.2-1 Example chase event while following an individual vehicle with the mobile laboratory. The volatile PM loadings are obtained with the AMS. Each peak in the CO_2 signal signifies a "capture" of the target vehicle's exhaust plume. The valleys between plume captures reflect ambient gas and PM loadings. The sharp dips in the CO_2 concentration arise from periodic N_2 purges of the inlet system that were used to measure background signal levels in the various instruments (*Canagaratna et al., 2004)*.

The correlated changes in PM and CO_2 shown in figure 6.2-1 are essential to the experiment as CO_2 is used as a tracer for the exhaust plume. The CO_2 concentration in raw gasoline exhaust, assuming a stoichiometric amount of air, is ~12.4% or 124,000 ppm. Diesel engines always operate with an excess of air, and the CO_2 concentration in diesel exhaust may range between ~ 2-3 % at low power and 10 % at high power [*Heywood*, 1988]. Typically, the CO_2 levels of the plumes sampled in this study ranged from 100 to 800 ppm, which suggests that the plume was diluted by a factor of about 100-1000 times by the time it entered the inlet of the mobile

laboratory. It is known from dilution tunnel studies of vehicle exhaust that particle mass tends to be conserved during the plume dilution process[*Kittelson*, 1998].

As with tunnel and remote sensing studies, since dilution is controlled by turbulent mixing, it is assumed that the different pollutants emitted by the vehicle are diluted to the same extent over the sampling volume and allows for the calculation of a PM emission index referenced to CO_2. This CO_2 –based emission ratio can then be converted to a fuel-use-based emission index because CO_2 emissions are proportional to fuel burned. A strict accounting of exhaust carbon species would require the addition of CO and total hydrocarbon (THC) emissions to CO_2, but it is known that for diesel vehicles these emissions are generally too small to significantly affect the carbon balance[*Yanowitz et al.*, 2000].

It is important to differentiate CO_2 plume captures belonging to the vehicle of interest from those from other vehicles. The identification of contaminated plume captures is primarily accomplished with the video images and operator notes obtained during each chase event. The video images are used to gauge the traffic level and to check for time periods in which other vehicles physically entered the space between the target vehicle and the mobile lab. Self-contamination from the exhaust of the gasoline-powered ARI mobile lab is a valid concern (especially during low mobile lab speeds), but it appeared to have a negligible effect during this study. Although self-contamination is not visible in the video images, it could be identified during diesel vehicle chases because the NO_X/CO_2 ratio in plume captures from gasoline and diesel-powered vehicles are distinctly different from each other. When contaminated plume captures are identified within a chase event, they are removed from the emission index calculation.

In addition, PM peaks that occur with no corresponding increase in CO_2 or that occur during time periods when other sources of PM could be identified in the video images were automatically removed from the chase event analysis. Differences in mass spectra and particle size distributions were also used to identify peaks in the PM mass time trend that are not due to the vehicle being chased by the mobile lab.

Calculation of Emission Ratios

The method used to calculate PM emission ratios for each vehicle chase event varied slightly between the two measurement phases of this experiment. The two methods were shown to agree within 15% with no systematic deviation.

Method 1: For the first phase of the measurement campaign the net change in PM concentration over the entire chase event relative to ambient background levels was divided by the analogous change in CO_2 to yield an emission ratio (ER) in units of $\mu g/m^{-3}$ PM /CO_2 ppm as follows:

$$ER = \sum_{i=StartTime}^{i=EndTime} (PM_i - PM_{bgd}) / \sum_{i=StartTime}^{i=EndTime} (CO_{2\,i} - CO_{2\,bgd}) \qquad (1)$$

The baseline ambient levels for each of these species were determined from time periods immediately before and after the chase event.

Method 2: The data from the summer intensive experiments were analyzed by performing a linear fit of the PM mass vs. CO_2 concentration over the entire chase event. Figure 6.2-2 shows this procedure as it is applied to the chase event data shown in figure 6.2-1. The linear fit is performed with the intercept fixed at representative ambient CO_2 and PM values for the event. Since more than 50% of the time during most vehicle chase events is spent measuring the ambient background (i.e. the valleys in between the peaks in Figure 6.2-1), the PM and CO_2 concentrations that were sampled most frequently during the chase were used as representative ambient background values for each of these species. For chase events that were short or did not have adequate time spent sampling background levels, ambient concentrations for each of these species were determined from appropriate time periods immediately before and after the chase event.

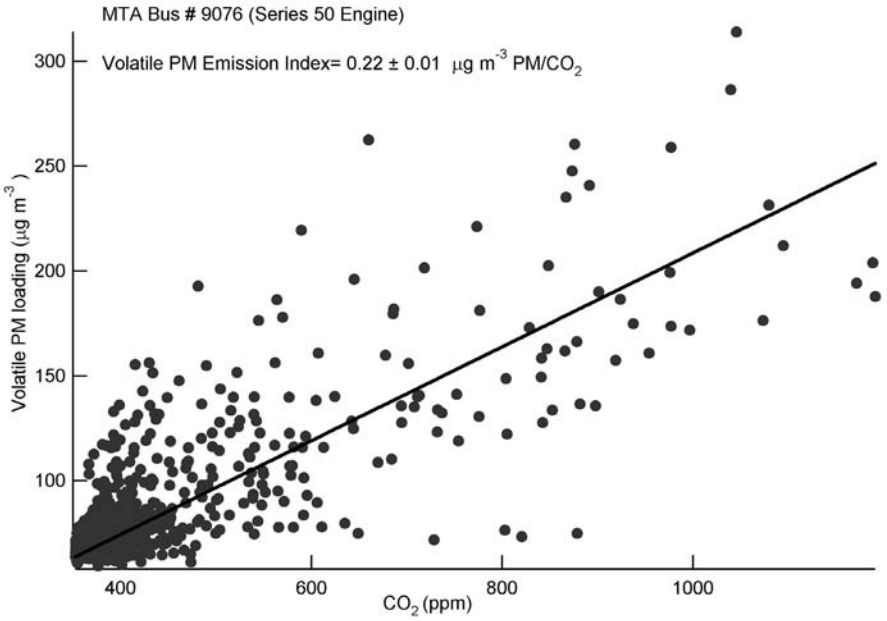

Figure 6.2-2 The correlation between PM and CO_2 signal used to obtain emission ratios in units of ugm^{-3} PM/ppm CO_2. The data in this figure is fit to a straight line passing through a fixed intercept corresponding to the ambient background PM and CO_2 concentrations (*Canagaratna et al., 2004).*

The detection limit for the exhaust plume PM measurements is determined by the AMS counting noise, from instrument and ambient background signal, at each m/z in the mass spectrum. An analysis of the noise level in the AMS time trends of total volatile PM mass and sulfate mass yields two-second detection limits of 6 μg/m3 and 7.5 μg/m3, respectively. Thus, for a typical vehicle plume capture with a CO_2 concentration increase of 400 ppm, the AMS detection limits for sulfate and total mass are 0.015 μg m^{-3}/ppm CO_2 and 0.019 μg m^{-3}/ppm CO_2. The single emission index determined from a chase event characterizes the average PM emission characteristics of the given vehicle over the entire measurement time period. For the chase event shown in figure 6.2-1 and analyzed in figure 6.2-2, for example, the fitted emission index is 0.22 μg m^{-3}/CO_2 with an uncertainty of 5%. The emission index values obtained for all vehicle chase events in this study had uncertainties that ranged from 2%-9%. While measurement noise contributes to this uncertainty, some of this variability in the emission index

for a given vehicle may be a function of variations in instantaneous driving conditions during the chase event. In the chase event shown in figure 6.2-1, for example, there appears to be an alternation between high particle mass and high particle number emission regimes during vehicle operation. This effect can be seen when comparing the time trends of total particle number concentration determined from the CPC with the trends in AMS mass concentration in sections A and B of figure 6.2-1. The low correlation between the AMS and CPC signal intensities in these sections can be explained by the fact that while the CPC particle number measurement is most sensitive to changes in the number of small (5-50 nm) particles, the AMS particle mass measurement is sensitive to changes in the number of larger (50-500 nm) particles.

The emission ratios (ER) that are obtained in units of μgm^{-3} PM/ppm CO_2 can be converted to emission indices (EI) in the more standard units of g PM/kg fuel by multiplying them by a factor of 1.77. This factor is derived by using the following equation:

$$EI = (ER/490.8)(10^3)\,(W_c) \qquad (2)$$

where the division of the emission ratio by 490.8 is used to convert the CO_2 concentration from units of ppm to units of μg of carbon m^{-3} ,and a W_c is the weight fraction of carbon in diesel fuel. A typical W_c value of 0.87 is used in the calculations[*Heywood*, 1988; *Kirchstetter et al.*, 1999].

Results of all the emissions ratios calculated and categorized by vehicle type are summarized in figure 6.2-3. The height of each bar denotes the average emission ratio calculated over all the relevant chase events that represent the particular vehicle class, while the error bar represents one standard error of the mean. The vehicle classes are broadly categorized as MTA buses, non-MTA buses, and other heavy-duty vehicles. Within the MTA fleet, buses were divided into diesel, CRT, and CNG categories, with each diesel bus further separated according to the Detroit Diesel Corporation engine model (6V-92 or Series 50) it used. The "Non-MTA buses" category consists of passenger buses used in the city that are operated by companies other than the MTA. The "other heavy-duty" vehicle category contains trucks as well as school and charter buses. The emission ratios calculated for a car emitting a large amount of blue smoke (divided by 10 to fit on the graph) and for mixed-traffic emissions in the Midtown tunnel are also presented. The reported non-refractory PM (NRPM) refers to PM components that volatize at temperature ≤ 600ºC. In this case, it is principally organic PM and does not include elemental carbon.

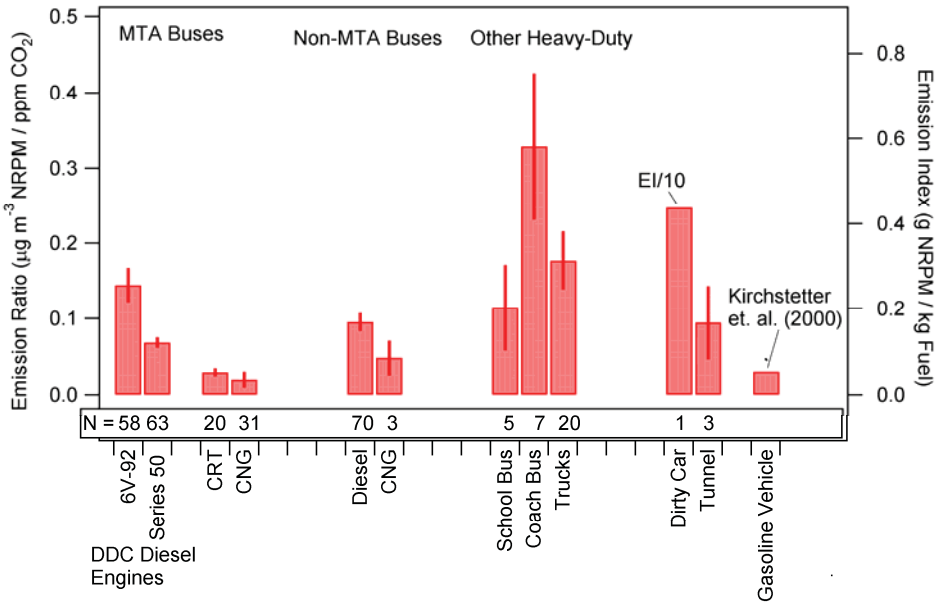

1

Figure 6.2-3 Classification of average non-refractory PM emissions by Vehicle Type. The height of each bar reflects the average emission ratio calculated over all the relevant chase events that represent the particular vehicle class. The error bar represents ± 1 standard error of the mean (*Canagaratna et al., 2004).*

Although the bulk of the vehicles sampled were diesel fueled, it is worth noting that on the occasions that CNG buses were sampled, their PM emissions were quite low and comparable to the CRT-DF equipped diesels.

Diesel and CNG Vehicle Emissions

The MTA diesel bus fleet has emissions of 0.12 and 0.25 g NRPM/kg fuel for the Series 50 and 6V-92 engine technologies, respectively. These engine models, which are manufactured by the Detroit Diesel Corporation, are widely used in bus fleets[*Prucz et al.*, 2001]. The 6V-92, a common bus engine used during the 1980s, is a two-stroke engine model. The Series 50 is a newer four-stroke engine model that has been used in buses since approximately 1993. The variability in measured emission indices of MTA diesel buses as a function of engine model year is presented in figure 6.2-4 and indicates that all model years of the Series 50 engine emit less PM than the 6V-92 models. Moreover, buses with Series 50 appear to have a smaller range of scatter in PM emissions than those with 6V-92 engines.

Recently Prucz et. al. (2001) published a comprehensive analysis of the Series 50 and 6V-92 bus engine chassis dynamometer measurements performed over the last decade. The analysis of the dynamometer data shows a reduction in the PM mass emissions and emission scatter for Series 50 engines compared to 6V-92 engines. The 50% PM mass emission reduction measured by the AMS in the current study is smaller, however, than the 70% reduction measured in the dynamometer studies. This discrepancy may be related to differences in drive cycle and vehicle operating conditions as well as individual vehicle maintenance conditions between the two studies. The dynamometer studies show a clear reduction in PM emissions as a function of year (particularly for the 1990-1992 6V-92 engines), which is not seen in this

study. It is important to note, however, that since the dynamometer analysis involved the compilation of individual measurements obtained over many years, it had better statistics than the current study. For example, each of the 1990-1992 6V-92 model engine years had an average of 100 individual measurements when compared to the 15-18 measurements obtained in this study.

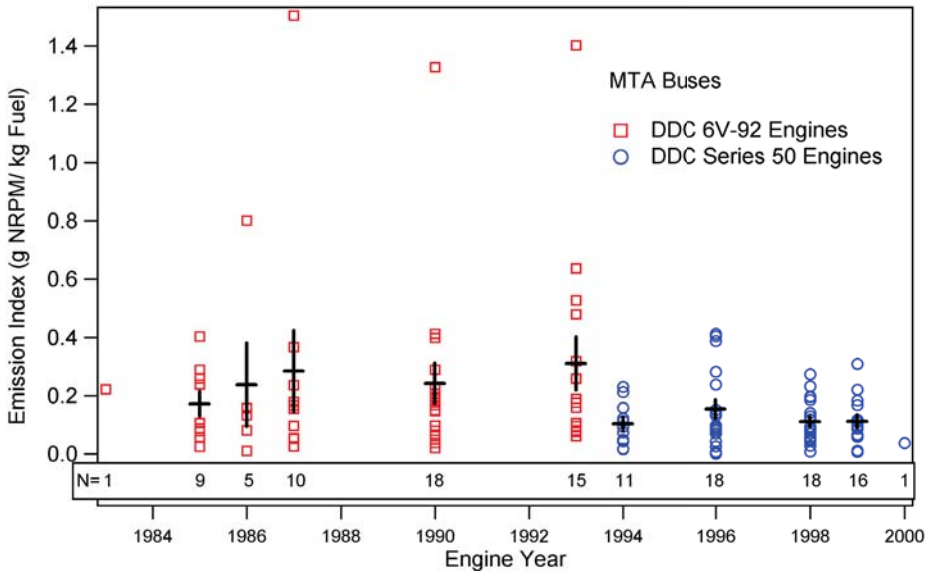

Figure 6.2-4 Comparison of MTA diesel bus emissions by engine year and model. The 6V-92 engine is an older model than the Series 50 engine. The horizontal lines show the emission index averages for each engine model year and the vertical lines reflect ± 1 standard error of the mean (*Canagaratna et al., 2004).*

Finding 6.2-1*: CNG- powered and CRT-DPF- equipped diesel buses show significant reduction in PM emissions as compared to their standard diesel counterparts (Herndon et al., 2005).*

Finding 6.2-2: *The comparison of vehicle chase study and dynamometer emissions for PM are consistent in the mean, but real-world in situ emission measurements suggest significantly more variation than dynamometer tests (Shorter et al., 2005).*

Another element of the chase studies was to identify the presence of any unexpected emission byproducts introduced by these new technologies (i.e. CNG fueled, diesel retrofit CRT-DF). Two hypotheses were posed for consideration, one pertaining to the formation of formaldehyde (H_2CO) during the combustion process in CNG powered buses, the second regarding the potential increase in NO_2 emissions in CRT-DF retrofitted vehicles as a result of NO_2 slip due to a stoichiometric imbalance in the catalytic destruction of filter trap carbon by NO_2.

Fast response gas measurements performed in the CNG -powered bus chase studies used a TILDAS instrument similar to that discussed in Section 6.1 for measurement of ambient ammonia. The instrument deployment in this application employed two IR tunable diode lasers (one for H_2CO and another for CH_4/SO_2). Figure 6.2-5 shows a representative chase study of a CNG-powered bus, with the times series of formaldehyde and CO_2 presented in the left panel

and correlation plots of these parameters in the right panel. The same analysis principals are applied as those outlined and discussed in the PM emissions calculations above. Similar analyses have been performed for SO_2 and CH_4 as well.

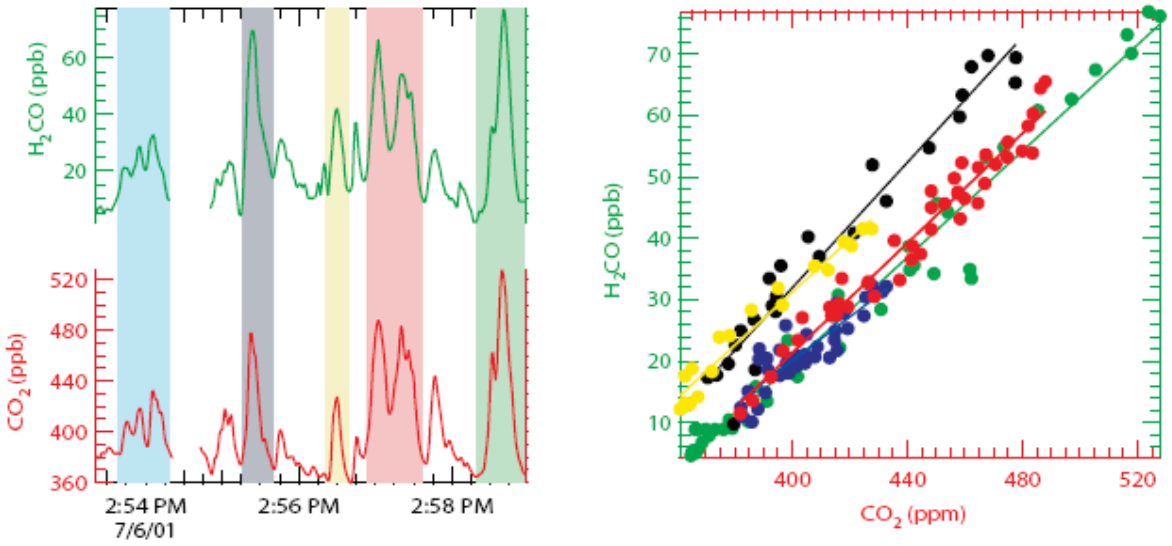

Figure 6.2-5 Time Series and Plume-by-Plume Analysis: The left panel shows the time series of measured H_2CO (upper trace-green) and CO_2 (lower trace-red) concentrations in ppb and ppm, respectively. The data were recorded while 'chasing' Long Island MTA 344, a CNG bus. Each pastel shaded region in the left panel corresponds to the darker colored sequence of points in the right panel. The gap in the time series data at 7/6/2001 14:54:20 lasting 30 seconds is due to the periodic purge, during which an excess of N_2 gas floods the sample inlet. The right panel depicts the correlation between the H_2CO and CO_2 concentrations for the various plumes identified by pastel coloring in the time series. For example the red points in the right figure correspond to the period of time shaded 'pink' in the left panel *(Herndon et al., 2005)*.

A summary of the overall findings for methane, formaldehyde, and sulfur dioxide emissions for each individual chase study event performed is shown in figure 6.2-6.

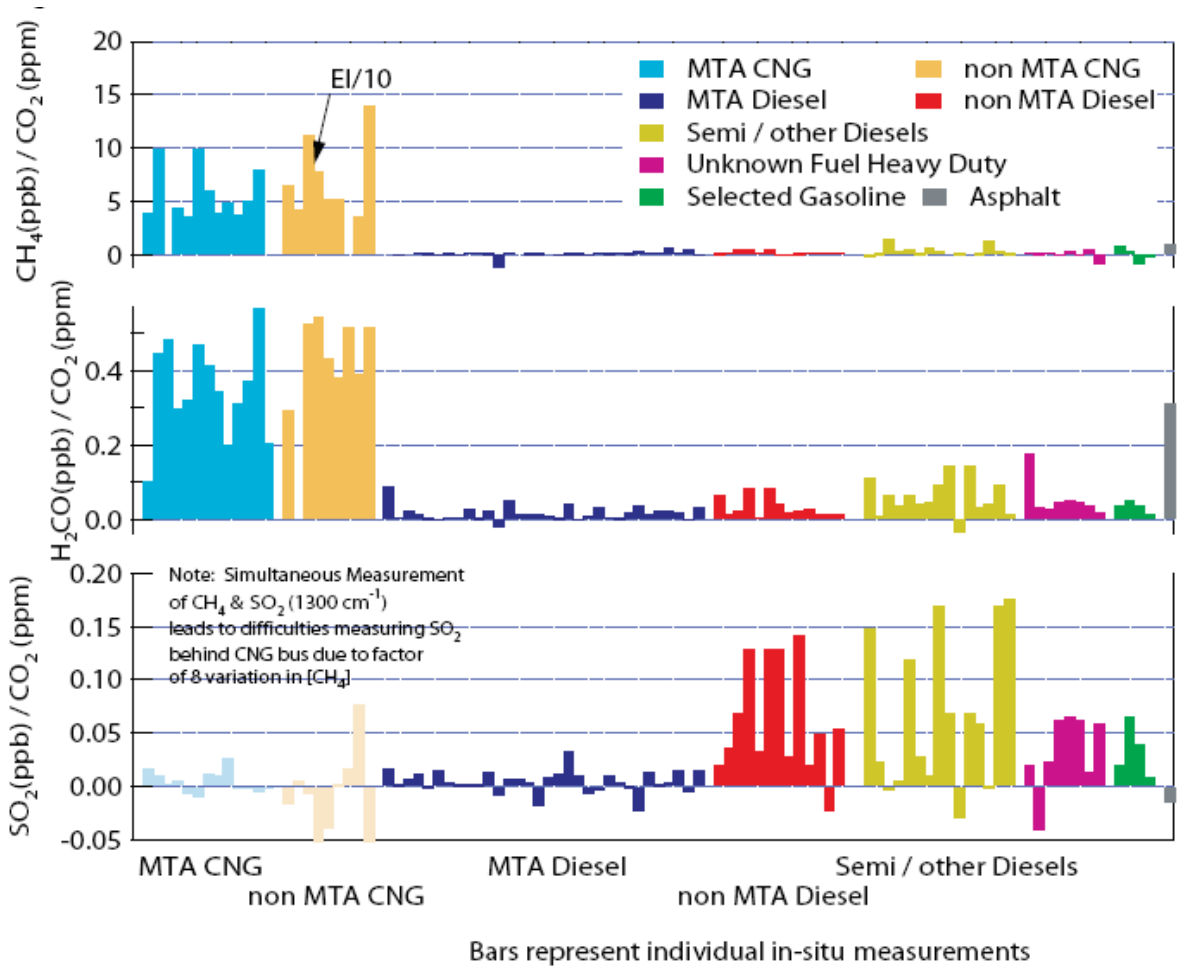

Figure 6.2-6 Molar Emission Ratios for Methane, Formaldehyde, and Sulfur Dioxide of Individually 'Chased' Vehicles. The emission ratios for CH4, H_2CO, and SO_2 determined from the chase period for individual vehicles are depicted in three different panels from top to bottom, respectively. The classes of vehicles from left to right are; MTA CNG, non-MTA CNG, MTA Diesel, non-MTA Diesel, 'Semi' and other Diesel, Other Heavy Duty, Heavy Duty Gasoline, and Asphalt Paving fumes. The results for SO_2 while chasing CNG vehicles are presented but are not considered valid due to SO_2 spectral line masking at high CH4 levels *(Herndon et al., 2005)*.

It can be seen in figure 6.2-6 that CNG- powered buses emit considerable amounts of CH_4 per CO_2 compared to the diesel buses. There is also evidence in these studies to suggest that a significant fraction of these emissions occur as a result of engine misfiring also noted in dynamometer tests (Lanni et al., 2003). Over the course of chasing 21 CNG buses on typical routes, the elevated CH_4 with no concomitant CO_2 'event' occurred nine times. The implication of these measurements is that the CNG buses chased in New York emit ~0.5% of their carbon as unburned fuel during normal operation. It is unclear from this work what the potential magnitude of these methane releases is relative to other emissions associated with CNG vehicles, such as losses during refueling, but given CH_4 significant greenhouse gas potential, a large fleet conversion to CNG would suggest careful consideration of this CH_4 emission source.

Finding 6.2-3: CNG- powered buses have significant methane emissions that are likely the result of engine misfiring and would likely require additional controls (EGR, oxy-catalyst) (*Herndon et al.*, 2005).

Formaldehyde emissions measured during chase studies were one tenth of the methane emissions on a per molecule basis. The general finding that CNG -powered buses emit high levels of H_2CO has been observed by others in chassis-dynamometer studies by *Lanni et al.* 2003 and *Kado et al.*, 2005. In the case of Kado et al., 2005, H_2CO emissions were greatly reduced as a result of the presence of an oxidation catalyst, which suggests a possible remedy for this potential toxic exhaust emission product from CNG fueled vehicles.

Finding 6.2-4: CNG- powered buses have significant formaldehyde emissions that will likely require additional controls (oxy-catalyst) (*Herndon et al.,* 2005).

In consideration of retrofitting its bus fleet with a diesel particulate trap technology termed Continuous Regenerating Technology (CRT), the New York Metropolitan Transit authority (MTA) decided to switch to ultra low sulfur fuel for its entire diesel fleet in September of 2000. Although the retrofitting would occur over several years, low sulfur fuel is necessary to protect the CRT catalyst from contamination by sulfur and maintaining separate fuel supplies was not practical. In addition, the introduction of low fuel diesel would have environmental benefits including reduced SO_2 and PM SO_4 emissions. Exhaust measurements of MTA buses using 30 ppm S fuel resulted in a bus class average of $(0.005 \pm 0.01) \times 10^{-3}$ moles SO_2 $mole^{-1}$ CO_2. In contrast, exhaust measurements of the non-MTA buses, which were burning fuel of unknown sulfur content resulted in an average of $(0.08 \pm 0.07) \times 10^{-3}$ moles SO_2 $mole^{-1}$ CO_2. It is assumed that the non-MTA buses were burning common diesel that nominally contains less than 300 ppm S. With the exception of one bus, the MTA diesel buses burning the ultra low sulfur fuel emitted less SO_2 than the non-MTA buses burning fuel of unknown specification. The MTA bus with a high sulfur emission ratio was measured during the October, 2000 measurements, and we presume that it was still using fuel from before the ultra-low sulfur switch over. The result for this bus was not included in bus class average for MTA buses.

It is important to note that the fuel specifications of 30 ppmS (ultra-low sulfur diesel) and 300 ppm S (low sulfur diesel) are regulatory limits. The actual sulfur content of the fuel delivered to the depot holding tanks is usually below the specified grade limit. The fuel used prior to MTA's program to phase in the CRT, 'low sulfur fuel' contained less than 300 ppm. If 30 and 300 ppm S fuel sulfur contents are converted to gaseous SO_2, the emission ratios for the ultra-low and low sulfur fuels are 0.013 and 0.13×10^{-3} moles SO_2 mole-1 CO_2, respectively assuming a CO_2 emission factor of 3180 g CO_2/kg fuel. This work demonstrated that both the MTA diesel and the non-MTA diesels buses have lower SO_2 emissions than would be suggested by the upper limits based on fuel sulfur content.

Diesel buses without a particulate filter exhaust (CRT) after-treatment convert over 70% of the fuel sulfur to gaseous SO_2. Though we did not observe a strong instantaneous relationship between gaseous SO_2 and particulate sulfate, the respective emission indices show a clear distinction. The gaseous SO_2 emission index and particulate sulfate loading (*Canagaratna et*

al., 2004*)* are both significantly lower for the MTA diesel buses using ultra-low sulfur diesel than the non-MTA buses burning low sulfur diesel.

Using the same fast response measurement technologies as previously discussed (TILDAS and LiCOR) chase studies were also performed to characterize the emissions of NO and NO_2 from the MTA bus fleet as well as non-MTA buses and trucks. A summary of the chase studies by vehicle type performed in this program is presented in Figure V.I.2-7, and a comparison of these emissions findings with others performed in chassis dynamometer experiments is presented Table V.I.2-1.

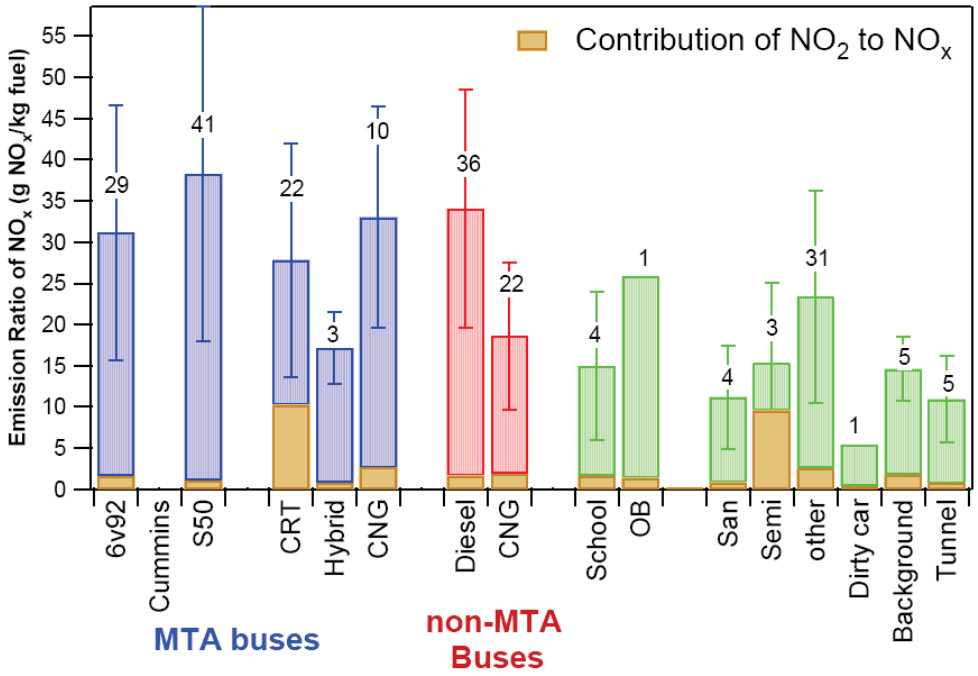

Figure 6.2-7. Classification of average NO_x ($NO + NO_2$) emissions by vehicle type. The height of each bar reflects the average emission ratio calculated over all relevant chase events that represent the particular vehicle class. Error bars represent ±1 standard error of the mean. The orange section ( ) of each bar represents the portion of total NO_x emission resulting from NO_2 emissions. OB = other buses; San = sanitation trucks; Semi = semitrucks; other = other light duty and heavy duty vehicles that do not fall in the other categories; Background = emissions in background urban area, when not directly sampling other vehicles; dirty car = a car with particularly high particulate emissions *(Shorter et al., 2005).*

As can be seen in Figure 6.2-7, the portion of NO_2 in NO_x for most vehicle samples are >5% with the exception of semi-truck class and CRT-DF equipped buses. We have no explanation for the high NO_2 fraction observed in NO_x emission in the semi-truck class, as this a somewhat anomalous result for diesel exhaust emissions. The high NO_2 fraction in the exhaust of CRT-DF equipped buses was hypothesized, as this technology requires the generation of NO_2 to burn off diesel organic and element particulate trapped on the catalytic surface. Figure 6.2-8 shows the comparison of chase study results from a standard bus and a CRT-DF retrofitted diesel buses. Both buses have similar NO_x to CO_2 emissions ratios, but as seen in Figure 6.2-8, the NO_2 emission for the CRT-DF equipped bus are factors of 10 to 100 times greater than the non-equipped bus.

Table 6.2-1 Comparison of Emission Data from Chase and Chassis Dynamometer Studies (Shorter et al., 2005)

ref	approach[a]	vehicle type	cycle	NO_x[b] (g NO_x/kg fuel)	sample size
Prucz, 2001	CD	transit buses			
		DDC 6V-92TA	CBD	40.2 ± 1.0[c]	612
		DDC Series 50	CBD	42.6 ± 1.3[c]	248
Yanowitz, 2000	CD	transit buses	multiple, including CBD, HCT, WVT	34.2 ± 1.6	> 100
Ramamurthy and Clark, 1999	CD	transit buses			
		DDC Series 50	CBD, WVT, 5-mile	33.7 ± 11.3[e]	5
Yanowitz, 1999	CD	transit buses	all cycles	49.7 (40.0–61.2)	4
			CBD cycle, only	48.2 (40.0–57.4)	4
		DDC 6V-92TA		55.6 (50.2–61.2)	2
		DDC Series 50		44.7 (40.0–48.8)	2
		school buses		27.8 (20.4–33.9)	2
Wang, 1997	CD	diesel buses	CBD	38.6 ± 2.4[c]	131
		CNG buses	CBD	44.4 ± 5.9[d]	60
Lowell, 2003	CD	diesel buses, standard fuel	CBD	33.7 ± 8.0[e]	6
		diesel buses, ULSD	CBD	30.2 ± 6.3[e]	5
		diesel buses with CRT	CBD	31.2 ± 5.4[e]	8
		diesel buses, standard fuel	NYB	32.7	1
		diesel buses with CRT	NYB	30.9 ± 5.5[e]	3
		CNG buses	CBD	26.4 ± 15.2[e]	13
		CNG buses	NYB	25.6 ± 20.7[e]	6
this work	mobile lab	MTA transit diesel buses			
		DDC 6V-92TA		31.2 ± 5.9 (8.1–72.0)	29
		Series 50		38.2 ± 6.2 (15.4–117.1)	41
		CRT	real world conditions, New York City	27.8 ± 6.3 (6.5–62.9)	22
		hybrid		17.2 ± 7.9 (12.6–21.3)	3
		CNG		33.0 ± 9.4 (16.7–62.7)	10
		non-MTA diesel buses		34.0 ± 4.7 (8.1–67.0)	36
		non-MTA CNG buses		18.7 ± 3.9 (7.9–41.3)	22
		school buses		15.0 ± 12.5 (5.6–23.4)	4

[a] CD = chassis dynamometer. [b] NO_x emissions reported as mean ± 95% confidence interval, unless otherwise noted. Values in parentheses are the range of results. [c] Assumes diesel bus fuel economy of 3.9 mile/gal (*45*) and fuel density of 7.1 lb/gal (=3.22 kg/gal). [d] Assumes CNG bus fuel economy of 3.4 mile/gal (*45*) and fuel density of 2.43 kg/gal. [e] 1σ standard deviation of the mean, determined from reported results.

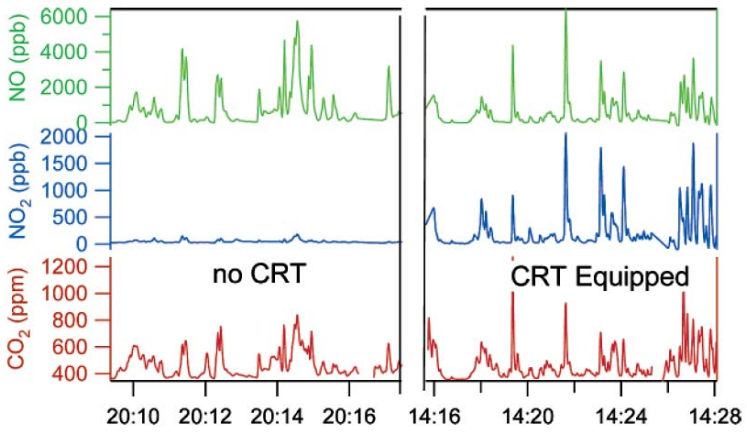

Figure 6.2-8. Comparison of typical NO, NO_2 and CO_2 chase data from a standard diesel bus (on left) and a CRT equipped diesel bus (on right). While the CO_2 and NO levels in the exhaust of both buses were comparable, the NO_2 emissions from the CRT bus are clearly higher *(Shorter et al., 2005).*

Finding 6.2-5: *CRT-DPF equipped diesel buses significantly change the NO_2/NOx ratio, which may affect traffic related NO_2 exposures and local ozone production and may have to be addressed in the long term (Shorter et al., 2005).*

Finding 6.2-6: *Ultra low sulfur fuels have significant direct benefits with respect to PM and SO_2 emissions, in addition to the control technology benefits requiring the use of these fuels (Herndon et al., 2005; Canagaratna et al., 2004). [Q7-Q8]*

Figure 6.2-9 shows an average of the PM organic and sulfate resolved size distributions provided by the AMS during the chase event. For each species, separate size distribution averages were obtained according to a CO_2 concentration-based data-processing filter that distinguished "in-plume" (plume capture) sampling from ambient background aerosol sampling. The "in-plume" and background size distributions are plotted as solid and dotted curves, respectively. The large dilution experienced by the exhaust plume when it exits the tailpipe means that even the "in-plume" size distributions are a combination of both exhaust and ambient aerosol distributions. For example, in Figure 6.2-9, the larger mode (vacuum aerodynamic diameter ~400 nm) of the "in-plume" sulfate distribution is dominated by ambient aerosols, while the smaller mode (~90 nm) is dominated by vehicle emissions. The small mode is also prominent in the "in-plume" organic distribution, and comparison with the background organic distribution indicates that this mode is largely due to exhaust aerosol.

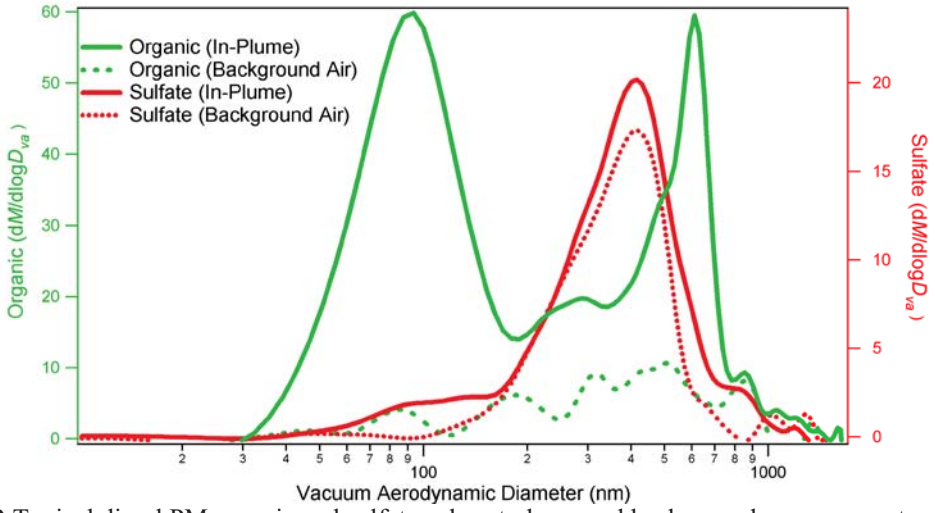

Figure 6.2-9 Typical diesel PM organic and sulfate exhaust plume and background measurements averaged over a chase event during summer 2001 field campaign in Queens, NY. The solid lines correspond to distributions averaged over time periods when the mobile laboratory was sampling the vehicle's exhaust plume. The dotted lines correspond to size distribution averages over time periods corresponding to ambient measurement conditions (*Canagaratna et al., 2004).*

Finding 6.2-7: *AMS diesel PM organic emissions measured in chase studies during the warm season in New York City show a bimodal distribution (70nm and 400nm modes) that is also reflected in ambient AMS measurements. Ambient AMS measurements made during the cold season at the same location showed a significantly diminished small particle mode. This may be the result of the broadened small particle wintertime size distribution masking the 70nm mean mode particles or the small particle mode source has shifted out of the particle transmission range of the AMS (i.e. 30nm(see section VII, figures VII.1-9 and VII.1-10)). These results suggest that low ambient temperatures affect the formation of lube oil particles either prior to or immediately after exiting the exhaust system (Weimer et al., 2006; Herndon et al., 2005; Drewnick et al., 2004a,b).*

Finding 6.2-8: *The observed diurnal pattern in ambient AMS PM organic measurements is consistent with other precursor emissions and indicates that a substantial portion of PM organic emission can be attributed to mobile sources (Drewnick et al., 2004a,b; Weimer, et al., 2006).*

Finding 6.2-9: *On-road vehicle emissions flux measurements of residual gases and PM mass, and chemical composition using a mobile measurement platform has been demonstrated as a viable means to sample large populations of in-use vehicles (Kolb et al., 2004, Canagaratna et al., 2004).*

6.3 Objective 3: Test and evaluate new measurement technologies and provide tech-transfer of demonstrated operationally robust technologies for network operation.

$PM_{2.5}$ Mass Measurement Monitors

The $PM_{2.5}$ National Ambient Air Quality Standard (NAAQS) is based on an integrated 24-hour filter measurement of fine particle mass, but there are known artifact issues – both positive and negative – with filter-based measurements. In addition, continuous PM mass measurement data is essential for near real-time public reporting, model comparison and evaluation, and study of intense short-term exposure to name just a few. In the course of this project we have undertaken a long-term and ongoing study and evaluation of continuous $PM_{2.5}$ mass measurement technologies. All of this work has been done in partnership with the NYSDEC, and much of it in partnership with Rupprecht & Patashnick, Inc. (now Thermo Electron, Inc.). This work has been reported on at two NYSERDA conferences, two AAAR conferences, the 2002 AWMA Symposium on Measurement Methods and Technology (Schwab et al., 2003), and has been the subject of three peer-reviewed papers (Schwab et al., 2004bc; Schwab et al., 2006a). The laboratory testing of continuous measurement methods is included in a different part of this report. This section will focus on the field evaluation of these methods.

Most of our effort comparing and evaluating continuous PM mass measurement technologies has concentrated on the Tapered Element Oscillating Microbalance or TEOM® method (Patashnick and Rupprecht, 1991). This method is based on the collection of non-volatile particulate matter onto a filter capsule mounted on a hollow thin glass tube. This glass "tapered element" is driven as a forced oscillator, and the frequency of the filter capsule/tapered element system is monitored as the mass accumulates on the filter. The instrument is widely used throughout the world under varying conditions and with many kinds of sample inlets and sample conditioning schemes. In this country the instrument is most widely deployed in the "standard" configuration; a size-selective sampling inlet to select $PM_{2.5}$ or PM_{10} is used, and the sample air and sensor are heated to 50ºC to reduce the interferences caused by water vapor. This instrument has known limitations when accuracy of a few micrograms per cubic meter is required, particularly when measuring $PM_{2.5}$, which has a larger fraction of volatile material than PM_{10}. The manufacturer has responded to these limitations by offering modified versions of the TEOM mass monitor.

Schwab et al. (2003) and Schwab et al. (2004c) characterized and evaluated the standard TEOM mass monitor and the Sample Equilibration System (SES) TEOM. The SES system used a reduced conditioning temperature of 30ºC for the sample air and sensor and added a dryer consisting of a bundle of semi-permeable Nafion® membrane tubes. These two implementations of the TEOM monitor were compared to each other and to the Federal Reference Method 24-hour filter samples analyzed gravimetrically. The measurements took place at the rural Pinnacle State Park site in Addison, NY, for a period of 29 months and at the urban NYSDEC site at PS219 in Queens (adjacent to Queens College) for a period of 18 months. Averaged over the whole study period, the standard TEOM and SES TEOM were biased low by 24% and 14% compared the FRM filter measurements, respectively, at the Pinnacle State Park site. For the urban Queens site the TEOM and SES TEOM were biased low by averages of 18% and 8% compared to the FRM, respectively. The SES TEOM captured 7-11% more $PM_{2.5}$ mass at these locations than did the standard TEOM.

The average bias values mask some important information about $PM_{2.5}$ seasonal composition and measurement error. Examining the measurement bias as a function of month, Schwab et al. (2004c) were able to glean additional insight into the likely composition of the fine PM at these locations. They used the slope and intercepts from monthly regression scatter plots of TEOM vs. FRM mass concentrations, combined with monthly average mass concentrations from the FRM measurements to calculate the bias at each site for each month:

$$Bias = b + (m - 1) * \overline{MC}_{FRM}$$

In this equation, b is the regression intercept, m is the regression slope, and MC_{FRM} is the average FRM mass concentration for the month under consideration. Figures 6.3-1 and 6.3-2 show the estimated monthly biases for the two sites calculated using the formula given above. The seasonal dependence of the bias for these New York State sites is clear – measurement bias is highest during the winter months for both locations, and there is a secondary maximum in the bias at the Pinnacle State Park site in Addison. The authors hypothesized that the winter bias at both sites may be caused in large part by volatilization of NH_4NO_3 from the TEOM sensor head. From the rural Addison site, they ventured further that the summer bias may be due to volatilization of photochemically produced organic species (secondary organic aerosols or SOA). At the Addison site the smallest biases occur during the spring and fall transition months. As can be seen in the figures, the wintertime bias is greater in Queens than in Addison. This is consistent with the greater nitrate component to the PM shown above (Schwab et al., 2004a). During the summer, the bias is more likely to be positive than negative, which indicates that this site has a quite different mix of semi-volatile compounds than the rural Addison site.

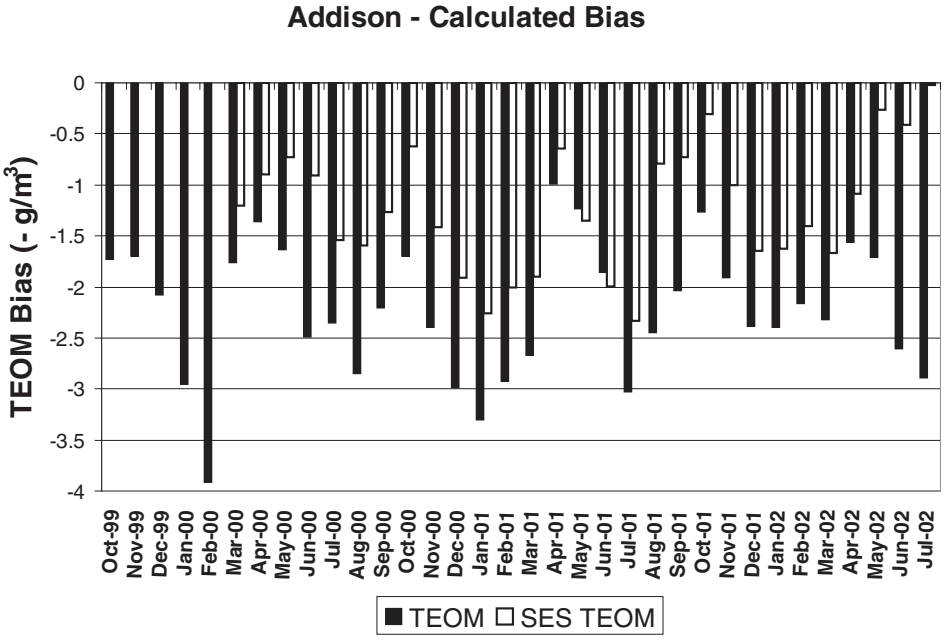

Figure 6.3-1. Estimated bias in μg/m^3 for the standard and SES equipped TEOM monitors with respect to the FRM filter mass concentrations at the Pinnacle State Park site in Addison, NY. Dark bars indicate the estimated bias of the standard TEOM monitor, and white bars indicate the estimated bias of the SES TEOM.

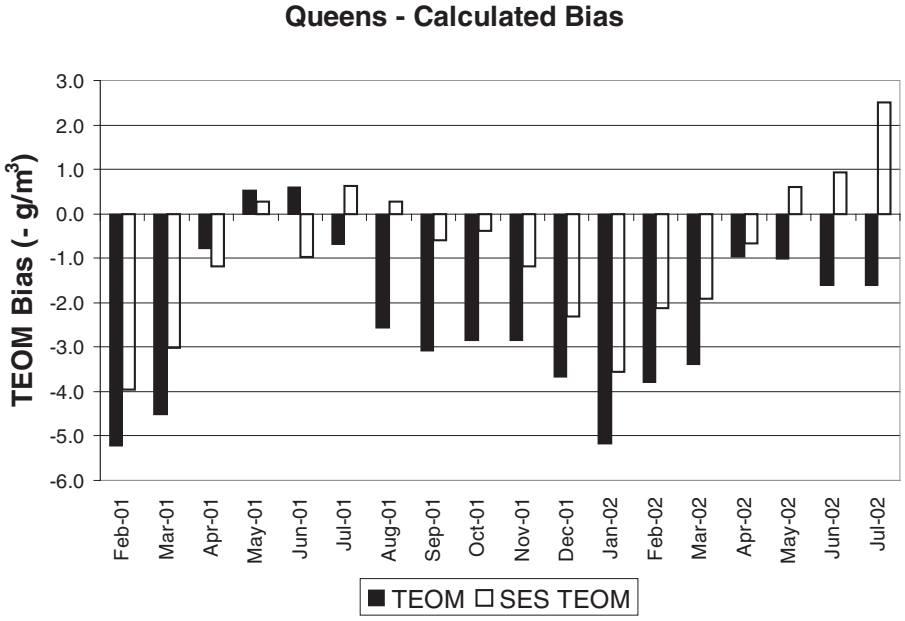

Figure 6.3-2. Estimated bias in μg/m^3 for the standard and SES equipped TEOM monitors with respect to the FRM filter mass concentrations at Queens College, in Flushing, NY. Dark bars indicate the estimated bias of the standard TEOM monitor, and white bars indicate the estimated bias of the SES TEOM.

The Filter Dynamics Measurement System (FDMS) TEOM was developed to account for volatilization and condensation artifacts in the TEOM monitor and to match the FRM standard measurements more closely. This technique uses a differential method similar in principle to that described by Patashnick et al. (2001). An attractive feature of this instrument is the simultaneous reporting of volatile and nonvolatile mass concentrations. The FDMS

measurement method and another commercially available continuous mass measurement method based on beta attenuation by PM (Beta Attenuation Monitor, BAM) were evaluated and compared to the FRM filter based measurements (Schwab et al., 2006a). These two methods showed a very high degree of correlation with each other at Queens, with a regression slope of 1.02, and an R^2 coefficient of 0.93. Figures 6.3-3a, b show the correlation scatter plots for each of these instruments versus the FRM measurements, again at the Queens site for the calendar year of 2004. The regression slopes indicate that the FRM method is missed, ~25% of the particle mass at the Queens site in New York City during 2004.

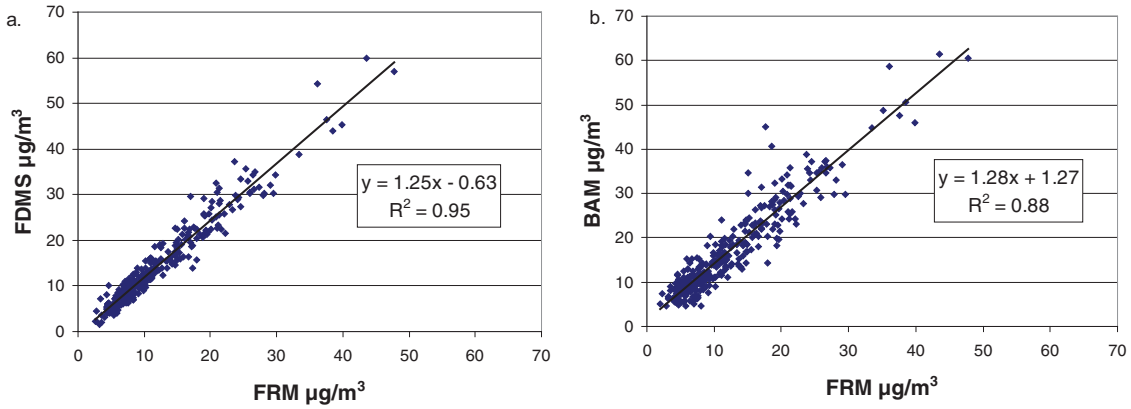

Figure 6.3-3. a.) Correlation plot for the 2004 24-hour averaged FDMS TEOM measurements vs. the FRM measurements at Queens. The fitted linear regression line and coefficients are also shown. b.) Correlation plot for the 2004 24-hour averaged BAM measurements vs. the FRM measurements at Queens. The fitted linear regression line and coefficients are also shown.

As noted above, the seasonally averaged analyses do not, in general, give a good picture of the true nature of the aerosol amount and composition, nor of our ability to measure it with known precision. To capture the simplest seasonal variation in $PM_{2.5}$ mass and various chemical components, Schwab et al. (2006a) calculated second order polynomial fits to various quantities, including FDMS, FRM, standard TEOM mass concentrations, and major chemical species form Speciation Trends Network (STN) filter samples. A reconstruction of $PM_{2.5}$ mass from the chemical species, along with an estimate for particle bound water, agreed to within about 10% of the FDMS measurement as shown in Figure 6.3-4. The agreement with the BAM is not as good. An attempt is also made in the paper to reconstruct the FRM mass using the same major species fits, this time including estimates of the amount of semi-volatile nitrate and OC lost from the FRM filter (and retained by the STN filters). Again, the reconstruction at Queens is close, but systematically low.

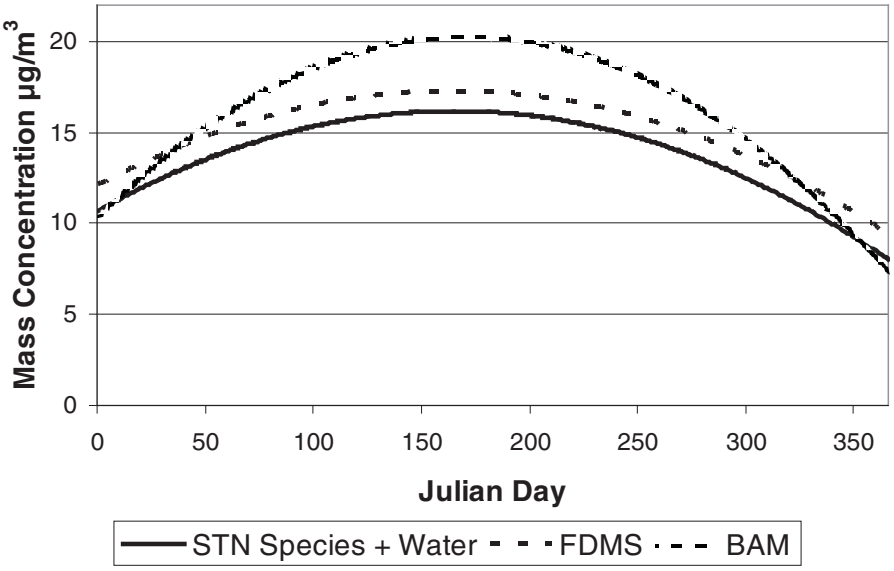

Figure 6.3-4. Reconstruction of the species mass contributions at Queens using the polynomial fits for individual species compared with the polynomial fit for the FDMS TEOM and the BAM. Species included in the reconstruction are sulfate, nitrate, ammonium, EC, OC*1.6, trace elements, and calculated water.

Finding 6.3-1: *Continuous PM mass measurement technologies (SES TEOM, FDMS-TEOM, and BAM) have shown continued progress in achieving the "true" measurement of PM mass. The designation of FRM as the mass measurement standard for the "true" ambient PM mass is now being challenged. Recent measurements based on FDMS technology indicate that the "true" PM mass is underestimated by the FRM, which loses NH4NO3 and semi-volatile organics. These losses exhibit significant seasonal dependence (Schwab et al., 2003; Schwab et al., 2004bc; Schwab et al., 2005a).*

$PM_{2.5}$ Sulfate Measurement Monitors

The ubiquitous nature and high concentration of fine particle sulfate in the Eastern U. S. has made development, evaluation, and deployment of continuous sulfate measurement systems a high priority for the PMTACS-NY project. Four semi-continuous sulfate instruments were deployed during the summer 2001 Queens intensive. These measurements were compared with each other and two sets of filter measurements, and reported on by Drewnick et al. (2003). Hogrefe et al. (2004) extended this analysis to include four sulfate methods at Whiteface Mountain during the summer 2002 intensive. As a complement to--and extension of--the intensive studies, Rattigan et al. (2006) presents a comparison at a remote and an urban site of one semi-continuous sulfate method with two filter based methods over a three-year period. Schwab et al. (2006b) reports on an extended comparison of a different semi-continuous method and the same two filter methods.

The intercomparison exercise for sulfate measurement systems that resulted from the summer 2001 Queens showed excellent agreement between the four semi-continuous instruments (Drewnick et al., 2003). The instruments involved were the Aerosol Mass Spectrometer (AMS),

the Particle Into Liquid Sampler coupled with Ion Chromatography (PILS-IC), the Rupprecht & Patashnick 8400S, and an early prototype version of the Thermo Electron 5020 (denoted and labeled as CASM in the figures). Figure 6.3-5 shows the time series of sulfate measurements from the four instruments during the summer 2001 intensive. The degree of agreement between these techniques was quite impressive, given the different collection and analysis techniques. Pair wise correlations between the instruments yielded multiple-R^2 values ranging from 0.87 to 0.94, slopes close to one, and intercepts close to zero $\mu g/m^3$.

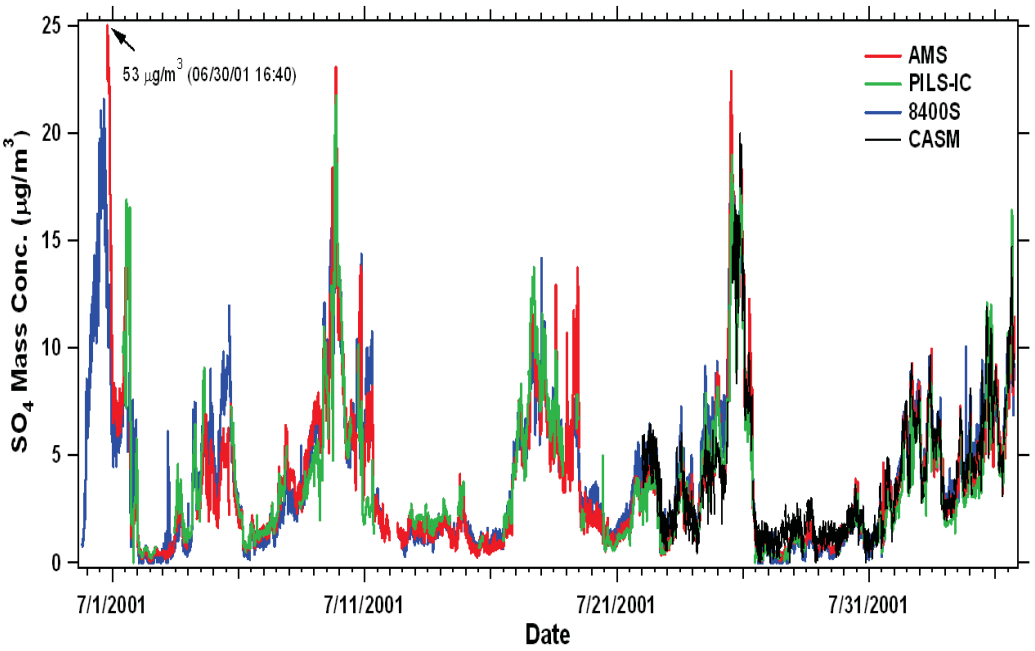

Figure 6.3-5. Fine PM sulfate mass concentration time series from the AMS, the PILS, the R&P 8400S, and the CASM for the whole PMTACS-NY summer 2001 campaign at Queens.

The semi-continuous data were also compared to four sets of filter samples collected on the site and at the adjacent PS219 site (roughly 100 m away across a playing field). These filter samples were analyzed using ion chromatography at two different laboratories and were very consistent, yielding R^2 values greater than .975 for all correlations and recovery coefficients that averaged to within 3% of unity. The comparison between the filters and the semi-continuous instruments highlighted a small, but persistent, systematic difference between the filter-based and semi-continuous measurements. The semi-continuous instruments averaged recovery values of 0.75 in comparison with the six-hour filters, and 0.85 in comparison with the 24-hour filters. Various causes that could contribute to the systematic under-measurement were present by Drewnick et al. (2003), but as noted below, three additional studies show this same systematic difference.

The same four instruments were deployed during a summer campaign in 2002 at the Whiteface Mountain Lodge level. Results of the intercomparison have been presented by Hogrefe et al. (2004). The time series of sulfate measurements is shown as Figure 6.3-6. The agreement between instruments during this campaign was less good than during the Queens 2001 campaign. There were problems with water purity for the PILS and with water condensation in

the zero cycle lines of the CASM. Of the six pair wise correlations, two (CASM vs. AMS and CASM vs. PILS-IC) yielded the relatively low R^2 values of 0.73; the other four correlations had an average R^2 of 0.91. The recovery coefficients comparing the semi-continuous instruments for this campaign ranged from 0.81 to 1.3. This is not the same excellent agreement found in Queens, with the largest deviations coming from comparisons involving the PILS-IC and CASM.

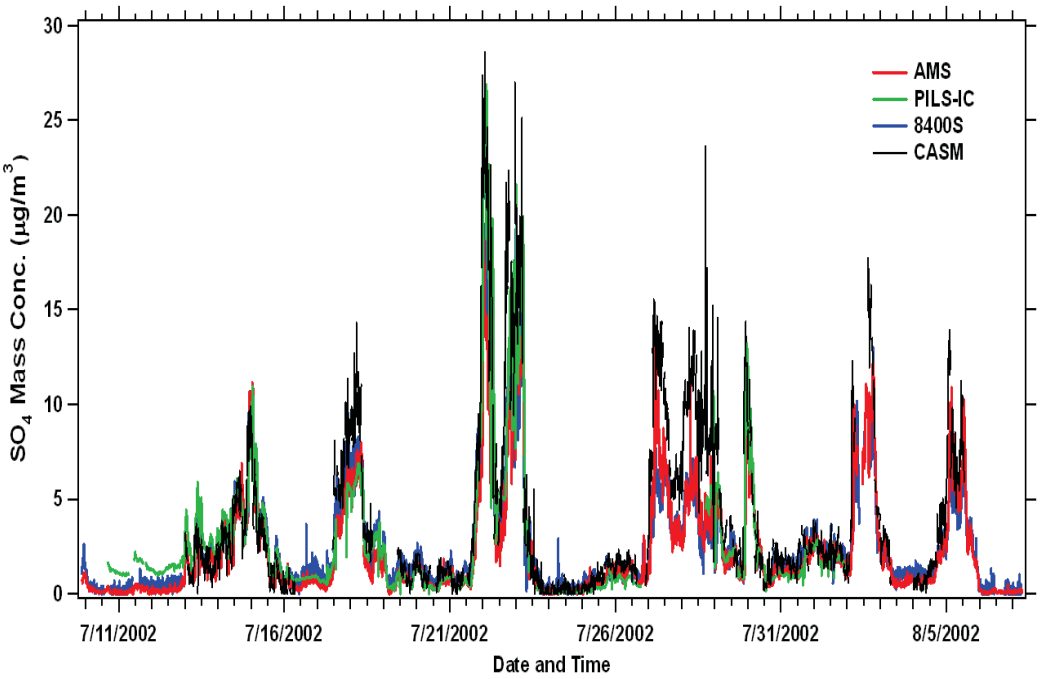

Figure 6.3-6. Time series of semi-continuous fine PM sulfate mass concentrations measured during the PMTACS-NY summer 2002 campaign at Whiteface Mountain Lodge.

There were three sets of 24-hour filter samples available for comparison during this campaign. Because of the instrument problem, the CASM data was not compared to the filters. The AMS, PILS-IC, and 8400S correlated very well with the 24-hour filters (R^2 values of 0.96, 0.96, and 0.97). However, the AMS and 8400S correlations yielded recoveries of 0.77 and 0.83 – consistent with the Queens values – while the PILS-IC correlation yielded a recovery coefficient of 1.07.

Of the four instruments compared in the above studies, only the R&P 8400S was commercially available in 2001 and suitable for routine deployment. Results from a three-year evaluation of this instrument and comparison with filter samples are presented by Rattigan et al. (2006). The instruments were deployed at the IS52 South Bronx site and at the Whiteface Mountain Lodge level. Comparisons with filter samples collected every third day as part of the EPA STN program, and daily as part of the PMTACS-NY activity are presented. Figure 6I.3-7 shows the 8400S data (averaged up to 24-hours) compared in a correlation scatter plot with the combined filter data. Table 6.3-1 summarizes the linear regression fits to the long-term data sets at both sites.

The intercepts are significant at the South Bronx site and are much smaller at the Whiteface site. The consistency of the intercepts for the two filter sets may indicate an as yet unknown positive artifact in the 8400S data. The slopes of these regression fits are quite consistent with values presented above from the summer intensive campaigns (excluding the PILS-IC at Whiteface). The authors also note that although they found the 8400S capable of providing a high data capture (>80%), its requirement for frequent (bi-weekly and often weekly) maintenance by trained personnel made its deployment at remote monitoring sites unfeasible.

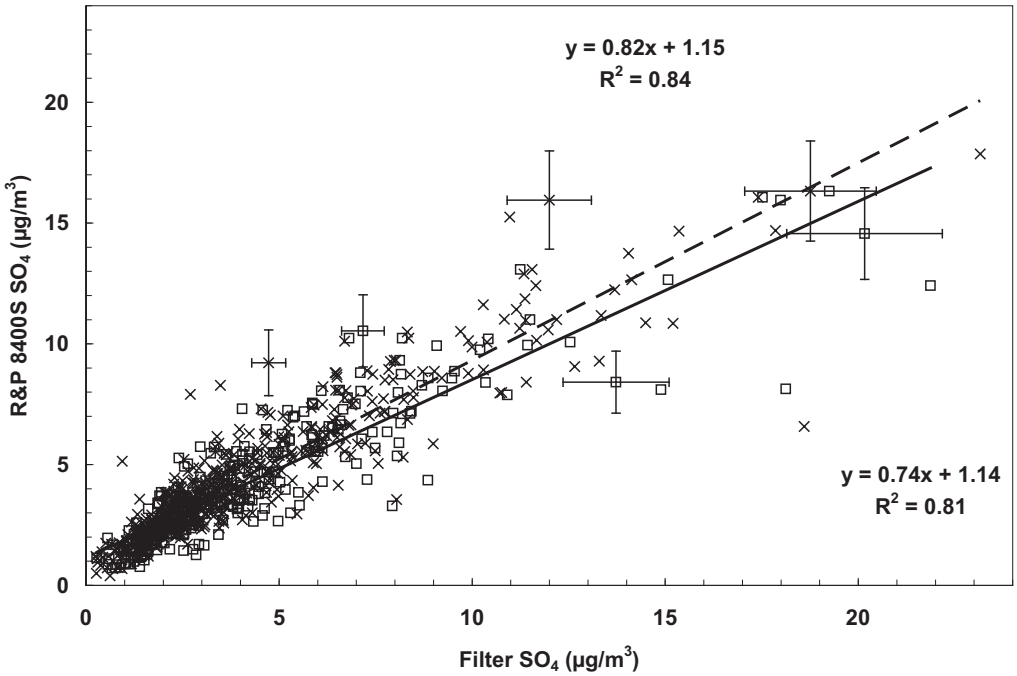

Figure 6.3-7. Comparison of 24-hr average R&P 8400S SO4 data at the South Bronx site with the corresponding collocated R&P ACCU (crosses) and R&P 2300 (open squares) 24-hr integrated filter data. The dashed and solid lines indicate the linear least squares regression fits to the crosses and squares, respectively.

Table 6.3-1.Summary of the linear regression between the SO_4 measured by the R&P 8400S and 24-hr filter instruments.

Correlated data	Site	Slope	Intercept	R^2	Data Points
8400S vs. ACCU	Bronx	0.82	1.15	0.84	513
8400S vs. 2300	Bronx	0.74	1.14	0.81	322
8400S vs. ACCU	WFM	0.75	0.22	0.95	207
8400S vs. 2300	WFM	0.78	0.17	0.85	198

Thermo Electron commercialized the 5020 Sulfate Particulate Analyzer in 2004. For the summer 2004 campaign at Pinnacle State Park, we obtained a manufacturer's prototype of this instrument. Laboratory evaluations of this instrument are presented elsewhere in this report. Here we report on the field evaluation of the prototype instrument for the 3 ½ month period from July 14 to November 1, 2004 at PSP in Addison (Schwab et al. 2006b). Figure 6.3-8 shows the times series plot of 24-hour averaged values from the 5020 and a combined filter data set, which included STN and ACCU filters. Figure 6I.3-9 shows the correlation plot of this 24-hour data.

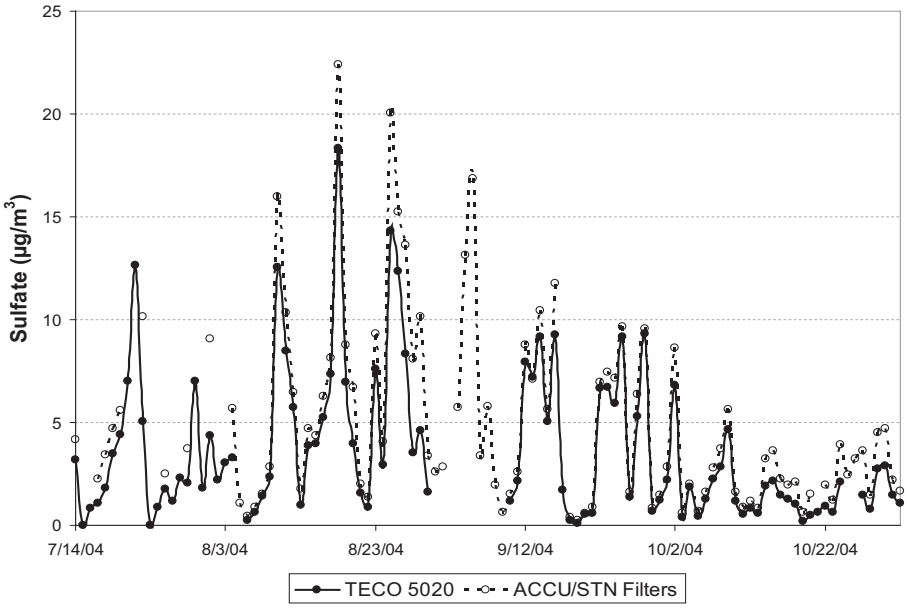

Figure 6.3-8. Time series plot of the 24-hour averaged 5020 sulfate and filter sulfate from the combined ACCU/STN data set collected at Pinnacle State Park in Addison, NY.

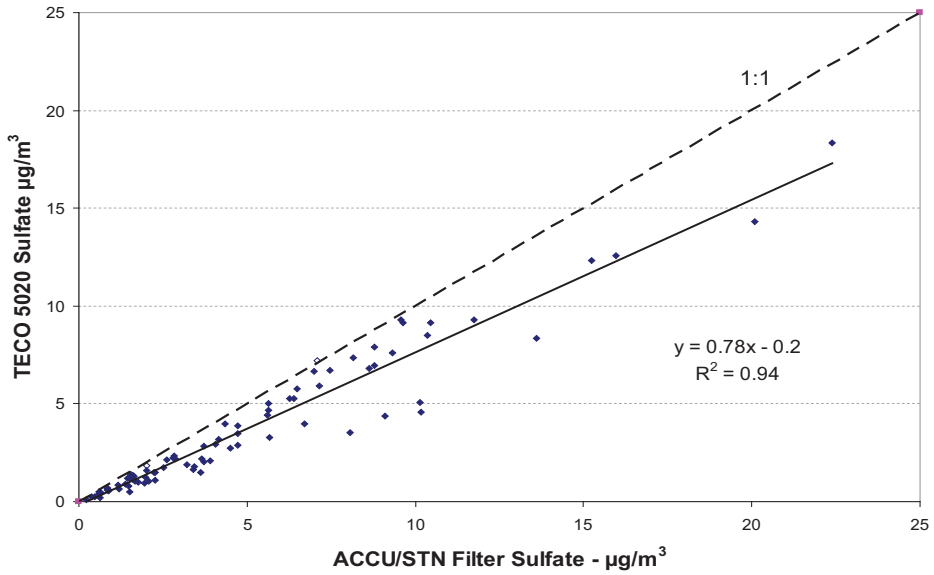

Figure 6.3-9. Correlation plot of the 24-hour data from Addison, along with the 1:1 line for reference and the linear regression line and equation.

The sulfate data from this study is more highly correlated than the data from the 8400S instruments in the South Bronx or at Whiteface, but the regression slope is very similar. It seems consistent from all these studies that the thermal methods used by these instruments to convert sulfate to SO_2 (or mass fragments in the case of the AMS) operates with about an 80% (±5%) efficiency at our sites in New York State. We have tested some hypotheses to explain this conversion efficiency, but we have been unable to explain it, and it remains an open question. The Thermo Electron 5020 proved itself during this study (and continues to do so while currently deployed at PSP and the South Bronx) as a preferred method for continuous sulfate measurements.

Finding 6.3-2: *Continuous PM sulfate measurement technologies (8400S and Thermo 5020) show promise for routine network deployment. Sulfate measurements are in good agreement with collocated instruments and consistently recover about 80% as much sulfate as 24 hr STN filters. Outstanding operational/maintenance issues with some systems remain to be resolved (Drewnick et al., 2003; Hogrefe et al., 2004; Rattigan et al., 2005; Schwab et al., 2005b).*

$PM_{2.5}$ Nitrate Measurement Monitors

Fine particle nitrate presents a greater measurement challenge because of its semi-volatile nature. Seasonally speaking, it is "complementary" to sulfate in the Northeastern U.S., as it peaks in the winter and is lower in the summer. In fact, it is quite often below detection limits in rural and remote locations during the summer period. Hogrefe et al. (2004) evaluated and compared three semi-continuous nitrate methods with STN filters for the summer 2001 Queens and summer 2002 Whiteface Mountain intensives. Rattigan et al. (2006) includes a three-year evaluation of a commercial semi-continuous nitrate method and comparison to STN filter measurements. As with sulfate, the instruments included an Aerodyne AMS, the PILS-IC, and a Rupprecht & Patashnick 8400N.

The time series of the nitrate mass concentrations is shown as Figure 6.3-10 (Hogrefe et al., 2004). The three instruments show reasonable correlation, but not nearly the level of agreement shown by the sulfate instruments in Figure 6.3-5. Still, the correlation R^2 values are high, ranging from 0.89 to 0.95. The PILS-IC reports the highest nitrate values and recoveries versus the PILS for the AMS and 8400N are 0.88 and 0.63, respectively. The only nitrate filter data available for comparison are from the STN, which are collected every third day. This means there are only seven or eight 24-hour samples available for comparison. The R^2 values for these comparisons are 0.99, 0.99, and 0.98; and the recoveries are 0.9 for the AMS, 0.65 for the 8400N, and 0.92 for the PILS-IC. It is clear from these comparisons that the 8400N has losses in the collection or conversion processes central to its operation. While it is not strictly quantitative, it does respond fairly linearly with particle nitrate, at least at low to modest loadings.

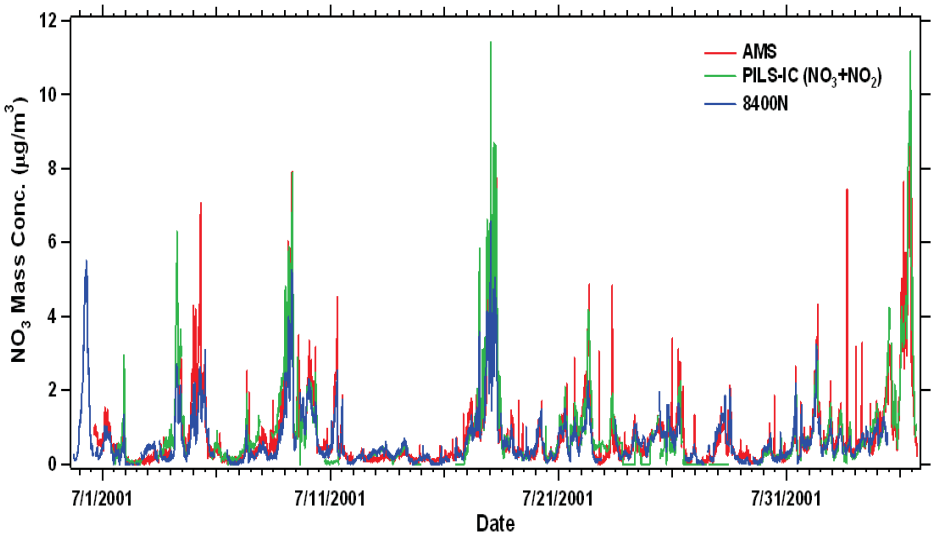

Figure 6.3-10. Fine PM nitrate mass concentration time series from the AMS, the PILS-IC, and the R&P 8400N for the PMTACS-NY summer 2001 campaign at Queens.

The time series data from the summer 2002 campaign at Whiteface Mountain Lodge is shown as Figure 6.3-11. The first thing to note is that the scale for this plot is a factor of 10 lower than the scale for Figure 6.3-10. A consistent observation based on both filter and semi-continuous data is that $PM_{2.5}$ nitrate in rural and remote areas is very low during the summer season. It is difficult to effectively compare the methods when so much of the data is near or below the detection limits (0.03 $\mu g/m^3$ for the AMS, 0.05$\mu g/m^3$ for the PILS-IC, and 0.15$\mu g/m^3$ for the 8400N). Hogrefe et al. (2004) does the correlation analysis, but the R^2 values are not terribly good (ranging from 0.46 to 0.83), so numerical values will not be presented here.

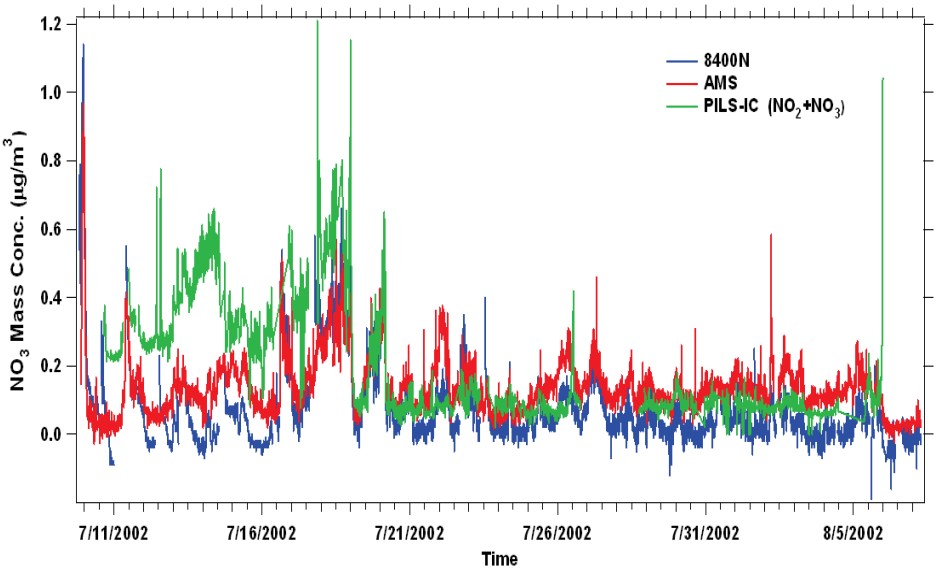

Figure 6.3-11. Time series of semi-continuous fine PM nitrate mass concentrations measured during the PMTACS-NY summer 2002 campaign at Whiteface Mountain Lodge.

The Rattigan et al. (2006) study examines a much larger data set for the 8400N instruments deployed at Whiteface Mountain and the South Bronx. Figure 6.3-12 shows the correlation scatter plot resulting from 305 valid comparisons of 24-hour averaged 8400N data and filter samples from the co-located STN sampler. The regression slope of 0.59 for this site is quite similar to the value of 0.65 obtained for the filter comparison obtained in the summer 2001 Queens campaign. Rattigan et al. (2006) note that out of 168 valid 24-hr filter NO_3 data at the Whiteface site there were 118 days when the R&P 8400N NO_3 was below the detection limit (approximately 70%). This in contrast to the South Bronx, where less than 5% of the data was below the detection limit and seven data points were flagged at this site for various reasons. The linear regression using some 40 points yielded an R^2 of 0.90, and intercept of 0.01, and a slope of 0.73. Although this slope is approximately 20% higher than observed at the South Bronx site (slope = 0.59), it is within the measured uncertainties. More notable than the different slopes is the widely different range of nitrate concentrations at these two sites. In particular, 95% of the Whiteface filter-NO_3 data lies below 1 $\mu g/m^3$ compared to 34% in the South Bronx. In addition, approximately 30% of the South Bronx 24-hr filter NO_3 data are above 2.7$\mu g/m^3$, with the highest value observed at Whiteface Mountain.

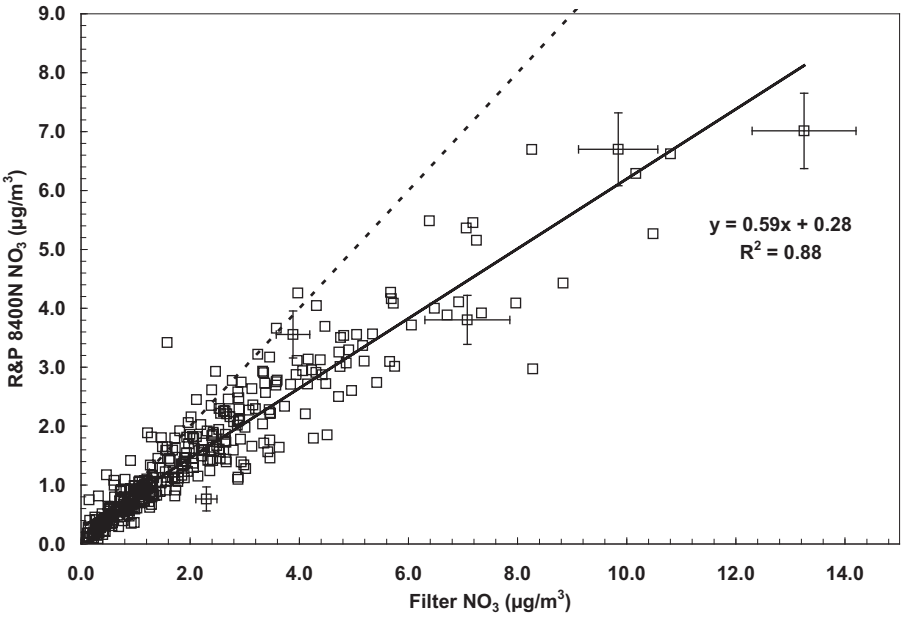

Figure 6.3-12. Comparison of 24-hr average R&P 8400N NO_3 at the South Bronx site with the corresponding collocated R&P 2300 24-hr integrated filter data. The solid and dashed lines indicate the linear least squares regression fit to the data set and the 1:1 line.

As with the 8400S, the instrument is capable of providing a high data capture (>80%) and reasonable correlation with filter measurements, but its requirement for frequent (bi-weekly and often weekly) maintenance by trained personnel makes its deployment at remote monitoring sites quite difficult. Comparison of the R&P 8400N with 24-hr integrated filter measurements shows that the R&P 8400N is on average biased low by 30%-40% compared to the filter data, which indicates that the R&P 8400N NO_3 to NO_x conversion process is sensitive to the aerosol composition or suffers from a systematic shortfall.

Finding 6.3-3: *Continuous PM nitrate measurement technology (8400N) shows promise for routine network deployment, but measured PM NO_3 levels are significantly lower (30-40%) than other collocated semi-continuous instruments and 24 hr STN filters. Some measurement data indicate a non-linear response with increasing PM nitrate levels which suggest a changing or limiting reductive capacity of the flash conversion system (Hogrefe et al., 2004; Hering et al., 2004;Rattigan et al., 2005).*

$PM_{2.5}$ Organic/Elemental Carbon Measurement Monitors

Measurement of carbonaceous material in $PM_{2.5}$ is a significant challenge, but it is of critical importance given its large fractional contributions, its ubiquitous nature, and its potential health effects. Field deployments of semi-continuous Sunset Labs EC/OC analyzers at South Bronx and Pinnacle State Park occurred much later than the deployments of the sulfate and nitrate analyzers. Comparison PM organic carbon mass measurements from an aerosol mass spectrometer and the Sunset Labs analyzer (Weimer et al., 2006) indicated a linear correlation of paired hourly data with an $R^2 = 0.66$ and slope = 3.28 and intercept = -4.18. This negative

intercept is likely a sampling artifact of the Sunset Labs analyzer resulting from the loss of volatile organic PM from the filter surface,which typically runs above ambient temperatures during the sampling cycle. In addition, the regression of the AMS OM to the Sunset Labs OC gives an indication of the nature of the organic aerosol, that is, whether it is fresh hydrocarbon dominated or more aged oxygenated material. The slope of the regression line for a zero intercept is 2.06 (Weimer et al., 2006), a number in agreement with recent results, suggesting that standard accepted multiple of 1.4 may be significantly under estimated (Zhang et al., 2005a, 2005b, Turpin et al., 2001).

Black carbon measured at Queens and at IS52 in the South Bronx during the winter 2004 intensive period is analyzed and compared by Venkatachari et al. (2006a). The regression of simultaneously measured BC at the two sites (9 km apart) produced an R^2 value of 0.30, which indicates a weak correlation. This indicates BC may be an even more local pollutant then had been previously assumed. The authors also found very little day-of-week trends in the BC data, as shown in Figure 6.3-13, but this finding must be qualified, given the limited period of the data set.

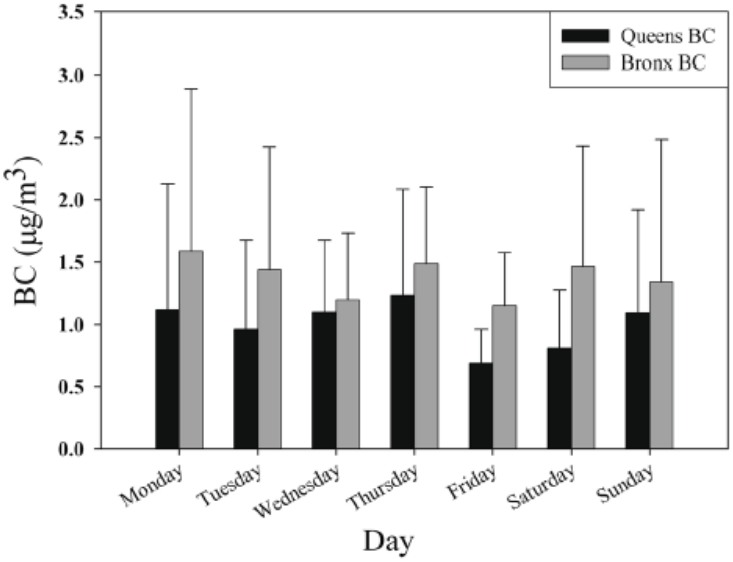

Figure 6.3-13. Day-of- week trends in BC concentrations at the two sites for the sampling period.

An intercomparison of measurement methods for carbonaceous aerosol was performed by Venkatachari et al. (2006b) using data collected during the Queens winter 2004 campaign. Instruments and parameters included in this study were the Sunset Labs EC/OC field instrument (EC and OC), the R&P 5400 Monitor (EC and OC), the Aerodyne Q-AMS (OM only), Magee Scientific AE-20 Aethalometer (BC only), and STN and ASRC 24-hour filters (EC and OC). In this study, the authors reported correlation coefficients (r – not R^2 as in the other works cited) and coefficients of divergence (COD). A COD of 0 denotes perfect agreement, and a COD of 1 denotes complete disagreement. They observed that the R&P 5400 total carbon (TC) tracked the filter measurements reasonably well (r = 0.91) but that EC and OC from the 5400 compared less well (r = 0.76 for OC and r = 0.88 for EC). The Sunset Labs EC/OC instrument, compared to the filter measurements yielded correlation coefficients of 0.88 for TC, 0.82 for OC, and 0.97 for EC. All of these comparisons are based on between 15 and 17 samples during January and February 2004.

The work of Venkatachari et al. (2006b) hints that the R&P 5400 may produce useful data that compares reasonably well (at least for total carbon) at the Queens site. Extended deployments of this instrument at the Whiteface Mountain Lodge and Pinnacle State Park sites did not produce data that was comparable to the STN filter data. In addition, there are questions about the collection method (it is based on an impact or design with a cut-off diameter of 0.14 μm which excludes a wide range of carbon particles) and about operational issues (numerous failures were experienced at the PSP site before the instrument was shut down). We have shut down all 5400s, and, as noted above, are currently operating two Sunset Labs EC/OC instruments.

Finding 6.3-4: *Continuous PM carbon measurement technology (Sunset Labs - EC/OC) shows promise for routine network deployment, indicating good agreement with collocated instruments and 24 hr STN filters and AMS – OC measurements. R&P 5400 EC/OC tracks total relative carbon well, but it is not quantitative, as it does not provide comparable EC/OC with 24 hr STN filters (Venkatachari et al., 2005; Weimer, et al., 2005).*

Aerosol Particle Sizing Instrumentation

The Scanning Mobility Particle Sizer (SMPS) is a multi-component instrument, which measures the size distribution of aerosols, thus providing information about the concentration of aerosol particles of various diameters in an analyzed air sample. For many routine field measurements it can be more practical to use a particle sizer, which: combines basic features of the SMPS yet is convenient to transport, deploy, and operate in field conditions; operates with a set of fixed parameters, thus producing data that are easy to compare with those from similar instruments at various locations; and requires even less maintenance than the conventional SMPS. A “single box” Scanning Mobility Particle Sizer (SMPS 3034, TSI Inc.) has the potential to function as such an instrument. The SMPS 3034 is an alternative to a conventional multi-component SMPS and houses a Differential Mobility Analyzer and butanol-based Condensation Particle Counter in one cabinet. There are also several modifications to the design of its individual components. The SMPS 3034 has been evaluated in the field for the first time during the Queens College Winter 2004 intensive field study [Hogrefe et al, 2006]. It appears that the SMPS 3034 captures the main features of a size distribution correctly and is also as sensitive to small particles (diameters 10-104 nm) as the Nano SMPS (Figure 6.3-14). It has been shown that the number median diameters measured by the SMPS 3034 and the Nano SMPS agree within 3 nm and that the total particle number concentrations measured by the SMPS 3034 agree within 16% with those from the conventional NanoSMPS (Figure 6.3-15) and are also highly correlated with those from a stand-alone Condensation Particle Counter (CPC 3022, TSI Inc.). It also has been shown that inferred mass concentrations from the SMPS 3034 are well correlated with mass concentrations from an R&P Inc. Filter Dynamic Measurement System TEOM mass monitor (Figure 6.3-15).

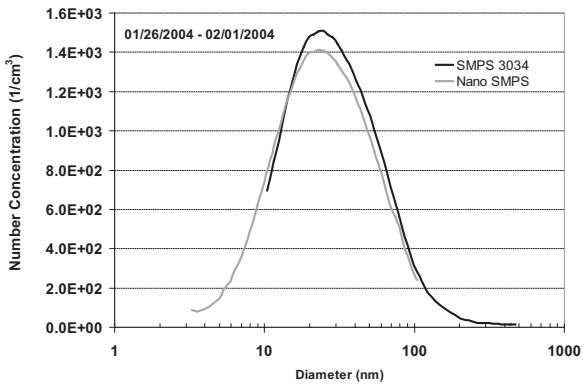

Figure 6.3-14. Weekly average (01/26/04-02/01/04) number size distributions as measured by the SMPS 3034 and the Nano SMPS.

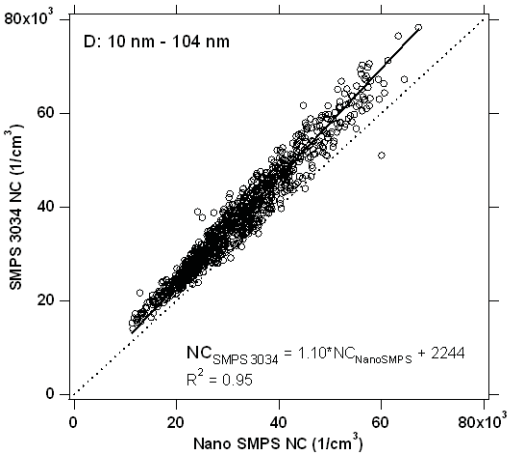

Figure 6.3-15. SMPS 3034 number concentration data (30-minute averages) plotted vs. data from SMPS 3936 with the Nano DMA. Only number concentrations from common size bins (10-104 nm) are considered in this comparison.

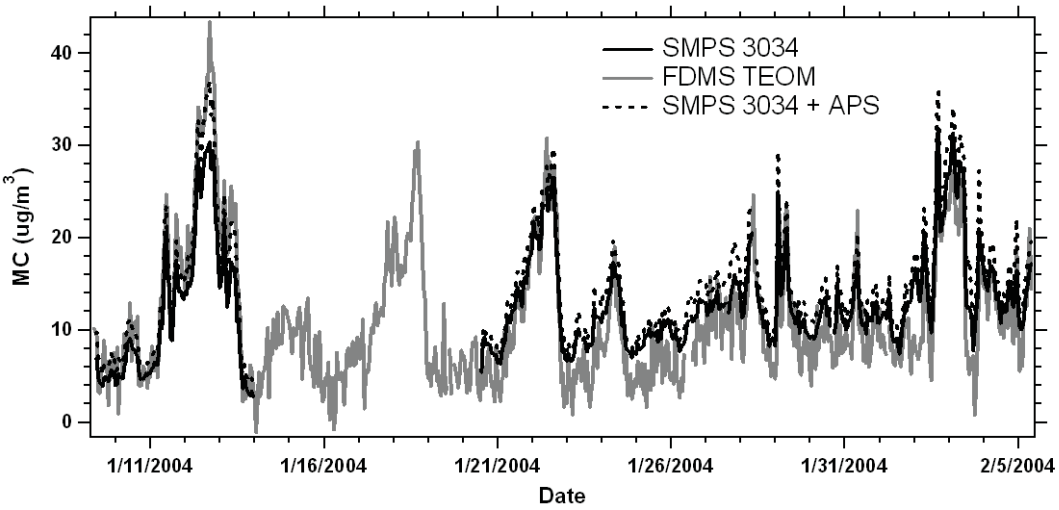

Figure 6.3-16. The time series of hourly aerosol mass concentrations from the SMPS 3034, the APS, and the FDMS TEOM. FDMS TEOM size cut-point is 2.5 μm. While the total mass concentration from the SMPS 3034 is shown, the APS data include only mass concentrations corresponding to the particle diameters of 480 nm to 2.0 μm (corresponds to aerodynamic diameter of 2.5 μm). Particle density (SMPS3034 and APS) was assumed to be 1.5 g/cm^3 (Pitz, et al., 2003).

It has been concluded that the SMPS 3034 can be used as an easy-to-operate and easy-to-transport alternative to the SMPS 3936, especially for long-term field measurements. In certain cases of ultrafine particle measurements, the SMPS 3034 can serve as a replacement for the combination of the Nano SMPS and SMPS with the LDMA, since it can measure particles in the diameter range of 10-487 nm. Although a compact design of the instrument makes moving and set up relatively easy, it can also make it harder to perform repairs in field conditions. Since operation parameters are fixed, it is much easier to start and run the instrument, as well as compare the data from several SMPS 3034 instruments. On the other hand, fixed flows (and consequently the diameter range over which the number concentrations are measured) and scan time may limit the use of the SMPS 3034 for research purposes.

Finding 6.3-5: *The" single box" Scanning Mobility Particle Sizer (SMPS 3034, TSI Inc.) for the measurement ambient aerosol size distributions is an easy-to-operate and easy-to-transport alternative to the SMPS 3936, especially for long-term field measurements. In some ultrafine particle measurement applications, the SMPS 3034 can serve as a replacement for the combination of the Nano SMPS and SMPS with the LDMA, but its time resolution may limit its use for research applications.*

Aerosol Particle Counter Instrumentation

A newly developed, laminar flow, water-based condensation particle counter (WCPC) was evaluated under field conditions during the Queens College Winter 2004 intensive field study [Hering et al. 2004a and 2004b]. The WCPC uses a unique "growth tube" technology that enables the enlargement of particles by water condensation in a laminar, thermally diffusive flow. It is an environment-friendly and researcher-friendly alternative to a conventional butanol-based CPC. The instrument tested, the Quant-400, was the prototype of the commercial version (CPC 3785, TSI Inc). During the tests, the basic operational principle of the WCPC - the warm wet walled condenser – was verified. Total ambient particle number concentrations were compared to a collocated conventional butanol-based condensation particle counter (CPC 3022, TSI Inc.). The WCPC agreed very well with the CPC 3022 when concentration data are derived from single particle counting (Figure 6.3-17).

Agreement was neither as good, nor as consistent, at ambient concentrations above 65,000cm^{-3}, when the WCPC values were derived from total scattering from the "cloud" of particles (photometric mode). This issue was a subject of subsequent research of Hering and colleagues. Capabilities of the WCPC as a component of the SMPS were also tested: the WCPC was placed downstream of an electrostatic classifier with a Nano DMA, where it was measuring concentrations of particles in individual size bins. Data from the WCPC were compared with those from the butanol-based ultrafine CPC 3025 (TSI Inc.). A typical size scan obtained using both condensation counters is shown in Figure 6.3-18. No systematic differences were found between the WCPC and the CPC 3025. The WCPC concentrations were generally within the statistical error of those reported by the CPC 3025 over the entire size range from 5 nm to 100 nm. Better statistics were observed with the WCPC, due to the fact that the flow rate of the latter is 16.7 higher than that of the CPC 3025.

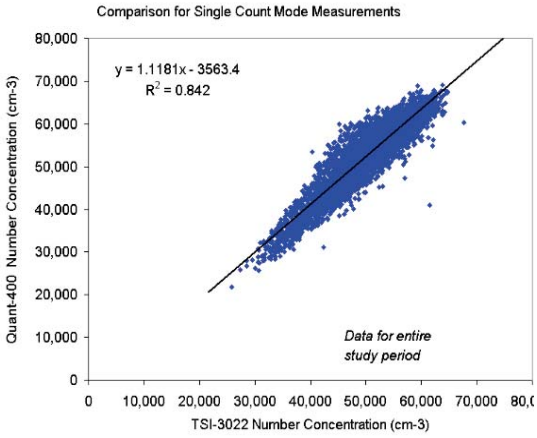

Figure 6.3-17. WCPC particle number concentration plotted vs. those from the CPC 3022.

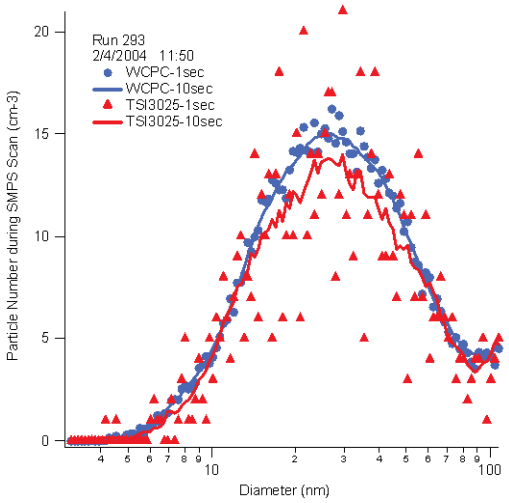

Figure 6.3-18. Size distributions obtained when the WCPC and the CPC 3022 were placed downstream of the Electrostatic Classifier with the Nano DMA.

Finding 6.3-6: *Water-based condensation particle counter technology provides comparable performance to that of the butanol-based condensation particle counters. The removal of butanol from the measuring environment is advantageous, as this volatile organic compound can be a significant source of local contamination..*

7 IMPLICATIONS FOR AIR QUALITY MANAGEMENT AND KNOWLEDGE GAPS

PMTACS-NY findings have provided insight into several aspects of the air quality management of $PM_{2.5}$ and photochemical oxidants. These include:

Control Technology and Measurement Technologies for Mobile Sources

The results from chase studies of heavy duty diesel buses retrofitted with diesel filter trap oxidation catalyst control technology suggest that implementation of a diesel truck retrofit filter trap control program would be an extremely effective means of reducing organic PM in major metropolitan areas (e.g. Boston to Washington corridor) through the reduction of direct primary EC/OC emission as well as the reduction of gas phase precursor VOCs contributing to SOA. In planning such a program, the impact on ambient air quality needs to be assessed and measurement strategies identified that allow tracking of air quality changes in response to the implementation of emission controls.

The demonstration of instrumentation for the measurement of on-road vehicle emissions fluxes of residual gases and PM mass and chemical composition, using aerosol mass and tunable diode laser differential absorption spectrometers, provides a viable means to sample large populations of in-use vehicles and effectively evaluate the performance. The instrumentation could also be used to collect data to assess the overall uncertainty of mobile emission model predictions. Overall, our studies suggest that the comparison of vehicle chase study and dynamometer emissions for PM are consistent in the mean, although real-world in situ emission measurements are significantly more variable than dynamometer tests (*Shorter et al.,* 2005). In-use testing also offers the opportunity to assess the impact of gross emitters of PM (poorly maintained high pollution vehicles) from both diesel and gasoline-fueled vehicles.

Atmospheric Processes and Secondary Aerosol Formation

Our studies have shown the strong linkage between summer ozone and OH concentrations in the atmosphere and the importance of OH reactions with precursors (e.g., SO_2, VOC and NO_2) in the secondary formation of PM sulfates, organics, and nitrates. The results indicate that the oxidant and PM control strategies must be considered in an integrated framework, recognizing that ozone mitigation directly effects (i.e. reduces) PM secondary production. It must be noted that strategies that consider controls only during the oxidant season (e.g. NO_x SIP call) do not benefit. One example is, PM winter time nitrate mitigation in the northeast. Although recent studies have indicated that biogenic emissions of isoprene and terpenes can be significant precursors to secondary organic aerosol production, we did not see evidence of this in our studies.

In addition, when secondary PM production is attenuated due to low photochemical activity during the cold season in the northeast, we find comparable PM mass levels and only a slight reduction in the percentage contribution of sulfate. This result suggests the presence of a significant cold season SO_2 transformation process (likely heterogeneous reactions) to sulfate, a processes that remains unevaluated (in summer or winter) in models due to very limited measurement studies.

Promising Methods for Ambient Air Quality Monitoring

Several new measurement systems were deployed and evaluated over the course of the PMTACS_NY Supersite program including the following commercial monitors: Sunset Labs-EC/OC, Magee Scientific AE20-BC, R&P 5400-EC/OC, TECO 5020-$PM_{2.5}$ Sulfate, R&P 8400S –$PM_{2.5}$ Sulfate, R&P 8400N-$PM_{2.5}$ Nitrate, R&P FDMS-$PM_{2.5}$ mass, and Met One BAM- $PM_{2.5}$ mass. The deployment experience gained by NYSDEC, our collaborative partner in this study and the published results from intercomparison and evaluation studies of these monitoring systems have benefitted air quality monitoring agencies in making informed decisions regarding the selection of advanced semi-continuous PM mass and PM component monitoring systems.

Over the course of the PMTACS-NY Supersite program, and as a result of findings therein, additional scientific questions as well as areas of uncertainty have surfaced that will need further attention. These findings, the knowledge gaps, and suggested recommendations for future work are briefly summarized as follows.

Characterization of Fine Particle Emission Sources

The warm season AMS diesel PM organic emissions measured in chase studies show a bimodal distribution (70nm and 400nm modes) that also was reflected in ambient AMS measurements in Queens, NY (Herndon et al., 2005, Drewnick et al., 2004a,b). Similar AMS chase studies of heavy duty diesel vehicles under cold season conditions should be performed to characterize the size distribution of diesel PM organic in the source plume. This would help resolve the loss of the distinct bimodal size distribution in the AMS PM organic fixed site measurements during the 2004 winter intensive field study was emissions related or the result of masking, due to an overall downward shift in mean mode size distribution of ambient PM.

Implications for Health Effects Research

The accurate determination of ambient $PM_{2.5}$ mass concentration is critically important to the development and implementation of $PM_{2.5}$ National Ambient Air Quality Standards. Recent instrumentation evaluation and intercomparison studies of $PM_{2.5}$ mass measurement devices performed as part of the PMTACS-NY Supersite program indicate that the “true” ambient PM mass is underestimated by the FRM, and the likely source of these differences is the loss of NH_4NO_3 and semi-volatile organics, which exhibit significant seasonal dependencies (*Schwab et al.,* 2003; *Schwab et al.,* 2004bc; *Schwab et al., 2005a*). These findings have significant implications in exposure assessment and in the interpretation of the epidemiological time series studies used in the development of the $PM_{2.5}$ NAAQS. Understanding the seasonal and regional differences in $PM_{2.5}$,mass as well as any associated measurement artifacts that may exist, are critically important to the health effects community that corrects for confounders (e.g. temperature), which also correlates with volatile $PM_{2.5}$ losses. The systematic loss of seasonally averaged semi-volatile components of $PM_{2.5}$ mass by the FRM measurement technique also raises questions as to the composition and toxicological importance of the volatized species.

Implications for Accountability

Tracking the trends in $PM_{2.5,}$ photochemical oxidants, and their precursor species in response to regulatory actions is critically important to the demonstration of accountability in air quality management system. Some notable examples of important measurement/analysis activities that must be sustained to address key air quality accountability issues include: 1) tracking the impact of the NO_x SIP call on trends in NO_y and ozone air quality; 2) tracking the impact of the national 2007 diesel sulfur rule regulation on local and regional SO_2, PM (sulfate and organic, size) air quality and in the case of New York City, where additional fuel sulfur regulations are being contemplated (in heating oil and off road and marine diesel), design experiments to demonstrate the effectiveness of these interventions; and 3) tracking the introduction of new control technologies (e.g. 2007 diesel engine standard, CRT-DF diesel engine retrofits, and the use of alternate fuels, such as CNG, ethanol, gasoline-oxygenate blends, and biodiesel) for anticipated improvements and potential negative impacts on air quality.

The accountability of the air quality management process entails maintaining measurement programs to track progress made in improving the air quality in urban and regional environments in response to regulatory actions. Such measurement programs require routine monitoring as well as strategic intensive measurement studies to track the actions outlined above.

To achieve accountability in this process requires a commitment to support several strategically placed “PM Supersite-like” monitoring systems capable of supporting advanced field intensive studies as needed. These sites would be placed within and downwind of affected source regions and would be kept operational for a decade or longer over the course of the regulations' expected effectiveness.

8 QUALITY ASSURANCE AND QUALITY CONTROL

A Quality Assurance Project Plan for the EPA Particulate Matter "Supersite": $PM_{2.5}$ Technology Assessment and Characterization Study in New York (PMTACS-NY) was developed and adopted by EPA and posted on the U.S. EPA website at http://www.epa.gov/ttn/amtic/files/ambient/super/nyqapp.pdf (QAPP Version 1.1, last revised July 15, 2002) and as such adopted for the NYSERDA Joint Enhanced Ozone and PM Precursor-PMTACS-NY program as well. It defined the Data Quality Objectives and audit responsibilities for the special intensive field studies for research methods (RM) and federal reference methods (FRM) measurements that were carried out in the summer of 2001 and winter of 2004. Accordingly, all measurements that are based on (FRMs) have been audited by New York State Department of Environmental Conservation, Division of Air Resources, Bureau of Technical Support Quality Assurance Section

Research measurements have associated research protocols (RPs) that have been developed and quality assessed through specially designed quality assurance experiments based on three approaches:

(1) Filter Comparison- these start with evaluations of the filter methods
(2) Laboratory Evaluations and Comparisons- these require a substantial investment and effort to establish a benchmark facility.
(3) Instrument Inter-comparisons- these can establish "comparability and/or "agreement" often require substantial effort and/or equipment investment.

Methodology/instrument inter-comparisons were performed at the ASRC reference laboratory and/or during the field experiments. The purpose of these activities was to characterize instrument performance with regard to possible interferences, minimum detection level, precision (root mean square error) and accuracy (trueness). For all instruments (FRM and RM) a Standard Operating Procedure (SOP) was developed, approved by the QA-Manager, and posted on the PMTACS-NY web site prior to their deployment in the field.

It must be recognized that no standard reference/calibration material or FRM procedure is available from EPA for suspended, atmospheric PM (specifically chemical composition, size distribution, number concentration etc). The establishment of an aerosol generation and calibration facility under this program was essential to meeting QA objectives. The facility is briefly described in Appendix C with a more detailed accounting provided in the program QA Report.

The final Quality Assurance Report summarizes the results obtained to April 2005 with special focus on the summer 2001and the winter 2004 intensive field campaigns and is posted on the U.S. EPA website at
http://www.epa.gov/ttn/amtic/files/ambient/super/PMTACS_QA_FinalRep2005_Version5.3.pdf

9 REFERENCES

Albritton, D.L. and D.S. Greenbaum. Atmospheric Observations: Helping Build the Scientific Basis for Decisions Related to Airborne Particulate Matter. Report of the PM Measurements Research Workshop, Chapel Hill, NC, 1998.

Atkinson, R., 1997. Gas-phase tropospheric chemistry of volatile organic compounds.1: Alkanes and alkenes, *Journal of Physical and Chemical Reference Data*, *26* (2), 215-290.

Atkinson, R., 2003. Kinetics of the gas-phase reactions of OH radicals with alkanes and cycloalkanes, *Atmospheric Chemistry and Physics*, *3*, 2233-2307.

Calvert, J.G., 2000. The mechanisms of atmospheric oxidation of the alkenes, viii, 552 pp., Oxford University Press, New York.

Calvert, J.G., 2002. The Mechanisms of atmospheric oxidation of aromatic hydrocarbons, x, 556 pp., Oxford University Press, New York.

Canagaratna, M. J., J. T. Jayne, D. Ghertner, S. Herndon, Q. Shi, J. L. Jimenez , P.J. Silva, P. Williams, T. Lanni, F. Drewnick, K. L. Demerjian, C. Kolb, D. Worsnop, 2004. Chase Studies of Particulate Emissions from in-use New York City Vehicles, *Aerosol Science & Technology*, 38, 555-573.

Drewnick, F., J.J. Schwab, J.J., Hogrefe, O., Peters, S., Husain, L., Diamond, D., Weber, R., Demerjian, K.L., 2003. Intercomparison and evaluation of four semi-continuous $PM_{2.5}$ sulfate instruments, *Atmospheric Environment*, 37, 3335-3350.

Drewnick, F., J. J. Schwab, J. T. Jayne, M. Canagaratna, D.R. Worsnop, and K.L. Demerjian, 2004a. Measurement of ambient aerosol composition during the PMTACS-NY 2001 campaign using an aerosol mass spectrometer. Part I: Mass concentrations, *Aerosol Science and Technology*, 38(SI), 92-103.

Drewnick, F., J.T. Jayne, M. Canagaratna, D.R. Worsnop and K.L. Demerjian, 2004b. Measurement of ambient aerosol composition during the PMTACS-NY 2001 campaign using an aerosol mass spectrometer. Part II: Chemically speciated mass distribution, *Aerosol Science and Technology*, 38(SI):104-117.

Drewnick, F., S.S. Hings, P.F. DeCarlo, J.T. Jayne, M. Gonin, K. Fuhrer, S. Weimer, J.L. Jimenez, K.L. Demerjian, S. Borrmann, D.R. Worsnop, 2005. A new time-of-flight aerosol mass spectrometer (ToF-AMS) – Instrument description and first field deployment. *Aerosol Science &. Technology*, 39:637–658

Dutkiewicz, V. A., S.Qureshi, A.R. Khan, V. Ferrara, J. Schwab, K. Demerjian, L. Husain, 2004. Sources of fine particulate sulfate in New York, *Atmospheric Environment*, 38, 3179-3189.

Dutkiewicz, V.A., S. Qureshi, A.R. Khan, L. Husain, J. J. Schwab, and K. L. Demerjian, 2006a. Field test data for 42 liter per minute $PM_{2.5}$ aerosol sampler used to collect 6-hr aerosols samples during the PMTACS-NY Intensives held at Queens College, Queens, NY, *Atmospheric Environment*, 40, S182-S191.

Dutkiewicz, V.A., S. Qureshi, L. Husain, J. J. Schwab, and K. L. Demerjian, 2006b. Elemental Composition of $PM_{2.5}$ Aerosols in Queens, New York: Evaluation of sources of fine-particle mass, *Atmospheric Environment*, 40, S347-S359.

Federal Register, Vol. 62(138), Friday July 18, 1997, 40 CFR Part 50.

Forstner, H.J.L., R.C. Flagan, and J.H. Seinfeld, 1997. Molecular speciation of secondary organic aerosol from photooxidation of the higher alkenes: 1-octene and 1-decene, *Atmospheric Environment*, *31* (13), 1953-1964.

Grosjean, D., and J.H. Seinfeld, Parameterization of the formation potential of secondary organic aerosols, *Atmospheric Environment*, *23* (8), 1733-1747, 1989.

Heard, D.E., and M.J. Pilling, Measurement of OH and HO_2 in the troposphere, 2003. *Chemical Reviews*, *103* (12), 5163-5198.

Hering, S., P.M. Fine, C. Sioutas, P.A. Jacques, J.L. Ambs, O. Hogrefe and K.L. Demerjian, 2004. Field assessment of the dynamics of the particulate nitrate vaporization using differential TEOM and automated nitrate monitors, *Atmospheric Environment*, 38, 5183-5192.

Hering, S., Hogrefe O., Lala G.G., Demerjian, K.L. (2004a). Field evaluation of the Quant-400 Laminar-Flow, water-based condensation particle counter (WCPC) Queen's College, NY. PMTACS-NY Queens College Winter 2004 Field Intensive Data Workshop, June 15, Albany, NY.

Hering, S.V., Hogrefe, O., Lala, G., Demerjian, K.L. (2004b). Field Evaluation of a Laminar-Flow, water-based condensation particle counter (poster). 23rd Annual AAAR Conference, Atlanta, Georgia, October 4-8.

Herndon, S. C., J.H. Shorter, M.S. Zahniser, D.D. Nelson, J.T. Jayne, R.C. Brown, R.C. Miake-Lye, I.A. Waitz, P. Silva, T. Lanni, K.L. Demerjian, C. E. Kolb, 2004. NO and NO_2 emissions ratios measured from in use commercial aircraft during taxi and rake-off, *Environmental Science and Technology*, 38, 6078-6084.

Herndon, S.C., T.B. Onasch, B.P. Frank, L.C. Marr, J.T. Jayne, R.C. Brown, R.C. Miake-Lye, I.A. Waitz, P. Silva, T. Lanni, K. L. Demerjian, C.E. Kobe, 2004, NO and NO_2 emissions ratios measured from in use commercial aircraft during taxi and take off, *Environmental Science and Technology,* 38, 6078-6084.

Herndon, S.C., J.H. Shorter, M. S. Zahniser, J. Wormhoudt, D. D. Nelson, K. L. Demerjian and C. E. Kolb, 2005. Real-time measurements of SO_2, CO and CH_4 emissions from in-use curbside passenger buses in New York City using a chase vehicle, *Environmental Science and Technology*, 39, 7984-7990.

Heywood, J.B., *Internal Combustion Engine Fundamentals*, McGraw-Hill, Inc., 1988.

Hoffmann, T., J.R. Odum, F. Bowman, D. Collins, D. Klockow, R.C. Flagan, and J.H. Seinfeld, 1997. Formation of organic aerosols from the oxidation of biogenic hydrocarbons, *Journal of Atmospheric Chemistry*, *26* (2), 189-222.

Hogrefe, O., F. Drewnick, G.G. Lala, J. J. Schwab, and K.L. Demerjian, 2004a. Development, operation and applications of an aerosol generation, calibration and research facility, *Aerosol Science and Technology*, 38(SI): 196-214.

Hogrefe, O., J. Schwab, F. Drewnick, K. Rhoads, G.G. Lala, H.D. Felton, O.V. Rattigan, L. Husain, V.A. Dutkiewicz, S. Peters, and K.L. Demerjian, 2004b. Semi-continuous $PM_{2.5}$ sulfate and nitrate

measurements at an urban and a rural location in New York: PMTACS-NY Summer 2001 and 2002 campaigns, *J. Air & Waste Manage. Assoc*., 54, 1040-1060.

Hogrefe, O., G. G. Lala, B.P. Frank, J.J. Schwab, K. L. Demerjian, 2006. Field evaluation of a TSI Model 3034 Scanning Mobility Particle Sizer in New York City: Winter 2004 Intensive Campaign, *Aerosol Science and Technology*, 40:753-762.

Horii, C. V., M. S. Zahniser, D. Nelson, J. B. McMannus, and S. C. Wofsy (1999), Nitric acid and nitrogen dioxide flux measurements: a new application of tunable diode laser absorption spectroscopy, *SPIE Proc*., 3758, 152-161.

Kado, N.Y., R.A. Okamoto, P.A. Kuzmicky, R. Kobayashi, A. Ayala, M.E. Gebel, P.L. Rieger, C. Maddox, L. Zafonte, 2005. Emissions of toxic pollutants from compressed natural gas and low sulfur diesel-fueled heavy-duty transit buses tested over multiple driving cycles, *Environmental Science & Technology*, 39(19), 7638-7649.

Kirchstetter, T.W., R.A. Harley, N.M. Kreisberg, M.R. Stolzenburg, and S. Hering, On-road measurement of fine particle and nitrogen oxide emissions from light and heavy-duty motor vehicles, *Atmospheric Environment*, *33*, 2955-2968, 1999.

Kittelson, D., Engines and Nanoparticles: A Review, *Journal of Aerosol Science*, *29* (5/6), 575-588, 1998.

Kim, E., P.K. Hopke, 2004. Improving source identification of fine particles in a rural northeastern U.S. area utilizing temperature-resolved carbon fractions, *J.Geophys. Res*., 109, D09204, doi:10.1029/2003JD004199.

Kleindienst, T.E., D.F. Smith, W. Li, E.O. Edney, D.J. Driscoll, R.E. Speer, and W.S. Weathers, 1999. Secondary organic aerosol formation from the oxidation of aromatic hydrocarbons in the presence of dry submicron ammonium sulfate aerosol, *Atmospheric Environment*, *33* (22), 3669-3681.

Kolb, C. E., S.C. Herndon, J.B. McManus, J.H. Shorter, M.S. Zahniser, D.D. Nelson, J.T. Jayne, M.R. Canagaratna, D.R. Worsnop, 2004. Mobile laboratory with rapid response instruments for real-time measurements of urban and regional trace gas and particulate distributions and emission source characteristics, environmental science and technology 21, 5694-5703.

Lala, G.G, Hogrefe, O., and Demerjian, K.L. (2005). Aerosol distributions: a comparison from summer and winter field campaigns in Queens, New York**.** particulate matter supersites program and related Studies**:** An AAAR International Specialty Conference, Atlanta, Georgia, February 7-11.

Lala, G.G., Hogrefe, O., Demerjian, K.L. (2003). Aerosol size distributions: A comparison of measurements from urban and rural sites (poster). AAAR Conference “Particulate Matter: Atmospheric Sciences, Exposure and the Fourth Colloquium on Particles and Human Health”, Pittsburgh, Pennsylvania, March 31 - April 4.

Lanni, T.; Frank, B. P.; Tang, S.; Rosenblatt, D.; Lowell, D., "Performance and emissions evaluation of compressed natural gas and clean diesel buses at New York City's Metropolitan Transit Authority", 2003, SAE Technical Paper 2003-2001-0300.

Li, Y.Q., K.L. Demerjian, M.S. Zahniser, D.D. Nelson, J.B. McManus and S.C. Herndon, 2004a. Measurements of formaldehyde, nitrogen dioxide, and sulfur dioxide at Whiteface Mountain using a dual tunable diode laser system, *J. Geophys. Res*. 109, D16S08, doi:10.1029/2003JD004091.

Li, Y.J. Schwab, K.L. Demerjian, 2006. Measurements of ambient ammonia using a tunable diode laser absorption spectrometer: characteristics of ambient ammonia emissions in an urban area of New York City, *J. Geophys. Res*. 111, D10S02, doi:10.1029/2005JD006275.

Li, Z., P.K. Hopke, L.Husain, S. Qureshi, V.A. Dutkiewicz, J.J. Schwab, F. Drewnick, and K.L. Demerjian, 2004b. Sources of fine particle composition in New York City, *Atmospheric Environment* 38, 6521-6529.

NARSTO, 2000. An Assessment of Tropospheric Ozone Pollution --A North American Perspective. NARSTO Management Office (Envair), Pasco, Washington.

Nelson, D. D., M. S. Zahniser, J. B. Mcmanus and J. H. Shorter (1996), Recent improvements in atmospheric trace gas monitoring using mid-infrared tunable diode lasers, *Proc. SPIE*, 2834, 148-159.

Odum, J.R., T. Hoffmann, F. Bowman, D. Collins, R.C. Flagan, and J.H. Seinfeld, 1996. Gas/particle partitioning and secondary organic aerosol yields, *Environmental Science & Technology*, *30* (8), 2580-2585.

Odum, J.R., T.P.W. Jungkamp, R.J. Griffin, R.C. Flagan, and J.H. Seinfeld, 1997. The atmospheric aerosol-forming potential of whole gasoline vapor, *Science*, *276* (5309), 96-99.

Pandis, S.N., R.A. Harley, G.R. Cass, and J.H. Seinfeld, 1992. Secondary organic aerosol formation and transport, *Atmospheric Environment Part a-General Topics*, *26* (13), 2269-2282.

Patashnick, H. and E.G. Rupprecht, 1991. Measurements using the tapered element oscillating microbalance, *J. Air & Waste Manage. Assoc.*, 41:1079-1083.

Patashnick, H., G. Rupprecht, J.L. Ambs, and M.B. Meyer, 2001. Development of a reference standard for particulate matter mass in ambient air, *Aerosol Sci. Tech*., 34:42-45.

Pitz, M., J. Cyrys, E. Karg, A. Wiedensohler, h.-E. Wichmann, J. Heinrich, 2003. Variability of apparent particle density of an urban aerosol, *Env. Sci. and Tech.*, *37* (19), 4336-4342.

Prucz, J.C., N.N. Clark, M. Gautam, and D.W. Lyons, 2001. Exhaust emissions from engines of the detroit diesel corporation in transit buses: A decade of trends, *Environmental. Science and Technology*, *35* (9), 1755-1764.

Qureshi, S., V. A. Dutkiewicz, K. Swami, K. X. Yang, L. Husain, J. J. Schwab, and K. L. Demerjian, 2006. Elemental composition of $PM_{2.5}$ aerosols in Queens, New York: Solubility and temporal trends, *Atmospheric Environment*, 40, S238-S251.

Rattigan, O.V., O. Hogrefe, H.D. Felton, J. J. Schwab, U. K. Roychowdhury and K. L. Demerjian, 2006. Multi-year urban and rural semi-continuous $PM_{2.5}$ sulfate and Nitrate measurements in New York State: Evaluation and comparison with filter based measurements, *Atmospheric Environment*, 40, S192-S205.

Ren, X., Harder, H., Martinez, M., Lesher, R.L., Oliger, Shirley, A.T., Adams, J., Simpas, J.B., Brune, W.H., 2003a. HOx concentrations and OH reactivity observations in New York City during PMTACS-NY 2001, *Atmospheric Environment*, 37, 3627-3637.

Ren, X., Harder, H., Martinez, M., Lesher, R.L., Oliger, Simpas, J.B., Brune, W.H., Schwab, J.J., Demerjian, K.L., He, Y., Zhou, X., Gao, H., 2003b. OH and HO_2 chemistry in the urban atmosphere of New York City, *Atmospheric Environment*, 37, 3639-3651.

Ren, X., W.H. Brune, J. M., M. J. Mitchell, R.L. Lesher, A.R. Metcalf, J. B. Simpas, J. J. Schwab, K. L. Demerjian, H.D. Felton, G. Boynton, Y. He, X. Zhou, and J. Hou, 2006. Behavior of OH and HO_2 in the winter atmosphere in New York City, *Atmospheric Environment*, 40, S252-S263.

Ren, X., William H. Brune, Angelique Oliger, Andrew R. Metcalf, James B. Simpas, Terry Shirley, James J. Schwab, Chunhong Bai, Utpal Roychowdhury, Yongquan Li, Chenxia Cai, Kenneth L. Demerjian, Yi He, Xianliang Zhou, Honglian Gao, and Jian Hou, 2006. OH, HO_2 and OH reactivity during the PMTACS–NY Whiteface Mountain 2002 campaign: Observations and model comparison, *J. Geophys. Res.*, 111, D10S03, doi:10.1029/2005JD006126.

Seinfeld, J.H and S.N. Pandis, 1998. Atmospheric Chemistry and Physics: From Air Pollution to Climate Change, John Wiley & Sons, Inc., New York, New York.

Sillman, S., 1995. The use of NO_y, VII.$1O_2$, and HNO_3 as indicators for O_3-NO_x-VOC sensitivity in urban areas, *J. Geophys. Res*. 100D:14175-14188

Schwab, J.J., J. Spicer, H.D. Felton, J.A. Ambs, and K.L. Demerjian, 2003. Long-term comparison of TEOM, SES TEOM and FRM measurements at rural and urban New York sites, in Symposium on Air Quality Measurements and Technology – 2002I, VIP-115-CD, ISBN 0-923204-50-4, Air and Waste Management Association, Pittsburgh, PA.

Schwab, J.J., H.D. Felton, and K.L. Demerjian, 2004a. Aerosol chemical composition in New York State from integrated filter samples: Urban/rural and seasonal contrasts, *J. Geophys. Res*., 109, D16S05, doi:10.1029/2003JD004078.

Schwab, J.J., J. Spicer, K.L. Demerjian, J.L. Ambs, and H.D. Felton, 2004b. Long-term field characterization of TEOM and modified TEOM samplers in urban and rural New York State locations, *J. Air & Waste Manage*., 54, 1264-1280.

Schwab, J.J., O. Hogrefe, K.L. Demerjian, J.L. Ambs, 2004c. Laboratory characterization of modified TEOM samplers, *J. Air & Waste Manage.*, 54, 1254-1263.

Schwab, J.J., Y.-Q. Li, and K.L. Demerjian, 2004d. Semi-continuous formaldehyde measurements with a diffusion scrubber/liquid fluorescence analyzer. In Symposium on air quality measurement methods and technology – 2004 [CD-ROM], Air and Waste Management Association, Pittsburgh, PA, USA.

Schwab, J.J., H.D. Felton, O.V. Rattigan, and K.L. Demerjian, 2006a. New York State urban and rural measurements of continuous $PM_{2.5}$ mass by FDMS TEOM and BAM J. *Air & Waste Manage. Assoc*. 56:372-383.

Schwab, J.J., O. Hogrefe, K. L. Demerjian, V. A. Dutkiewicz, L. Husain, H. D. Felton, 2006b. Field and Laboratory Evaluation of the Thermo Electron 5020 Sulfate Particulate Analyzer, *Aerosol Sci. Tech.*, 40(S1): 36-44.

Shorter, J.J, S.C. Herndon, M. S. Zahniser, D. D. Nelson, J. Wormhoudt, K.L. Demerjian, C. E. Kolb, 2005. Real-time measurements of Nitrogen Oxide emissions from in-use New York City transit buses using a chase vehicle, *Environmental Science and Technology*, 39, 7991-8000.

Tang, M, An estimation of SOA yield from VOC oxidation in NYC, University at Albany, Department of Earth and Atmospheric Science, MS Thesis April 2006.

Turpin, B.J., and H.J. Lim (2001), Species contributions to $PM_{2.5}$ mass concentrations: Revisiting common assumptions for estimating organic mass, *Aerosol Science & Technology 35*, 602–610.

Venkatachari, P., L. Zhou, P. K. Hopke, H. D. Felton, O. Rattigan, J. J. Schwab, K. L. Demerjian, 2006a. Spatial and temporal variability of black Carbon in New York City, *J. Geophys. Res*., 111, D10S05, doi:10.1029/2005JD006314.

Venkatachari, P., L. Zhou, P.K. Hopke, J.J. Schwab, K.L. Demerjian, S. Weimer, O. Hogrefe, D. Felton, O. Rattigan, 2006b. An intercomparison of measurement methods for carbonaceous aerosol in the ambient air in New York City, *Aerosol Sci. Tech*., 40(S1): 1-8.

Weimer, S., F. Drewnick, O. Hogrefe, J. J. Schwab, K. Rhoads, D. Orsini, M. Canagaratna, D. R. Worsnop, K. L. Demerjian, Size-selective non refractory ambient aerosol measurements during the PMTACS-NY 2004 Winter Intensive in New York City, *J. Geophys. Res*. 111, D18205, doi10.1029/2006JD007215.

Yanowitz, J., R.L. MCCormick, and M.S. Graboski, In-use emissions from heavy-duty diesel vehicles, *Env. Sci. and Tech.*, *34* (5), 729-740, 2000.

Zahniser, M.S., D.D. Nelson, J.B. McManus, and P.L. Kebabian, Measurement of trace gas fluxes using tunable diode laser spectroscopy, *Phil. Trans. R. Soc. Lond. A*, *351*, 371-382, 1995.

Zhang, Q., M.R. Alfarra, D.R. Worsnop, J.D. Allan, H. Coe, M.R. Canagaratna, and J.L. Jimenez, Deconvolution and quantification of hydrocarbon-like and oxygenated organic aerosols based on aerosol mass spectrometry, *Environmental Science & Technology*, *39* (13), 4938-4952, 2005.

Zhang, Q., M.R. Canagaratna, J.T. Jayne, D.R. Worsnop, and J.L. Jimenez (2005a), Time and size-resolved chemical composition of submicron particles in Pittsburgh – Implications for aerosol sources and processes, *Journal of Geophysical Research 110*, D07S09, doi: 10.1029/2004JD004649.

Zhang, Q., D.R. Worsnop, M.R. Canagaratna, and J.L. Jimenez (2005b), Hydrocarbon-like and oxygenated organic aerosols in Pittsburgh: Insights into sources and processes of organic aerosols, *Atm.Chem. Phys. Discuss 5*, 8421- 8471.

Graduate Students Mentored under this Program:

Sarah Peters, MS Thesis Title: “Performance of a Particle Into Liquid Sampler with Ion Chromatography with Field and Laboratory Analyses”, Graduation Fall 2002.

Rachelle Jenkins, MS Thesis Title: “An Analysis of IMPROVE data from 1988 through 2003 and an Analysis and Comparison of two New York State Sites for Ozone Production Efficiency”, Graduation Spring 2006.

Mingyu Tang, MS Thesis Title: “An Estimate of SOA Yield from VOC Oxidation in NYC”, Graduation Spring 2006.

Chenxia Cai, PhD Thesis Title: “Implementation and Performance Evaluation of An Air Quality Forecast Modeling System (AQFMS) For Northeastern USA”, Graduation Spring 2006

.

APPENDIX A. SCIENCE POLICY QUESTIONS AND RELATED HYPOTHESES

A series of outstanding $PM_{2.5}$ science policy questions raised by the scientific and regulatory communities provided the basis for three objectives of the Joint Enhanced Ozone and PMTACS-NY program. The project in turn identified a series of hypotheses associated with these science-policy questions to be tested under the program. The linkage between the science-policy questions and hypothesis are presented in Table A.1. As the program evolved and scientific results emerged, some of the initial proposed hypothesis became less relevant and new hypotheses were considered.

Table A.1. Joint Enhanced Ozone/PMTACS-NY Science Policy Questions and Related Hypotheses

1. Will urban/regional atmospheres have a non-linear response of PM10/$PM_{2.5}$ mass or composition to changes in precursor source gases (NOx, SO_2, VOCs)?
   H1.Trends in historical and PMTACS measurements of PM mass and SO_4= and NO_3- species provide direct evidence for a nonlinear response to Title IV emission reduction, and H2. PM10/$PM_{2.5}$ *sulfate and nitrate production efficiencies are directly proportional to ozone production efficiencies.*

2. Can chemical source signatures be effectively applied to attribute specific source contributions to monitored species components (e.g. SO_4=, NO_3- or carbon)? Can source attribution and/or multivariate/factor analysis techniques distinguish the contribution of local production versus regionally transported $PM_{2.5}$ mass?
   H3. PM Fe/Mg ratios provide an effective signature of oil derived combustion aerosol; H4. PM V/Se ratios provide an effective signature of coal vs. oil derived aerosol on the regional scale; H5. PM As/Se ratios provide an effective signature of mid-western vs. Canadian derived aerosols; and H6. Enhanced PM composition and gas phase measurements provide an effective means for distinguishing the contribution of local vs. regional source types/classes within the study region.

3. What are the sources of $PM_{2.5}$ affecting NY city/Upstate NY regional air quality?
   H7. NYC summertime SO_4 is dominated by local SO_2 gas to particle transformation; and H8. Regional SO_4 in New York State is dominated by long range transport of transformed SO_2 emissions from out of state sources.

4. What fraction of the urban/regional $PM_{2.5}$ mass is semi-volatile organic matter? Are biogenic emissions a significant source of the semi-volatile organic matter $PM_{2.5}$ mass fraction found in urban/regional atmospheres?
   H9. Biogenic hydrocarbons represent a significant source of the semi-volatile organic matter mass fraction of warm season regional $PM_{2.5}$ *mass.*

5. Is NH3 concentration a limiting reagent in the production of NH_4NO_3 in the urban/regional environment? If so, will reductions in SO_2 through Title IV controls and proposed reductions in sulfur in fuels result in an increased fraction of $PM_{2.5}$ mass as nitrate?
   H10. Changes in ambient PM sulfate mass fraction are anti-correlated with changes in the ambient PM nitrate mass fraction.

6. What are the air quality benefits (or negative consequences) of a CNG Bus Fleet and CRT-DPF Diesel Fleet Deployment?
   H11. CNG-fueled buses in New York City show measurable reductions of vehicle NO, SO_2 and PM emissions, with minimal negative consequences (i.e. increases in CO and PM Ultrafine) as compared with their diesel counterparts; and H12. CRT control technology with low sulfur fuels in retrofitted diesel buses in New York City shown measurable reductions of vehicle NO, SO_2 and PM emissions, with minimal negative consequences (increases in CO and PM Ultrafine) as compared with standard diesel buses.

7. Are there observable changes in NO_2, SO_2, CO and PM air quality as a result of the CNG/CRT vehicle fleet deployments?
H13. The deployment of CNG-fueled and CRT-retrofitted diesel fleets show measurable reductions in ambient NO, SO2, CO, and PM concentrations at the one or more of the PMTACS urban monitoring sites.

8. Is the EPA designate FRM for $PM_{2.5}$ mass an accurate measurement of the mass of atmospheric $PM_{2.5}$? Does the measurement method have any systematic bias, and if so, is it species correlated?
H14. The EPA designated filter based reference method underestimates the actual atmospheric PM2.5 *mass by more than 30% as a result of volatile species losses; and H15. Water management and temperature control of existing continuous automated mass, total sulfur, and nitrogen species measurement systems represent a major improvement in* PM2.5 *measurement technology.*

9. Is $PM_{2.5}$ mass an appropriate surrogate measurement for characterizing regional haze?
H16. Measurements of the optical properties of the atmosphere (aerosol light scattering and absorption) using fixed and remote sensing systems provide an effective means for verifying the existence and extent of regional haze and correlate with surface measurements of PM2.5 *mass.*

10. Are aerosols an effective delivery mechanism for specific gaseous pollutants (e.g. air toxics, oxidants) into the deep lung? What is the role of liquid water in this delivery mechanism?
H17. Quantitative amounts of gaseous pollutants (e.g. PAH, CO, xylene, trichloroethylene, etc.) are absorbed on PM and are detectable by Aerosol Mass Spectrometer (AMS) and Single Particle Laser Ablation Time of Flight Mass Spectrometer (SPLAT-MS) analytical techniques; H18. PM chemical composition varies by aerodynamic size, which in turn varies in time and with temperature and season resulting in complex variations in chemical inhalation exposures; and H19. Heterogeneous processes contribute to the oxidizing capacity of the atmosphere resulting in significant production of PM2.5 *mass.*

The results from this study have been organized around long -term research measurement at two regional monitoring sites at Pinnacle State Park and Whiteface Mountain, two urban monitoring sites in metropolitan New York (IS-52 and Queens College), and three intensive field study campaigns performed during the PMTACS-NY program.

The findings presented are associated with citations to papers from research conducted within the program objectives and the related science policy questions. Although most of the science policy questions have been addressed, some results are inconclusive and those questions that remain outstanding require additional data and/or further analyses to answer.

Hence, the results and findings summarized in this report highlight the most prominent and expeditious analyses that support the identified program objectives and proposed hypotheses and science policy questions.

APPENDIX B. MEASUREMENTS SYSTEMS AND OPERATION SCHEDULES

The regional air quality research measurements have been operational at this Whiteface Mountain since 1988 and Pinnacle State Park since 1995. The measurements covered by this contract included the period 1998-2005 for the Whiteface Mountain and Pinnacle State Park sites and July 2001 to December 2005 for the two urban sites. The baseline suite of measurements in 1998 consisted of ozone, ozone precursor gases, sulfur dioxide, and supporting micrometeorology parameters. The major emphasis at that point was ozone and oxidant production. Details of the gaseous measurements are listed in Table B.1. With the promulgation of the fine particle ($PM_{2.5}$) standard in 1997-98, a second major measurement focus on fine particulate matter was added at these sites starting in 2000 at the regional/rural sites and in 2001 at the urban sites.

These included continuous measurements of fine particle mass (sometimes as many as four simultaneous instruments), FRM filters for $PM_{2.5}$ mass, sets of filters for chemical composition by both the STN and IMPROVE networks, continuous measurement of fine particle sulfate and carbon, and aerosol scattering using a white light nephelometer. The details of the integrated filter measurements, the continuous $PM_{2.5}$ measurements, and the micrometeorology measurements are listed in Tables B.2, B.3, and B.4, respectively.

Table B.1. Ozone and ozone precursor gas measurements at Whiteface Mountain and Pinnacle State Park

Trace Gas	Instrument Manufacturer and Model	Measurement Method	Dates of Measurement	Data Frequency	Measurement Range	Minimum Detection Limit
Ozone (O_3)	Thermo Model 49	UV Absorption	7/1/1995 – present	five-Minute/ Hour averages	1-1000 ppbv	2 ppbv
Nitric Oxide (NO)	Thermo Model 42S	Chemi-luminescence (CL)	7/1/1995 – present	five-Minute/ Hour averages	0-50 ppbv	0.06 ppbv
Nitrogen Dioxide (NO_2)	Photolysis and Thermo Model 42S	Arc Lamp Photolysis of NO_2 followed by CL	7/1/1997 - present	five-Minute/Hour averages	0-50 ppbv	0.15 ppbv
Total Oxides of Nitrogen (NO_Y)	Molybdenum Converter and Thermo Model 42S	Heated molybdenum converter followed by CL	7/1/1995 - present	five-Minute/Hour averages	0-50 ppbv	0.12 ppbv
Nitric Acid (HNO_3)	Denuder, molybdenum converter and Thermo 42S	NaCl denuder, heated molybdenum converter and CL	12/16/1999 - present	five-Minute/Hour averages	0-50 ppbv	0.25 ppbv
Carbon Monoxide (CO)	Thermo Model 48S	Non-dispersed Infrared (NDIR) gas filter correlation with native zeroing	7/1/1995 – present (Native zero began 5/96)	five-Minute/Hour averages	0-1000 ppbv	10 ppbv
Sulfur Dioxide (SO_2)	Thermo Model 43BS	Pulsed Fluorescence	7/1/1995 - present	five-Minute/Hour averages	0-50 ppbv	0.06 ppbv

Ozone and ozone precursor measurements are also available from NYSDEC at IS52 South Bronx and Queens College sites.

Table B.2. Ongoing integrated filter measurements at the Whiteface Mountain, Pinnacle State Park, South Bronx(IS-52) and Queens College sites*

Program	Start Date	Frequency	Duration	Target Species
EPA FRM[1]	8/1999	Daily	24 hour	$PM_{2.5}$ mass
EPA STN[2]	2/2001	Every 3rd day	24 hour	$PM_{2.5}$ mass, EC/OC, ions, and elements
IMPROVE[3]	4/2001	Every 3rd day	24 hour	$PM_{2.5}$ mass, PM_{10} mass, EC/OC, ions, and elements

Table 2 Notes:

1. Environmental Protection Agency, Federal Reference Method (in collaboration with New York State Department of Environmental Conservation – NYSDEC).
2. Environmental Protection Agency Speciation Trends Network (in collaboration with NYSDEC). Whiteface Mountain frequency every 6th day
3. Interagency Monitoring of Protected Visual Environments (in collaboration with NYSDEC), Pinnacle State Park and IS-52 SB sites only

Table B.3. Ongoing continuous and semi-continuous aerosol measurements during Joint NYSERDA-EPA PMTACS-NY Supersite Monitoring

9.1.1 Parameter	Sites	Dates of Measurement	Method	Time Resolution	Detection Limit
$PM_{2.5}$ Mass	WFML, PSP, SB, QC	8/1999 - present	TEOM Mass Monitor	10 minute running avg.	1.5 $\mu g/m^3$
$PM_{2.5}$ Mass	PSP, SB, QC	3/2003 - present	FDMS TEOM (Filter differential method)	12 minute switched	1.5 $\mu g/m^3$
PM_{10} Mass	PSP, SB, QC	7/2005 - present	TEOM Mass Monitor	10 minute running avg.	1.5 $\mu g/m^3$
$PM_{2.5}$ EC/OC	PSP, SB	7/2004 - present	Sunset Labs Carbon Aerosol Analyzer	1 hour	0.2 $\mu gC/m^3$
$PM_{2.5}$ Sulfate	WFML[1], PSP, SB[1], QC	7/2004 – 11/2004; 10/2005 - present	Thermo 5020 Sulfate Particulate Analyzer	15 minute or 1 hour	0.3 $\mu g/m^3$
Aerosol Scattering Coefficient	WFML, PSP, SB	7/2001 - present	Integrating white light nephelometer with $PM_{2.5}$ size selective inlet	10 minutes	0.8 Mm^{-1}

*Sites: Whiteface Mountain Summit and Lodge: WFMS, WFML; Pinnacle State Park, Addison, NY: PSP, I.S. 52 South Bronx: SB; Queens College: (QC) permanent shelter to be constructed (eta -May 15, 2005) on QC campus until then 8x8 trailer QC and PS 219 roof QC(PS219).

[1] Operating R&P8400S

Table B.4. Supporting micrometeorological measurements at WFM and PSP

9.1.2 Parameter	Dates of Measurement	Method	Time Resolution	Detection Limit
Temperature	7/1995 – present	Solid State Thermistor	1 minute	N/A
RH	7/1995 – present	Thin Film Capacitor	1 minute	N/A
WS/WD	7/1995 – present	Cup Anemometer / Wind Vane	1 minute	N/A
BP	7/1995 – present	Solid State Transducer	1 minute	N/A
Precipitation	5/1996 – present	Tipping Bucket	1 minute	N/A
Solar Radiation	7/1995 - present	Pyranometer	1 minute	N/A

Data for all continuous and semi-continuous measurements are processed and archived at ASRC. Over the duration of the contract, three different data analysts have worked at ASRC reducing, validating and archiving these data. Data base files prepared prior to 2000 are available in a

format established under the NARSTO-Northeast program (The Addison site was originally established as a NARSTO-Northeast surface measurement station.). Data base files prepared in 2000 and later are available in the NARSTO-Northeast format, and the hour-averaged data is available in the revised NARSTO data base format established for the EPA PM Supersites Program. The data from 2000-2005 has been submitted to the PM Supersites Data Management Team, where it is reviewed for consistency with all data base requirements and Quality Assurance checks and submitted to NARSTO Quality Systems Science Center (QSSC). A description of and access to the archived data files is provided in Appendix D.

APPENDIX C. ASRC AEROSOL FACILITY AND APPLICATIONS

The accurate measurement of atmospheric trace components typically requires calibration standards of known quality to challenge the analytical system performing the measurement. Calibration standards for atmospheric trace gases are directly available from the National Institute Standards and Technology or third parties that prepare traceable secondary standards. There are no such traceable standards for particulate matter/aerosols. In anticipation of expanding research measurement programs into the areas of particulate matter mass and composition as well as aerosol characterization, the Atmospheric Science Research Center, U-Albany embarked on the development of an aerosol generation, calibration, and research facility in 1998. The major purpose for developing the facility was to provide aerosol calibration standards under controlled environmental conditions through the application of reproducible aerosol generation and chemical and physical characterization techniques. These calibration standards would be used for evaluating aerosol instrumentation, including quality assurance testing, intercomparison, performance evaluation, and calibration of aerosol sizing, bulk, and speciated mass-measuring instruments. In addition, the aerosol facility was designed to provide excellent opportunities to carry out basic aerosol research including the study of photochemical secondary organic aerosol formation.

The Aerosol Generation, Calibration and Research Facility is described in detail in Hogrefe et al., 2004 and consists of two major components: 1) a PM Laboratory (PMLab), which is equipped to generate, characterize and transform (photochemical and thermal) aerosols with diameters >40 nm (Figure C-1); and 2) a Small Particle Laboratory (SPLab) equipped to generate and sample test aerosols in the 5-500 nm diameter range. Main components of the Aerosol Generation, Calibration, and Research Facility are shown in Figure C-2.

Figure C-1. Aerosol Generation, Calibration and Research Facility.

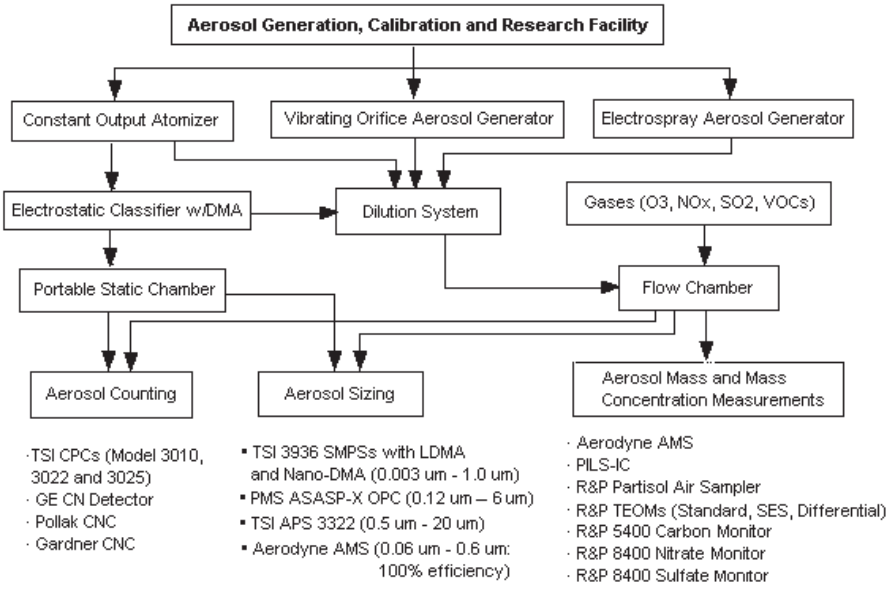

Figure C-2. Schematic of the Aerosol Generation, Calibration, and Research Facility; generation methods for small insoluble particles (propane torch, hot tungsten wire) are not shown here**.**

The aerosol facility has capabilities for generation of aerosols of various composition (organic, inorganic, mixed), solubility, size (3nm <D< 20 μm), and concentration (5-1000 $\mu g/m^3$). Depending on study objectives, polydisperse or monodisperse aerosol can be generated. In most cases stable concentrations of aerosols can be generated for several hours and even days (if needed). Some of generated aerosols can be used for instrument calibration (see next section).

Generation system is used to produce polydisperse aerosols using a spray-atomization method. This aerosol can be further sized to produce monodisperse particles. Other methods of particle generation include using a Vibrating Orifice Generator (TSI Inc., Model 3450), Electrospray Generator (TSI Inc., Model 3480), hot tungsten wire, and propane torch burning. Both laboratories are equipped with ducts to access outside air if needed.

The aerosol facility also includes a dilution system; a slow-flow, a fast flow and a portable static aerosol chamber; aerosol measurement and characterization instrumentation; and data acquisition, storage, and processing equipment (Figure C-2). A schematic of a main aerosol generation and dilution system is shown in Figure C-3. Particle-free filtered air from an oil free compressor is used for aerosol generation and dilution. This air is also ideal for an accurate determination of instrument blank corrections.

The generated aerosols are always conditioned and equilibrated in one of the aerosol chambers prior to sampling. The fast-flow chamber and/or the portable, static chamber are used for experiments with aerosol particles in 0.005 – 0.2 μm diameter range. These particles are mainly used for calibration and evaluation of the performance of aerosol counting and sizing instrumentation.

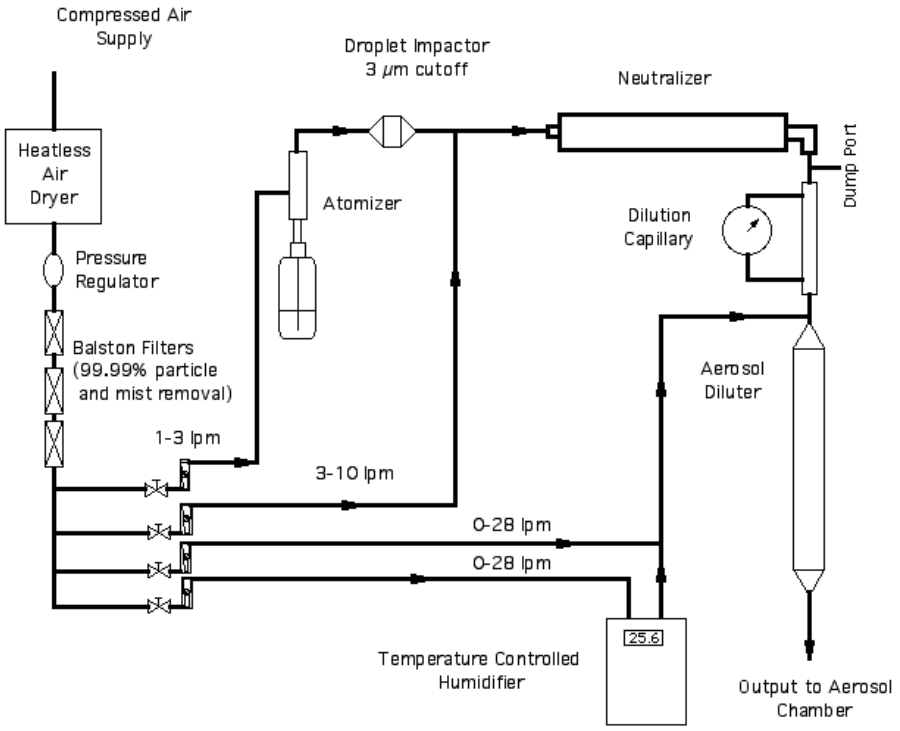

Figure C-3. The PMLab aerosol generation and dilution system.

The 450L glass slow-flow chamber is used mainly for the dilution, equilibration, and controlled humidification of generated primary aerosol particles larger than 50 nm as well as for the generation of secondary aerosols through the choice of appropriate precursor reactants.

ASRC Aerosol Facility was used in the Joint Enhanced Ozone and PM Precursor/$PM_{2.5}$ Technology Assessment and Characterization Study in New York to:

1) Evaluate and test new instrumentation prior to field and laboratory deployments
2) Test instrumentation following field campaigns to help interpret field data
3) Calibrate conventional and new instrumentation before and after field campaigns for quality assurance
4) Intercompare instrumental methods for the measurement of aerosol size and composition
5) Optimize operating conditions for aerosol and PM instrumentation

The full description of Aerosol Facility and the details of the instrument performance evaluations performed under this study can be found in the final Quality Assurance Report for this Joint NYSERDA/U.S. EPA program which, is posted on the U.S. EPA website at http://www.epa.gov/ttn/amtic/files/ambient/super/PMTACS_QA_FinalRep2005_Version5.3.pdf.

APPENDIX D. ARCHIVED DATA SETS

The following data files reside in the NARSTO permanent archive web-site: http://eosweb.larc.nasa.gov/PRODOCS/narsto/table_narsto.html#new_york. The archive includes metadata details and all measurements collected under the NYSERDA/U.S. EPA sponsored program.

1. EPA_SS_NY_IS52_P+G_DEC_CAMS_20000101_182_V1.csv
2. EPA_SS_NY_IS52_P+G_DEC_CAMS_20000701_184_V1.csv
3. EPA_SS_NY_IS52_P+G_DEC_CAMS_20010101_181_V1.csv
4. EPA_SS_NY_IS52_P+G_DEC_CAMS_20010701_184_V1.csv
5. EPA_SS_NY_IS52_P+G_DEC_CAMS_20020101_365_V1.csv
6. EPA_SS_NY_IS52_P+G_DEC_CAMS_20030101_356_V1.csv
7. EPA_SS_NY_IS52_P+G_DEC_CAMS_20040101_366_V1.csv
8. EPA_SS_NY_IS52_PRT_DEC_FRM_20000101_366_V1.csv
9. EPA_SS_NY_IS52_PRT_DEC_FRM_20010101_365_V1.csv
10. EPA_SS_NY_IS52_PRT_DEC_FRM_20020101_365_V1.csv
11. EPA_SS_NY_IS52_PRT_DEC_FRM_20030101_365_V1.csv
12. EPA_SS_NY_IS52_PRT_DEC_FRM_20040101_182_V1.csv
13. EPA_SS_NY_IS52_P+M_DEC_SPECIATION_20001115_1824_V1.csv
14. EPA_SS_NY_IS52_PRT_SULFATE_AIR_FILT_20020119_347_V1.csv
15. EPA_SS_NY_MDBS_P+G_DEC_CAMS_20000101_182_V1.csv
16. EPA_SS_NY_MDBS_P+G_DEC_CAMS_20000701_184_V1.csv
17. EPA_SS_NY_MDBS_P+G_DEC_CAMS_20010101_165_V1.csv
18. EPA_SS_NY_MDBS_PRT_DEC_FRM_20000101_366_V1.csv
19. EPA_SS_NY_MDBS_PRT_DEC_FRM_20010101_181_V1.csv
20. EPA_SS_NY_P219_G+M_DEC_CAMS_20010712_173_V1.csv
21. EPA_SS_NY_P219_GPM_DEC_CAMS_20020101_365_V1.csv
22. EPA_SS_NY_P219_GPM_DEC_CAMS_20030101_365_V1.csv
23. EPA_SS_NY_P219_GPM_DEC_CAMS_20040101_365_V1.csv
24. EPA_SS_NY_P219_P+M_DEC_SPECIATION_20010326_1690_V1.csv
25. EPA_SS_NY_P219_PRT_CARBON_5400_20040108_30_V1.csv
26. EPA_SS_NY_P219_PRT_METAL-AIR-FILT_20010807_147_V1.csv
27. EPA_SS_NY_P219_PRT_METAL-TOTAL-AIR_20010630_93_V1.csv
28. EPA_SS_NY_P219_PRT_METAL-TOTAL-AIR_20011001_92_V1.csv
29. EPA_SS_NY_P219_PRT_METAL-TOTAL-AIR_20020101_181_V1.csv
30. EPA_SS_NY_P219_PRT_METAL-TOTAL-AIR_20020701_184_V1.csv
31. EPA_SS_NY_PSP__GPMR_CONT_AQ_20010101_90_V1.csv
32. EPA_SS_NY_PSP__GPMR_CONT_AQ_20010401_91_V1.csv
33. EPA_SS_NY_PSP__GPMR_CONT_AQ_20010701_92_V1.csv
34. EPA_SS_NY_PSP__GPMR_CONT_AQ_20011001_92_V1.csv
35. EPA_SS_NY_PSP__GPMR_CONT_AQ_20020101_90_V1.csv
36. EPA_SS_NY_PSP__GPMR_CONT_AQ_20020401_91_V1.csv
37. EPA_SS_NY_PSP__GPMR_CONT_AQ_20020701_92_V1.csv
38. EPA_SS_NY_PSP__GPMR_CONT_AQ_20021001_92_V1.csv
39. EPA_SS_NY_PSP__GPMR_CONT_AQ_20030101_90_V2.csv
40. EPA_SS_NY_PSP__GPMR_CONT_AQ_20030401_91_V2.csv
41. EPA_SS_NY_PSP__GPMR_CONT_AQ_20030701_92_V2.csv
42. EPA_SS_NY_PSP__GPMR_CONT_AQ_20031001_92_V2.csv

43. EPA_SS_NY_PSP__GPMR_CONT_AQ_20040101_90_V1.csv
44. EPA_SS_NY_PSP__GPMR_CONT_AQ_20040401_91_V1.csv
45. EPA_SS_NY_PSP__GPMR_CONT_AQ_20040701_92_V1.csv
46. EPA_SS_NY_PSP__GPMR_CONT_AQ_20041001_92_V1.csv
47. EPA_SS_NY_PSP__GPMR_CONT_AQ_20050101_90_V1.csv
48. EPA_SS_NY_PSP__GPMR_CONT_AQ_20050401_91_V1.csv
49. EPA_SS_NY_PSP__GPMR_CONT_AQ_20050701_92_V1.csv
50. EPA_SS_NY_PSP__GPMR_CONT_AQ_20051001_92_V1.csv
51. EPA_SS_NY_PSP__PRT_TEOMD_20040101_90_V1.csv
52. EPA_SS_NY_PSP__PRT_TEOMD_20040401_91_V1.csv
53. EPA_SS_NY_PSP__PRT_TEOMD_20040701_92_V1.csv
54. EPA_SS_NY_PSP__PRT_TEOMD_20041001_92_V1.csv
55. EPA_SS_NY_PSP__PRT_TEOMD_20050101_90_V1.csv
56. EPA_SS_NY_PSP__PRT_TEOMD_20050401_91_V1.csv
57. EPA_SS_NY_PSP__PRT_TEOMD_20050701_92_V1.csv
58. EPA_SS_NY_PSP__PRT_TEOMD_20051001_92_V1.csv
59. EPA_SS_NY_PSP__PRT_METAL-AIR-FILT_20010704_34_V1.csv
60. EPA_SS_NY_PSP__PRT_METAL-AIR-FILT_20010807_147_V1.csv
61. EPA_SS_NY_PSP__PRT_METAL-AIR-FILT_20020101_365_V1.csv
62. EPA_SS_NY_PSP__PRT_METAL-AIR-FILT_20030101_365_V1.csv
63. EPA_SS_NY_PSP__PRT_METAL-AIR-FILT_20040101_365_V1.csv
64. EPA_SS_NY_PSP__PRT_METAL-TOTAL-AIR_20010704_34_V1.csv
65. EPA_SS_NY_PSP__PRT_METAL-TOTAL-AIR_20020101_181_V1.csv
66. EPA_SS_NY_PSP__PRT_METAL-TOTAL-AIR_20020701_184_V1.csv
67. EPA_SS_NY_PSP__P+M_DEC_SPECIATION_20010206_1741_V1.csv
68. EPA_SS_NY_PSP__PRT_DEC_FRM_20000101_366_V1.csv
69. EPA_SS_NY_PSP__PRT_DEC_FRM_20010101_365_V1.csv
70. EPA_SS_NY_PSP__PRT_DEC_FRM_20020101_365_V1.csv
71. EPA_SS_NY_PSP__PRT_DEC_FRM_20030101_365_V1.csv
72. EPA_SS_NY_PSP__PRT_DEC_FRM_20040101_182_V1.csv
73. EPA_SS_NY_QBCC_GAS_DEC_CAMS_20000101_182_V1.csv
74. EPA_SS_NY_QBCC_GAS_DEC_CAMS_20000701_184_V1.csv
75. EPA_SS_NY_QBCC_GAS_DEC_CAMS_20010101_181_V1.csv
76. EPA_SS_NY_QBCC_GAS_DEC_CAMS_20010701_180_V1.csv
77. EPA_SS_NY_QBCC_PRT_DEC_FRM_20000101_364_V1.csv
78. EPA_SS_NY_QCOL_GAS_HONO_HNO3_20010628_36_V1.csv
79. EPA_SS_NY_QCOL_GAS_HNO3_20040116_19_V1.csv
80. EPA_SS_NY_QCOL_GAS_HONO_20040116_22_V1.csv
81. EPA_SS_NY_QCOL_GAS_OH-HO2_20010630_34_V1.csv
82. EPA_SS_NY_QCOL_GAS_OH-HO2_20040110_28_V1.csv
83. EPA_SS_NY_QCOL_GAS_TDLAS_HNO3_1HOUR_20040112_25_V1.csv
84. EPA_SS_NY_QCOL_GAS_TDLAS_NH3_1MIN_20040112_25_V1.csv
85. EPA_SS_NY_QCOL_GPM_DEC_CAMS_20010315_108_V1.csv
86. EPA_SS_NY_QCOL_GPM_DEC_CAMS_20010701_184_V1.csv
87. EPA_SS_NY_QCOL_GPM_DEC_CAMS_20020101_365_V1.csv
88. EPA_SS_NY_QCOL_GPM_DEC_CAMS_20030101_365_V1.csv
89. EPA_SS_NY_QCOL_GPM_DEC_CAMS_20040101_366_V1.csv
90. EPA_SS_NY_QCOL_P+M_NO3_MASS_8400N_20010629_36_V1.csv
91. EPA_SS_NY_QCOL_PRT_NO3_MASS_8400N_20040108_30_V1.csv
92. EPA_SS_NY_QCOL_P+M_SO4_MASS_8400S_20010629_37_V1.csv
93. EPA_SS_NY_QCOL_PRT_SO4_MASS_8400S_20040108_30_V1.csv

94. EPA_SS_NY_QCOL_PRT_CARBON_SUNSET_20040112_25_V1.csv
95. EPA_SS_NY_QCOL_PRT_CARBON_5400_20010629_039_V1.csv
96. EPA_SS_NY_QCOL_PRT_IONS_MASS_AMS_20010630_37_V1.csv
97. EPA_SS_NY_QCOL_PRT_IONS-PILS-IC_20010701_36_V1.csv
98. EPA_SS_NY_QCOL_PRT_IONS-PILS-IC_20040108_26_V1.csv
99. EPA_SS_NY_QCOL_PRT_METAL-AIR-FILT_20010707_28_V1.csv
100. EPA_SS_NY_QCOL_PRT_METAL-AIR-FILT6_20010629_39_V1.csv
101. EPA_SS_NY_QCOL_PRT_METAL-TOTAL-AIR_20010707_28_V1.csv
102. EPA_SS_NY_QCOL_PRT_METAL-TOTAL-AIR_20040108_30_V1.csv
103. EPA_SS_NY_QCOL_PRT_METAL-TOTAL-AIR-6H_20010629_39_V1.csv
104. EPA_SS_NY_QCOL_PRT_METAL-TOTAL-AIR-6H_20040108_30_V1.csv
105. EPA_SS_NY_QCOL_PRT_NH4_SIZE_AMS_20010630_37_V1.csv
106. EPA_SS_NY_QCOL_PRT_NO3_SIZE_AMS_20010630_37_V1.csv
107. EPA_SS_NY_QCOL_PRT_NUMBER_CONC_CPC_20010628_39_V1.csv
108. EPA_SS_NY_QCOL_PRT_NUMBER_CONC_CPC_20040108_29_V1.csv
109. EPA_SS_NY_QCOL_PRT_ORG_SIZE_AMS_20010630_37_V1.csv
110. EPA_SS_NY_QCOL_PRT_SIZE_APS_20010629_38_V1.csv
111. EPA_SS_NY_QCOL_PRT_SIZE_APS_20040108_29_V1.csv
112. EPA_SS_NY_QCOL_PRT_SIZE_NanoSMPS_20010629_34_V1.csv
113. EPA_SS_NY_QCOL_PRT_SIZE_NanoSMPS_ASRC_20040108_28_V1.csv
114. EPA_SS_NY_QCOL_PRT_SIZE_NanoSMPS_DEC_20040108_28_V1.csv
115. EPA_SS_NY_QCOL_PRT_SIZE_SMPS_20010629_37_V1.csv
116. EPA_SS_NY_QCOL_PRT_SIZE_SMPS_20040108_28_V1.csv
117. EPA_SS_NY_QCOL_PRT_SO4_HSPH_20010722_015_V1.csv
118. EPA_SS_NY_QCOL_PRT_SO4_SIZE_AMS_20010630_37_V1.csv
119. EPA_SS_NY_QCOL_PRT_DEC_FRM_20010101_365_V1.csv
120. EPA_SS_NY_QCOL_PRT_DEC_FRM_20020101_365_V1.csv
121. EPA_SS_NY_QCOL_PRT_DEC_FRM_20030101_365_V1.csv
122. EPA_SS_NY_QCOL_PRT_DEC_FRM_20040101_182_V1.csv
123. EPA_SS_NY_WFML_GAS_HNO3_20020712_31_V1.csv
124. EPA_SS_NY_WFML_GAS_HONO_20020712_31_V1.csv
125. EPA_SS_NY_WFML_GAS_OH-HO2_20020709_30_V1.csv
126. EPA_SS_NY_WFML_GAS_TDLAS_NO2_SO2_10MIN_20020710_29_V1.csv
127. EPA_SS_NY_WFML_GAS_TDLAS_NO2_SO2_1MIN_20020710_29_V1.csv
128. EPA_SS_NY_WFML_GAS_TDLAS_NO2_SO2_HCHO_20020709_30_V1.csv
129. EPA_SS_NY_WFML_GPM_DEC_CAMS_20000101_182_V1.csv
130. EPA_SS_NY_WFML_GPM_DEC_CAMS_20000701_184_V1.csv
131. EPA_SS_NY_WFML_GPM_DEC_CAMS_20010101_181_V1.csv
132. EPA_SS_NY_WFML_GPM_DEC_CAMS_20010701_184_V1.csv
133. EPA_SS_NY_WFML_GPM_DEC_CAMS_20020101_1096_V1.csv
134. EPA_SS_NY_WFML_PRT_CARBON_5400_20020712_31_V1.csv
135. EPA_SS_NY_WFML_PRT_DEC_FRM_20000101_366_V1.csv
136. EPA_SS_NY_WFML_PRT_DEC_FRM_20010101_365_V1.csv
137. EPA_SS_NY_WFML_PRT_DEC_FRM_20020101_365_V1.csv
138. EPA_SS_NY_WFML_PRT_DEC_FRM_20030101_365_V1.csv
139. EPA_SS_NY_WFML_PRT_DEC_FRM_20040101_182_V1.csv
140. EPA_SS_NY_WFML_P+M_DEC_SPECIATION_20010525_1630_V1.csv
141. EPA_SS_NY_WFML_P+M_NO3_MASS_8400N_20020709_30_V1.csv
142. EPA_SS_NY_WFML_P+M_SO4_MASS_8400S_20020709_30_V1.csv
143. EPA_SS_NY_WFML_PRT_IONS_MASS_AMS_20020709_30_V1.csv
144. EPA_SS_NY_WFML_PRT_IONS-PILS-IC_20020710_24_V1.csv

145. EPA_SS_NY_WFML_PRT_METAL-AIR-FILT_20010630_38_V1.csv
146. EPA_SS_NY_WFML_PRT_METAL-AIR-FILT_20010807_147_V1.csv
147. EPA_SS_NY_WFML_PRT_METAL-TOTAL_AIR_20020101_181_V1.csv
148. EPA_SS_NY_WFML_PRT_METAL-AIR-FILT_20030101_365_V1.csv
149. EPA_SS_NY_WFML_PRT_METAL-AIR-FILT_20040101_365_V1.csv
150. EPA_SS_NY_WFML_PRT_METAL-TOTAL-AIR_20010630_38_V1.csv
151. EPA_SS_NY_WFML_PRT_METAL-TOTAL-AIR_20010807_147_V1.csv
152. EPA_SS_NY_WFML_PRT_METAL-TOTAL-AIR_20020710_30_V1.csv
153. EPA_SS_NY_WFML_PRT_NH4_SIZE_AMS_20020709_30_V1.csv
154. EPA_SS_NY_WFML_PRT_NO3_SIZE_AMS_20020709_30_V1.csv
155. EPA_SS_NY_WFML_PRT_ORG_SIZE_AMS_20020709_30_V1.csv
156. EPA_SS_NY_WFML_PRT_NUMBER_CONC_CPC_20020709_27_V1.csv
157. EPA_SS_NY_WFML_PRT_SIZE_APS_20020709_27_V1.csv
158. EPA_SS_NY_WFML_PRT_SIZE_NanoSMPS_20020709_30_V1.csv
159. EPA_SS_NY_WFML_PRT_SIZE_SMPS_20020709_30_V1.csv
160. EPA_SS_NY_WFML_PRT_SO4_SIZE_AMS_20020709_30_V1.csv
161. EPA_SS_NY_WFMS_GPM_ASRC_CAMS_20020101_365_V1.csv
162. EPA_SS_NY_WFMS_GPM_ASRC_CAMS_20040101_366_V1.csv

Meta data files:

1. EPA_SS_NY_5400_CPM_QA_REPORT.pdf
2. EPA_SS_NY_8400N_OPERATION.pdf
3. EPA_SS_NY_8400S_OPERATION.pdf
4. EPA_SS_NY_PILS_IC_QA_report.pdf
5. EPA_SS_NY_QCOL_AMS_METADATA_REPORT.pdf
6. EPA_SS_NY_SO4_HSPH_QA_REPORT.pdf
7. EPA_SS_NY_TDLAS_OPERATION.pdf
8. EPA_SS_NY_WFML_AMS_METADATA_REPORT.pdf

For information on other
NYSERDA reports, contact:

New York State Energy Research
and Development Authority
17 Columbia Circle
Albany, New York 12203-6399

toll free: 1 (866) NYSERDA
local: (518) 862-1090
fax: (518) 862-1091

info@nyserda.org
www.nyserda.org

Results and Findings from the Joint Enhanced Ozone and PM Precursor - $PM_{2.5}$ Technology Assessment and Characterization Study in New York (PMTACS-NY)

Final Report 09-10

State of New York
David A Paterson, Governor

New York State Energy Research and Development Authority
Vincent A. DeIorio, Esq., Chairman
Francis J. Murray, Jr., President, and Chief Executive Officer

NYSERDA

Results and Findings from the Joint Enhanced Ozone and PM Precursor - $PM_{2.5}$ Technology Assessment and Characterization Study in New York (PMTACS-NY)

NYSERDA Final Report 09-10